STRUCTURAL MONITORING AND ANALYSIS OF STEEL TRUSS RAILROAD BRIDGES

A THESIS SUBMITTED TO
THE GRADUATE SCHOOL OF NATURAL AND APPLIED SCIENCES
OF
MIDDLE EAST TECHNICAL UNIVERSITY

BY

TUĞBA AKIN

IN PARTIAL FULFILLMENT OF THE REQUIREMENTS
FOR
THE DEGREE OF MASTER OF SCIENCE
IN
CIVIL ENGINEERING

SEPTEMBER 2012

Approval of the thesis:

STRUCTURAL MONITORING AND ANALYSIS OF STEEL TRUSS RAILROAD BRIDGES

Submitted by **TUĞBA AKIN** in partial fulfillment of the requirements for the degree of **Master of Science in Civil Engineering Department, Middle East Technical University** by,

Prof.Dr. Canan Özgen
Dean, Gradute School of **Natural and Applied Sciences** _____

Prof.Dr.Güney Özcebe
Head of Department, **Civil Engineering** _____

Assoc.Prof.Dr Ahmet Türer
Supervisor, **Civil Engineering Department** _____

Examining Committee Members:

Prof. Dr Çetin Yılmaz
Civil Engineering Dept., METU _____

Assoc. Prof. Dr. Ahmet Türer
Civil Engineering Dept., METU _____

Prof.Dr. Uğurhan Akyüz
Civil Engineering Dept., METU _____

Assoc.Prof. Dr. Alp Caner
Civil Engineering Dept., METU _____

Dr. Varol Akar
Bridges Dept., TCDD _____

Date: _____

I hereby declare that all information in this document has been obtained and presented in accordance with academic rules and ethical conduct. I also declare that, as required by these rules and conduct, I have fully cited and referenced all material and results that are not original to this work.

Name, Last Name: TUĞBA AKIN

Signature:

ABSTRACT

STRUCTURAL MONITORING AND ANALYSIS OF
STEEL TRUSS RAILROAD BRIDGES

Akın, Tuğba

M.Sc., Department of Civil Engineering
Supervisor: Assoc. Prof. Ahmet Türer

September 2012, 217 pages

Railroad bridges are the most important connection parts of railroad networks. These bridges are exposed to heavier train loads compared to highway bridges as well as various detrimental ambient conditions during their life span. The railroad bridges in Turkey are mostly constructed during the late Ottoman and first periods of the Turkish Republic; therefore, they are generally close to about 100 years of age; their inspection and maintenance works are essential. Structural health monitoring (SHM) techniques are widely used around the world in order to increase the effectiveness of the inspection and maintenance works and also evaluate structural reliability. Application of SHM methods on railway bridges by static and dynamic measurements over short and long durations give important structural information about bridge members' load level and overall bridge structure in terms of vibration frequencies, deflections, etc. Structural Reliability analysis provides further information about the safety of a structural system and becomes even more efficient when combined with the SHM studies.

In this study, computer modeling and SHM techniques are used for identifying structural condition of a steel truss railroad bridge in Uşak, Turkey, which is

composed of six spans with 30 m length each. The first two spans of the bridge were rebuilt about 50 years ago, which had construction plans and are selected as pilot case for SHM and evaluation studies in this thesis. Natural frequencies are obtained by using 4 accelerometers and a dynamic data acquisition system (DAS). Furthermore, mid span vertical deflection member strains and bridge accelerations are obtained using a DAS permanently left on site and then compared with the computer model analyses results. SHM system is programmed for triggering by the rail load sensors developed at METU and an LVDT to collect mid span deflection high speed data from all sensors during train passage. The DAS is also programmed to collect slow speed data (once at every 15 minutes) for determination of average ambient conditions such as temperature and humidity and all bridge sensors during long term monitoring. Structural capacity and reliability indices for stress levels of bridge members are determined for the measured and simulated train loads to determine structural condition of bridge members and connections. Earthquake analyses and design checks for bridge members are also conducted within the scope of this study.

Keywords: Structural Health Monitoring, Capacity Index, Reliability Index, Steel Truss, Bridge, Earthquake.

ÖZ

ÇELİK MAKAS DEMİRYOLU KÖPRÜLERİNİN
YAPISAL İZLEME VE ANALİZİ

Akın, Tuğba
Yüksek Lisans, İnşaat Mühendisliği Bölümü
Tez Yöneticisi: Doç.Dr.Ahmet Türer

Eylül 2012, 217 sayfa

Demiryolu köprüleri, demiryolu ağlarının en önemli bağlantı noktalarıdır. Bu köprüler, karayolu köprülerine göre daha ağır yüklere, bunun yanı sıra çeşitli hasar verici çevresel koşullara maruz kalmaktadır. Türkiye'nin mevcut demiryolu köprüleri büyük çoğunluğu 100 yaşın üzerinde olan; Osmanlı Devleti'nin son dönemi ve Türkiye Cumhuriyeti'nin ilk yıllarında inşa edilmiş köprülerdir, bu sebep ile bu köprülerin bakım ve onarım çalışmaları büyük önem taşımaktadır. Yapısal sağlık izleme (YSİ) teknikleri demiryolu köprüleri bakım ve onarım çalışmalarının etkinliğini arttırmak ve yapı mevcut durumunu değerlendirmek amacı ile dünya çapında kullanılan tekniklerdir. Demiryolu köprülerinde kullanılan YSİ teknikleri kısa ve uzun süreli; statik ve dinamik ölçümler ile yapı elemanları yükleme durumları ve titreşim frekansları, deplasmanlar gibi köprü geneli hakkında önemli yapısal bilgiler sağlanmaktadır. Yapısal güvenilirlik analizleri, yapı mevcut güvenlik durumu hakkında bilgi vermektedir; bu analizlerin YSİ çalışmaları ile birlikte yürütülmesi analizlerin etkinliğini arttırmaktadır.

Bu çalışmada, Türkiye Uşak sınırları içinde olan 30'ar metrelik altı açıklığı bulunan çelik makas demiryolu köprüsünde yapı mevcut durum tespiti amacı ile YSİ teknikleri, bilgisayar modellemesi ve güvenilirlik analizleri uygulamaları yapılmıştır. Demiryolu köprüsünün yaklaşık 50 önce yeniden inşa edilmiş olan ilk

iki açıklığı, teknik çizimlerinin var olması sebebi ile YSİ ve yapı değerlendirmesi için pilot açıklıklar olarak seçilmiştir. Yapı doğal frekansları 4 adet ivmeölçer ve dinamik data toplama sistemi ile tespit edilmiştir. Bunlara ek olarak açıklık ortası deplasmanı, eleman birim deformasyonları, köprü ivme değerleri uzun süreli veri toplama sistemi ile tespit edilmiş ve bilgisayar modeli analizleri ile karşılaştırılmıştır. YSİ sistemi, ODTÜ tarafından geliştirilmiş olan ray yük sensörleri ve LVDT ile tetikleme yapabilmesi için programlanmış ve sistemin hızlı data okuma yapabilmesi sağlanmıştır, ayrıca sistem çevre koşullarının (sıcaklık, nem vb.) tespiti için tüm sensörlerden yavaş (15 dakikada bir) data okuyabilecek şekilde programlanmıştır. Köprü açıklık elemanları ve bağlantıları, eleman gerilmeleri bakımından, yapısal durumunun belirlenmesi amacı ile yapısal kapasite ve güvenilirlik indisleri, ölçüm ve tasarım yüklemeleri altında belirlenmiştir. Köprü elemanları deprem analizleri ve tasarım kontrolleri çalışma kapsamında tamamlanmıştır.

Anahtar Kelimeler: Yapısal Sağlık İzleme, Kapasite İndisi, Güvenilirlik İndisi, Çelik Makas, Köprü, Deprem.

To My Family

ACKNOWLEDGEMENTS

This study was conducted under the supervision of Assoc.Prof.Dr. Ahmet Türer. I would like to express sincere appreciation to Assoc.Prof.Dr. Ahmet Türer for his support, guidance, advice, encouragement and insight throughout the study.

I would like to express my thanks to Assoc.Prof.Dr. Alp Caner and Res.Asst.Mustafa Can Yücel for their precious helps during study.

I would like to express my special thanks to Dr.Varol Akar due to his invaluable suggestions and guidance since the beginning of the study.

I also would like to thank Turkish State Railways (TCDD) officials and personnel for their helps during study.

I would like express my thanks to my friend Özge Alper Gür for his contributions to this study.

My colleagues Tamer Fenercioğlu, Fatih Cinek, Mert Fenercioğlu in Veni Engineering Company deserve special thanks for their valuable supports during thesis study.

I am grateful to my family for their encouragement, confidence in me and support.

TABLE OF CONTENTS

APPENDICES

LIST OF TABLES

TABLES

LIST OF FIGURES

FIGURES

CHAPTER 1

INTRODUCTION

1.1 General

Railroad bridges are the most important connection parts of the railroad networks. These bridges are exposed to heavier train loads compared to highway bridges as well as various detrimental ambient conditions during their life span. The railroad bridges in Turkey are mostly constructed during the late Ottoman and the first periods of the Turkish Republic; therefore, they are generally about close to 100 years of age; their inspection and maintenance works are essential.

There are several types of inspection techniques including tabulated visual inspection form based inspection, basic deflection measurement based inspection, vibration measurement based inspection. The most commonly used technique is visual inspection which quite subjective based on the mood of the inspector, environmental conditions during inspection etc. Measurement based techniques can be categorized under general structural health monitoring (SHM); whereas, the monitoring technique may be rapid & short term or slow & long term. The number of measurement locations and measurement types can greatly vary from case to case. In general, SHM techniques are widely used around the world, in order to increase the effectiveness of the inspection, improve objectivity in the evaluation, impose quantitative evaluation rather than qualitative, and optimize maintenance works while improving structural reliability. Application of SHM methods on railroad bridges by static and dynamic measurements over short and long durations

provide important structural information about bridge members' strain and load level as well as overall bridge resonant vibration frequencies and span deflections. Combining SHM methods with finite element modeling (FEM) and structural reliability analyses yields even more efficient condition assessment of a bridge.

1.2 Objectives

In this study, computer modeling and SHM techniques will be used for identifying structural information of steel truss Railroad Bridge located on Basmane-Dumlupınar railroad route Km: 199+352 in Uşak, Turkey. Bridge composed of six spans with 30 m length. The first two spans of the bridge were rebuilt about 50 years ago. The first span of bridge is selected as pilot span for SHM and evaluation studies which had construction plans. By dynamic measurements, bridge span acceleration information during train cross and span natural frequencies; by static measurements, mid span vertical deflection and member strains will be obtained and compared with computer model analyses results. Additional measurements will be done for determination of ambient conditions such as wind speed and direction, temperature and humidity. SHM system will be programmed for triggering by the invented rail sensors and LVDT to collect high speed data during train passage and, also programmed to collect slow speed data for determination of average ambient conditions during long term monitoring. FEM will be the completing part of study for the purpose of SHM measurement and FEM analyses result comparison to determine SHM system reliability, and also loading condition assessment tool for the members of structure that are not monitored. At the end of study, computer modeling and SHM measurements will be lead to determination of structural capacity and reliability indices of bridge members to evaluate structural condition of bridge. Bridge condition of bridge members are conducted for measured and simulated loads. In another part of study FEM is used for earthquake analyses and design checks for bridge pier and span frame members with two different analyses method namely time history analysis and response spectrum analysis.

This study is conducted as a part of joint research project of Middle East Technical University and Turkish State Railways (TCDD). DSIM 10-03-03-2-06-06 coded joint project name is “Structural Monitoring and performance evaluation of railroad bridges under train traffic, and developing inspection and maintenance procedures for railroad bridges that is used by TCDD”.

1.3 Scope

Thesis study is started with the SHM studies conducted, introduced in chapter 2. Properties and environmental conditions of bridge are identified by site visits and technical drawings. Preliminary 2D FEM is used to decide critical member which should be monitored according to assumptions and loading conditions. Critical member determination is lead to sensor types and location decision making and also sensor development studies. Completed sensor types and location works is continued with the purchasing SHM system parts such as sensors, data logger and programming studies to complete SHM system. At the end SHM studies are completed by SHM system installation to the selected bridge span.

Thesis study continued with the FEM studies, introduced in chapter 3. 2D FEM of span one truss is created as first modeling step. Connection condition of steel trusses of bridge span is determined by the analysis of 2D FEM. 3D FEM is created and analyzed then compared with the 2D FEM and decided to continue with simpler 2D FEM. FEM studies is continued with the influence lines construction of bridge truss members, floor beams, lateral braces, and vertical braces. FEM studies are completed with the comparison of analysis results and SHM measurements data.

Thesis study third step is the determination of Capacity indices (CI) of bridge span steel members, introduced in chapter 4. CI determination done according to steel design regulations stated in Eurocode-3. Loads used in calculations are chosen according to both design regulations and service loading conditions.

Thesis study fourth step is the determination of Reliability indices (β) of bridge span steel members, introduced in chapter 5. β determination done for evaluation of real condition of bridge span structure. Loads used in calculations are chosen according calculated service loading from design loading condition and real service conditions.

Thesis study fifth step is the proposing instrumentation based evaluation principles for application to all types of railroad bridges, introduced in chapter 6.

Thesis study last step is the earthquake analyses and design checks of bridge piers and spans members, introduced in chapter 7.

Thesis study is concluded with the related summary, outcomes, and conclusions for the analyses and sub studies performed in the scope of the study, introduced in chapter 8.

1.4 Literature Survey

Many research studies are conducted on structural reliability, structural health monitoring and in some cases researchers combined two to improve condition estimation of bridge structures. Some of studies conducted and took part in literature are presented in following paragraphs.

Nowak,A.S. and Collins,K.R. (2000),introduced reliability concepts in their book, Reliability of Structures. Part of their subject was introducing the concept of probability of failure (P_f). They classified load (Q) and resistance (R) as random variables and derived probability of failure with the probability density functions of these random variables (Figure: 1.1).

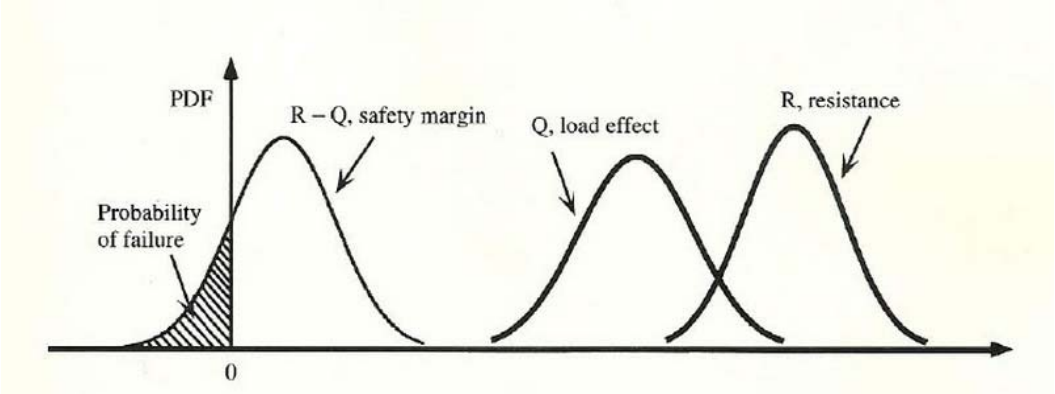

Figure 1.1: PDFs of load, resistance and safety margin (from Reliability of Structures, 2000)

Nowak,A.S. and Collins,K.R. (2000) presented reliability index calculations in their book. First they converted random variables Q and R to non-dimensional reduced variables Z_Q and Z_R respectively. Authors defined limit state function g(R, Q) = R-Q in terms of reduced variables. If the new limit state function $g(Z_R,Z_Q)$ equal to 0 then this line is the border line that between safe and failure domain. Authors presented a definition first introduced by Hasofer and Lind (1974) for reliability index (β) as "the shortest distance from the origin of reduced variables to the line g (ZR, ZQ) = 0" (Figure 2.1), which is the formulated as (Equation 1.1);

$$\beta = \frac{\mu_R + \mu_Q}{\sqrt{{\sigma_R}^2 + {\sigma_Q}^2}} \qquad (1.1)$$

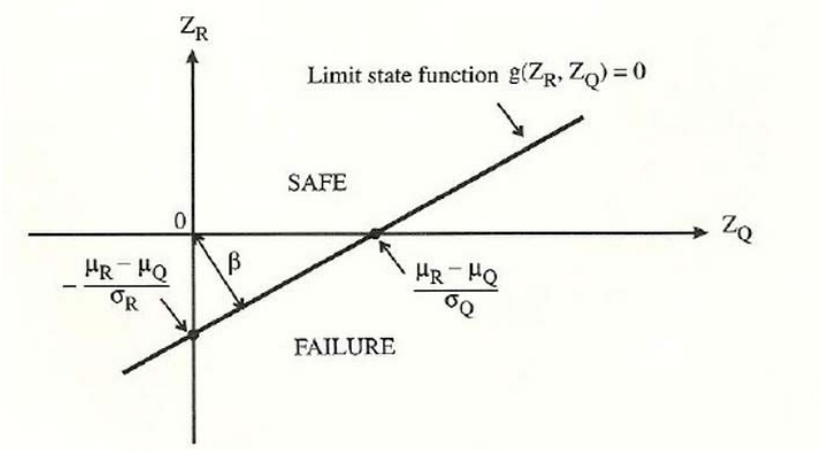

Figure 1.2: Reliability index definition in graphical form (from Reliability of Structures, 2000)

Dissanayake P.B.R, and Karunananda, P. A. K. (2008), proposed reliability based methodology for condition assessment of aging bridges. First step of their study was the determination of critical failure criteria depending on type of bridge evaluated. Based on critical criteria, acceptable safety margin was defined. Authors assumed that the statistical distribution of quantities, which are defined for critical failure criteria, was a normal distribution. Under this assumption they calculated element reliability indices and failure probabilities of element. Element based reliability indices and failure probabilities are concluded with the system reliability index and failure probability of structure, in the period of time under consideration.

For the interests of study; one of the longest and busiest railroad bridge in Sri Lanka was chosen as case study bridge. It is eight spans, with two lane railroad traffic, warren type steel truss bridge. Fatigue and corrosion were chosen as critical failure criteria for evaluated bridge. Study concluded that the bridge was in excepted safety margin for current loading condition. Another result of research is that the reliability analysis is useful approach for evaluation of current condition of bridges.

Czarnecki,A. A.,Nowak, A. S. (2007), studied on structural reliability of steel girder bridges. They proposed that reliability of structure should be represented by complete structure, rather than element level. Authors stated that structural reliability depends on the load sharing and ductility level of structure. During study it is observed that load carrying capacity of complete structure is much higher than that element based designed load carrying capacity. Therefore authors focused on system reliability. They studied on steel girder bridge case study. During study both system reliability indices and element level reliability indices are obtained and compared. Bridge is two lanes, single span, and multi girder steel bridge designed according to AASTHO LRFD code. Study concluded that as expected by authors system has reserved structural safety due to load sharing, while girder of bridge has reached its ultimate level of load carrying. End of study authors proposed that

reliability differences between girder and system can be considered as measure of bridge degree of redundancy.

Enckell-El Jemli,M., Karoumi, R. and Lanaro,F. (2003) studied on structural health monitoring of the bridge that was under construction during study. Bridge is optimized and complex ten span pre-stressed concrete bridges. Purposes of study were monitoring bridge during construction and service life in 10 year period and compare traditional strain transducers and newly invented fiber optic sensors. Bridge SHM system was consist of 24 strain transducers, 6 accelerometers, 1 LVDT, 46 fiber optic sensors and 9 temperature sensors. Data collecting system was consist of four steps; as first step, statistical preliminary data analyses in field, second step, main analyses, graphical result obtaining and documentation in monitoring office, third step, data transferring by broadband, and last step, long term data base construction.

Catbas,F. N., Susoy, M., Frangopol, D. M. (2008) have conducted reliability estimation and SHM study on Commodore Barry Highway Bridge since 1999. Purposes of study were reliability estimation of main truss component and entire structural system and monitoring critical member stresses, structural movements, determination of strengthening needs of one of the longest cantilever steel truss bridge over the world.

Authors constructed SHM system with 2 weight sensors and speed sensors, 1 climate station, 4 ultrasonic wind sensors, 36 inclinometer, 17 LVDT, 16 capacitive accelerometers, 204 strain transducers, 201 thermistors and 4 data collecting units. Finite element model (FEM) was created in 2D, 3D and calibrated with the monitored data. Calibrated FEM used for reliability analysis of bridge structure. Dead, live, wind load effects are used load cases during reliability analysis. First order reliability method was chosen to estimate reliability of bridge under considered load effects. Reliability indices of lower chord members, upper chord members, vertical truss members, tower and hanger elements calculated.

Uzgider,E. et al (2004), carried out “safety evaluation of railroad bridges” named project. Subject of the project was determining the reliability condition of the bridges located in one of the railroad route in Turkey for the maximum allowable axle load specified by Turkish State Railways. In the scope of project reliability of 24 sample bridges are examined among 1777 bridges. Sample bridges was chosen according to construction material and structural type (steel, steel-encased-concrete, concrete arch, masonry arch and reinforced concrete), year of construction, span length, standards used for design, strengthening experiences of bridge.

During project, reliability studies were started with the finite element model (FEM) creation of each sample. Calibrations of FEMs were done with the acceleration monitoring studies of bridges. Acceleration measurements were done during test train cross. With the measured accelerations modal frequencies and modal shapes were obtained, then coincided the FEMs’ modal frequencies and modal shapes by calibrations. After FEM studies, project was continued with the reliability indices calculations. Member stresses were calculated for LM71 type and Turkish State Railroad chosen type train moving loads. After members stresses calculation, for each type of construction material of bridge different reliability indices calculation approach were used and obtained reliability indices.

Large scale study concluded that bridges, which were the subject of project, have reliability indices greater that the allowable reliability index value of 3 specified by the Turkish State Railway.

Sustainable Bridges project is the one of the largest scale project, conducted by 31 partners from Europe. Project was started in 2003 and continued for 4 years. Project subject was searching the condition of European railroad bridges and evaluation of bridges that sustainable enough under the demands of the year 2020 such as heavier axle load, more passenger amount, speed up trains etc. Main aims of projects were reaching allowable axle load to 33 tons for good transportation, allowable speed to 350 km/hour, residual life time 25% more and better

strengthening and repair system. For the purposes of project nine work packages were completed. End of the project four guidelines were published. One out of four guidelines was for monitoring of railroad bridges.

Monitoring of Railway Bridges Guideline were included four sub guidelines as monitoring of steel railway bridges, estimating structural damping of railway bridges, corrosion monitoring systems for reinforced concrete bridges and estimating reliability of monitoring systems of bridges.

First guideline, which is in thesis concerns, were included guides for methods and tools to design and install monitoring systems on steel railway bridges. Guideline first introduced definitions of inspection and technical monitoring concepts. Than continued with the codes and guidelines exist in literature. Thirdly guided for design of technical monitoring in details and gave the hints of using sensor technologies, communication networks, data loggers and processing, requirements and complete health monitoring systems in condition assessments of bridge structure. After design of sensors, guideline expressed technical monitoring of steel railway bridges. In this chapter monitoring options were summarized and gave opportunity to reader to understand the monitoring options that differs according to study duration, kind, and application. Authors of guideline introduced also service life analysis methods as “classical” und “adaptive” approach, action models, structural modeling, damage models, general approach for service life analysis with the help of monitoring, and approach using operation time interval. Guideline continued with the guides for identification of critical members; in this chapter guideline give detail information that used while determination of critical member study is carried out, such as critical member decision should be make according to age of bridge, structural design of bridge etc. Before the sample case studies presentations, guideline concluded with the damage groups and potentiality of technical monitoring. In this part of guideline damage groups were classified such as contamination, deformation etc, investigation and technical monitoring were presented as destructive testing and non-destructive testing, lastly summary of parameters and measurement methods were presented. Guideline for monitoring of

steel railway bridges concluded with application studies of steel railway bridges. For case applications firstly riveted steel railway bridges introduced, in this case visual inspection and monitoring studies combined to determine the cracks initiated in different parts of structures. Then use of monitoring for steel railway bridges presented. In this part bridge built in second decade of the 20^{th} century is consulted, bolts' strains and main girder's vertical web strain measurements were conducted. Last case was measurement for estimation of susceptibility to corrosion. In this part of guideline present that closed area under the railroad track measurements conducted to investigate the corrosion problem existence in the area closed. Temperature and humidity measurement was the monitoring application.

CHAPTER 2

STRUCTURAL HEALTH MONITORING (SHM) STUDIES ON THE SELECTED BRIDGE

2.1 Properties of the Selected Bridge

Selected bridge structure is a six span steel truss bridge (Figure 2.1). Each span is 30 meters long. Five piers are made of steel and 2 abutments are made of masonry. Bridge was constructed over 100 years and first two spans and 19 m pier were rebuilt about 50 years ago.

Total length of the bridge structure is 180 meters long; its width is 3.2 meters, maximum depth of each truss 4.5 meters. Detailed information of bridge is given in following subsections.

Figure 2.1: General view of bridge structure

2.1.1 Location of Bridge

Bridge structure is located on Basmahane-Dumlupınar Railroad route km:199+352, between Uşak, Turkey and Alaşehir, Manisa, Turkey. The satellite view of bridge location is given in the figures below (Figure 2.2 and Figure 2.3).

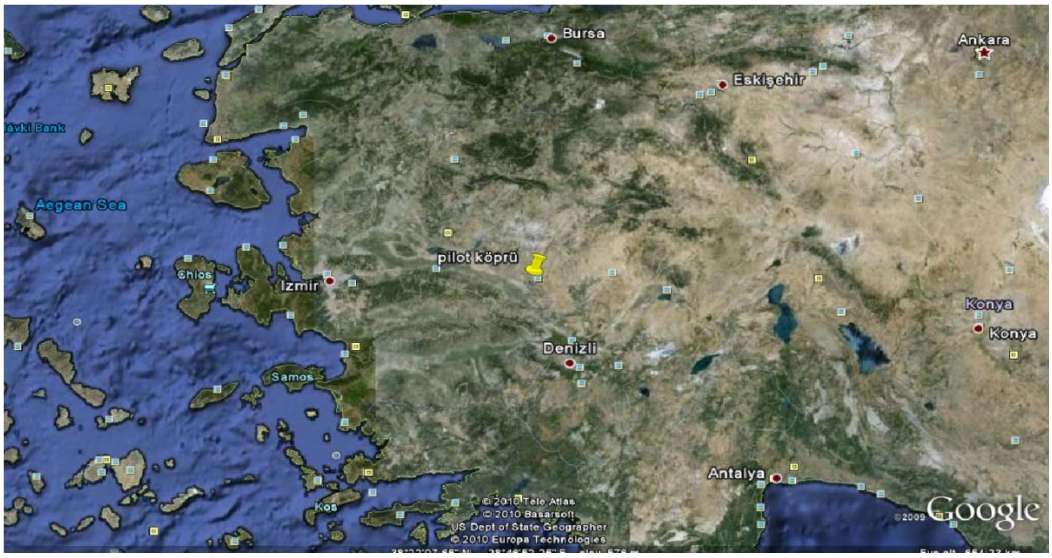

Figure 2.2: Satellite view of location of bridge-1

Figure 2.3: Satellite view of location of bridge-2

2.1.2 Superstructure of Bridge

S49 type railroad track used in superstructure of bridge Expansion joints exist to eliminate temperature changes created stresses on railroad tracks (Figure 2.4).

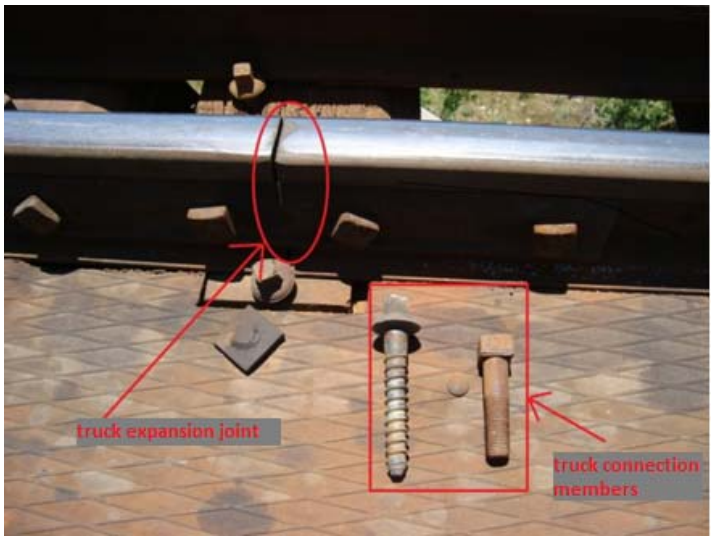

Figure 2.4: S49 Railroad track, expansion joint and railroad track connection members

Railroad sleepers are made of wood and protective sheet metals are used above sleepers to avoid spunk created during train cross (Figure 2.5).

Figure 2.5: Railroad wood sleepers and protective sheet metals

2.1.3 Substructure of Bridge

Bridge substructure, composed of 6 spans with 30 m span length, which are aligned with 300 m radius horizontal curve, super elevation and % 2.5 vertical slope (Figure 2.6).

Figure 2.6: Bridge horizontal curve, vertical slope and super elevation view

Bridge 6 spans are constructed by steel trusses. Each span is composed of two main trusses and designed as simply supported beams (Figure: 2.7). Each truss has six tension members as bottom chord, five compression members as top chord, and eight diagonals. Trusses are symmetrical with respect to their vertical midpoint (Figure 2.8).

Figure 2.7: Bridge trusses supports

Figure 2.8: Bridge one span general view

Bridge spans have supported by five steel piers with maximum height of pier is 52 meters which is middle pier (Figure 2.9).

Figure 2.9: Middle pier view

Bridge piers are connected to foundation with one pin supports and three roller supports (Figure 2.10); one of them is moving bridge longitudinal direction; one of them is moving bridge transverse direction (Figure 2.11) and one of them moving both directions.

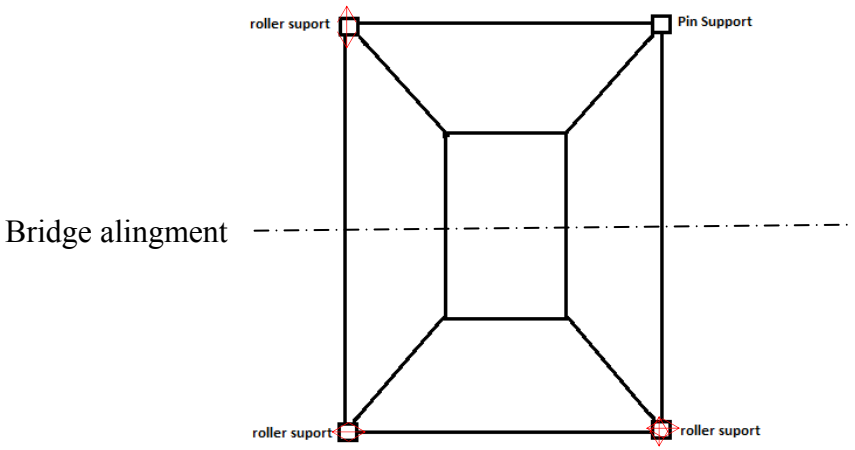

Figure 2.10: Pier support conditions

Figure 2.11: Transverse direction moving roller support

Bridge piers are connected foundation by steel large scale anchorages (Figure 2.12).

Figure 2.12: Foundation anchorage

2.2 Critical Members Determination

SHM studies conducted on the selected bridges are started with the determination of critical members within truss members. Critical members' determination is done according to Eurocode-3 and under LM71 moving train load stated in Eurocode-1 part 2: Traffic Loads on Bridges and self-weight of truss.

Structural analyses of truss are conducted with a simple connection model of truss members which is explained in chapter 3.Train moving load is simulated by locating train load statically with 0.4 m apart loading steps on 2D FEM of truss detailed explanation of loading explained in following chapters.

Detailed calculation of members loading condition calculations are given in Chapter 4. Critical member determination calculations are not included impact and distribution factors, whereas calculations are included application coefficient as 1.4 by multiplying vertical train load by this coefficient.

Material strength properties are 280 MPa for yield strength, 364 MPa for ultimate strength according to laboratory tests.

2.2.1 Critical Compression Members Determination

There are seven compression members in each truss (Figure 2.13). Critical compression members' determination is done according to compression member check stated in EC3 part: 2 equation: 6.9 (Equation 2.1). In accordance with the equation ratios are obtained under train moving load and the self-weight of truss. Members U1U2 and U1'U2', which have closest ratios to the boundary value of 0.9 are the critical compression members. Same maximum ratios are obtained for both critical compression members U1U2 and U1'U2' as 0.474.

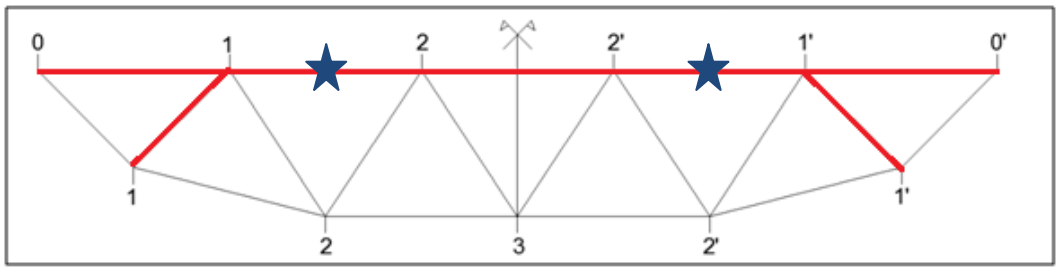

Figure 2.13: Compression members of truss

$$\frac{N_{Ed}}{X_y \frac{f_y \cdot A_{eff}}{\gamma_{M1}}} + C_{mi,o} \cdot \left(\frac{M_{y,Ed} + N_{Ed} \cdot e_{Ny}}{\frac{f_y \cdot W_{eff,y}}{\gamma_{M1}}} \right) \leq 0,9 \qquad (2.1)$$

Where;

γ_{M1}=1.1

f_y =280 MPa (From Laboratory Tests)

2.2.1.1 Graphical Results of Stress Ratios for Compression Members

Compressive stress ratios due to train load and self-weight of truss are presented in graphs as stress ratios calculated by equation 2.1 vs. loading steps (Figure 2.14).

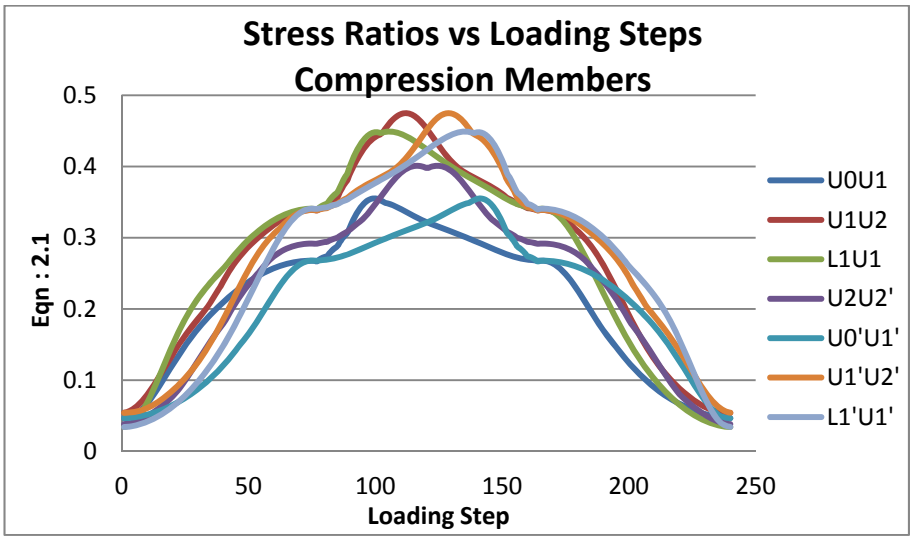

Figure 2.14: Compression members stress ratios with Eqn: 2.1 (max = 0.474 from members U1U2 and U1'U2')

2.2.2 Critical Tension Members Determination

There are six tension members in each truss (Figure 2.15). Critical tension members' determination is done according to tension member check stated in EC3 part:1-1 equation:6.44 (Equation 2.2). In accordance with the equation, ratios are obtained under train moving load and the self-weight of truss. Members L2L3 and L2'L3, which have closest ratios to the boundary value of 1.0 are the critical tension members. Same maximum ratios are obtained for both tension members L2L3 and L2'L3 as 0.423.

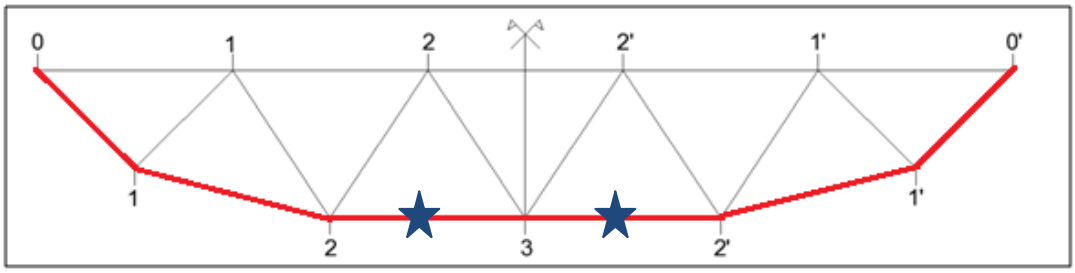

Figure 2.15: Tension members of truss

$$\frac{N_{Ed}}{\frac{f_y \cdot A_{eff}}{\gamma_{M0}}} + \frac{M_{y,Ed} + N_{Ed} \cdot e_{Ny}}{\frac{f_y \cdot W_{eff,y}}{\gamma_{M0}}} \leq 1,0 \qquad (2.2)$$

Where;

γ_{M0}=1.0

f_y =280 MPa (From Laboratory Tests)

2.2.2.1 Graphical Results of Stress Ratios for Tension Members

Tensile stress ratios due to train moving load and self weight of truss are presented in graphical representation as by equation 2.2 vs. loading steps for tension members (Figure 2.16).

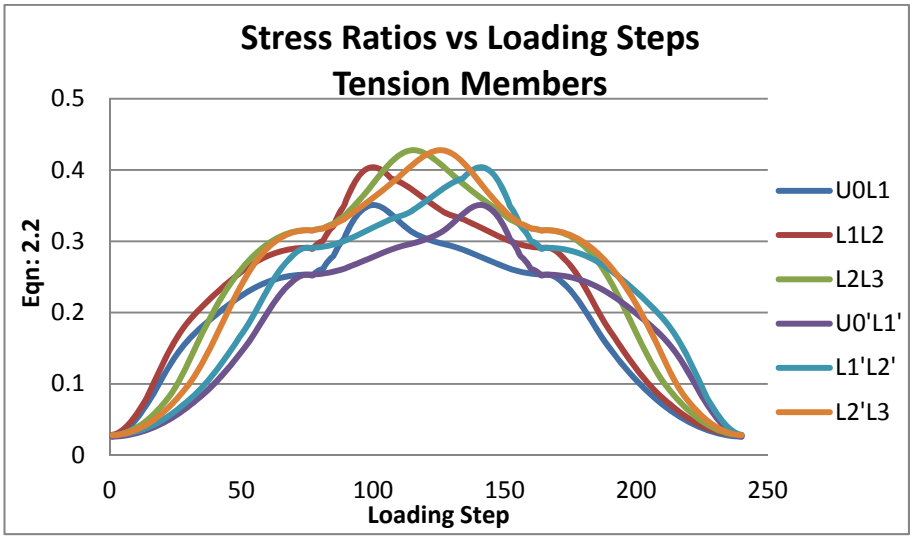

Figure 2.16: Tension members stress ratios with Eqn: 2.2 (max = 0.423 from members L2L3 and L2'L3)

2.2.3 Critical Compression-Tension Members Determination

There are six compression-tension members in each truss (Figure 2.17). Critical compression-tension members' determination is done according to its loading situation, if it is under compression, it is treated as compression member, if not it is treated as tension member. Members U1L2 and U1'L2', most exposed to tension compression change is named as critical compression-tension members because of the fatigue concerns. Members U1L2 and U1'L2' have stress ratios as 0.252 for compression and 0.249 for tension which yields 0.252 + 0.249 = 0.501 stress ratio change from eqn:2.1 and eqn:2.2.

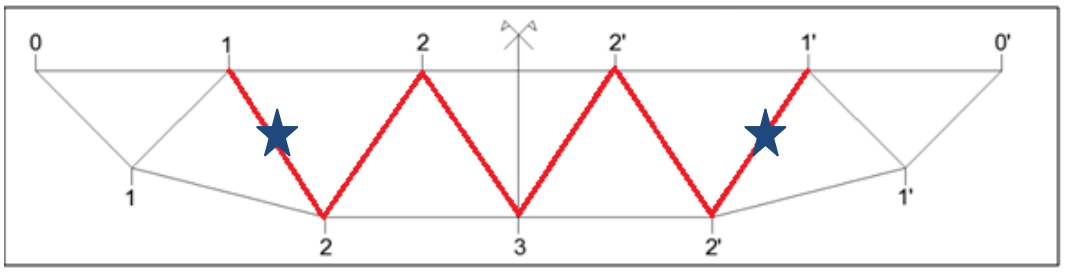

Figure 2.17: Compression-Tension members of truss

2.2.3.1 Graphical Results of Stress Ratios for Compression-Tension Members

Compressive and tensile stress ratios due to train moving loading and self weight of truss are presented in graphical representation as stress ratios vs loading steps (Figure 2.18). Stress ratios are calculated by equation 2.1 if member is under compressive load and equation 2.2 if member is under tensile load. Negative ratios are corresponds to compressive stress ratios, positive ratios are corresponds to tensile stress ratios.

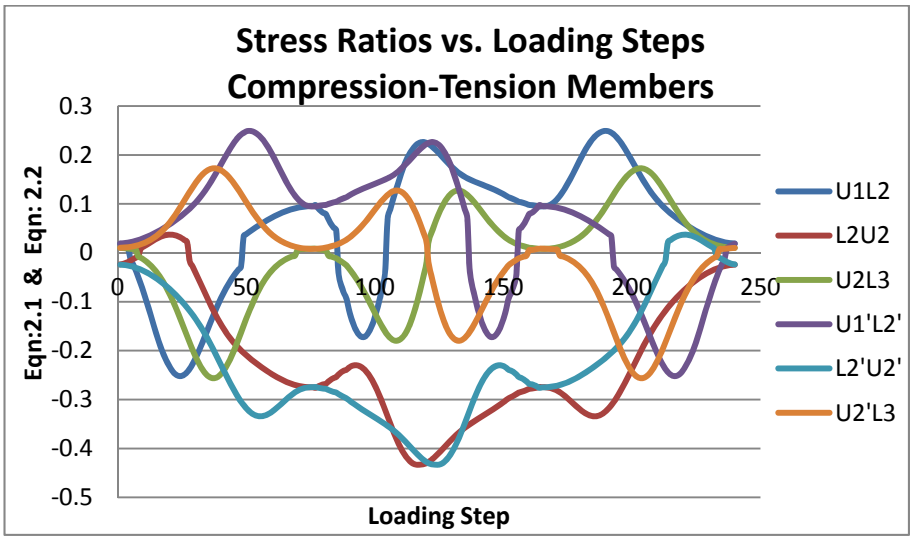

Figure 2.18: Compression-tension members stress ratios with Eqn: 2.1 and Eqn:2.2 (max stress ratio change = 0.501 from members U1L2 and U1'L2')

2.3 Sensor Types and Locations

Bridge structure and critical members are monitored with different type of monitoring sensors. Sensor type and location decisions are made according to purpose of monitoring such as determination of strains in members, deflections of span, vertical strains on web of rail during train crossing the bridge, and environmental conditions. Sensor type, installed location and purpose are summarized in Table: 2 1 below and Figure 2.19 also detailed technical information given following subsections.

Table 2.1: Sensor type, installed location data logger channel and purpose

Data Logger Channel	Type	Location	Purpose of measurement
2	BDI strain transducer (BDI 2269)	U1L2 top flange	strain in compression-tension member
3	BDI strain transducer (BDI 2268)	U1L2 bottom flange	
4	BDI strain transducer (BDI 2270)	L2L3 web	Strain in tension member
6	OMEGA strain transducer (Gage16)	L2L3 web	
7	OMEGA strain transducer (Gage7)	L2L3 top flange	
5	OMEGA strain transducer (Gage 18)	L2L3 bottom flange	
9	OMEGA strain transducer (Gage 5)	U1U2 + shape upper point	strain in compression member
8	OMEGA strain transducer (Gage 17)	U1U2 + shape lower point	
1	Railroad track strain gauges	1.5 m before span	system trigger, strain in truck
14	Railroad track strain gauges	first span second support	
12	LVDT	lower midpoint of span	system trigger, span midpoint deflection
20	Accelerometer	Joint U2	acceleration of span during train cross
19	Accelerometer	Joint L2	
18	Kyowa Strain transducer	lower member of 19 m pier	strain in pier member
13	Wind direction vane	tube section welded to railing	wind direction
Pulse Counter	Anemometer	tube section welded to railing	wind speed
Digital	Temperature and relative humidity probe	tube section welded to railing	temperature and humidity

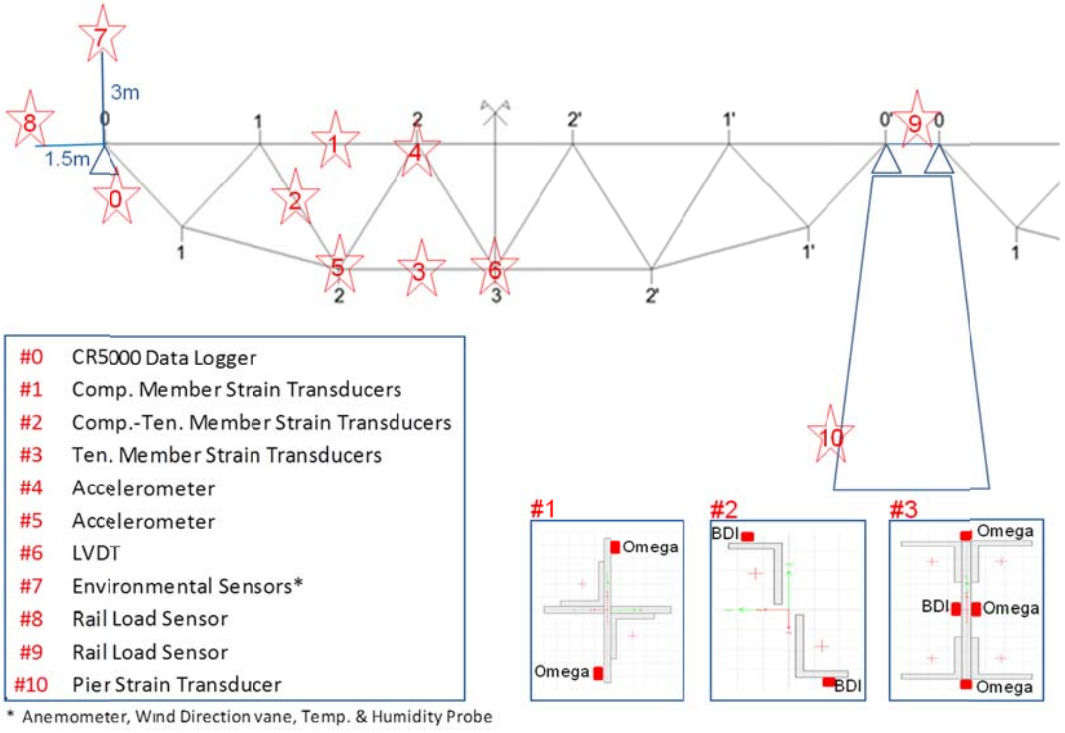

Figure 2.19: Sensor types and locations

2.3.1 BDI Strain Transducer

Three BDI ST-350 type strain transducers are used during studies (Figure 2.20). BDI gages have 76.2 mm effective gage length, full wheatstone bridge with four active 350 W foil gages, ±2 % accuracy in ±4000 με (for aluminum) strain range and 500 με/mV/V sensitivity.

Figure 2.20: Installed BDI ST-350 strain transducer

2.3.2 KYOWA Strain Transducer

One Kyowa BCD-E70S strain transducer is installed during studies (Figure 2.21). Strain transducer has 70 mm of effective gage length, with full wheatstone bridge, 2% tensile strain, 0.5% compressive strain measuring range with 10% accuracy.


Figure 2.21: Installed Kyowa BCD-E70S strain transducer

2.3.3 LVDT

One Opkon LPM type potentiometrical LVDT is installed during studies (Figure 2.22). LVDT has 5 K ohm resistance with ±20% resistance tolerance, 50 to 500 mm measuring range and 100 million cycle mechanical life.

Figure 2.22: Installed Opkon LPM potentiometrical LVDT

2.3.4 Environmental Sensors

One Campbell Scientific CS215 Type Temperature and Relative Humidity Probe is installed during studies (Figure 2.23). Probe has 0 to 100 % Relative Humidity measuring range with ±2-4 accuracy, -40 °C to +70 °C temperature measuring range with ±0.3-0.9 °C accuracy and also 0.03% RH and 0.01 °C output resolution.

Figure 2.23: Installed Campbell Scientific CS215 Temperature and Relative Humidity Sensor

One NRG SYSTEMS #40C type anemometer is installed during studies (Figure 2.24). Anemometer has 1 m/s to 90 m/s measuring range.

Figure 2.24: Installed NRG #40C Anemometer

One NRG SYSTEMS #200P type wind direction vane is installed during studies (Figure 2.25). Wind direction vane has 360° mechanical, continuous rotation measuring range with 8° maximum 4° typical accuracy.

Figure 2.25: Installed NRG #200P Wind Direction Vane

2.3.5 Accelerometers

Two Kyowa AS-5GB type accelerometers are installed during studies (Figure 2.26). Accelerometers have ±5g measuring range with ±5% accuracy and ±4% transverse sensitivity.

Figure 2.26: Installed Kyowa AS-5GB Accelerometer

2.3.6 Data Logger

Campbell Scientific CR5000 type data logger is used as data collecting unit (Figure 2.27). Properties of equipment are;

- Analog Channel : 40 single-ended (20 differential)
- Switched Excitation Channels : 4 voltage , 4 current
- Pulse Counters : 2
- Analog Voltage Range : ± 5000 mV
- Analog Voltage Accuracy : ± 0.05 % (full scale range), 0° to 40°
- Analog to Digital converter (A/D) : 16 bits
- Scan Rate : 1667 Hz
- Measurement Resolution : 167 μV for ± 5000 mV input range
- Current Drain : sleep mode :1.5 mA, 1 Hz sample rate : 4.5 mA, 5 kHz sample rate : 200 mA
- Control Ports : 8 I/Os , 1 SDM
- Memory : 128 kbytes (program storage), 2 Mbytes (data storage)
- Expanded memory : PCMCIA type I, type II or type III card (2GB PCMCIA card is used during study)

To complete data collecting unit GSM modem and antenna, 12 V dry battery, data sim card and data logger connector cable.

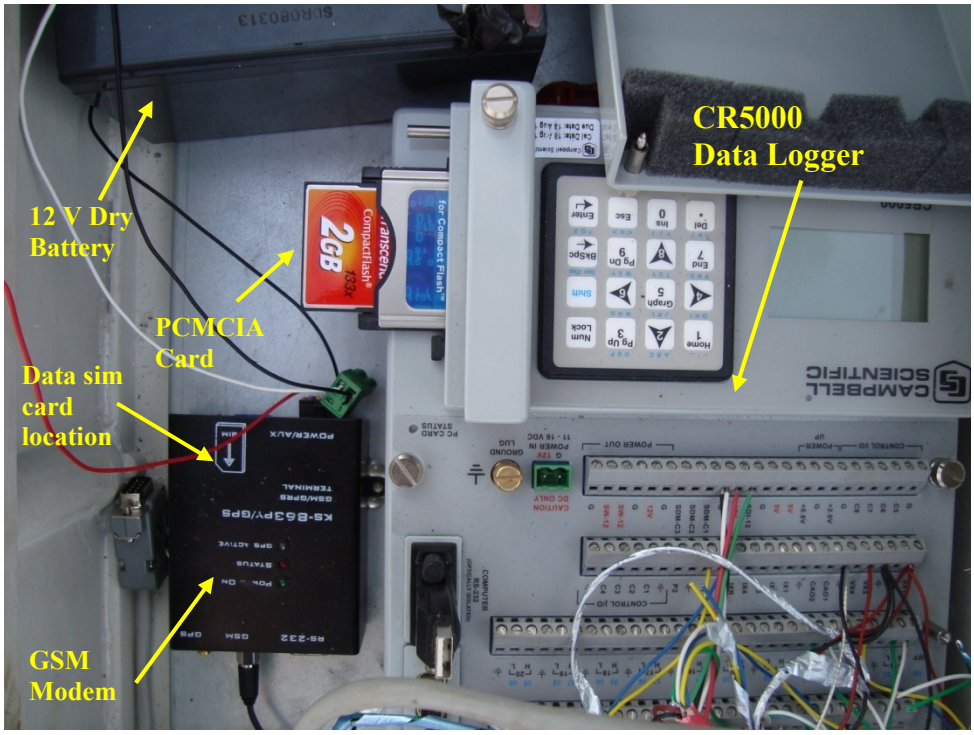

Figure 2.27: CR5000 data logger and complete data collection unit

2.4 Sensor Development Studies

Additional sensors were developed to be used in conjunction with the professional sensors available in the market.

2.4.1 Omega Sensors

Custom made omega strain transducers are installed during studies (Figure 2.28). Omega sensors were developed during the previous study called TÜBİTAK MAG-104I108 “Research, development, and application of preventive structural health monitoring methods, tools, and strategies”.

Omega sensors consist of full wheatstone bridge with four active strain gages system for bending strain measurement which is thermally compensated. Working principle of omega gages is that member axial strain due to loading creates bending strain on the top of omega shaped steel part of transducer which strain gage installed part. Foil strain gages measure this strain and by calibration with the known dimension of transducer, member strain is computed.

The advantages of omega sensors are easy availability and low cost of production materials, high resolution results, due to certainty about working principle, ease of application.

There is another important advantages in compared with the BDI gages. BDI gages were made out of aluminum causing strain shifts due to temperature differences between day and night as well as seasonal shifts. Custom made sensors were made of steel which had the same thermal expansion coefficient as the bridge; therefore, there are not temperature caused virtual strain shifts in measurements.

Figure 2.28: Installed and painted omega sensor on web of tension member L2L3

2.4.2 Rail Load Sensors

Rail load sensor was developed and used to measure relative axle loads of trains as well as trigger the data logger system. Development study is done in the scope of METU Civil Engineering Department CE742 "Structural Health Monitoring" course term project in METU Civil Engineering Department Structural Engineering Laboratory. Study consist of four preparation steps, that are five installation and test steps, FE modeling step, analysis and evaluation of results step.

2.4.2.1 Preparation Steps

Sensor development study is started with the obtaining the railroad track sample used in bridge superstructure. The railroad track is obtained from METU

Metallurgical and Material Engineering Department laboratory. The dimensions and material properties of railroad track are given in Table 2.2 below;

Table 2.2: S49 Railroad Track Dimensions and Material Properties

S49 Railroad Track Dimensions	
Height	149 mm
Top Flange Width	67 mm
Bottom Flange Width	125 mm
Top Flange Thickness	40 mm
Bottom Flange Thickness	10.5 mm
Web Thickness	14 mm
Section modulus	240 cm^3
Moment of Inertia	1819 cm^4
Area	62.97 cm^2
Material Properties	
Elastic Modulus	2100 t/cm^2
Unit mass	7.85 t/m^3
Poisson's ratio	0.3

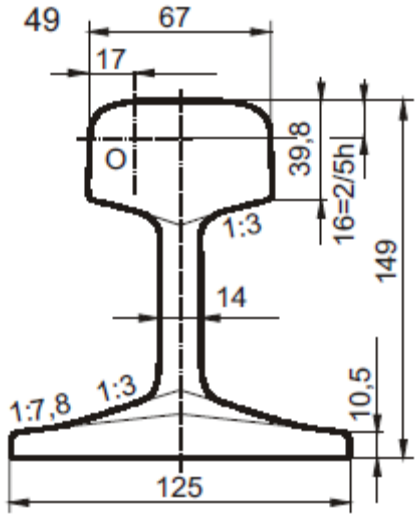

Second step of preparation is Wheatstone bridge design with four foil strain gages for measuring vertical axial strain on web of railroad track section. Four active gages are used for constructing wheatstone bridge as orthogonal 4-active-gage-system (Figure 2.29). This system is used for compensate temperature and eliminate bending strains. KFG-10-120-C1-11 Kyowa type foil strain gages for strain measurements and CR10X Campbell Scientific data logger for data collection are used during measurements. Properties of strain gages and data logger are given in Table 2.3. Sample strain gage configuration figure and wheatstone bridge structure are given in Figure 2.30.

Table 2.3 : Foil Strain Gage and Datalogger Properties

Strain Gage KFG-10-120-C1-11 Kyowa:	
Type	BF120-30 AA
Ohms	119.2±0.1%
Gage Factor	2.0±1%

Data Logger CR10X Campbell Scientific:	
Type	Campbell Scientific CR10X
Storage	62000 data points
A/D Bits	13
# of Channels	6 Diff/12 SE
Range	±2.5 V
Resolution	0.67 mV
Accuracy	± 5 mV

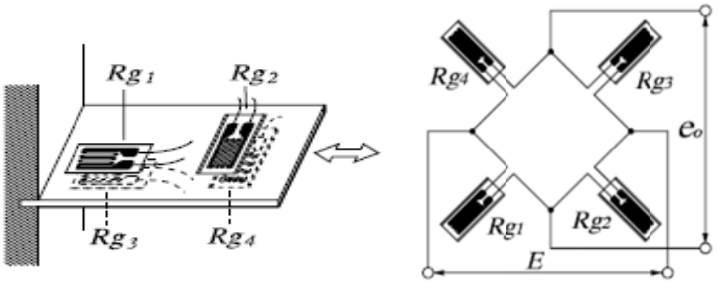

Figure 2.29: Sample strain gage configuration (left) and wheatstone bridge structure (right)

Third step of preparation is making decision of loading condition of railroad track. Decision is made according to TCDD maximum allowable axle load criteria (20 tons). It is assumed that two railroad tracks are loaded equally and maximum allowable axle load 20 tons is divided in two equal loads of 10 tons. Railroad track is loaded axially until 10 tons with 0.5 ton increments and this loading repeated two times. In second loading maximum load of 10 tons is increased to 20 tons to study capacity and behavior of railroad track.

Last step of preparation in addition to rail road type, strain gage orientation and loading condition decision step; during study, it is decided that sleepers and train wheel should be simulated during test. For simulation of sleepers 20x20 cm and 25x25 cm steel plates used, and for simulation of wheels 2 cm wide steel plate are used.

2.4.2.2 Installation and Test Steps

First step of installation is removing impurities from the web of railroad track, gage installation faces. It is done by firstly mechanical cleaning by sander (Figure 2.30 left), and then chemical solutions (Figure 2.30 right).

Figure 2.30: Removing impurities by mechanically (left) and chemically (right)

Second step of installation is placing (Figure 2.31 left) and fixing strain gages (Figure 2.31 right) for full bond between gages and web of railroad track, according to decided configuration.

Figure 2.31: Placing (left) and fixing strain gages (right)

Thirdly terminals which are connecting strain gages' cables to copper connecting cables are installed (Figure 2.32 left). Then strain gages' cables are welded to terminals (Figure 2.32 right).

Figure 2.32: Placing (left) and welding terminals (right)

Fourth step is connecting copper cables to the terminals and data logger according to wheatstone bridge configuration (Figure 2.33).

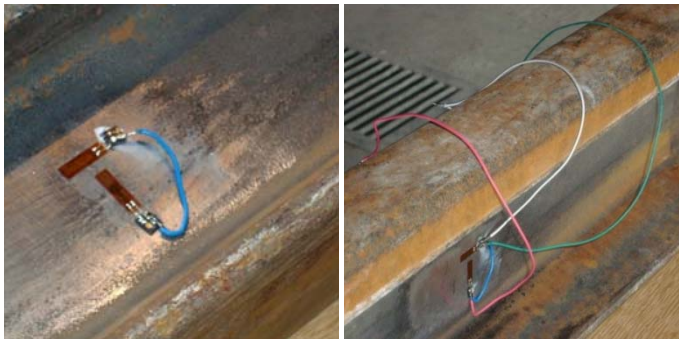

Figure 2.33: Connecting strain gages with other gages according to strain gage configuration

Last step of installation is completing test set up (Figure 2.34 and Figure 2.35) by locating instrumented web of railroad track in to loading machine and loading by 0.5 tons increment till 10 tons for first test and 20 tons for second test.

Figure 2.34: General view of test set up

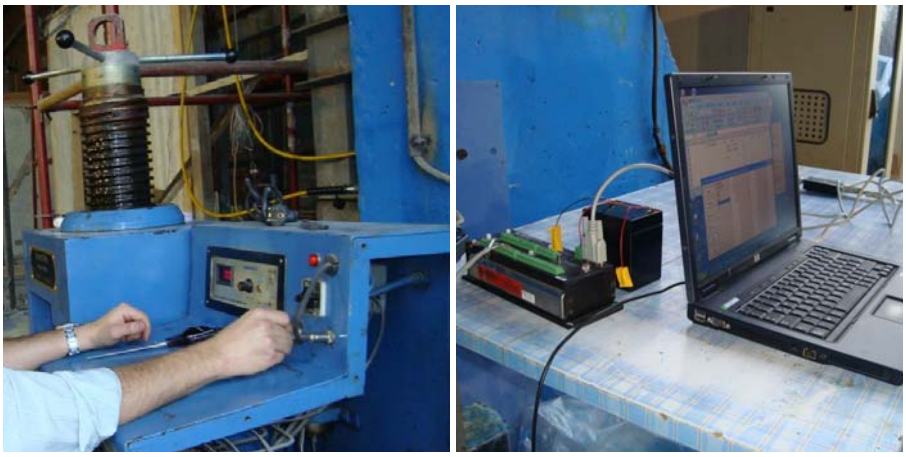
Figure 2.35: Loading (left), Datalogger and computer connection (right)

2.4.2.3 FEM Step

In order to determine correctness of test results, railroad track sample is modeled in structural analysis program SAP2000 by solid elements. Dimensions of each solid element are 4mm x 5mm in plan with 6.25 mm height and 1 m long. With the selected dimensions 35000 solid elements are modeled. Cross section of railroad track is symmetrical with respect to its centerline (Figure 2.36) therefore it is determined by analysis that half cross section analysis are given same stress distribution with the whole section stress distribution (Figure 2.37) with defined

proper end condition and symmetry axis. Structural analysis is continued with the half section structural analysis in order to reduce model size and increase speed of analysis.

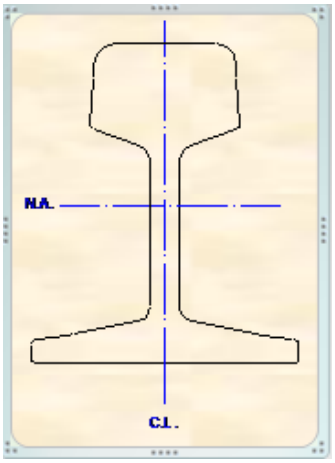

Figure 2.36: Axis of railroad track

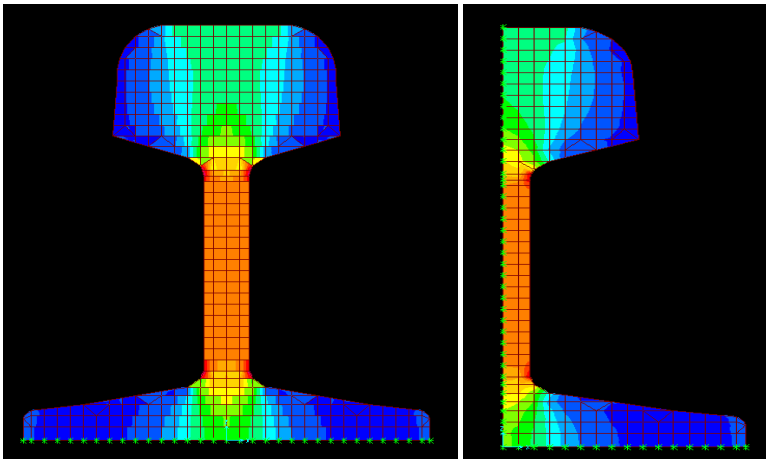

Figure 2.37: Stress distribution of full section (right) and half section model (left)

Railroad track structural analysis loading condition is defined same with the laboratory test set up loading conditions. Half of 10 tons and 0.25 increments are used to determine stress and strain due to used half cross section model.

In addition to solid modeling of railroad track, plates used to simulate sleepers and wheel are modeled in FE modeling.

2.4.2.4 Analysis and evaluation of results step

Measurements for each loading (0.5 loading increments) are collected by data logger in the unit of volts. By the mathematical relationship (Equation 2.3), it is converted to strain units.

$$e_o = \frac{(1+\nu)\,E}{2} K_s \varepsilon_o \tag{2.3}$$

Where;

e_0: Voltage output

ν: Poisson's ratio

E: elastic modulus

Ks: Strain gage coefficient

Railroad track web vertical strain values and loading relationships for different plates are found very close to linear correlation which is expected. Correlation of load and the strains is 99.8% for 20x20 plate (Figure 2.38) and 99.5% for 25x25 plate (Figure 2.39).

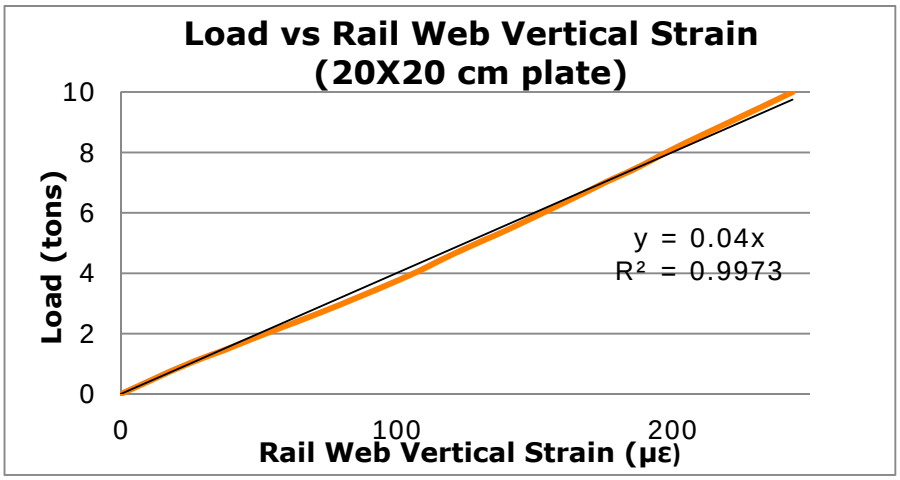

Figure 2.38: Strain vs. Load graph for 20x20 cm plate correlation 99.8%

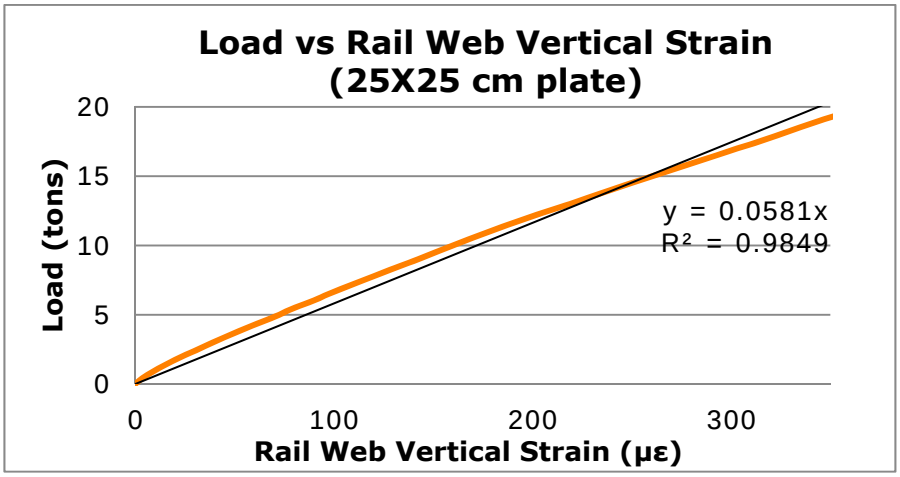

Figure 2.39: Strain vs. Load graph for 20x20 cm plate correlation 99.5%

Together with the rail web vertical strain loading relationship, FEM analysis results and test results are compared. Correlation coefficient is nearly 1.0 namely results are good correlated. (Figure 2.40 and 2.41)

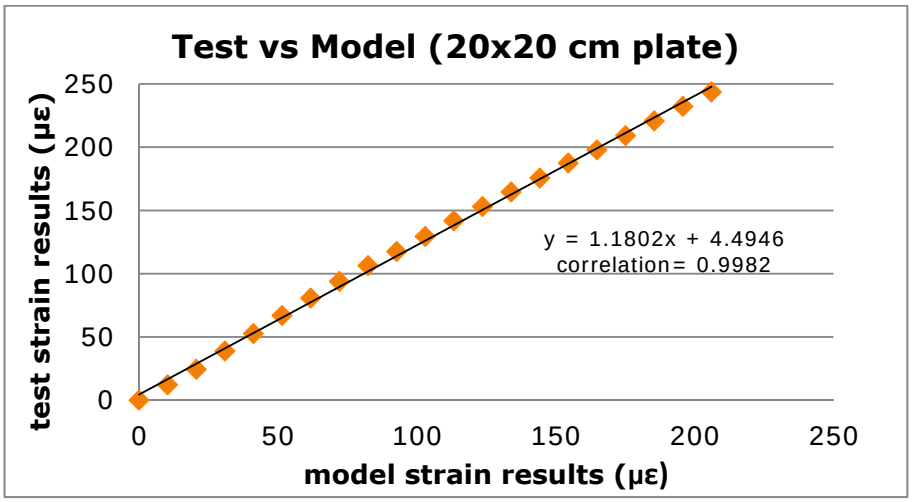

Figure 2.40: Model vs. Test strain results graph for 20x20 cm plate correlation 99.8%

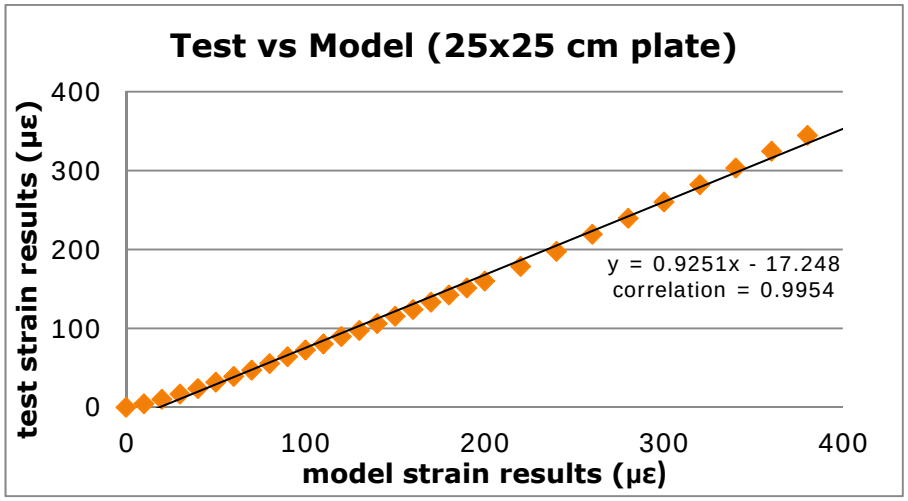

Figure 2.41: Model vs. Test strain results graph for 25x25 cm plate correlation 99.5%

According to rail load sensor development study it is shown that with similarly installed wheatstone bridge, strain measurements on web of railroad tracks can reflect the axle load of train crossing through sensor installed railroad track web.

2.5 Installation Studies

Installation studies are conducted in three field studies. First field study is bridge and bridge environmental identification studies, second field study is installation of first part of instruments and last field study is installation of second part of instruments and transferring collected data by data logger during term between second and third field study.

2.5.1 First Field Study

Purpose of first field study is identification of real structural application of bridge and making comparison with technical drawing. During first field study dynamic measurements are also conducted and analyses are made to identify modal properties of bridge structure.

Technical drawings of first two spans from Uşak side, which are prepared in 1960s for rebuilt of these two spans, are compared with the real application and confirmed during first field study.

Dynamic measurements are conducted with the two types of accelerometers, three triaxial wireless accelerometers and one uniaxial cabled accelerometer. Three dynamic data sets are collected through measurements. First data set is collected during passenger train cross from İzmir to Uşak, second is collected with the test locomotive cross from Uşak to İzmir, third is collected with the test locomotive cross from İzmir to Uşak.

2.5.1.1 Dynamic measurements during first field study

Dynamic measurements are conducted with the two types of accelerometers, three triaxial wireless accelerometers (Node229, Node237, Node242) with data collection speed as 512 Hz and duration as 120 seconds, and one uniaxial cabled accelerometer with data collection speed as 2048 Hz and duration as approximately 9 seconds. Cabled accelerometer has more sensitive (fast) data collection capability but duration is lower compared with the wireless accelerometers. Accelerometers locations are presented in Figure 2.42.

Figure 2.42: Location of wireless and cabled accelerometers used during first field study

Throughout dynamic measurement study, three measurements are conducted with wireless accelerometers and one measurement by two triggering is conducted with cabled accelerometer during train crosses. First field study measured dynamic data and analyses given in following subsection 2.7.1.

2.5.2 Second Field Study

Purpose of first field study is installation of first set of instruments and data logger programming.

2.5.2.1 Installation of instruments

- **Strain transducers**

Two types of strain transducers, omega and BDI, are installed to critical members of bridge already determined. Two omega type strain transducers are installed upper and lower part of critical compression member U1U2, "+" shaped (Figure 2.43).

Figure 2.43: Installed two omega gages on critical compression member U1U2

Two BDI type strain transducers are installed upper and lower parts of critical tension-compression member U1L2 composed of two angle section (Figure 2.44).

Figure 2.44: Installed two BDI gages on critical tension-compression member U1L2

Three omega type and one BDI type strain transducers are installed to the critical tension member L1L2. One omega to upper flange, one omega to bottom flange, one omega and one BDI to web of member L1L2 (Figure 2.45-46).

Figure 2.45: Installed one omega gage on bottom flange and one BDI gage on web of critical tension member L1L2

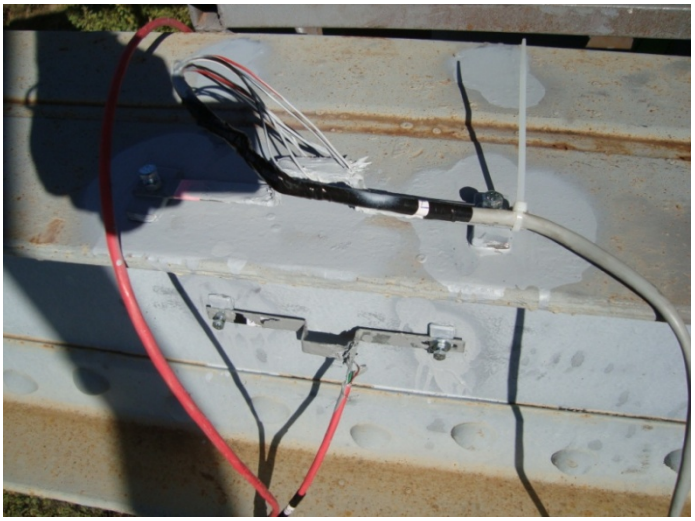

Figure 2.46: Installed one omega gage on top flange and one omega gage on web of critical tension member L1L2

- **LVDT**

One potentiometrical LVDT is installed at the middle of first span's bottom chord (Figure 2.47). Rod of LVDT is opened with the help of two springs to maximum measurement length and fix to ground by tension cable. It is designed to record data by closing rod while deflection of span created by any external load. Therefore instead of measurements recorded while opening of rod, reversed measurement recorded while closing of rod.

Figure 2.47: Installed LVDT mechanism on middle of first span's bottom chord

- **Rail load sensors**

Developed two railroad sensors are installed on railroad tracks' webs. Rail load sensors are installed for identification of crossing train types and relative axle load measurements, and triggering fast measurement system. Location of rail load sensors are decided due to sensors triggering purpose, one sensor is located on rail road track at 1.5 m before first span entrance (Figure 2.48) and second sensor on rail road track at the first 1.9 m pier location namely exit of first span (Figure 2.49). These sensors are triggered monitoring system for fast reading when threshold strain value exceeded e.g. when train cross.

Figure 2.48: two foil strain gages of rail load sensor located on outer web of rail at entrance of first span

Figure 2.49: two foil strain gages of rail load sensor located on inner web of rail at exit of first span

- **Environmental instruments and Solar panel**

Three types of environmental instruments are attached to 2.5 m length ø 50 x 3mm tube section. Then Tube section is welded to railing of first span to measure environmental condition data. Instruments are one anemometer to measure wind speed, one wind direction vane to measure wind direction and one temperature and relative humidity probe to measure temperature and humidity (Figure 2.50).

40 watt solar panel is also attached to tube section welded to railing with environmental instruments (Figure 2.50).

Figure 2.50: Installed environmental sensors and solar panel

- **Data collection box**

Under the abutment of span, waterproof data collection box is located. In data collection box Data logger, GSM modem, 12 V dry battery, data sim card, data logger connector cable, and GSM antenna are glued with hot glue (Figure 2.51).

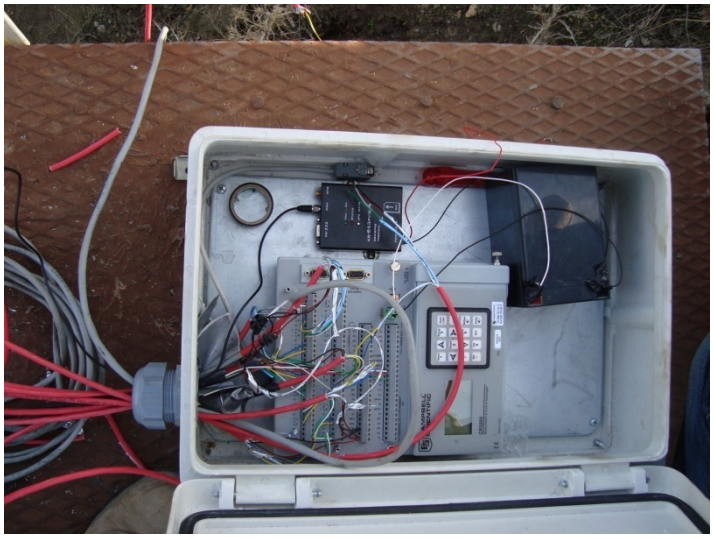

Figure 2.51: Data collecting box and sensor connection cables

- **Covering sensors**

To prevent external conditions sensors are covered by half PVC tubes (Figure 2.52). All sensors` steel connecting plates, omega type strain transducers, rail load sensors are painted to prevent corrosion.

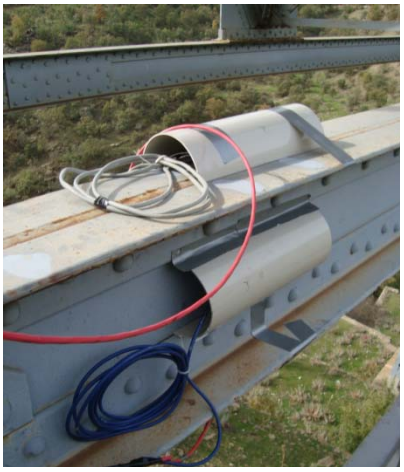

Figure 2.52: Example view of sensor covering

2.5.2.2 Programming and check of system

- **Programming**

First programming of data logger is done in second field study details of programming works are given in section 2.6.

- **Check of system**

Check of system is done by giving external compression and tension to sensors and checking of values. According to given force direction calibration values multiplied by -1 if values read reverse by force direction.

2.5.3 Third Field Study

Purpose of first field study is installation of last of instruments and last programming of data logger.

2.5.3.1 Installation of instruments

- **Accelerometers**

Two accelerometers are installed one at the joint L2 (Figure 2.53) and one at the joint U2 (Figure 2.54).

Figure 2.53: Installed accelerometer at the joint L2

Figure 2.54: Installed accelerometer at the joint U2

- **Strain transducer**

One kyowa strain transducer is installed on 19m pier (Figure 2.55).

Figure 2.55: Installed strain transducer on 19 m pier.

2.5.3.2 Check of second field study's installed instruments and programming

- **Strain transducers**

Some strain transducers on critical members are lost their functioning due to external conditions. Working strain transducers are one omega on critical compression member, two BDI on critical compression-tension member, one omega and one BDI on critical tension member. At least one strain transducer is functioning at each critical member therefore needed strain measurements can be done with these transducers.

- **LVDT and environmental measurement sensors**

LVDT and environmental measurement sensors are functioning properly. Although due to memory problem long term measurements cannot be recorded by environmental measurement sensors.

- **Rail load sensors**

Rail load sensor aligned on the second support of first span is lost its functioning due to external conditions therefore it is not triggering fast measurements. Rail load sensor aligned 1.5 m before first support of first span is lost its calibration but it is continuing to trigger fast measurements.

2.5.3.3 Programming

Second programming of data logger is done in third field study details of programming works are given in section 2.6.

Triggering mechanism is changed because of function lost of rail load sensor, triggering mechanism connected LVDT and rail load sensor located 1.5 m behind entrance of the first span.

2.6 Trigger mechanisms and programming

Data logger programming is done during second and third field study for data reading and storage. Program has two types of data collection and storage mode. The first mode is reading and storing fast data collection mode in short term. Duration of fast data collection mode is 2.5 minutes; speed of data collection is 50 Hz (e.i.50 sample/second). Member strains, rail web vertical strains, accelerations and span midpoint deflections data are read and stored by this mode. Fast data collection mode is achieved by triggering system with the rail load sensor or LVDT recorded data. Triggering can be explained as; system continuously reading rail load sensor`s strain measurements and LVDT`s deflection measurements, if the one of measurement values is passed the defined threshold values, system is started fast

data reading and storage. The second mode is reading and storing slow data collection mode in long term. There is no duration limitation of slow data collection mode, system is read and stored data in every 15 minutes. Slow data collection mode is read and store data from same sensors with fast data collection mode and also environmental condition data which are wind speed, wind direction, temperature and humidity data. Slow speed mode data storage cannot be achieved, due to memory problems of data logger are not solved during studies.

Representative flow chart of program is given in Figure 2.56

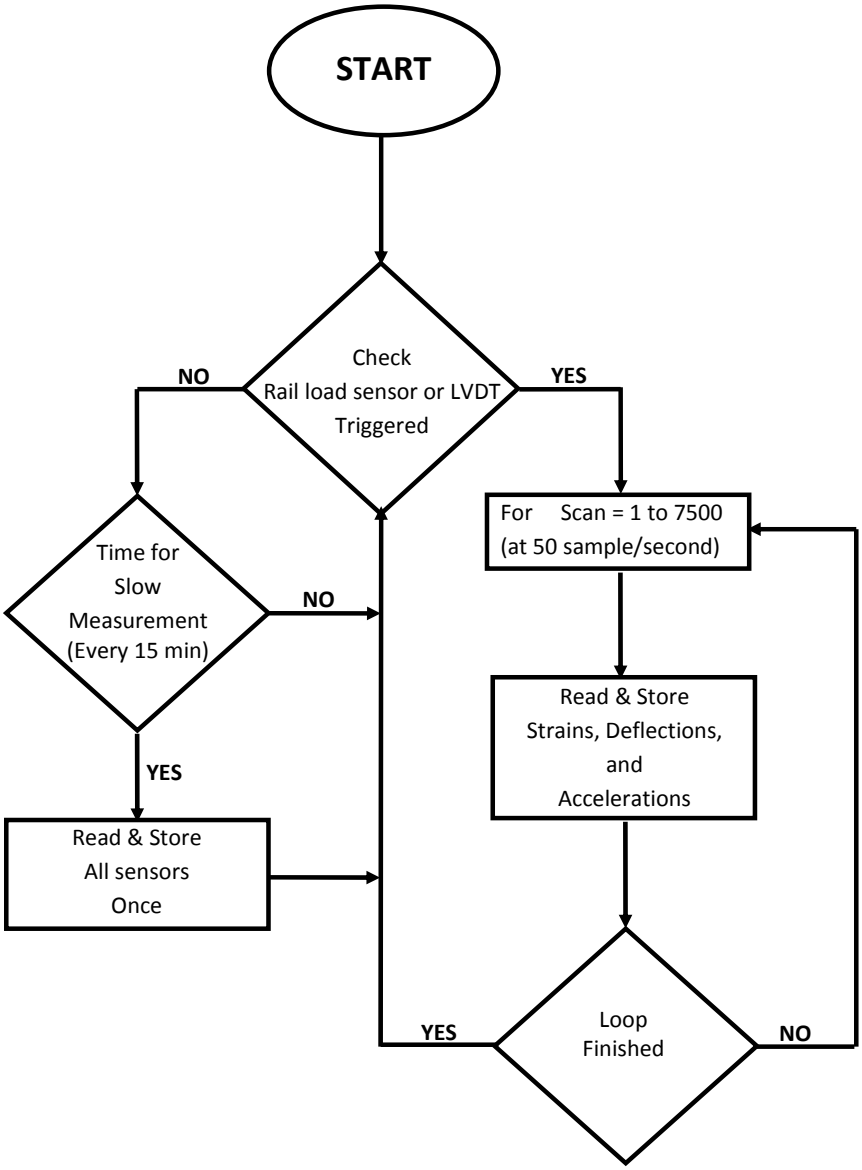

Figure 2.56: Data logger program flow chart

2.7 Test train records and data analysis

2.7.1 First Field Study Train Records

During first field study bridge acceleration measurements conducted during trains and locomotive crossing. Data analyses are done with collected acceleration data. Three dynamic measurements are conducted with wireless accelerometers; the first data set is collected during passenger train cross, the second and the third data sets are collected during test locomotive crosses. One dynamic measurement is conducted with cabled accelerometer with two triggering during passenger train cross. Analyzed data sets are given following figures, remaining acceleration measurements given in Appendix A.

Two types of analyses are conducted. Fist analyses purpose is that the determination of the first gravitational direction natural frequency of bridge span. Fast Fourier Transform (FFT) analyses are conducted for determination of gravitational direction natural frequencies. Analyses are done by the matlabR2008a software.

FFT analyses are done with different parts of data sets. External electrical noises created difficulties for determination of natural frequencies. By cabled accelerometers, two frequencies are determined from first triggered measurement (Figure 57) and second triggered measurement (Figure 58) during first measurement data set. According to the FFT analysis of two measurements, the first natural gravitational direction frequency of span is equal to 8.197 Hz. This result is obtained from data between 5 and 6 seconds for first triggered data set (Figure 59) and between 4 and 5 seconds for second triggered data set (Figure 60).

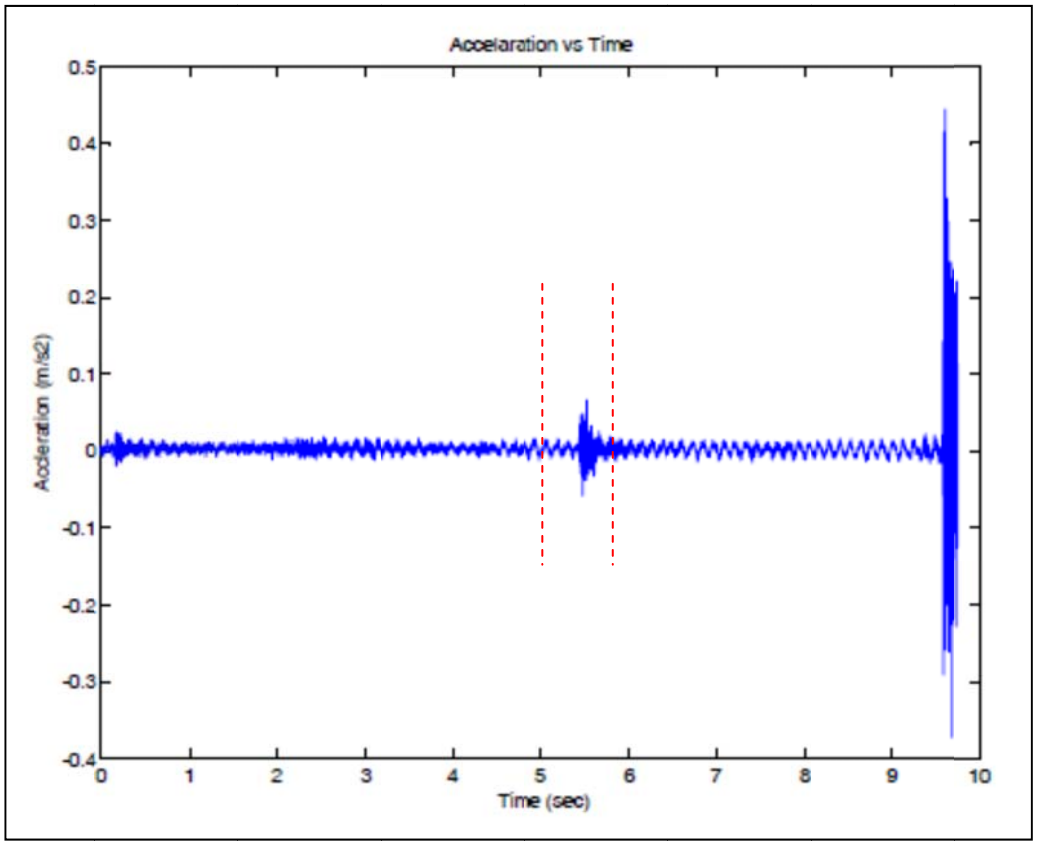

Figure 2.57: Acceleration vs. Time graph of first measurement first triggering from cabled sensor

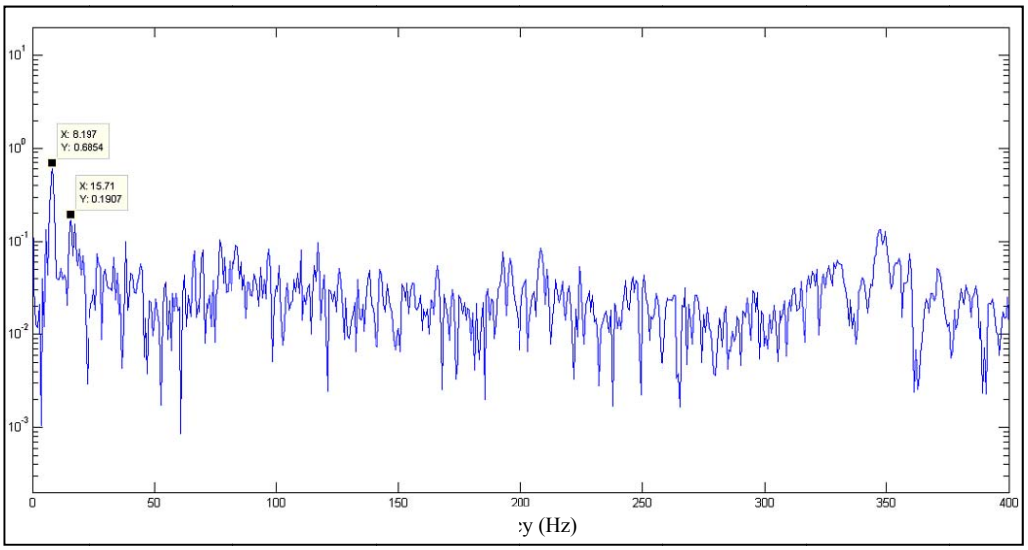

Figure 2.58: FFT analysis result of first measurement first triggering from cabled sensor data between 5 and 6 seconds

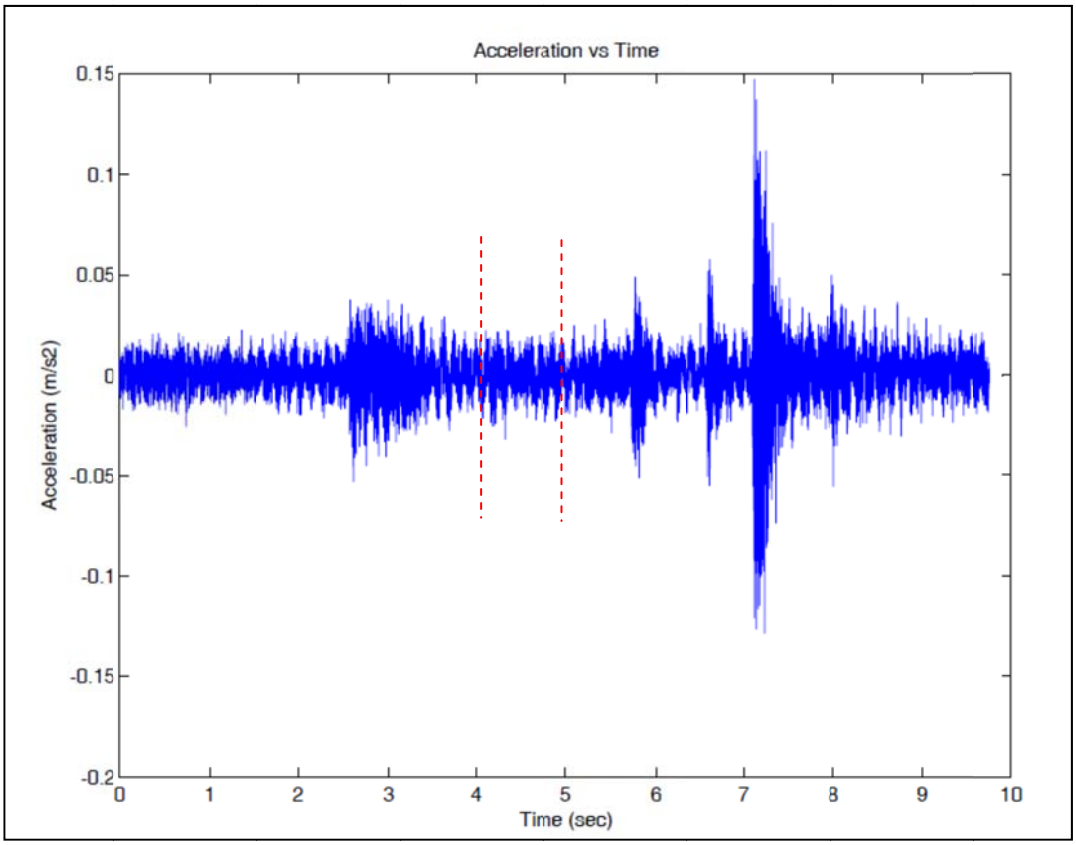

Figure 2.59: Acceleration vs. Time graph of first measurement second triggering from cabled sensor

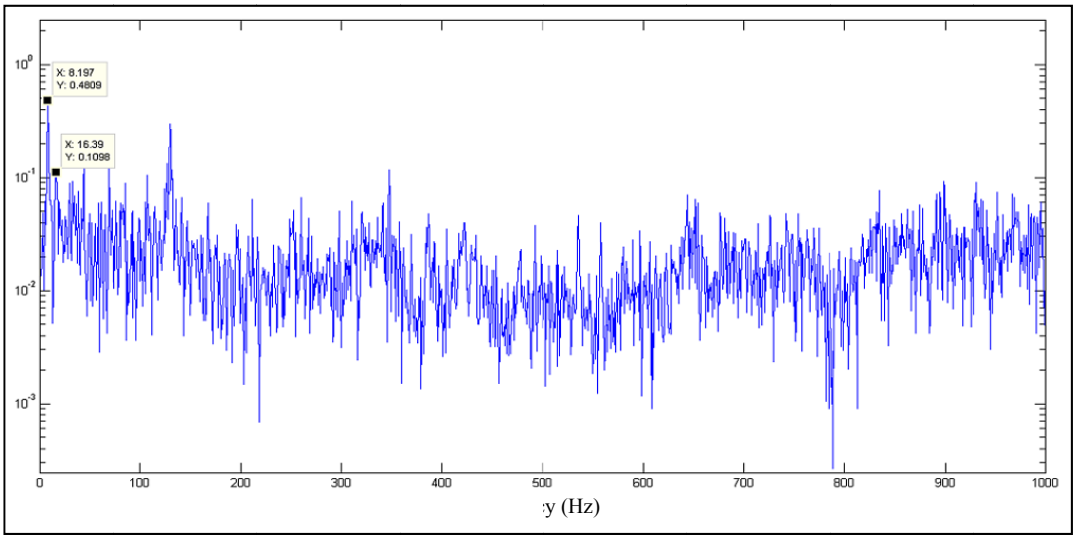

Figure 2.60: FFT analysis result of first measurement first triggering from cabled sensor data between 4 and 5 seconds

By node242 wireless sensors, one frequency is determined from first measurement (Figure 61) and is presented in figure 62. According to the FFT analysis first natural frequency of span is equal to 8.192 Hz. This result is obtained from gravitational direction data between 39 and 43 seconds.

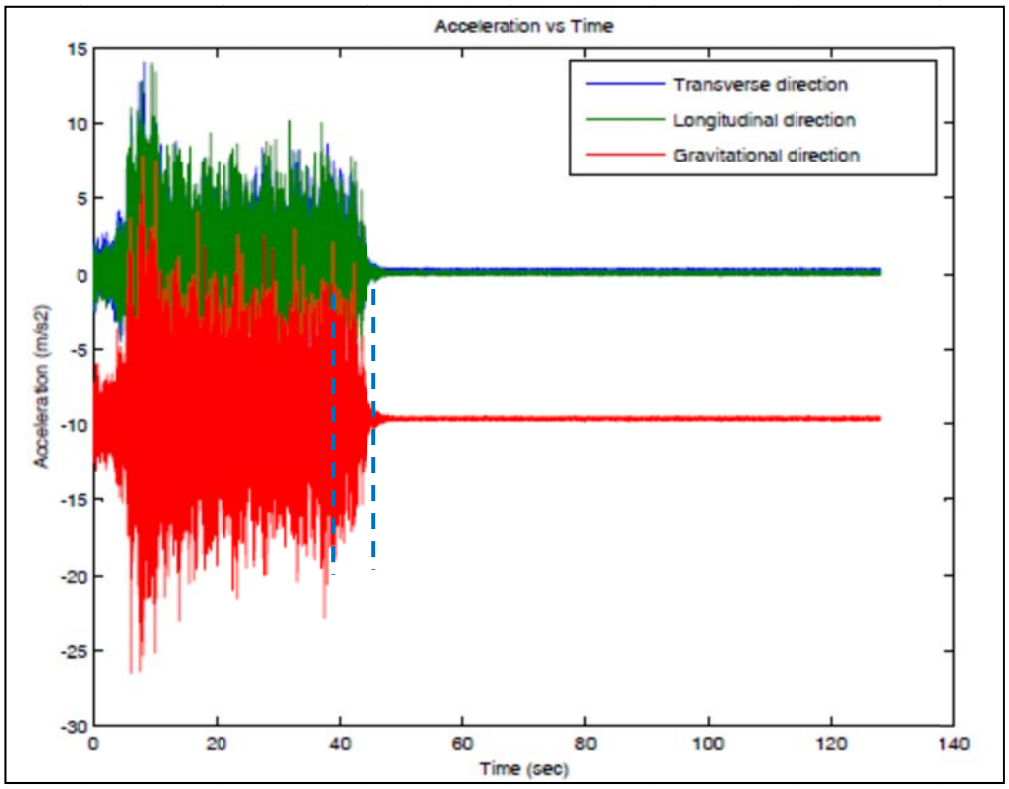

Figure 2.61: Acceleration vs. Time graph of first measurement from wireless sensor node242

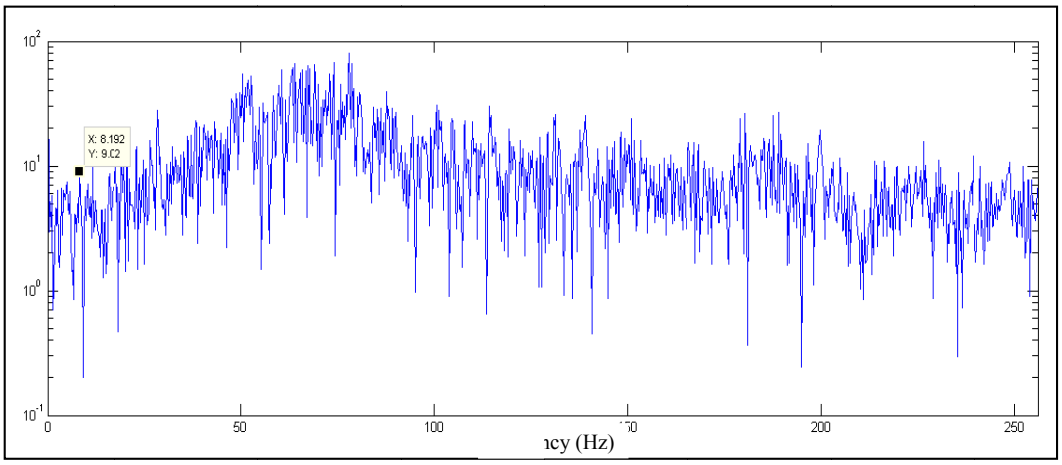

Figure 2.62: FFT analysis result of first measurement wireless sensor node242 data between 40 and 43 seconds

Second analyses purpose is that the determination of mode shape of bridge span. Software called Artemis is used for these analyses. The wireless sensors' collected data are used due to need of multiple locations collected data. Analyses results figures are given below. (Figure 63 and Figure 64)

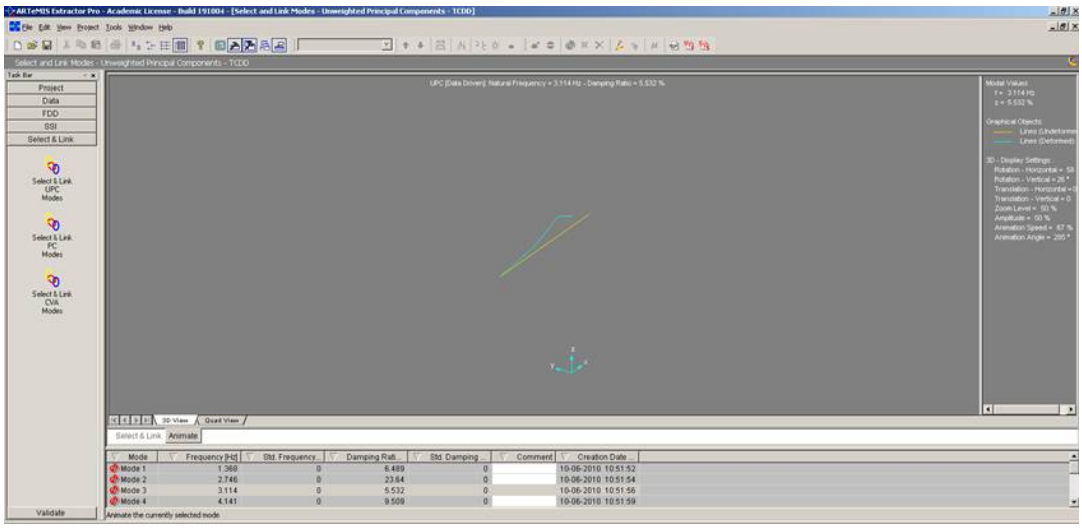

Figure 2.63: Obtained Lateral mode shape view

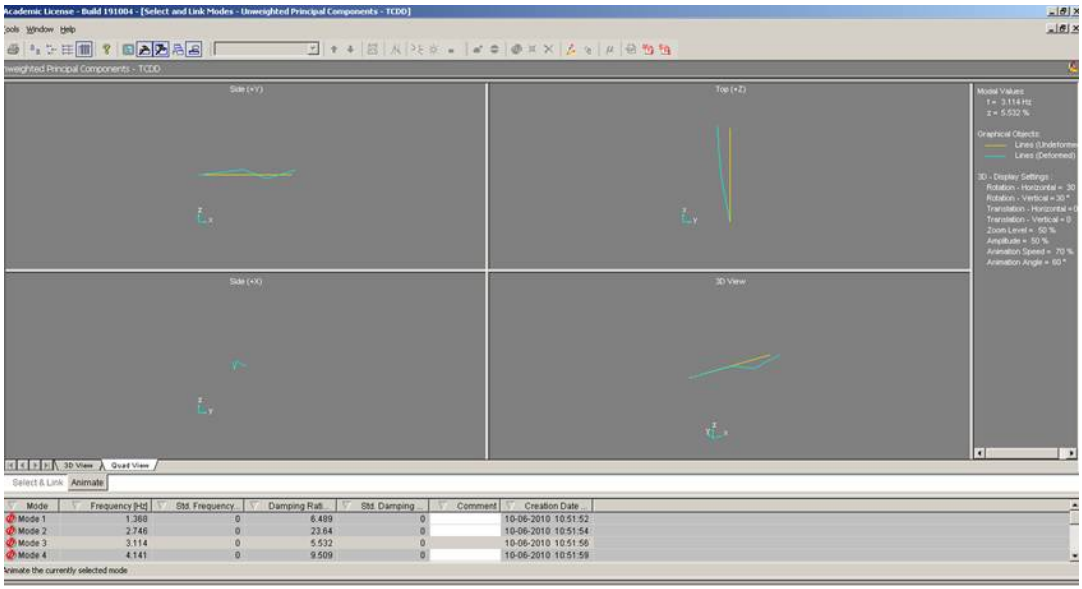

Figure 2.64: Obtained Lateral mode shape 3D and Plan views

2.7.2 Second Field Study Train Records

During second field study, one data set is collected while goods train crossing the bridge on 08.11.2010 at 12:52. This train has 18 wagons and two locomotives that the one of them is in front of the wagons and the other is behind of the wagons. Collected data and calculated member stresses are given as graphs (Figure 2.65-75) and maximum values are tabulated below (Table 2.4).

Rail web vertical strain vs. Time graph is shown that the each peak point represents an axle of train. Higher peaks represent two locomotives' axles, 6 peaks for each locomotive, in front of the wagons and behind the wagons (Figure 65).

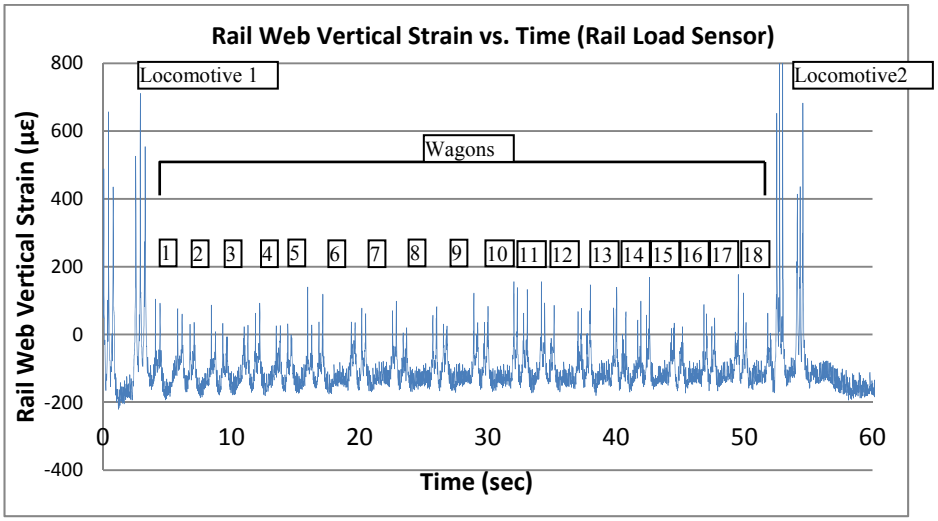

Figure 2.65: Rail Load Sensor rail web vertical strain measurements results

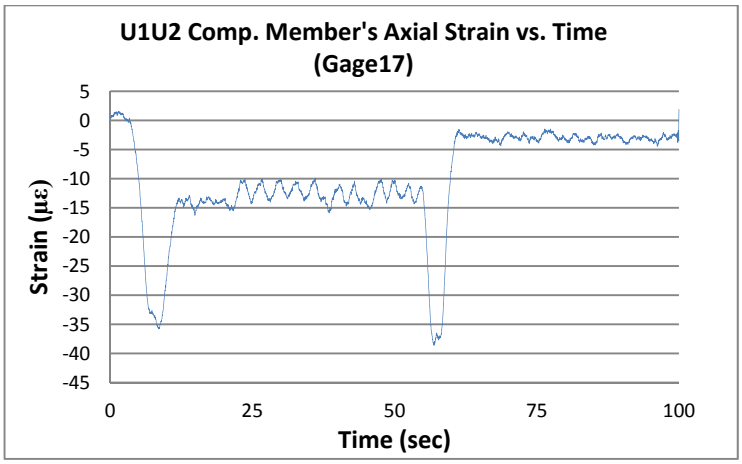

Figure 2.66: Compression member Gage17 strain measurements results

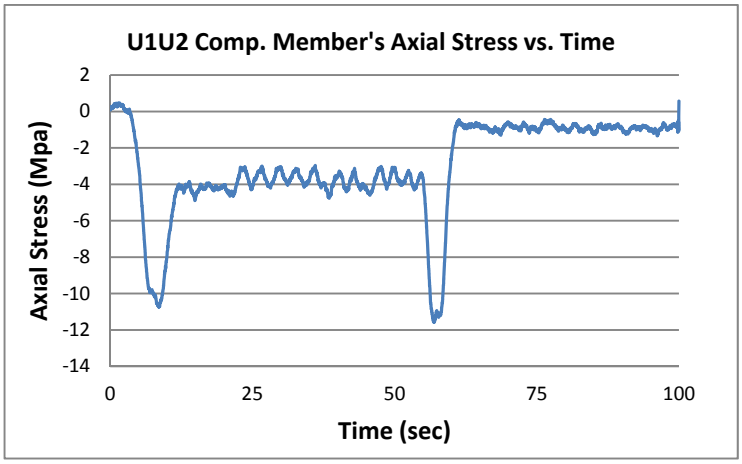

Figure 2.67: Compression member calculated stress by strain measurements results

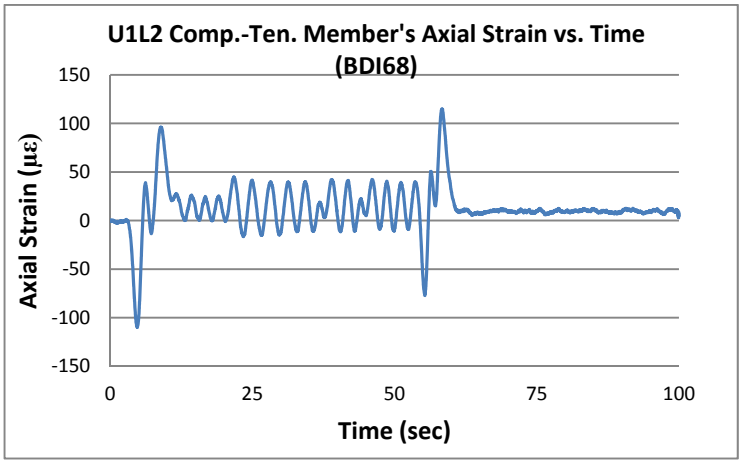

Figure 2.68: Comp-ten member BDI68 strain measurements results

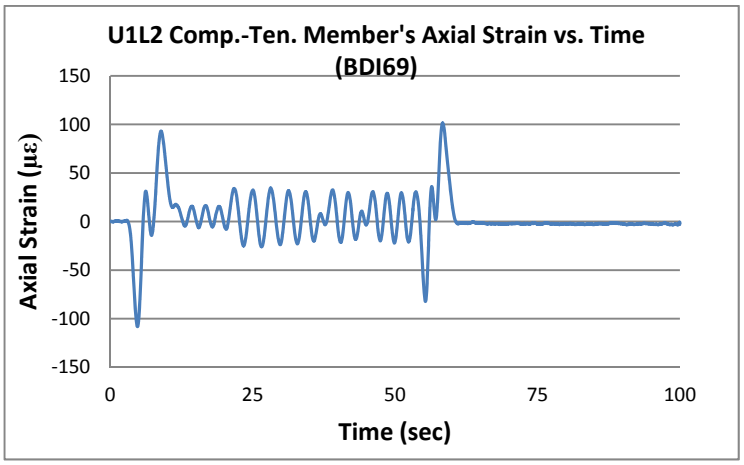

Figure 2.69: Comp-ten member BDI69 strain measurements results

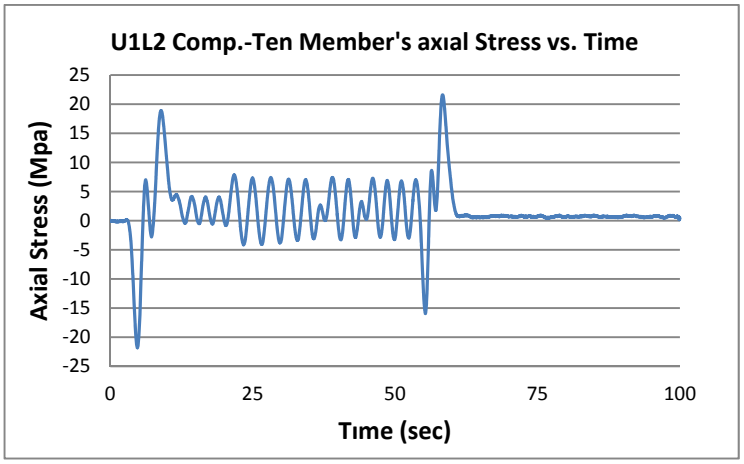

Figure 2.70: Comp-ten member calculated stress by strain measurements results

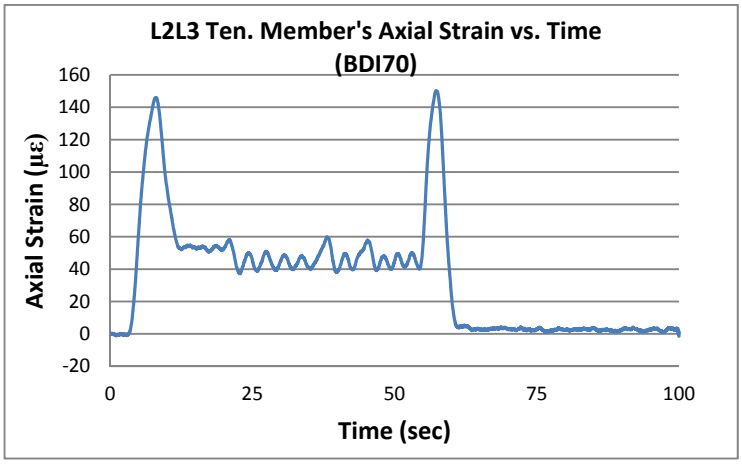

Figure 2.71: tension member BDI70 strain measurements results

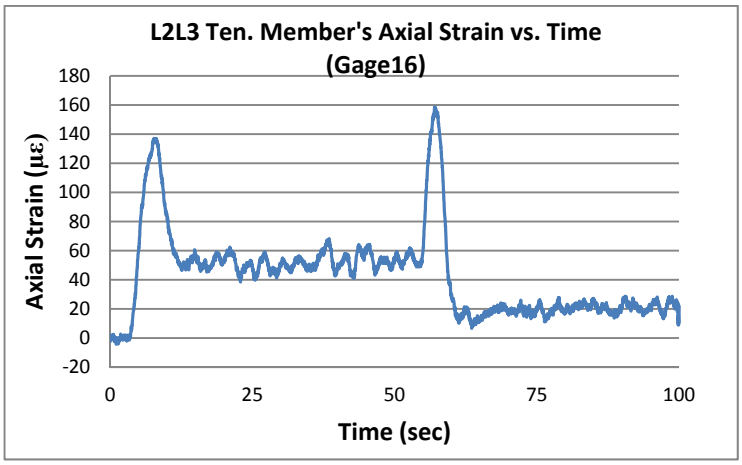

Figure 2.72: Tension member Gage16 strain measurements results

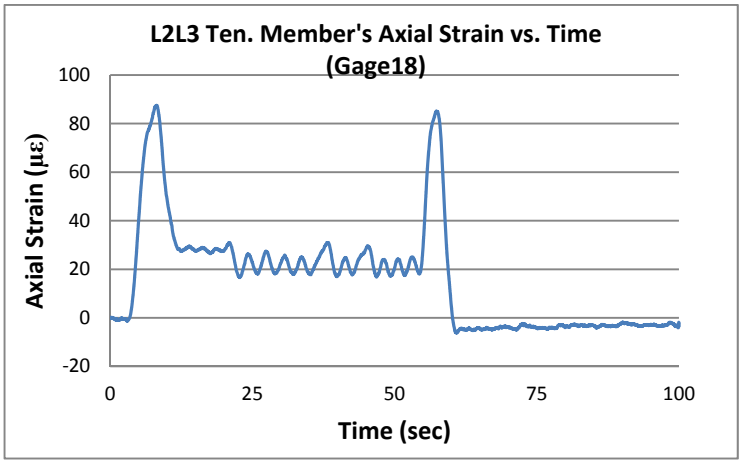

Figure 2.73: Tension member Gage18 strain measurements results

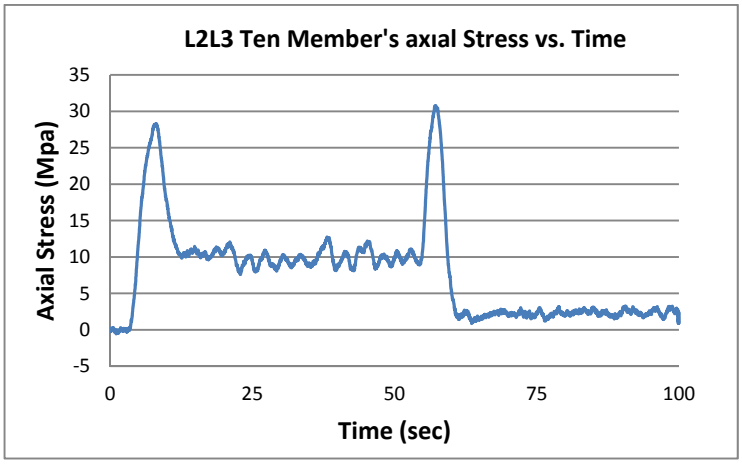

Figure 2.74: Comp-ten member calculated stress by strain measurements results

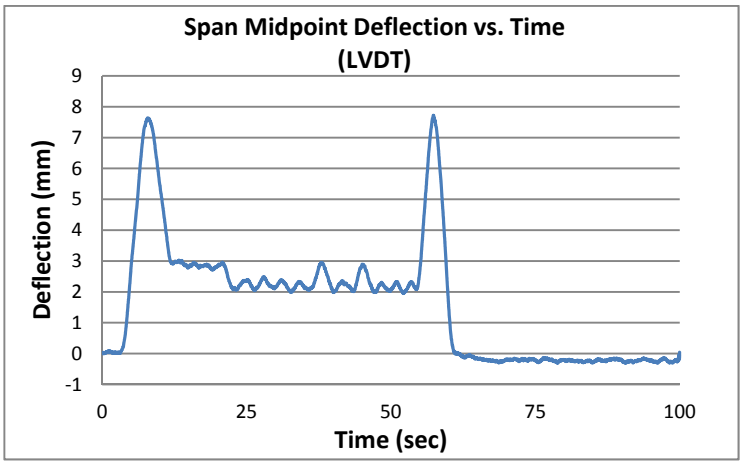

Figure 2.75: Truss midpoint deflection measurements results

Table 2.4: Measured maximum values during second field study

Date	Time	Train Type	Maximum Axial Stress (MPa)[2]				Maximum Deflection (mm)	Maximum Acceleration (m/s^2)	
			U1U2	U1L2	L2L3	Pier		U2	L2
08.11.2010	12:52	Goods	-11.68	-21.80	30.76	-[1]	7.72	-[1]	-[1]

1) Pier strain measurements and truss acceleration measurements are started after completing installation studies during third field study therefore same values can not be included in table.
2) Negative stress values correspond to compression, possitive stress values correspond to tension

2.7.3 Third Field Study Train Records

During third field study, six train cross data sets are collected, after installation studies are completed. One example set of collected data is given as graphs (Figure 2.76-90) and maximum values for whole trains crosses are tabulated below (Table 2.5). Remaining graphical data sets are given in appendix A.

Example data set belongs to goods train that crossed the bridge on 17.12.2010 at 22:48.

Rail web vertical strain vs. Time graph is shown that the each peak point represents an axle of train and higher peaks represent heavy axle loads of wagons as nearly equal to axle load of the locomotives' axles at the start and end of train (Figure 2.76).

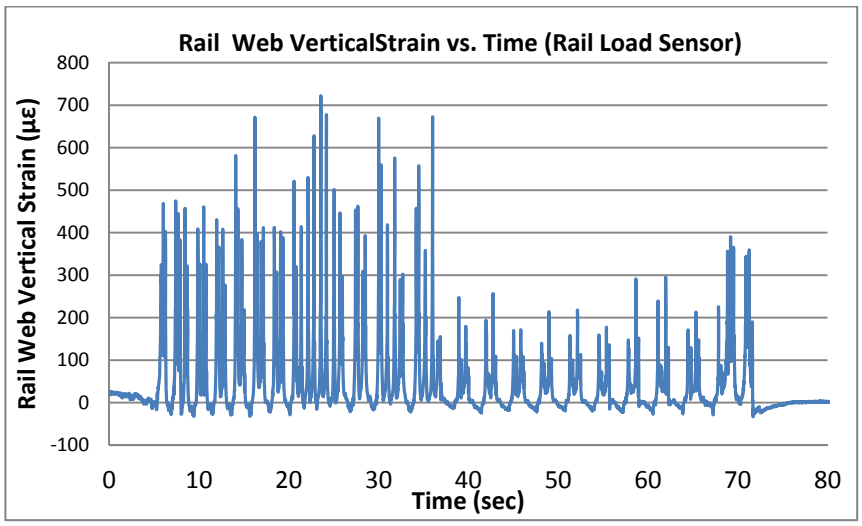

Figure 2.76: Rail Load Sensor rail web vertical strain measurements results

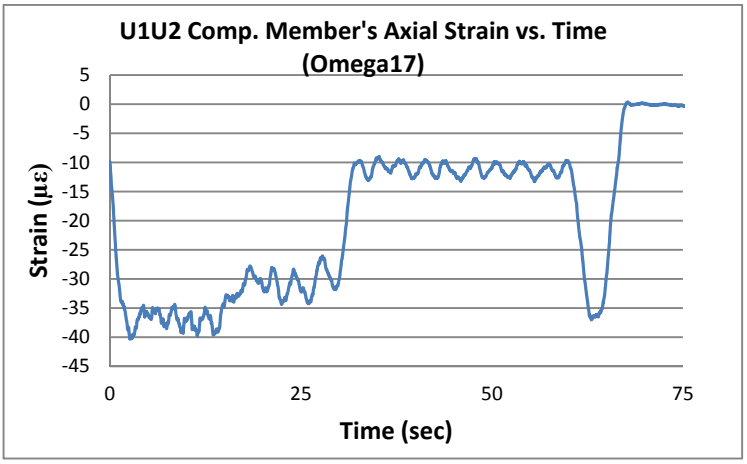

Figure 2.77: Compression member Gage17 strain measurements results

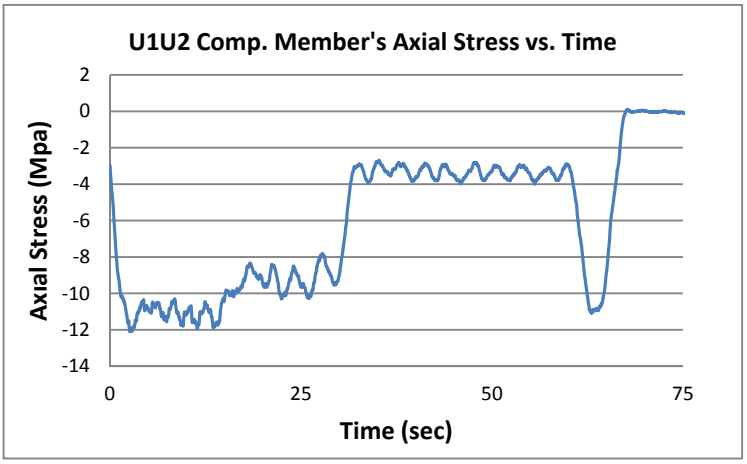

Figure 2.78: Compression member calculated stress by strain measurements results

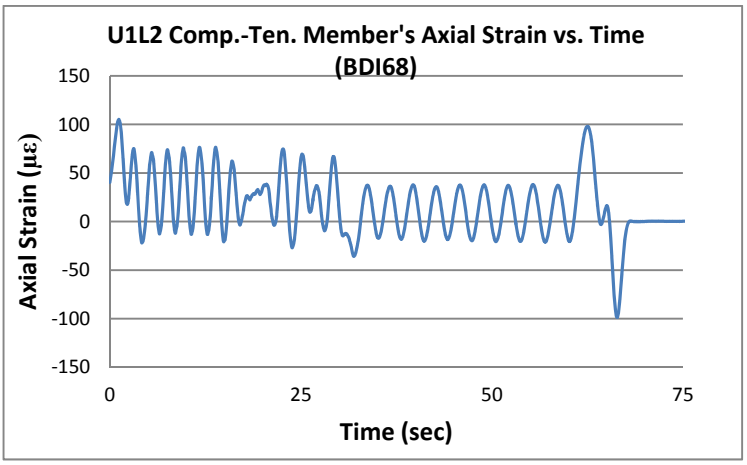

Figure 2.79: Comp-ten member BDI68 strain measurements results

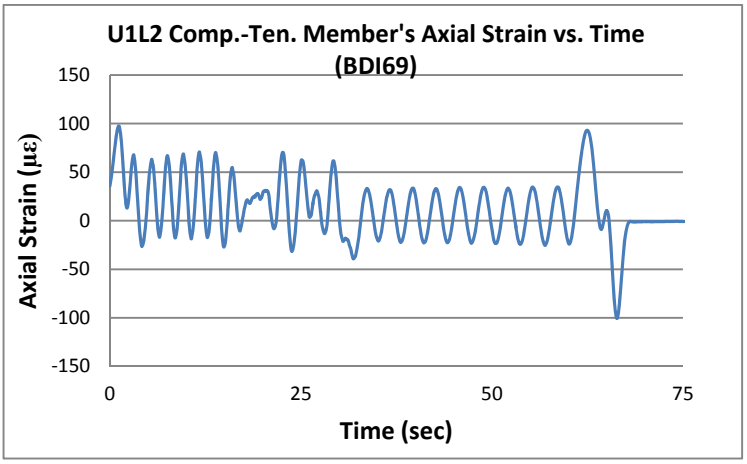

Figure 2.80: Comp-ten member BDI69 strain measurements results

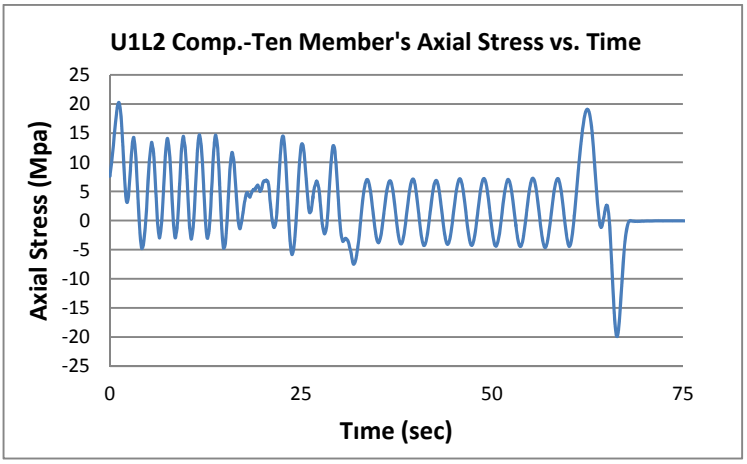

Figure 2.81: Comp-ten member calculated stress by strain measurements results

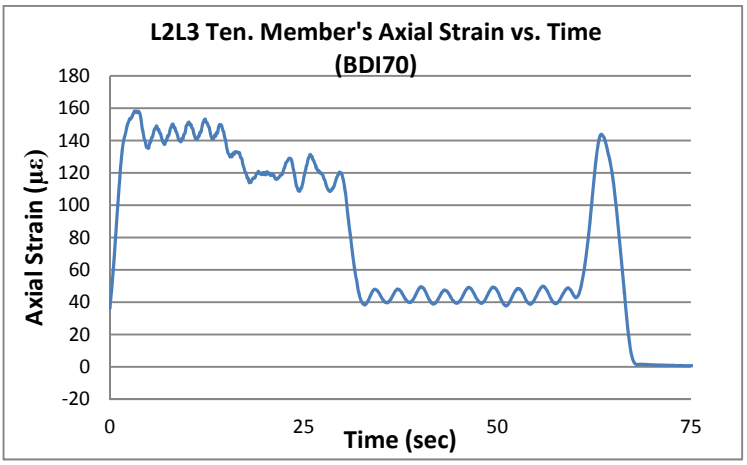

Figure 2.82: Tension member BDI70 strain measurements results

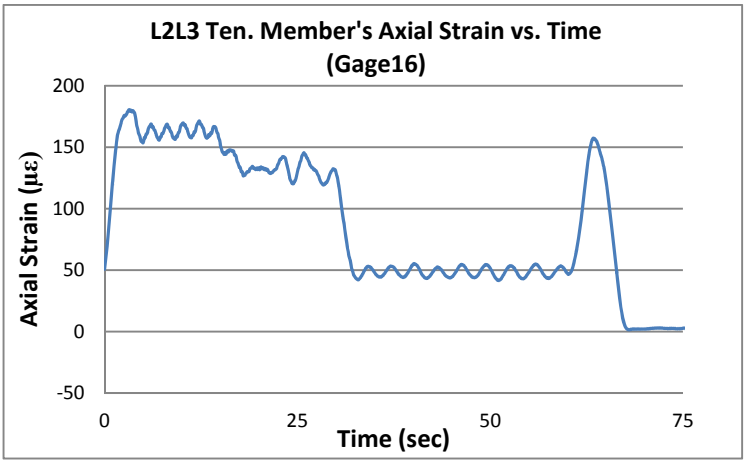

Figure 2.83: Tension member Gage16 strain measurements results

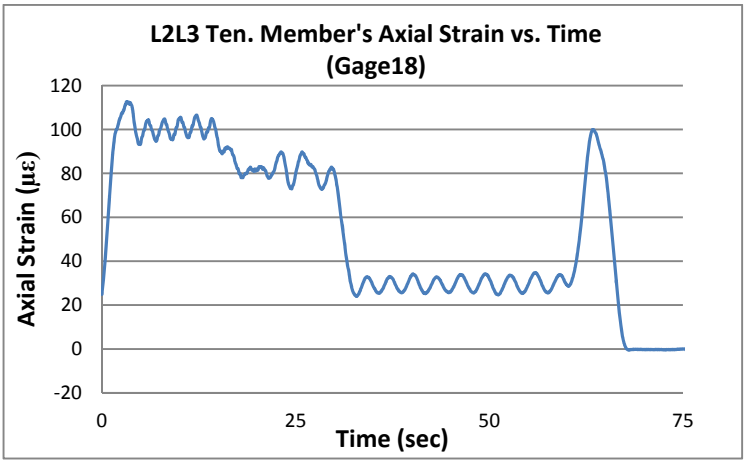

Figure 2.84: Tension member Gage18 strain measurements results

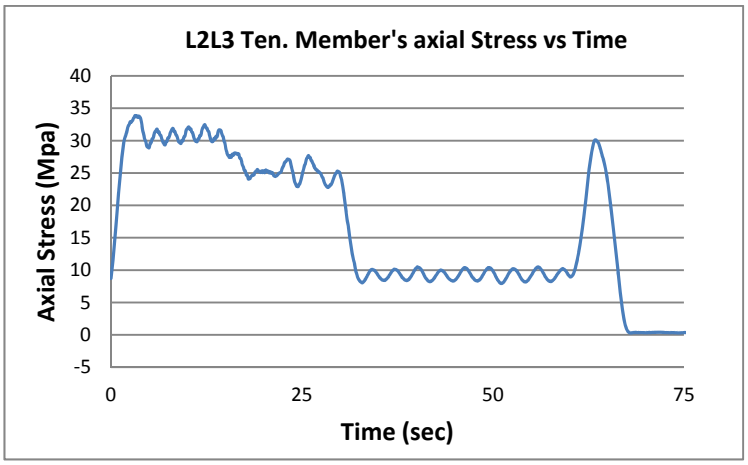

Figure 2.85: Tension member calculated stress by strain measurements results

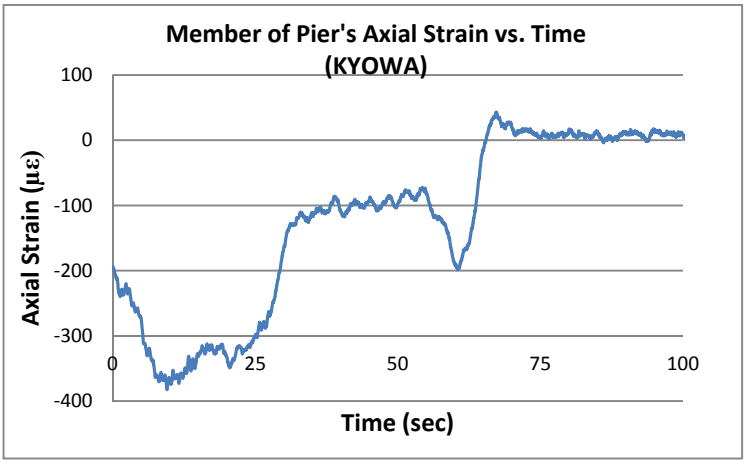

Figure 2.86: Member of pier Kyowa gage strain measurements results

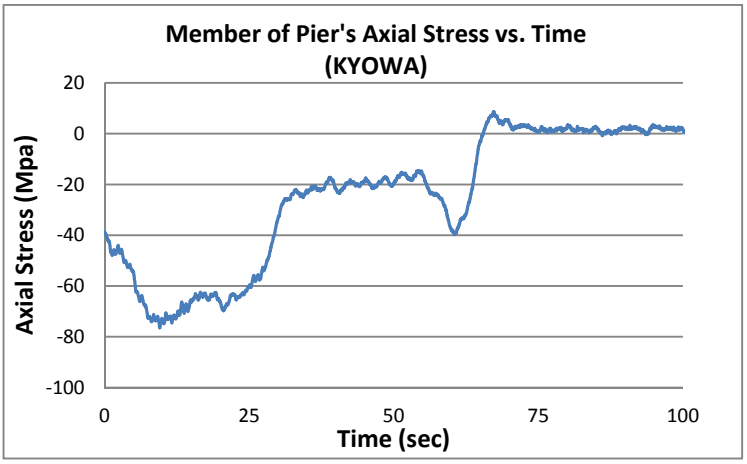

Figure 2.87: Member of pier calculated stress by strain measurements results

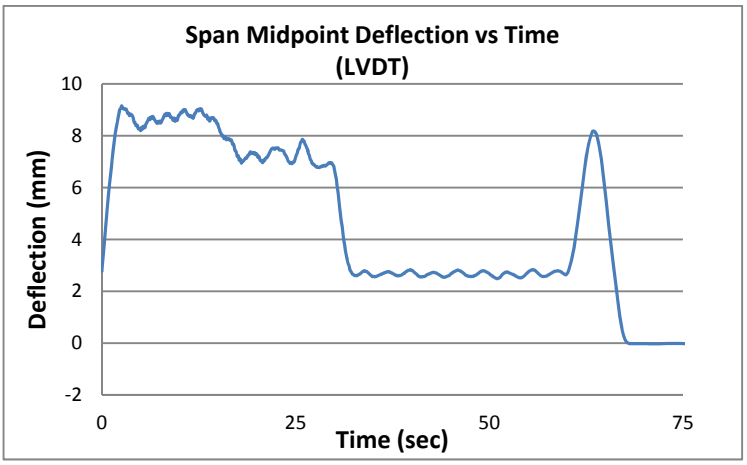

Figure 2.88: Truss midpoint deflection measurements results

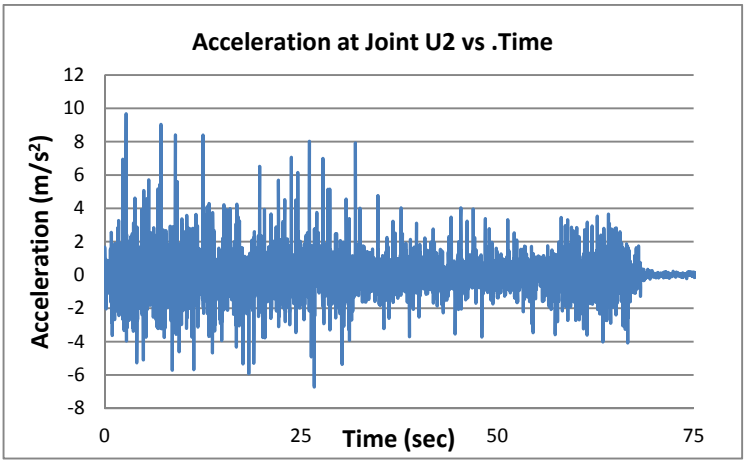

Figure 2.89: Joint U2 acceleration measurements results

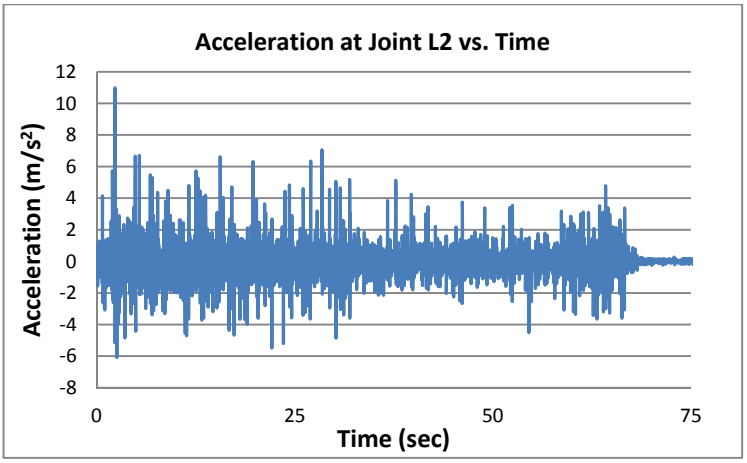

Figure 2.90: Joint L2 acceleration measurements results

Table 2.5: Measured maximum values during third field study

Date	Time	Train Type	Maximum Axial Stress (MPa)[2]				Maximum Deflection (mm)	Maximum Acceleration (m/s^2)	
			U1U2	U1L2	L2L3	Pier		U2	L2
17.12.2010	12:08	Passenger	-11.56	22.35	29.82	-[1]	8.37	-[1]	-[1]
17.12.2010	12:50	Goods	-13.54	-23.30	37.52	-[1]	9.66	-[1]	-[1]
17.12.2010	14:51	Goods	-13.87	-21.69	36.46	-[1]	10.00	6.34	-[1]
17.12.2010	22:58	Goods	-12.09	20.27	33.87	-76.46	9.15	9.65	10.97
18.12.2010	02:36	Locomotive	-11.48	21.64	28.98	-46.63	8.15	5.31	2.88
18.12.2010	04:30	Goods	-11.40	19.64	31.14	-49.46	8.53	7.74	9.27

1) Pier strain measurements and truss acceleration measurements are started after completing installation studies during third field study therefore some values can not be included in table.

2) Negative stress values correspond to compression, possitive stress values correspond to tension

2.8 Specimen Laboratory Test

During field study small specimen from bridge railing is collected. This material used for tensile test in METU Metallurgical Engineering Department Laboratory. According to test results, material average yield strength is equal to 280 MPa and ultimate tensile strength is equal to 364 MPa, from three specimens.

CHAPTER 3

FINITE ELEMENT MODELING AND TRAIN SIMULATION OF THE SELECTED BRIDGE

3.1 2D Finite Element Modeling (FEM)

Finite element modeling of selected bridge structure is started with the 2D FEM. Members of trusses are modeled as frame members. Purpose of this study is to determine degree of loading during train crossing the bridge and to decide how to model connection region of truss. In 2D FEM horizontal curve, super elevation, slope of actual bridge structure are not modeled. Cross sections of each member are modeled according to the technical drawing of two rebuilt spans in 1963. Loading of model is done according to standard LM71 moving train load stated in Eurocode-1 part 2: Traffic Loads on Bridges.

3.1.1 2D FEM Connection Region

2D FEM member connection regions are modeled as semi rigid connection, pin connection, simple connection, and simple pin connection. Purpose of this study is to determine the both closest and simplest connection simulation with the real connection application.

3.1.1.1 Semi Rigid Connection

In this type of model real application of drawings is modeled. Such as all connection plates, reinforcing plates are added to cross sections and new cross sections created and modeled in connection regions. It is assumed that connection

plates and reinforcing plates are increasing rigidity of connection region in semi rigid connection model. It is also assumed that most accurate model is the semi rigid connection model due to same structural condition to real application. There are no moment releases at the joints.

3.1.1.2 Pin Connection

This type of connection is same as the semi rigid connection model except pins are introduced at joints, by moment releases.

3.1.1.3 Simple Connection

In this type of connection, connection plates and reinforcing plates are not modeled. Cross sections are kept constant between joints. It is assumed that all members can transfer moment at the joints, moment releases are not defined.

3.1.1.4 Simple Pin Connection

This type of connection is same as the simple connection model, except moment releases are defined at joints..

3.1.2 2D FEM and Cross Section Views

General view of 2D FEM with cross section names is introduced (Figure 3.1) and un-stiffened regions' cross section namely main cross sections' views are given (Figure 3.2). Cross-sectional properties are given table 3.1.

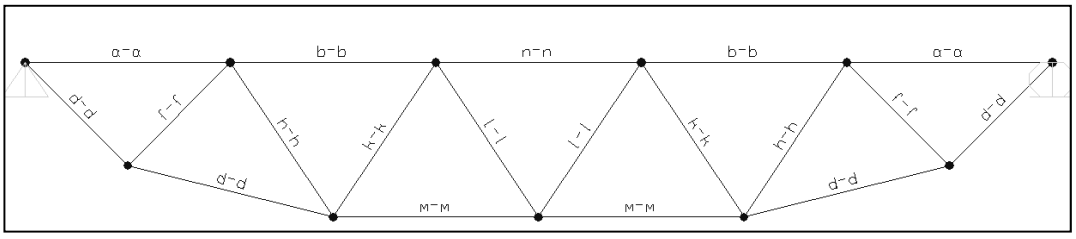

Figure 3.1: 2D FEM view with cross section names

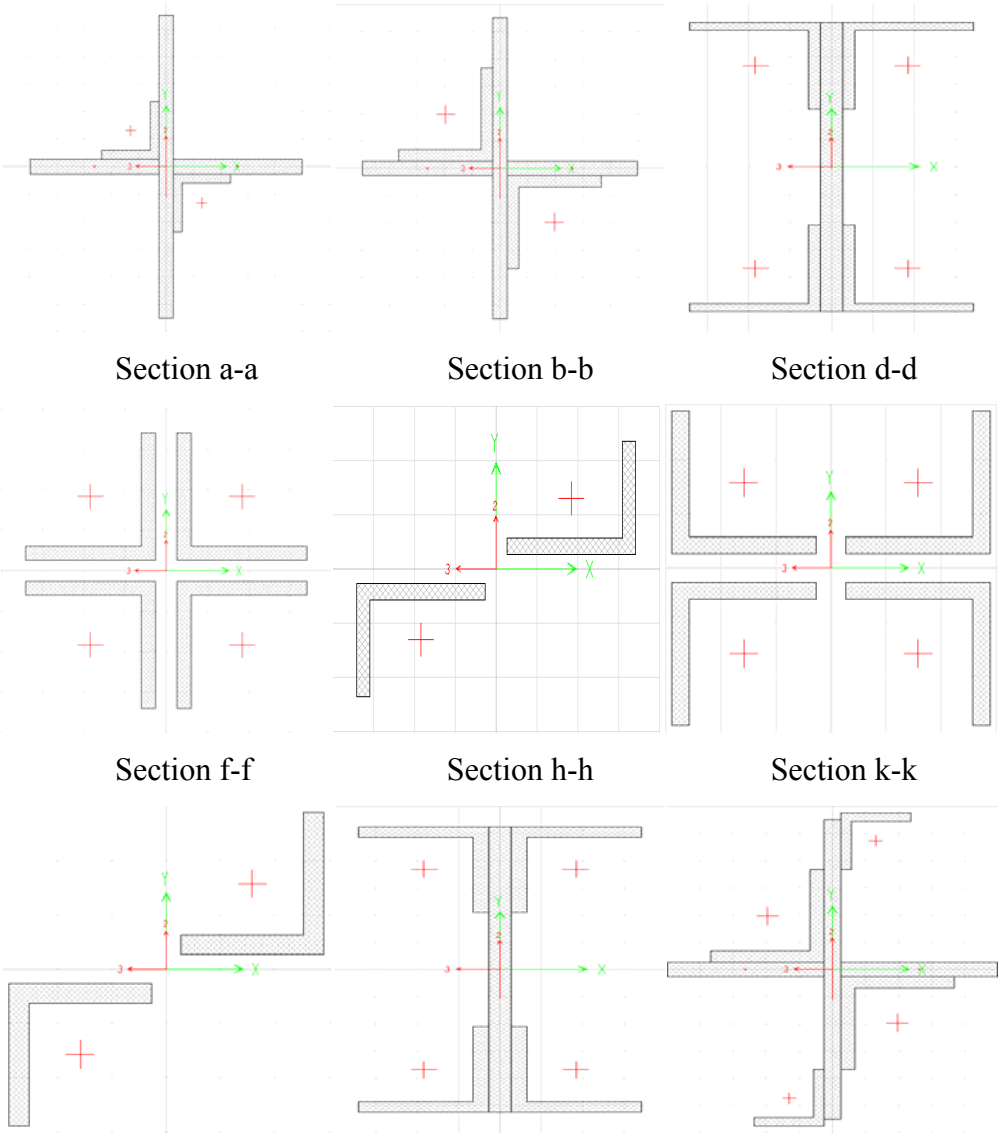

Figure 3.2: 2D FEM Cross Section views

Table 3.1: Truss members cross-sectional properties

Section Name	Area	TorsConst	I33	I22	AS2	AS3	S33	S22	Z33	Z22	R33	R22
	cm2	cm4	cm4	cm4	cm2	cm2	cm3	cm3	cm3	cm3	cm	cm
a-a	191.52	524.61	12998.14	9798.14	112.78	107.57	618.96	515.69	1040.11	884.11	8.24	7.15
b-b	234.08	933.91	15423.84	12223.84	147.03	139.76	734.47	643.36	1295.66	1139.66	8.12	7.23
d-d,d'-d'	180.76	573.24	39797.29	3367.53	98.02	71.42	1989.86	259.04	2472.02	483.94	14.84	4.32
f-f	118.04	67.25	3965.72	3965.72	87.73	87.73	305.06	305.06	528.61	528.61	5.80	5.80
h-h	45.12	21.92	4268.12	651.87	33.54	37.89	328.32	72.43	403.97	137.47	9.73	3.80
k-k	90.24	41.95	6701.75	2241.20	58.49	73.63	609.25	203.75	727.30	355.58	8.62	4.98
l-l	52.08	34.66	3799.91	1314.86	34.09	44.79	345.45	119.53	416.02	208.94	8.54	5.02
m-m	215.00	915.00	48999.92	4623.42	102.96	103.52	2450.00	355.65	3020.75	654.25	15.10	4.64
n-n	269.60	1041.88	29222.91	12849.98	165.34	168.76	1328.31	676.31	1990.51	1261.78	10.41	6.90

3.1.3 2D FEM Loading Information

In 2D FEM loading conditions; Load model 71 (Figure 3.3) presented in EN1991-2-2003 is used as gravitational moving train load and application coefficient is assumed as 1.4. In addition; it is assumed that train load is distributed equally to symmetric two trusses and 2D FEM is loaded with half of load model 71 (LM71) by defining load scale factor as 0.5.

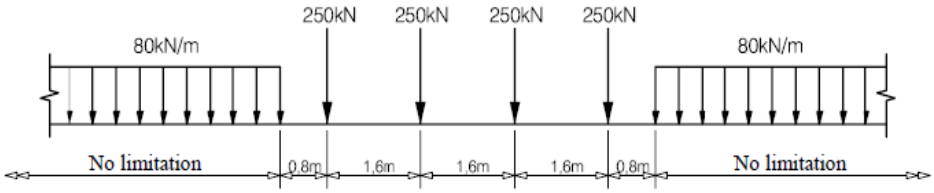

Figure 3.3: Load Model 71 (LM71) and characteristic values of vertical loads presented in EN1991-2-2002

In 2D FEM steel truss is loaded with LM71 at three different loading conditions for determination of connection region condition.

3.1.3.1 L/6 Loading Condition

LM71's four point loads' center is located at the 5th meter of 30 meters long truss (Figure 3.4).

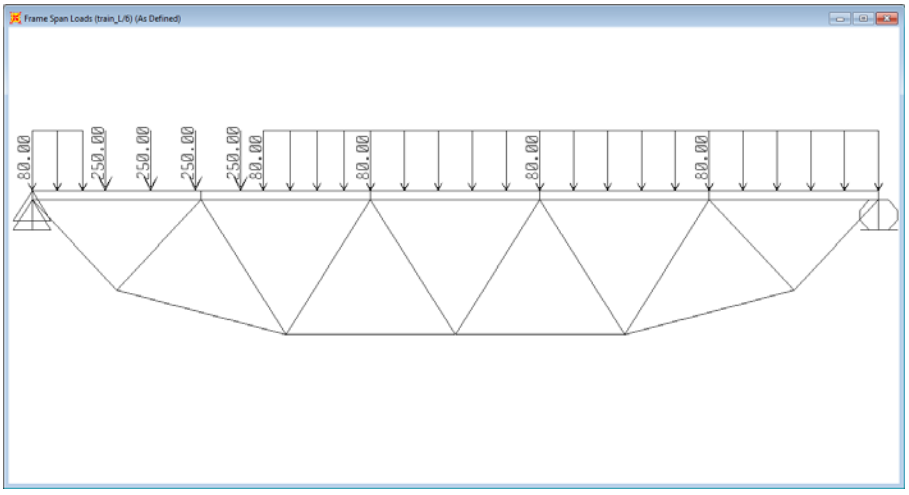

Figure 3.4: L/6 Loading condition model view

3.1.3.2 2L/6 Loading Condition

LM 71's four point loads' center is located at the 10th meter of 30 meters long truss (Figure 3.5).

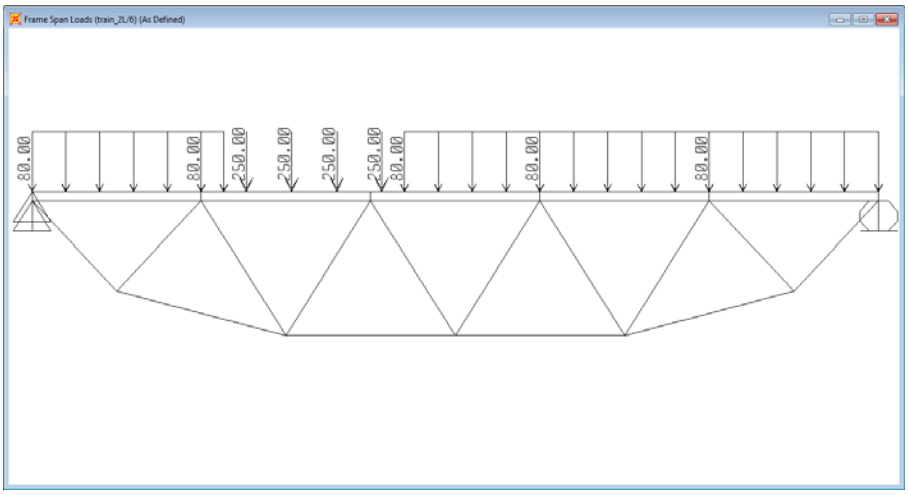

Figure 3.5:2L/6 Loading condition model view

3.1.3.3 3L/6 Loading Condition

LM 71's four point loads' center is located at the 15th meter of thirty meter long truss (Figure 3.6). (i.e. Symmetric loading and maximum deflection condition)

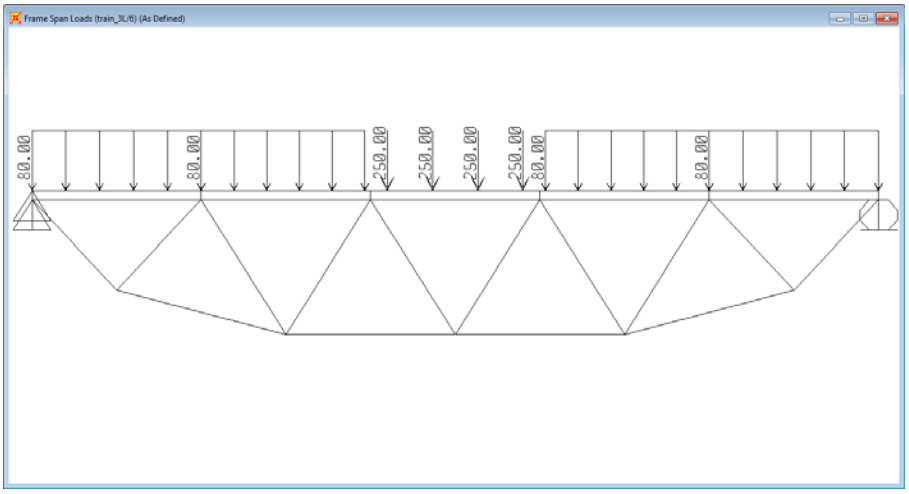

Figure 3.6: 3L/6 Loading condition model view

3.1.4 2D FEM Structural Analysis for Connection Regions Information

According to definitions and assumptions, four different 2D FEM (semi rigid, pin, simple, simple pin) are analyzed, under three different loading conditions (L/6, 2L/6, 3L/6). Truss midpoint deflection and member stresses are obtained. These parameters are used to compare three different models with the semi rigid connection model that is the real application model. Semi rigid vs. pin connection, semi rigid vs. simple connection and semi rigid vs. simple pin connection models comparisons are completed and presented in following subsections. As a result of comparison of models, connection property of 2D and 3D FEM models are decided.

Truss midpoint deflections are compared under train loading for each loading condition. Forces are obtained as result of analysis and recorded at five locations for each member. After that, forces are converted to the stress results, depend on cross-sectional properties. These five locations for each members are connection joints (start and end locations of member), midpoint, and section changing locations (ends of connection and reinforcing plates). Stresses' data point intervals (5 point for each member) and corresponding member ids are given in table 3.2.

Table 3.2: Data point intervals and corresponding member ids

Data Point Interval	Member
1-5	U0U1
6-10	U0'U1'
11-15	U1U2
16-20	U1'U2'
21-25	U0L1
26-30	U0'L1'
31-35	L1L2
36-40	L1'L2'
41-45	L1U1
46-50	L1'U1'
51-55	U1L2
56-60	U1'L2'
61-65	L2U2
66-70	L2'U2'
71-75	U2L3
76-80	U2'L3
81-85	L2L3
86-90	L2'L3
91-95	U2U2'

3.1.5 2D FEM Structural Analysis for Connection Regions Results

In this section analysis results are compared and presented as tabular form for midpoint deflection and graphical forms for member stresses at force output locations, introduced before in table 3.2. Stress outputs are combined in same graphs for three different loading conditions, the first 95 data points corresponds to L/6 loading condition; the second 95 data points corresponds to 2L/6 loading condition; the last 95 data points corresponds to 3L/6 loading condition.

3.1.5.1 Model Comparisons

3.1.5.1.1 Truss Midpoint Deflection Comparisons

Truss maximum midpoint deflection under 3L/6 train loading is 2.214 cm for semi rigid connection, 2.228 cm for pin connection, 2.459 cm for simple connection, 2.475 cm for simple-pin connection models. (Table 3.3). There is maximum 0.63% difference between semi rigid connection and pin connection; maximum 1.07%

difference between semi rigid connection and simple connection; 1.79% difference between semi rigid connection and simple-pin connection.

Table 3.3: Models Mid-point Deflection Comparisons

		DEFLECTION	COMPARISON
		Semi Rigid	Model/ Semi Rigid
COMBINATION	LOADING	cm	%
SEMI RIGID	L/6	1.879	-
	2L/6	2.109	-
	3L/6	2.214	-
PIN	L/6	1.889	100.53
	2L/6	2.121	100.57
	3L/6	2.228	100.63
SIMPLE	L/6	2.078	110.59
	2L/6	2.338	110.86
	3L/6	2.459	111.07
SIMPLE-PIN	L/6	2.089	111.18
	2L/6	2.352	111.52
	3L/6	2.475	111.79

3.1.5.1.2 Member Stresses Comparisons

Graphical representations of stresses are presented in this section for semi rigid vs. other models loading conditions. Stress comparisons are completed in two steps. The first step is, calculated total stresses of semi rigid and other models vs. data point are compared in graphical representation. The second step is; axial and total stresses for semi rigid and simple model are calculated and moment contributions in each model's stresses results are determined.

- **Total Stress Comparison of Semi Rigid Connections and Other Models**

Total stresses are calculated under three different train loading conditions. All calculated stresses are plotted in same graph for each model. Figure 3.7 is the graph of total stresses of semi rigid and pin model stresses. These stresses are shown that semi rigid connection model members have higher stresses due to moment contributions.

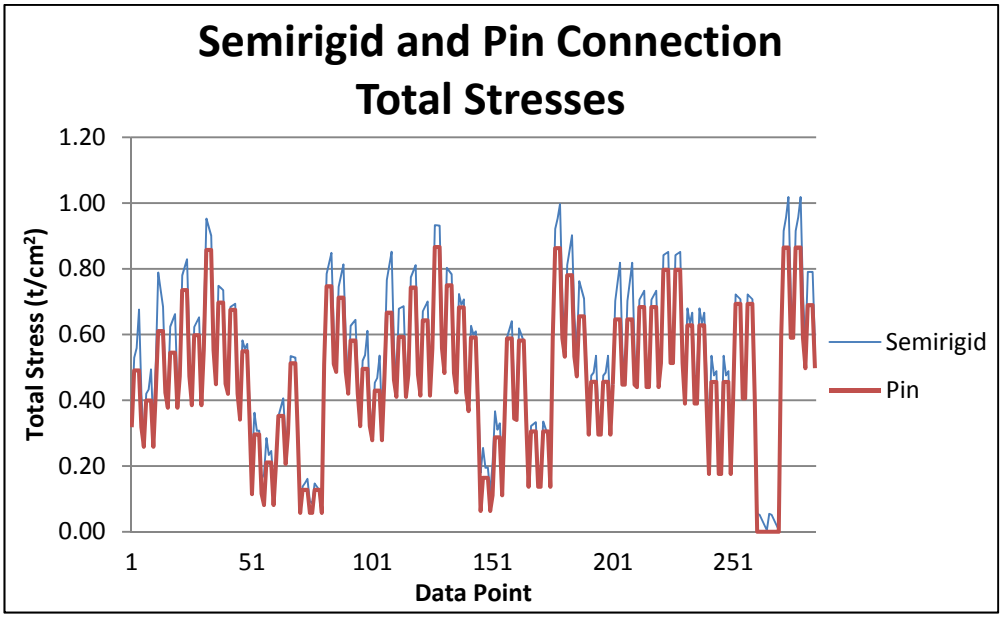

Figure 3.7: Semi Rigid and Pin Connection Models Total Stresses

Figure 3.8 is the graph of total stresses of semi rigid and simple model stresses. These stresses are shown that simple connection model members have same maximum total stress values with the semi rigid connection model members' maximum total stress values. There are differences in connection regions due to cross sectional property changes.

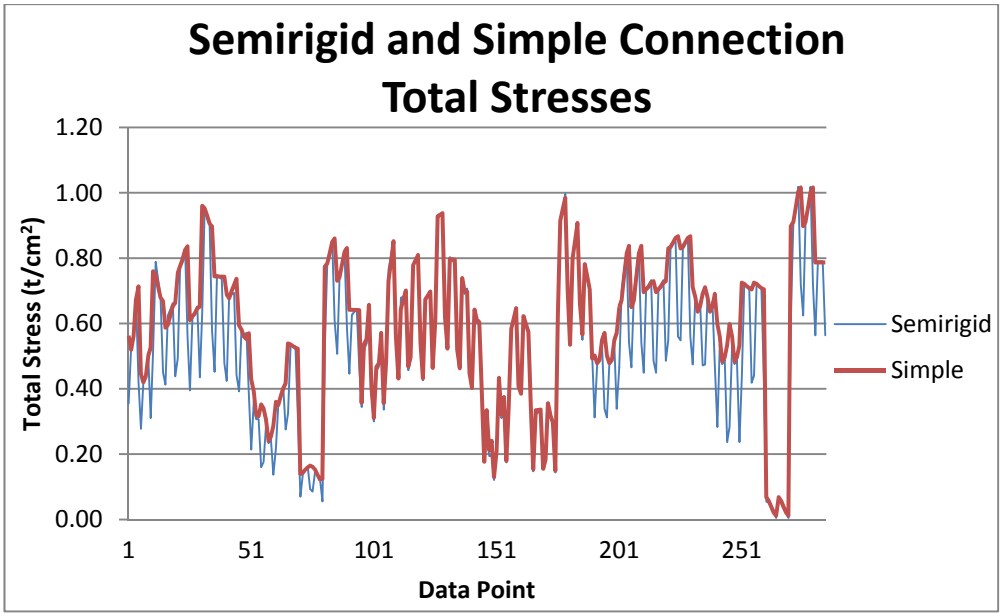

Figure 3.8: Semi Rigid and Simple Connection Models Total Stresses

Figure 3.9 is the graph of total stresses of semi rigid and simple pin model stresses. These stresses are shown that semi rigid connection model members have higher stresses due to moment contributions. There are also differences in connection regions due to cross sectional property changes.

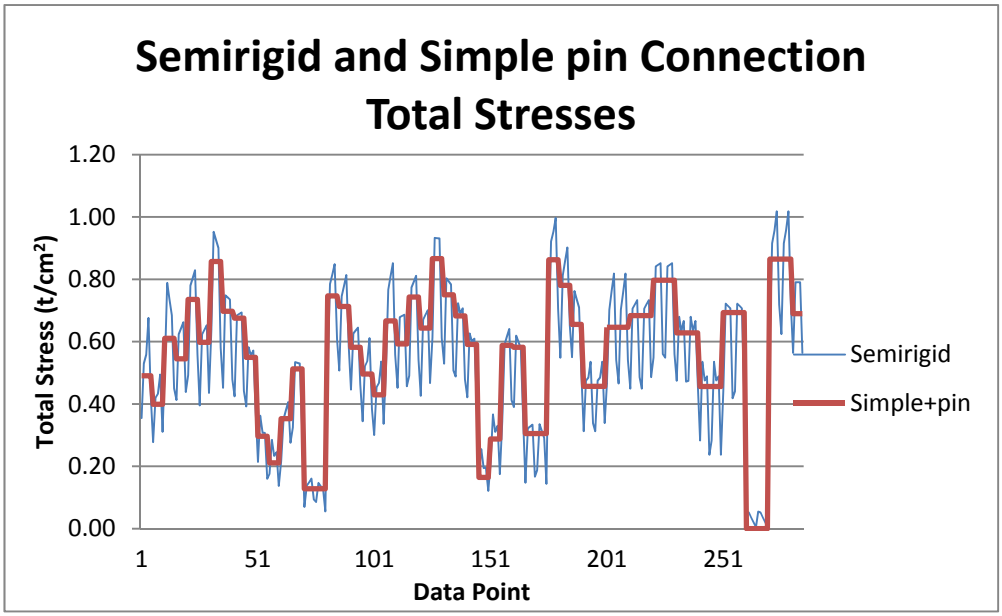

Figure 3.9: Semi Rigid and Simple Connection Models Total Stresses

- **Axial and Total Stress Comparison of Semi Rigid Connections and Simple Connections**

Second step of model comparisons is comparison of moment contribution in total stresses. Axial stresses and total stresses of semi rigid connection model and simple model are plotted in graphs for all loading conditions and presented in figure 3.10 and 3.11. According to analyses average of moment contributions in semi rigid connection model are 11% for compression members, 8% for tension members and 20% for tension-compression members; average of moment contributions in simple connection model are 11% for compression members, 7.5% for tension members and 19% for tension-compression members.

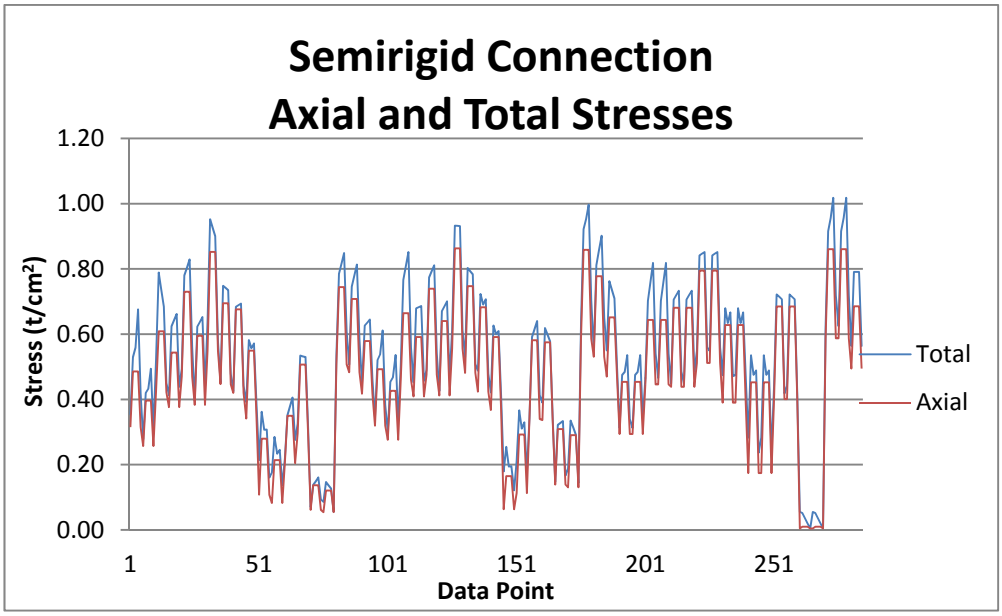

Figure 3.10: Semi Rigid Connection Axial and Total Stresses

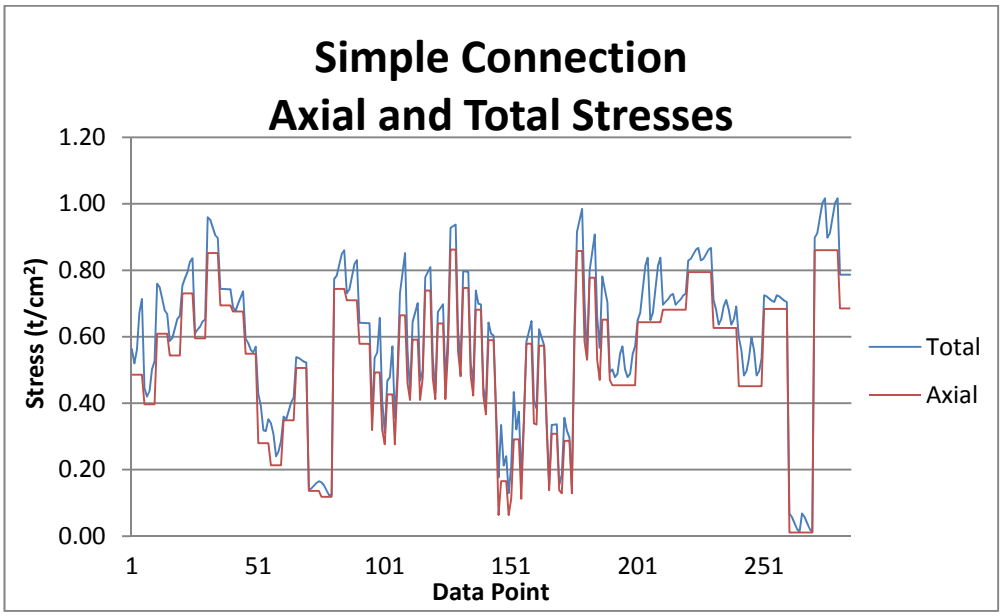

Figure 3.11: Simple Connection Axial and Total Stresses

- **General Conclusions of Results**

It is shown that by analyses moment effect cannot be determined by using pin connection model or simple pin connection models. Therefore using these models result underestimated the stress results. Simple connection model results showed that maximum stresses in members can be estimated equally with the semi rigid

connection model. Although higher stresses within connection regions are obtained in simple connection than the semi rigid connection, these results yield conservative condition assessments which are the following parts of study namely capacity index and reliability index calculation studies.

3.1.6 2D FEM Structural Analysis Results Evaluations

Out of four FEM the semi-rigid connection model has been found to be the closest FEM to the actual condition. However it is decided that, this type of FEM and its analysis process is not appropriate for 2D and 3D FEM analysis because of its complex and error-prone nature.

Simple connection 2D FEM has been found to be the closest model to the semi rigid connection 2D FEM in terms of member stresses. In addition to the stresses, there is 1.07% midpoint deflection difference between two models, which is acceptable in consideration of environmental conditions and effects. Simple connection modeling is chosen to be used in 2D and 3D FEM, due to the above two evaluation and its simplicity.

3.2 3D Finite Element Modeling (FEM)

As mentioned in 2D FEM sections, 3D FEM (Figure 3.25 and Figure 3.26) created with frame member with simple moment resisting connection. In contrast with 2D FEM, 3D FEM is completed with bridge 300 m radius horizontal curve (Figure 3.27), super elevation and % 2.5 vertical slope. In addition to the span structure one steel pier is modeled (Figure 3.28). LM71 loading condition is used in 3D FEM as 2D FEM.

3.2.1 3D FEM Views

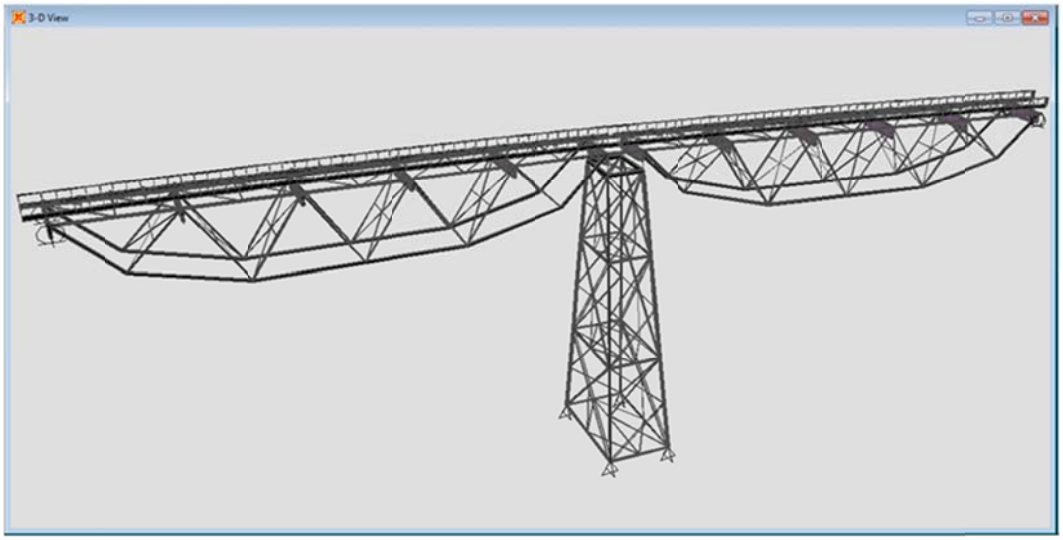

Figure 3.12: 3D FEM (two span and 19 m pier)

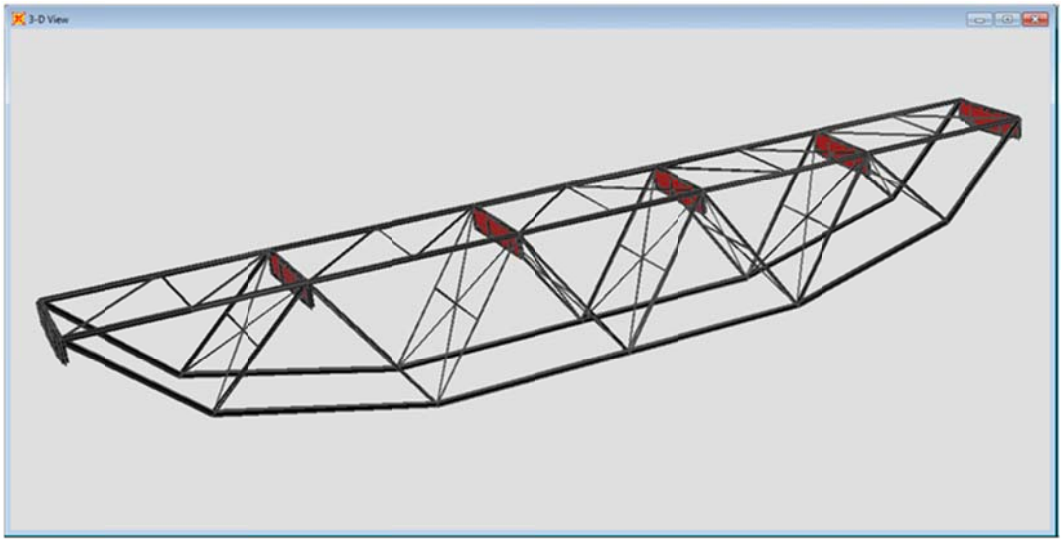

Figure 3.13: FEM truss members, lateral and vertical bracing and floor beams

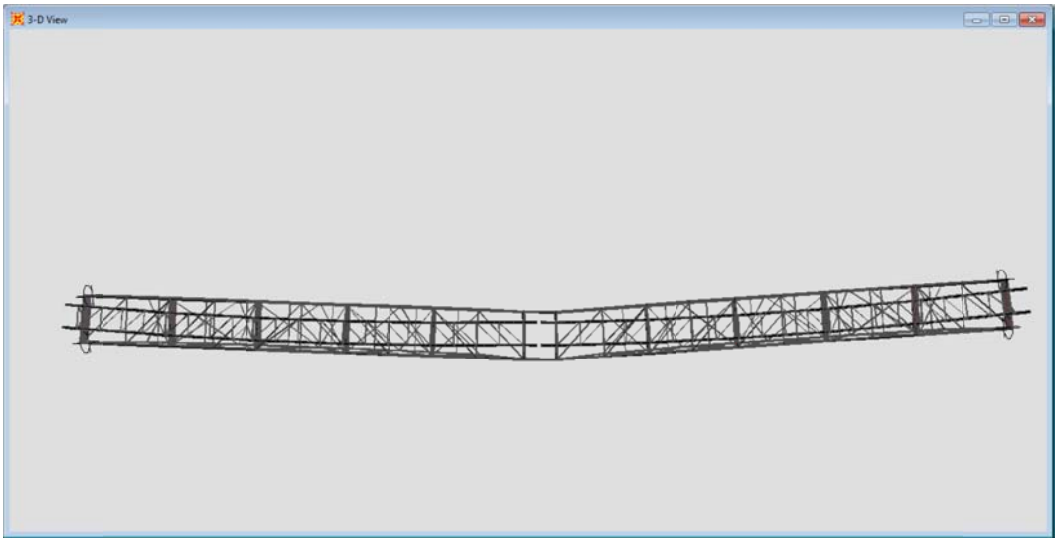

Figure 3.14: 3D FEM horizontal curve view

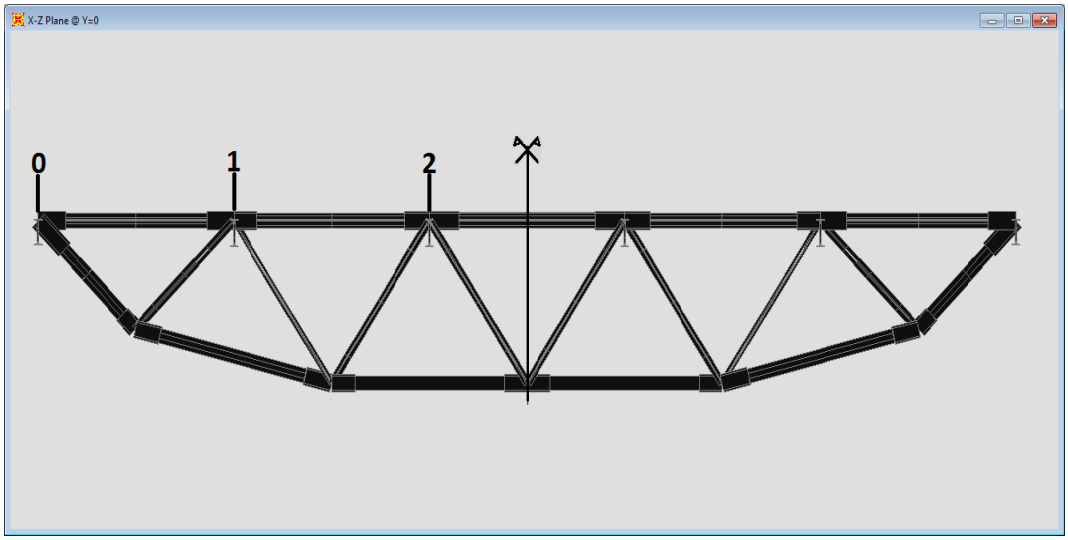

Figure 3.15: 3D FEM symmetry axis of truss and panel points numbering

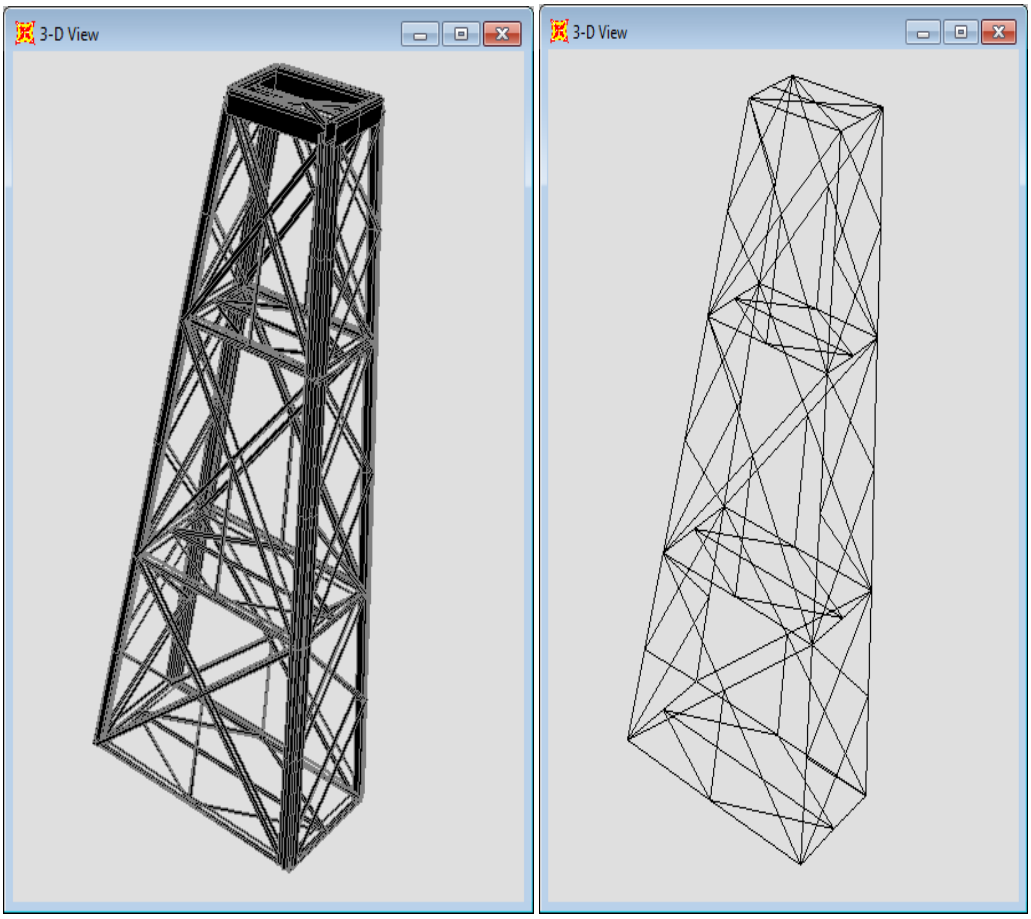

Figure 3.16: 3D FEM 19 m pier view

3.3 Influence Lines and Train Loading Simulation

Influence lines of member forces for 2D FEM are obtained, in order to determine train loading simulation. Influence lines are generated by independently applying a unit load at several points on 2D FEM and the value of the force functions are determined due unit load. Totally 74 different loading cases are created with 0.4 meters interval of 30 meters long steel truss 2D FEM. End moments and axial load functions are determined. Influence lines of member forces for end moments, about strong axis of cross section, are presented as moments-1 and moments-2, and axial forces presented as axial forces in graphical representation. Members are classified as compression members, tension members and compression-tension members depend on their axial load conditions. Sign convention for axial forces is assumed as tension is positive, compression is negative.

3.3.1 Compression Members Influence Lines

Compression members` 2D FEM view (Figure 3.30) and influence lines functions graphical representation are given for end moments, moment-1 (Figure 3.31) and moment-2 (Figure 3.32), and axial forces (Figure 3.33). It is obvious that about symmetry axis forces are equal for each symmetrical member; except for member U2U2` there is not symmetrical member, equal influence line does not exist.

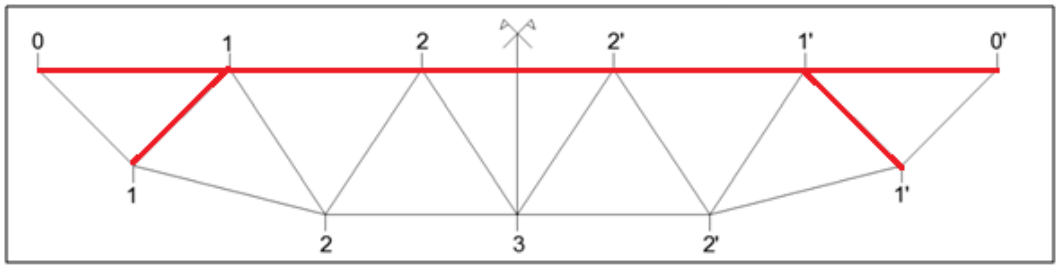

Figure 3.17: Compression members' 2D FEM view

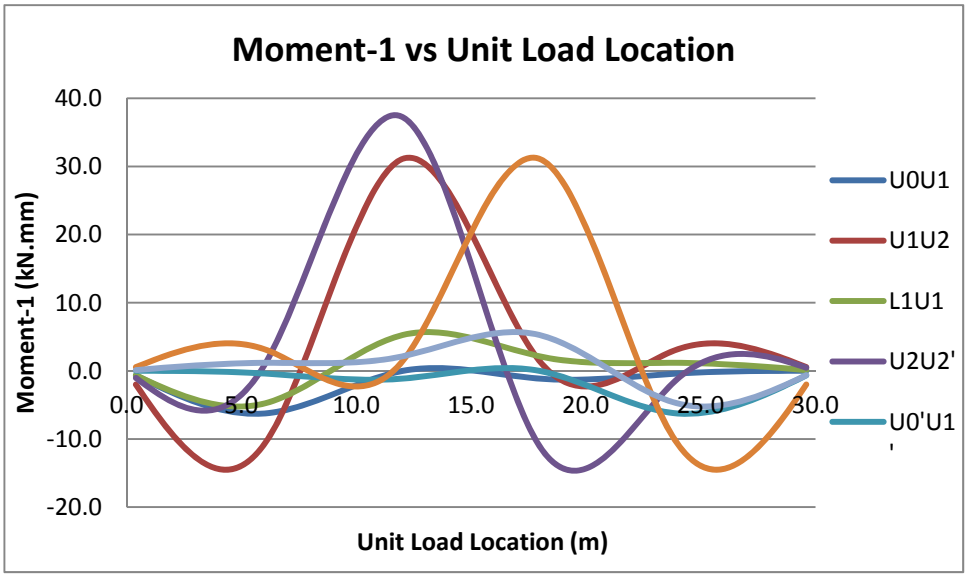

Figure 3.18: Compression members' Moment-1 influence lines

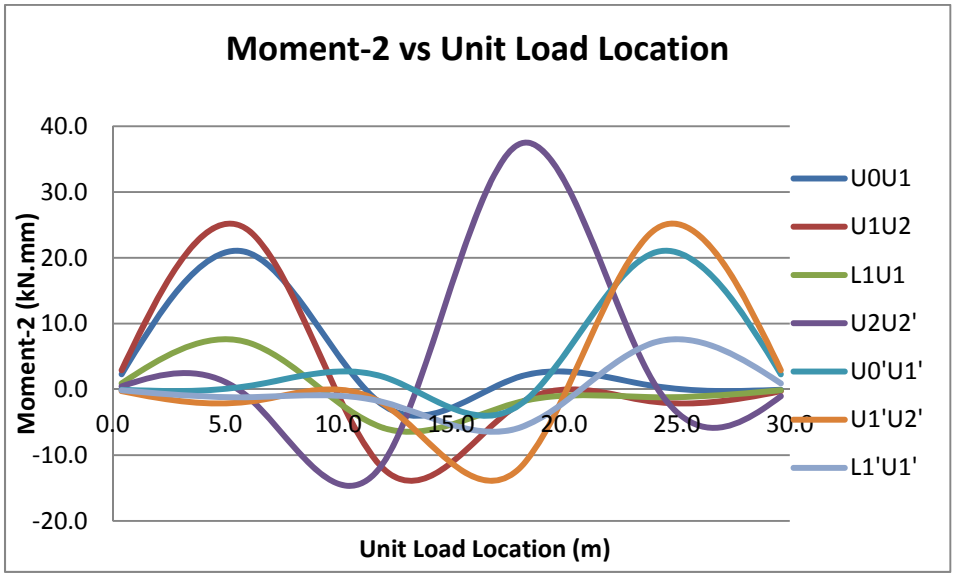

Figure 3.19: Compression members' Moment-2 influence lines

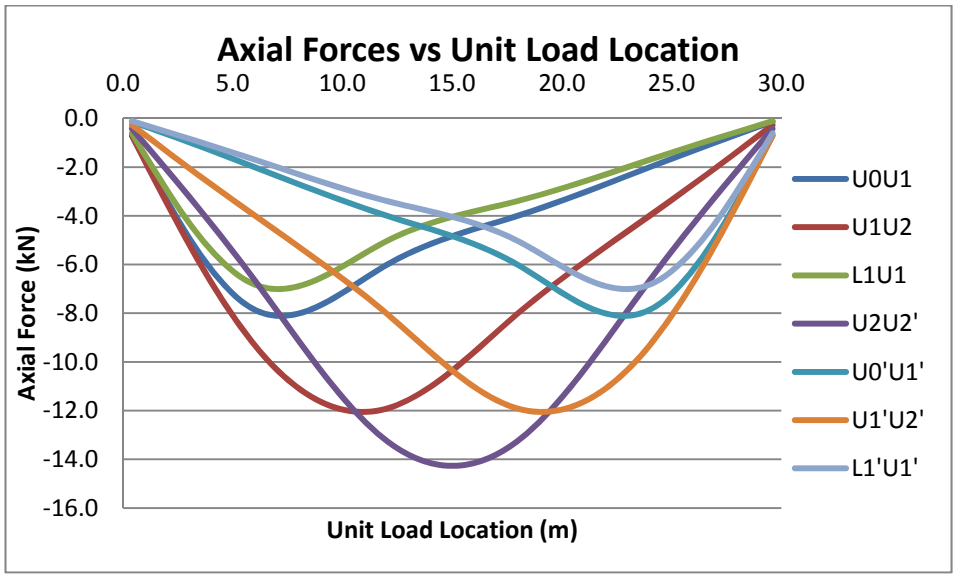

Figure 3.20: Compression members' axial force influence lines

3.3.2 Tension Members Influence Lines

Tension members` 2D FEM view (Figure 3.34) and influence lines functions graphical representation are given for end moments, moment-1 (Figure 3.35) and moment-2 (Figure 3.36), and axial forces (Figure 3.37). It is obvious that about symmetry axis forces are equal for each symmetrical member.

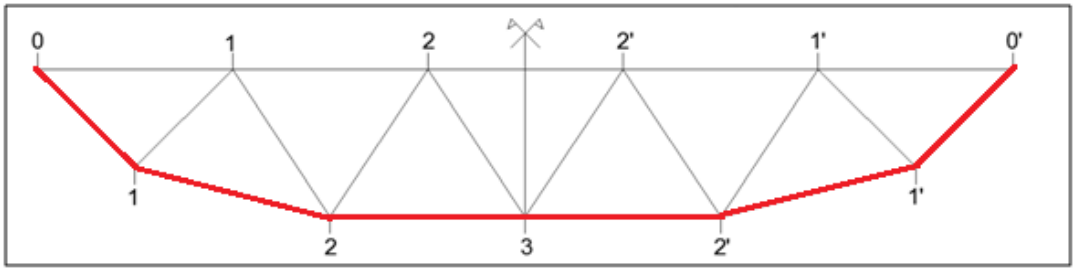

Figure 3.21: Tension members' 2D FEM view

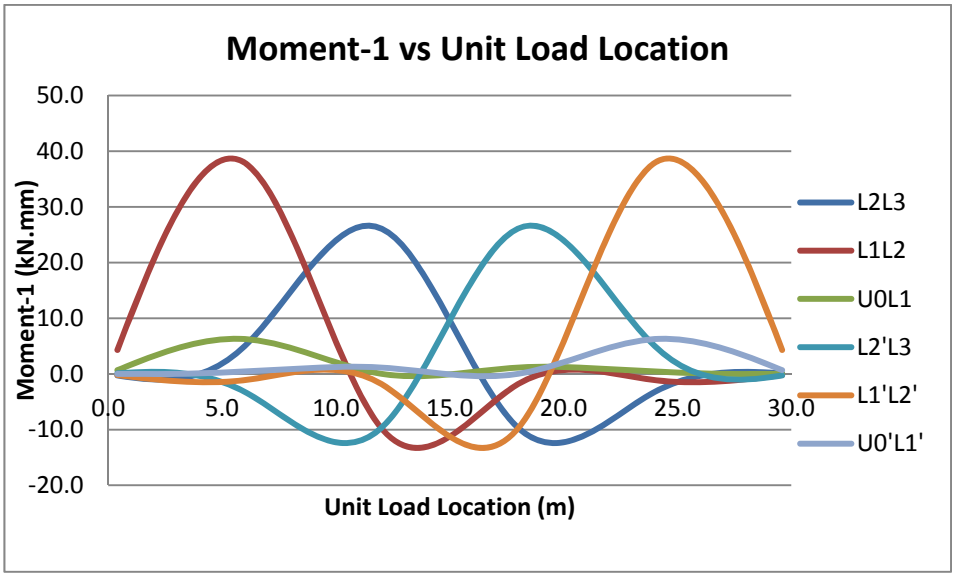

Figure 3.22: Tension members' Moment-1 influence lines

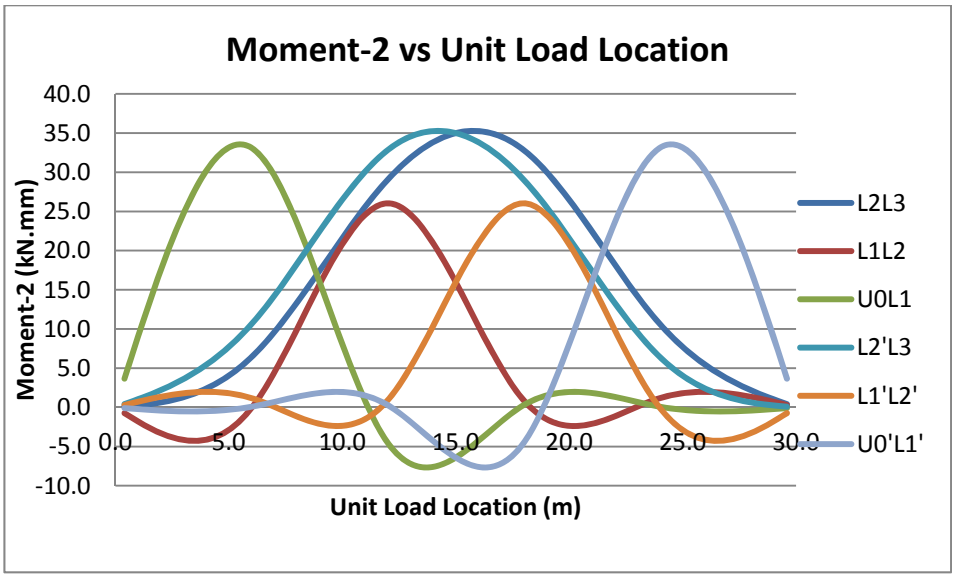

Figure 3.23: Tension members' Moment-2 influence lines

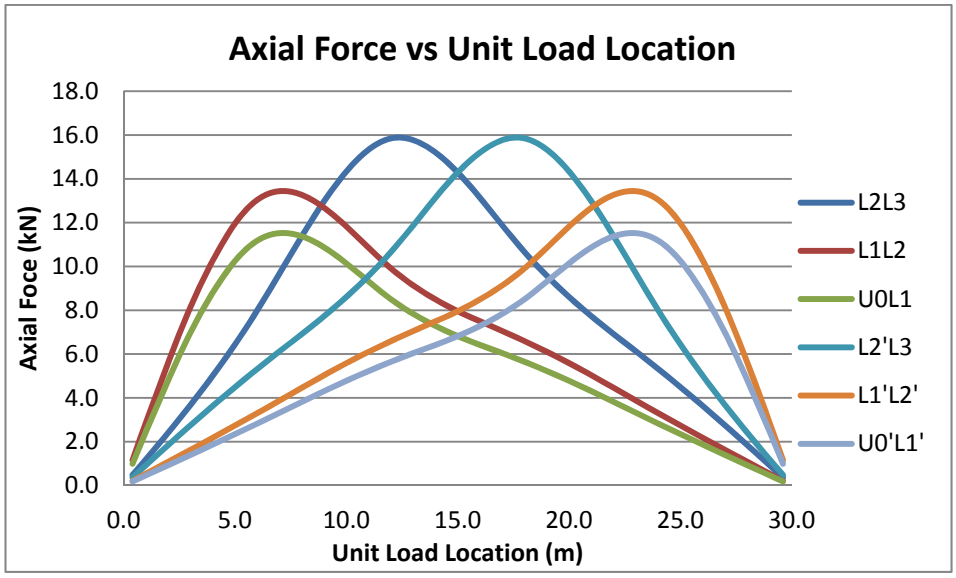

Figure 3.24: Tension members' axial forces influence lines

3.3.3 Compression-Tension Members Influence Lines

Compression-tension members` 2D FEM view (Figure 3.38) and influence lines functions graphical representation are given for end moments, moment-1 (Figure 3.39) and moment-2 (Figure 3.40), and axial forces (Figure 3.40). It is obvious that about symmetry axis forces are equal for each symmetrical member. Sharp changes seen in graphs are due to the force shifts between tensile and compressive forces.

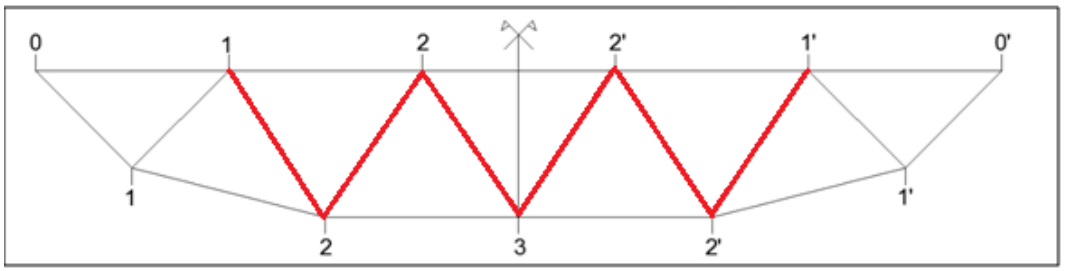

Figure 3.25: Compression-Tension members' 2D FEM view

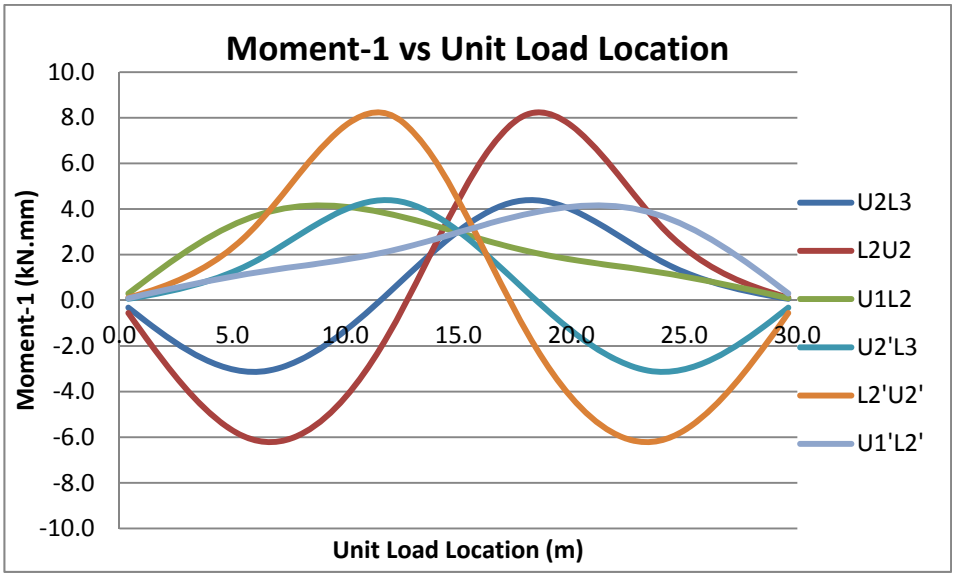

Figure 3.26: Compression-tension members' Moment-1 influence lines

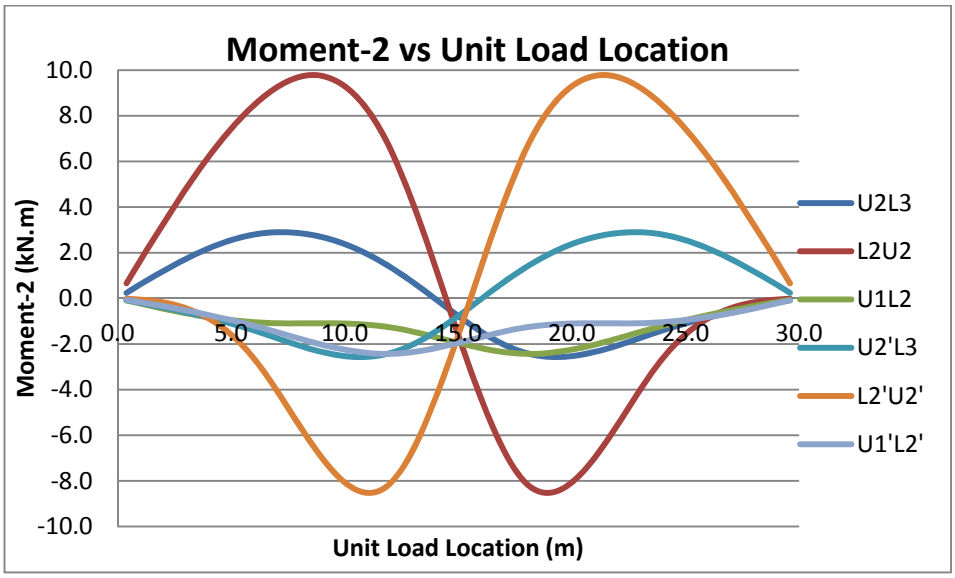

Figure 3.27: Compression-tension members' Moment-2 influence lines

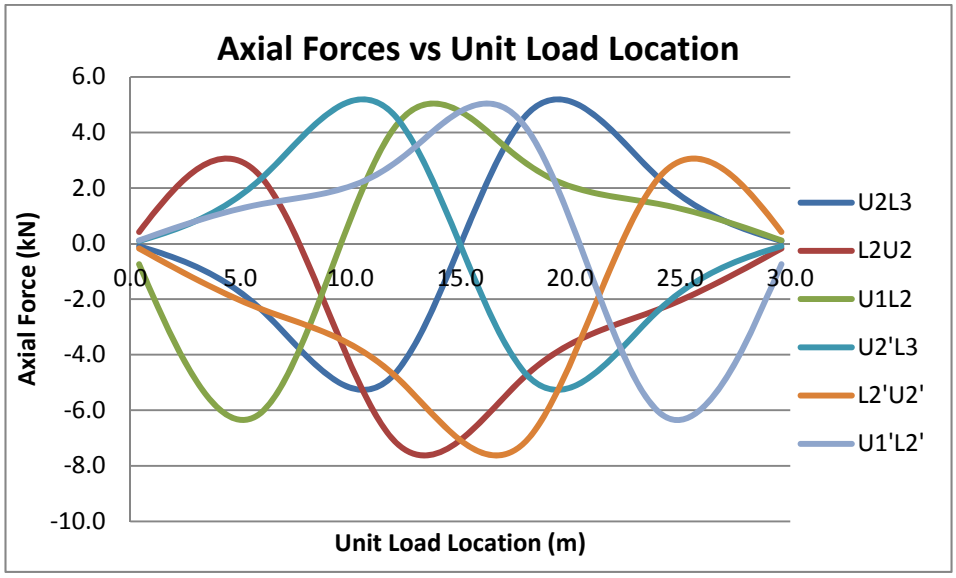

Figure 3.28: Compression-tension members' axial forces influence lines

3.4 Comparison of Measured Data vs. Simulated Data

Comparison of measured data vs. simulated data is done with collected data of good train cross, during second field study. Comparison measurements are axial strain measurements of critical members, and midpoint displacement measurements of monitored span of bridge. Train loading information is gathered from TCDD. Gathered loading information is applied to FEM of bridge span. Dead, wind, brake and acceleration forces are excluded from loading combinations in FEM analysis, for the purpose of comparison; centrifugal forces and dynamic factor are included. Results of measurements and FEM model simulation are given below.

Recorded maximum midpoint deflection value of span is 7.71 mm (Figure 3.42) and corresponding maximum midpoint deflected found from FEM analysis is 7.91 mm (Figure 3.43). Error is calculated as 2.53%. Possible reasons of error calculated are undetermined environmental conditions such as wind, assumed structural properties in FEM etc. It is agreed that, Error order is acceptable.

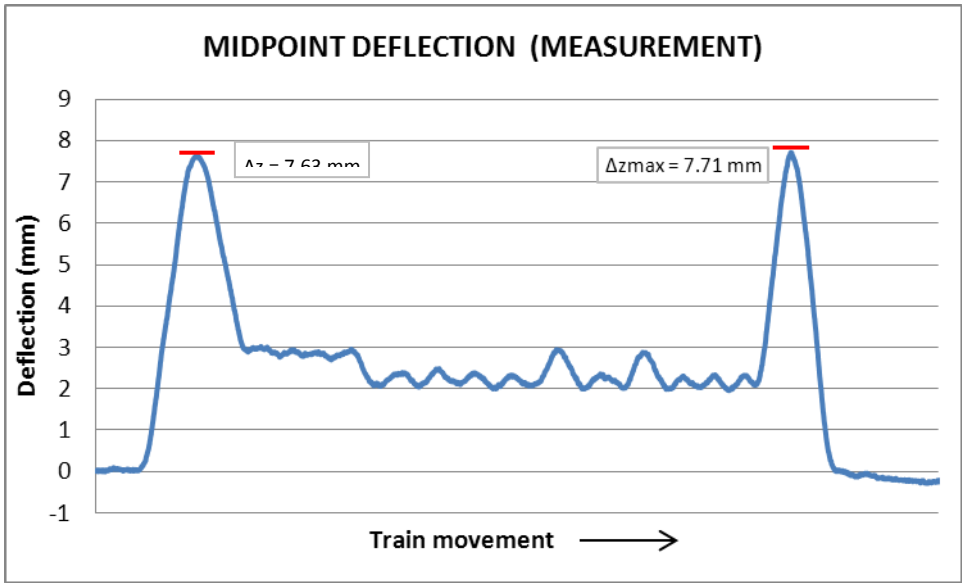

Figure 3.29: Measured midpoint deflection (Δzmax = 7.71 mm)

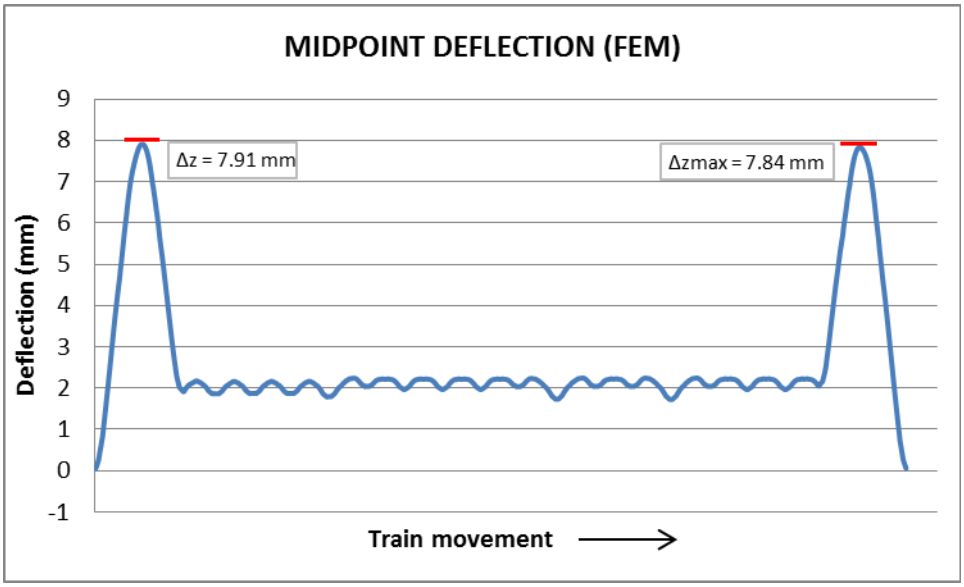

Figure 3.30: FEM analysis result midpoint deflection (Δzmax = 7.71 mm)

Absolute maximum recorded axial strain values of critical members U1U2 (Critical compression member), U1A2 (critical compression-tension member), A2A3 (Critical tension member) and absolute maximum axial strain values obtain from FEM analysis for corresponding members are tabulated (Table 3.6). Graphical representation of recorded data (Figure 3.44) and FEM analysis results (Figure 3.45) for train crossing is given below. Error is calculated as 45.95 % for compression member, 21.11% for compression-tension member, 1.80% for tension

member. Possible reasons of error calculated are undetermined environmental conditions such as wind, structural properties assumed in FEM etc. Error order is higher compared with deflection comparison due to more uncertainties existing in strain measurements, such as material properties are more effective in strain measurements. Whereas the maximum value comparison, from graphical representation behavior of strain in members, while train cross is observed adequate for representing span with FEM. As a result strain measurements are assumed in acceptable ranges.

Table 3.4: Measurements vs FEM analysis maximum strain results

	Measurement	FEM	Error
	με	με	%
U1U2 (comp)	58.28	107.82	45.95
U1A2 (comp-tens)	133.55	169.28	21.11
A2A3 (tens.)	158.89	161.8	1.80

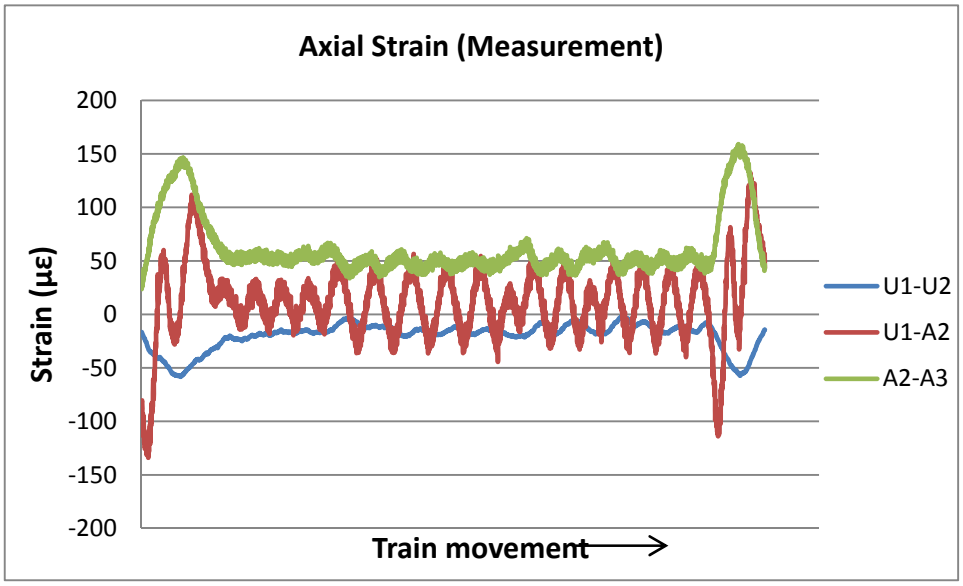

Figure 3.31: Measurement results axial strain values

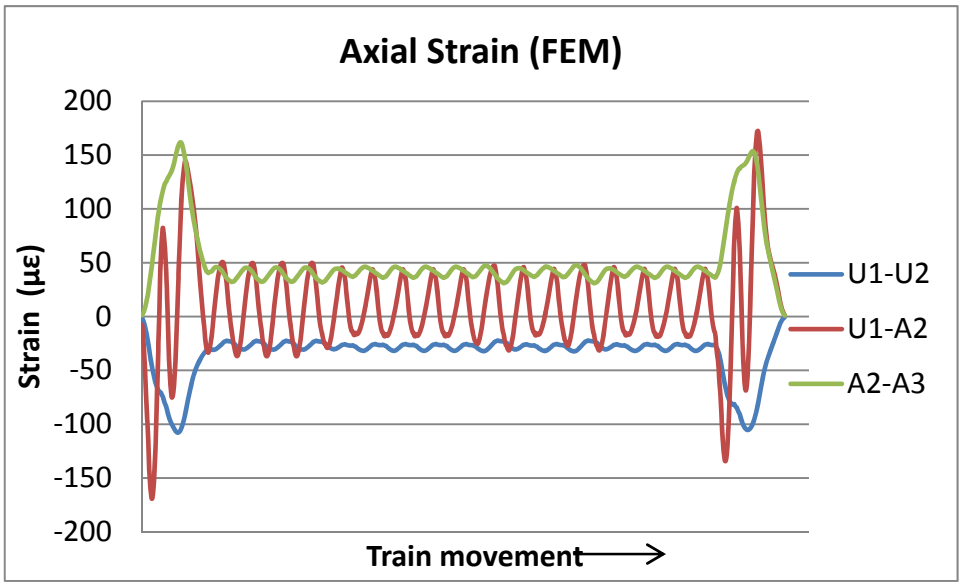

Figure 3.32: FEM analysis result axial strain values

CHAPTER 4

CAPACITY INDEX (CI) CALCULATIONS

4.1 Introduction

Upon the study scope, bridge existing structural state is studied. This study has two parts, the first one is capacity indices (CI) calculations and second one is reliability indices (β) calculations. CI calculations are included in chapter 4.

CI's are the ratio values that are reflecting the capacity state of members under design and service moving loading such as design, maximum possible service train loading and actual train loading, corresponding centrifugal forces, brake and acceleration forces, and wind loading (during train crossing the bridge and without train crossing the bridge).

CI calculations are done according to regulations stated in Eurocode (EC)-3 part: 2: Steel Bridges and EC-3 Part: 1-1: General rules and rules for buildings for members, EC-3 Part: 1-8: Design of joints for connections. In addition to members and connections capacity calculations, loading calculations are done according to EC-1 Part: 2: Actions on structures and EC-1 Part-1-4: Wind actions. Detailed information and calculations' results are given following subsections.

4.1.1 Design Regulations Stated in EC-3

Structural members that are exposed to both axial and rotational stresses are examined according to regulations stated in EC-3 part: 2 and EC-3 part: 1-1.

4.1.1.1 Truss members, Lateral Bracing Members, Floor Beams

Compression members buckling check (EC3 part: 2 eqn: 6.9)

$$\frac{N_{Ed}}{X_y \frac{f_y \cdot A_{eff}}{\gamma_{M1}}} + C_{mi,o} \cdot \left(\frac{M_{y,Ed} + N_{Ed} \cdot e_{Ny}}{\frac{f_y \cdot W_{eff,y}}{\gamma_{M1}}} \right) \leq 0,9 \qquad (4.1)$$

Where;

γ_{M1}=1.1

f_y =280 MPa (from laboratory test results)

Tension members yielding check (EC3 part: 1-1 eqn: 6.44)

$$\frac{N_{Ed}}{\frac{f_y \cdot A_{eff}}{\gamma_{M0}}} + \frac{M_{y,Ed} + N_{Ed} \cdot e_{Ny}}{\frac{f_y \cdot W_{eff,y}}{\gamma_{M0}}} \leq 1,0 \qquad (4.2)$$

Where;

γ_{M0} =1.0

f_y =280 MPa (from laboratory test results)

4.1.1.2 Vertical bracing members

Vertical bracing members are assumed to carry only axial tension force due to external loads. Self weights of braces are neglected. Vertical bracing members are analyzed according to regulation stated in EC-1 part-1.

Vertical bracing members yielding check (EC3 part: 1-1 eqn: 6.5)

$$\frac{N_{Ed}}{\frac{f_y \cdot A_{net}}{\gamma_{M0}}} \le 1,0 \qquad (4.3)$$

4.1.1.3 Connections

All connections of bridge structure are riveted. Design resistances of riveted joints are calculated according to EC-1 part: 8: Design of joints, table: 3.4 and section 3.10.2 and EC-1 part: 1: section 6.2.3.

Connections are analyzed and compared only with maximum axial load carried by connected members for simplicity. Moment actions are neglected.

Material and strength properties of connection materials are assumed to be equal to the members' material and strength properties (Fy=280 MPa, Fu= 364 MPa).

It is assumed that the connection is safe, only if it is not failed under axial load that transferred from connected members.

Shear resistance per rivet per plane (EC3 part: 1-8, table 3.4)

$$F_{V,Rd} = \frac{0,6 \cdot F_{ur} \cdot Ao}{\gamma_{M2}} \qquad (4.4)$$

Bearing resistance per rivet (EC3 part: 1-8, table 3.4)

$$F_{b,Rd} = \frac{k_1 \alpha_b F_u \cdot d_o \cdot t}{\gamma_{M2}} \qquad \alpha_b = \min\left(\alpha d, \frac{fur}{fu}, 1\right) \qquad (4.5)$$

Where;

Edge rivets:

$$\alpha_d = \frac{e_1}{3 \cdot d_o}$$

and

Inner rivets:

$$\alpha_d = \frac{p_1}{3 \cdot d_o} - \frac{1}{4}$$

$$k_1 = \min\left(2.8 \cdot \frac{e_2}{d_o} - 1.7, 2.5\right)$$

$$k_1 = \min\left(1.4 \cdot \frac{e_2}{d_o} - 1.7, 2.5\right)$$

Where;

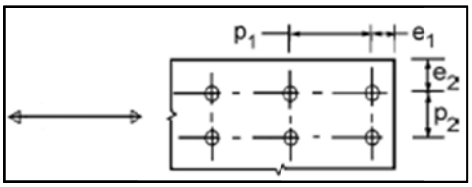

Yielding of gross section (EC3 part: 1-1 eqn: 6.6)

$$N_{pl,Rd} = \frac{A \cdot F_y}{\gamma_{M0}} \tag{4.6}$$

Fracture of net section (EC3 part: 1-1 eqn: 6.7)

$$N_{u,Rd} = \frac{0.9 \cdot A_{net} \cdot F_u}{\gamma_{M2}} \tag{4.7}$$

Block shear failure of gusset plate (EC3 part: 1-8 eqn: 3.9)

$$V_{eff,Rd} = \frac{F_u \cdot A_{nt}}{\gamma_{M2}} + \frac{1}{\sqrt{3}} \cdot \frac{Fy \cdot A_{nv}}{\gamma_{M0}}$$

$$A_{nv} = A_v - (n - 0.5) \cdot d_o \cdot t$$

$$A_{nt} = A_t - (n - 1) \cdot d_o \cdot t \tag{4.6}$$

4.1.2 Loads Stated in EC-1 Part: 2 and EC-1 part: 1-4

4.1.2.1 Train Moving Load (Q)

Three different train loads are determined for analyses LM71 train moving load defined in EC-1 Part: 2, ultimate service goods train which the train have locomotive and wagons which are heaviest locomotives and wagons used in Turkey, and last train load is actual goods train load crossing the bridge that data collection is done while this train cross in second field study.

During train load calculations application coefficient 1.4 defined in section 3.1.3 is not used in CI and RI calculations.

There is horizontal superelevatıon exists between railroad tracks, due to curved layout of bridge. Unequal force distributions between railroad tracks exist due to this superelevation. This unequal force distribution is included by distribution coefficients for inner railroad track and outer railroad track with respect to layout of the railroad. For inner (left) railroad track distribution coefficient value is 0.57584 and for outer (right) railroad track this coefficient value is 0.42416. In addition to distribution factors, impact factor, according to EC-1 part-2, calculated as 1.14.

Total load distribution factors calculated as;

Inner (left) Railroad Tracks	= 1.14*0.57584	= 0.6565
Outer (Right) Railroad Tracks	= 1.14*0.42416	= 0.4835

Applied moving loads are multiplied with the above coefficients during member force calculations, on the contrary with the 2D FEM connection condition determination.

4.1.2.1.1 LM71 (Design Train) Train Moving Load (EC-1 Part: 2)

LM71 type train moving load is explained in section 3.1.3, identical loads is used for CI calculations with distribution factors explained above.

4.1.2.1.2 Ultimate Service Goods Train Load

Maximum service goods train loading simulation is achieved by choosing shortest and heaviest wagons and locomotives, according to "TCDD goods wagons" catalog. Designed ultimate service goods train load is composed of three loaded fal-wu type wagons and two DE33000 type locomotives. Locomotives' and wagons' axle distance are given in Figure 4.1 and Figure 4.2 respectively. Ultimate service goods train load used both CI and β calculation with the multiplication factors explained above.

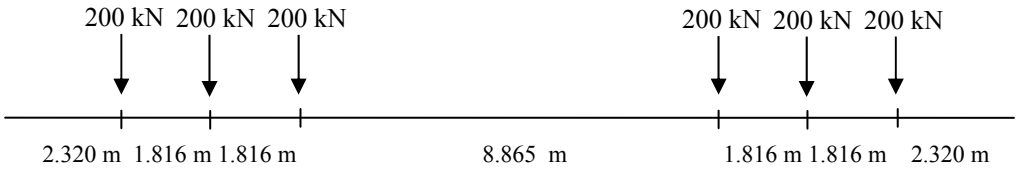

Figure 4.1: DE33000 type locomotive axle load and distances

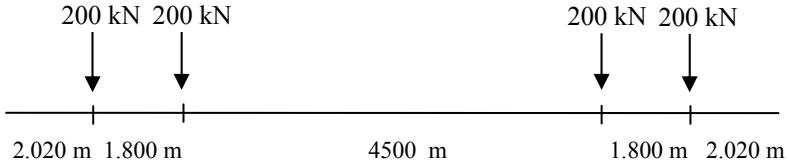

Figure 4.2: Loaded Fal-wu type wagon axle load and distances

4.1.2.1.3 Actual Goods Train Load Crossing the Bridge

Actual goods train is the train that data's collected from SHM system in second field study during train crossing the bridge. Actual train axle load and distances information is gathered from TCDD recorded loading data. This train is 339 m long and nearly 710 tones with 2 locomotives and 18 wagons. Actual goods train load crossing the bridge used both CI and β calculation with the distribution factors explained above

4.1.2.2 Centrifugal forces (EC-1 Part: 2) (Q_c)

Centrifugal forces are calculated for the maximum allowed velocity 20 km/h. Furthermore, these forces are multiplied by the same distribution coefficients with train moving load.

- Centrifugal force $= \frac{Q*V^2}{g*R} = 0.11\ Q$ (4.7)

Where;

V = allowable train velocity = 20 m/s

g = gravitational acceleration = 9.81 m/s^2

R = horizontal curve radius = 300 m

4.1.2.3 Wind Forces (EC-1 Part: 1-4) (W)

Characteristic wind speed, during train crossing through bridge structure is assumed as 25 m/s (90 km/hr), and is assumed without train crossing the bridge as 44.44 m/s (160 km/hr).

Wind forces are applied upper chord and lateral braces for both train crossing the bridge situation and without train situation.

$$F_w = P_w \cdot A_{ref} \tag{4.8}$$

$$P_w = \frac{1}{2} \cdot \rho \cdot \left(V_b\right)^2 \cdot C \tag{4.9}$$

$$V_b = C_{dir} \cdot C_{season} \cdot V_{b,0} \tag{4.10}$$

Where,

p = 1.25 kg/m^2

C = 3.6

C_{dir} = 1

C_{season} = 1

4.1.2.4 Break and Acceleration Forces (EC-1 Part: 2)

Acceleration force (A) : *Q*lak = 33 [kN/m] *L*a,b [m] _ 1000 [kN]

Break force (B) : *Q*lbk = 20 [kN/m] *L*a,b [m] _ 6000 [kN]

4.1.3 Load Combinations

Defined loads in section 4.1.2 combined to determine actual state of bridge. Impact factor is applied just train moving load and centrifugal load. First four of combinations are train moving load combinations and last two of them is wind only combination which are without train cross.

CombI) $Q + Q_c + W_{+y} + B + Self$

CombII) $Q + Q_c + W_{+y} + A + Self$

CombIII) $Q + Q_c + W_{-y} + B + Self$

CombIV) $Q + Q_c + W_{-y} + A + Self$

Moving load combinations

CombV) $W_{+y} + Self$

CombVI) $W_{-y} + Self$

Wind only combinations

4.2 LM71 (Design Train Moving Load) CI Results

According to regulation and assumptions CI analysis are completed for LM71 (Design Train Moving Load). CI Results of critical moving load combination are tabulated with maximum and minimum values. Tabulated CI values are given for truss members (Figure 4.3), lateral braces, floor beams (Figure 4.4), and vertical braces. Graphs of whole train cross are given for truss members. CI results of connections and wind load only combinations are also tabulated. In addition, the CI results of members for other combinations are given Appendix B as table of maximum and minimum values and graphs of whole cross of train.

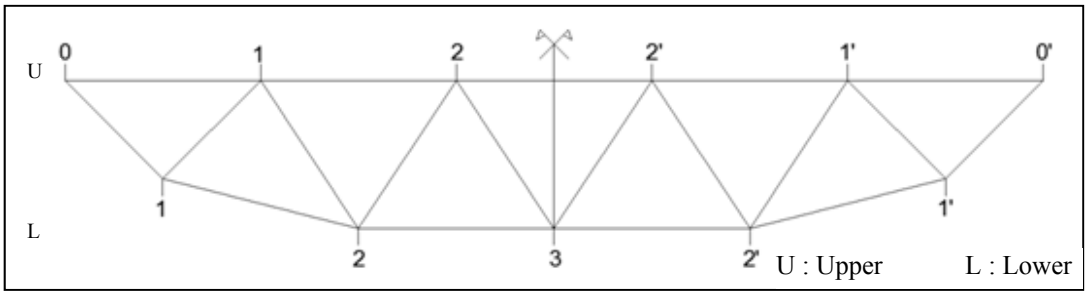

Figure 4.3: Representative view of truss members

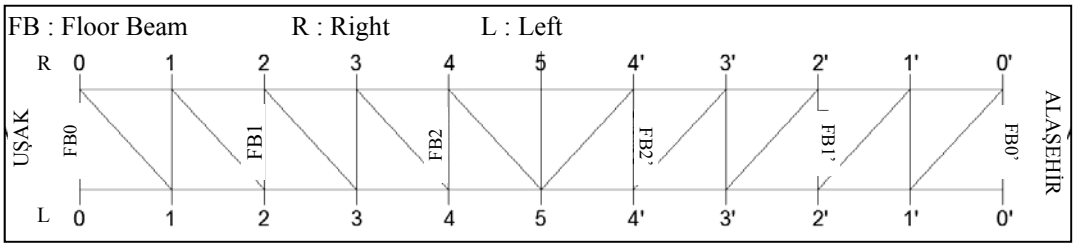

Figure 4.4: Representative view of lateral braces and floor beams members

Upon analysis for LM71 train loading, critical combination for truss members is CombIV **(**$Q + Q_c + W_{-y} + A +$ Self**)**. For CombIV combination obtained maximum CI value is 0.402 from L2L3 tension member and minimum CI value is -0.477 from U1U2 compression member (Table 4.1).

Table 4.1: CombIV CI Results for Truss Members

	Member	**Max**	**Min**		**Member**	**Max**	**Min**
RIGHT TRUSS	U0-U1	-0.048	-0.344	**LEFT TRUSS**	U0-U1	-0.128	-0.309
	U1-U2	-0.080	-0.477		U1-U2	-0.074	-0.334
	U0-L1	0.331	0.026		U0-L1	0.246	0.026
	L1-L2	0.382	0.029		L1-L2	0.284	0.028
	L1-U1	-0.037	-0.459		L1-U1	-0.036	-0.347
	U1-L2	0.228	-0.234		U1-L2	0.178	-0.168
	L2-U2	0.033	-0.407		L2-U2	0.023	-0.303
	U2-L3	0.162	-0.241		U2-L3	0.122	-0.176
	L2-L3	0.402	0.028		L2-L3	0.301	0.028
	U2-U2'	-0.067	-0.404		U2-U2'	-0.028	-0.275
	System	**0.402**	**-0.477**		**System**	**0.301**	**-0.347**

Upon analysis for LM71 train loading, critical combination for truss members is CombIV **(**$Q + Q_c + W_{-y} + A +$ Self**)** for this combination obtained CI results are presented in graphical form for whole train cross for right truss (Figure 4.5) and left truss (Figure 4.6).

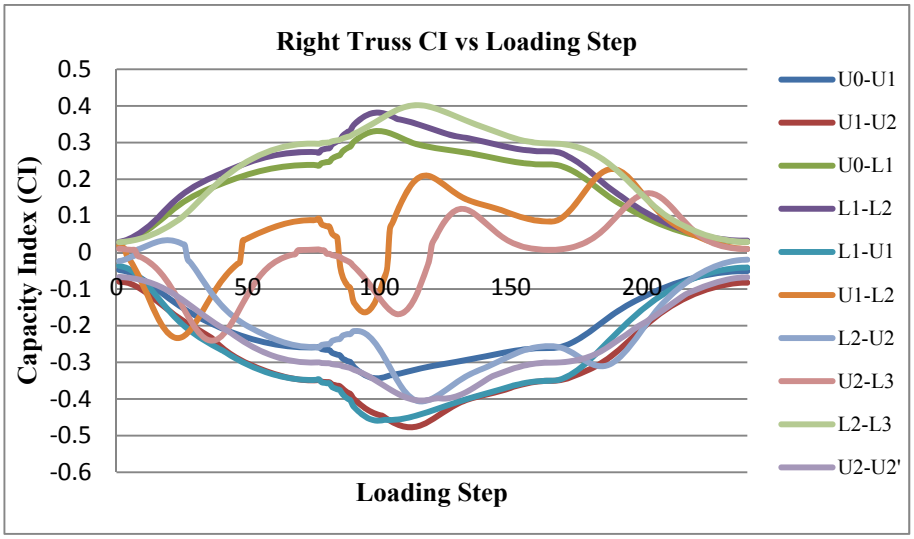

Figure 4.5: CombIV Right Truss CI vs Loading Step (max=0.402, min=-0.477)

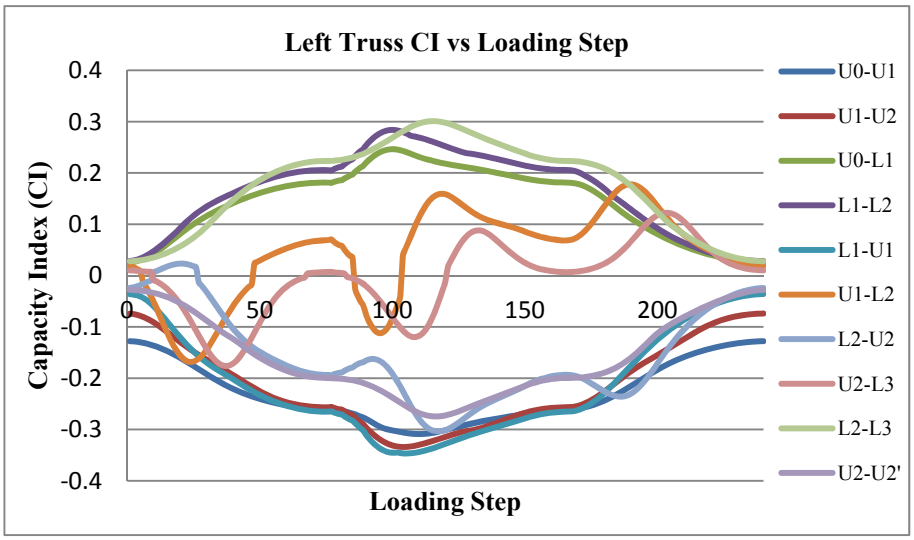

Figure 4.6: CombIV Left Truss CI vs. Loading Step (max=0.301, min=-0.347)

Upon analysis for LM71 train loading, critical combination for floor beams and lateral brace members is CombIV (Q + Q_c + W_{-y} + A + Self); for this combination, obtained maximum CI value is 0.318 from R0L1 and R1L2 and minimum CI value is -0.248 from R1L1 (Table 4.2).

Table 4.2: CombIV CI Results for Floor Beams and Lateral Braces

Member	Max	Min
FB0	0.048	0.044
R0L1	0.138	0.129
R1L 1	-0.225	-0.248
R1L2	0.138	0.129
FB1	-0.022	-0.024
R2L 3	0.097	0.090
R3L3	-0.083	-0.092
R3L 4	0.088	0.081
FB2	-0.014	-0.015
R4L 5	0.060	0.057
R5L 5	-0.026	-0.026
System	**0.138**	**-0.248**

Upon analysis for LM71 train loading, critical combination for vertical members is CombIV **(**$Q + Q_c + W_{-y} + A + Self$); for this combination, obtained maximum CI value is 0.082 fromL2U2 (Table 4.3).

Table 4.3: CombIV CI Results for Vertical Braces

Member	Max	Min
L1-U1	0.024	0.021
U1-L2	0.076	0.069
L2-U2	0.082	0.074
U2-L3	0.009	0.008
System	**0.082**	**0.008**

Upon analysis for LM71 train loading for all combinations, maximum CI value for truss members' connection is 0.613 from U2U2' (Table 4.4).

Table 4.4: CI Results for Connections

Member	Maximum Axial Member Force (kN)	Connection Capacity (kN)	Capacity Index (CI)
U0-U1	1066.01	2825.06	0.377
U1-U2	1672.69	2897.65	0.577
U0-L1	1373.83	2796.36	0.491
L1-L2	1595.67	3081.66	0.518
L1-U1	817.10	2032.57	0.402
U1-L2	257.65	893.17	0.288
L2-U2	611.96	2032.57	0.301
U2-L3	210.55	1027.35	0.205
L2-L3	1890.74	3152.98	0.600
U2-U2'	1995.25	3254.27	0.613
		System	**0.613**

Upon analysis wind only combinations', CombV **(**W_{+y} + Self) and CombVI **(**W_{-y} + Self), results are maximum 0.125 for right truss member U1U2 and minimum -1.191 for right truss member U0U1 for CombV; minimum -1.192 for left truss member U0U1 for CombVI (Table 4.5).

Table 4.5: CombV and VI CI Results for Truss Members

	Member	V)+Y wind	VI)-Y wind
RIGHT	U0-U1	-0.191	-0.153
	U1-U2	0.125	-0.175
	U2-U2'	0.060	-0.180
LEFT	U0-U1	-0.151	-0.192
	U1-U2	-0.171	-0.095
	U2-U2'	-0.160	-0.076
	System max	**0.125**	**-0.076**
	System min	**-0.191**	**-0.192**

Upon analysis wind only combinations', CombV **(**W_{+y} + Self) and CombVI **(**W_{-y} + Self), results for floor beams and lateral brace members are maximum 0.080 from member R1L1 and minimum -0.344 member R0L1 for CombV; maximum 0.159 from member R0L1 and minimum -0.248 member R1L1 for CombVI (Table 4.6).

Table 4.6: CombV and VI CI Results for Floor Beams and Lateral Braces

Member	**v)+Y wind**	**vi)-Y wind**
FB0	0.035	0.032
R0L1	-0.344	0.159
R1L 1	0.080	-0.248
R1L2	-0.255	0.127
FB1	0.027	-0.028
R2L 3	-0.277	0.113
R3L3	0.033	-0.080
R3L 4	-0.133	0.070
FB2	0.014	-0.015
R4L 5	-0.165	0.082
R5L 5	0.018	-0.048
System max	**0.080**	**0.159**
System min	**-0.344**	**-0.248**

4.3 Ultimate Service Goods Train Load CI Results

According to regulation and assumptions CI analysis are completed for ultimate service moving load. CI Results of critical moving load combination are tabulated with maximum and minimum values. Tabulated CI values are given for truss members (Figure 4.3), lateral braces, floor beams (Figure 4.4), and vertical braces. Graphs of whole train cross are given for truss members. CI results of connections and wind load only combinations are also tabulated. In addition, the CI results of members for other combinations are given Appendix B as table of maximum and minimum values and graphs of whole cross of train.

Upon analysis for ultimate service goods train loading, critical combination for truss members is CombIV (Q + Q_c + W_{-y} + A + Self). For CombIV combination, obtained maximum CI value is 0.243 from L2L3 tension member and minimum CI value is -0.296 from L1U1 tension-compression member (Table 4.7).

Table 4.7: CombIV CI Results for Truss Members

	Member	Max	Min		Member	Max	Min
RIGHTTRUSS	U0-U1	-0.048	-0.226	**LEFTTRUSS**	U0-U1	-0.128	-0.237
	U1-U2	-0.080	-0.292		U1-U2	-0.074	-0.227
	U0-L1	0.206	0.026		U0-L1	0.158	0.026
	L1-L2	0.238	0.028		L1-L2	0.179	0.028
	L1-U1	-0.036	-0.296		L1-U1	-0.036	-0.227
	U1-L2	0.195	-0.249		U1-L2	0.149	-0.180
	L2-U2	0.042	-0.271		L2-U2	0.029	-0.204
	U2-L3	0.142	-0.207		U2-L3	0.108	-0.151
	L2-L3	0.243	0.028		L2-L3	0.184	0.028
	U2-U2'	-0.067	-0.248		U2-U2'	-0.028	-0.161
	System	**0.243**	**-0.296**		**System**	**0.184**	**-0.237**

Upon analysis for ultimate service goods train loading, critical combination for members is CombIV (Q + Q_c + W_{-y} + A + Self). For CombIV combination obtained CI results are presented in graphical form for whole train cross for right truss (Figure 4.7) and left truss (Figure 4.8).

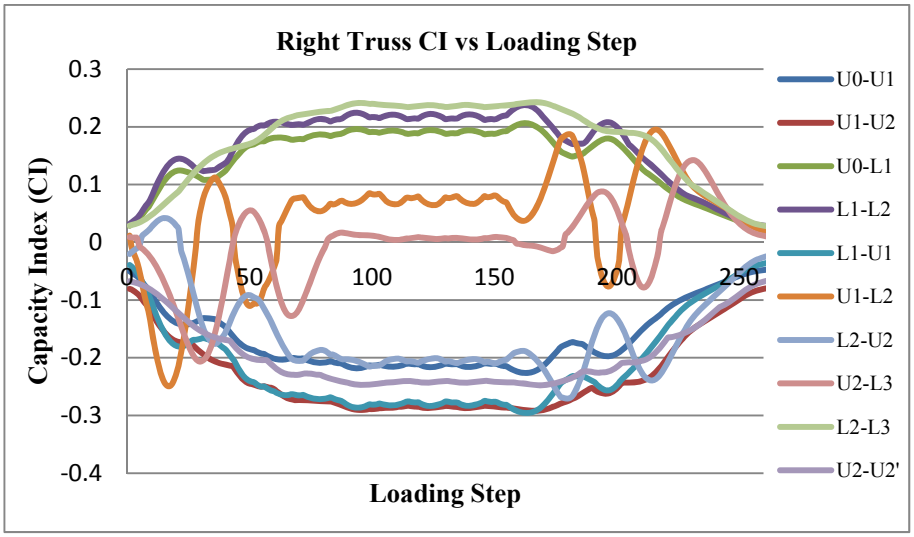

Figure 4.7: CombIV Right Truss CI vs. Loading Step (max=0.243, min=-0.296)

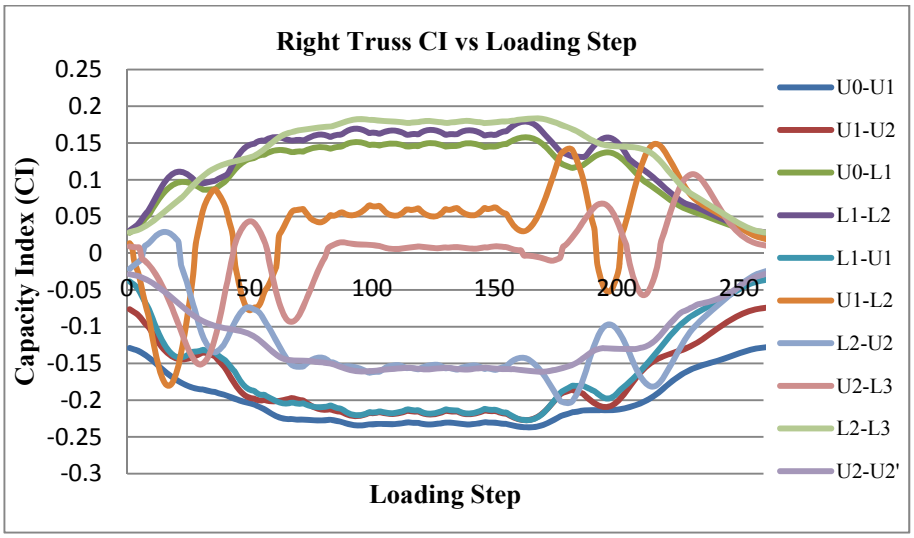

Figure 4.8: CombIV Right Truss CI vs. Loading Step (max=0.184, min=-0.237)

Upon analysis for ultimate service goods train loading, critical combination for floor beams and lateral brace members is CombIV (Q + Q_c + W_{-y} + A + Self). For CombIV combination obtained maximum CI value is 0.135 fromR0L1 and R1L2 and minimum CI value is -0.239 from R1L1 (Table 4.8).

Table 4.8: CombIV CI Results for Floor Beams and Lateral Braces

Member	Max	Min
FB0	0.047	0.044
R0-L1	0.135	0.129
R1-L 1	-0.225	-0.239
R1-L2	0.135	0.129
FB1	-0.022	-0.023
R2-L 3	0.094	0.090
R3-L3	-0.083	-0.088
R3-L 4	0.085	0.081
FB2	-0.014	-0.014
R4-L 5	0.059	0.057
R5-L 5	-0.026	-0.026
System	**0.135**	**-0.239**

Upon analysis for ultimate service goods train loading, critical combination for vertical members is CombIV **(**$Q + Q_c + W_{-y} + A +$ Self). For CombIV combination obtained maximum CI value is 0.116 from L2U2 (Table 4.9).

Table 4.9: CombIV CI Results for Vertical Braces

Member	Max	Min
L1-U1	0.033	0.030
U1-L2	0.108	0.101
L2-U2	0.116	0.109
U2-L3	0.012	0.012
System	**0.116**	**0.012**

Upon analysis for ultimate service goods train loading for all combinations, maximum CI value for truss members' connection is 0.397 from U2U2' (Table 4.10).

Table 4.10:CI Results for Connections

Member	Maximum Axial Member Force (kN)	Connection Capacity (kN)	Capacity Index (CI)
U0-U1	714.600	2825.062	0.253
U1-U2	1096.636	2897.651	0.378
U0-L1	876.725	2796.364	0.314
L1-L2	1015.778	3081.656	0.330
L1-U1	516.894	2032.573	0.254
U1-L2	225.525	893.169	0.252
L2-U2	409.235	2032.573	0.201
U2-L3	186.177	1027.354	0.181
L2-L3	1157.217	3152.979	0.367
U2-U2'	1291.399	3254.266	0.397
		System	**0.397**

4.4 Actual Train Crossing the Bridge CI Results

According to regulation and assumptions CI analysis are completed for actual train crossing the bridge. CI Results of critical moving load combination are tabulated with maximum and minimum values. Tabulated CI values are given for truss members (Figure 4.3), lateral braces, floor beams (Figure 4.4), and vertical braces. Graphs of whole train cross are given for truss members. CI results of connections and wind load only combinations are also tabulated. In addition, the CI results of members for other combinations are given Appendix B as table of maximum and minimum values and graphs of whole cross of train.

Upon analysis for actual train loading, critical combination for truss members is CombIV **(**$Q + Q_c + W_{-y} + A + Self$). For CombIV combination obtained maximum CI value is 0.200 from L2L3 tension member and minimum CI value is -0.251 from U1U2 compression member.

Table 4.11: CombIV CI Results for Truss Members

	Member	Max	Min		Member	Max	Min
RIGHTTRUSS	U0-U1	-0.055	-0.185	**LEFTTRUSS**	U0-U1	0.068	-0.112
	U1-U2	-0.034	-0.208		U1-U2	-0.079	-0.202
	U0-L1	0.172	0.026		U0-L1	0.132	0.026
	L1-L2	0.200	0.029		L1-L2	0.151	0.029
	L1-U1	-0.037	-0.246		L1-U1	-0.037	-0.190
	U1-L2	0.196	-0.242		U1-L2	0.149	-0.175
	L2-U2	0.040	-0.241		L2-U2	0.028	-0.182
	U2-L3	0.143	-0.203		U2-L3	0.108	-0.149
	L2-L3	0.197	0.029		L2-L3	0.150	0.028
	U2-U2'	-0.017	-0.161		U2-U2'	-0.066	-0.171
	System	**0.200**	**-0.246**		**System**	**0.151**	**-0.202**

Upon analysis for actual train loading, critical combination for members is CombIV (Q + Q_c + W_{-y} + A + Self). For CombIV combination obtained CI results are presented in graphical form for whole train cross for right truss (Figure 4.9) and left truss (Figure 4.10).

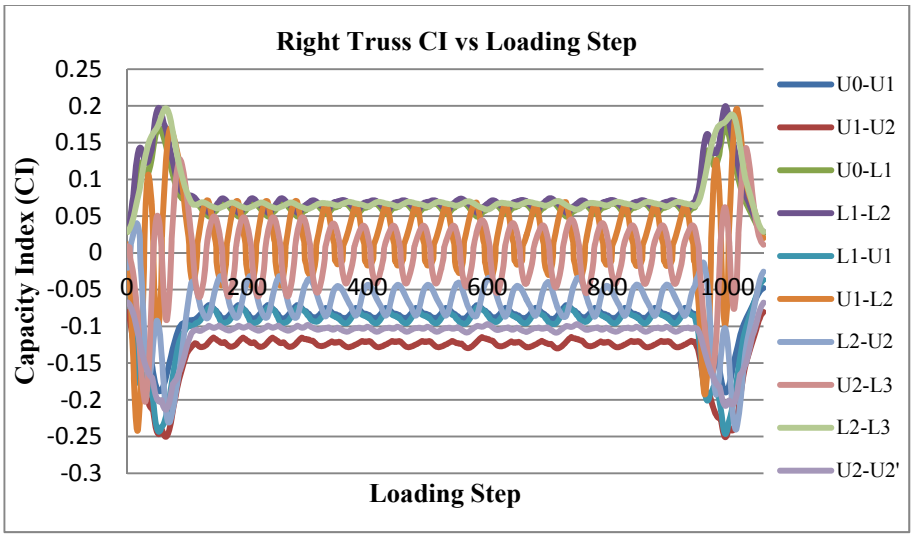

Figure 4.9: CombIV Right Truss CI vs. Loading Step (max=0.200, min=-0.246)

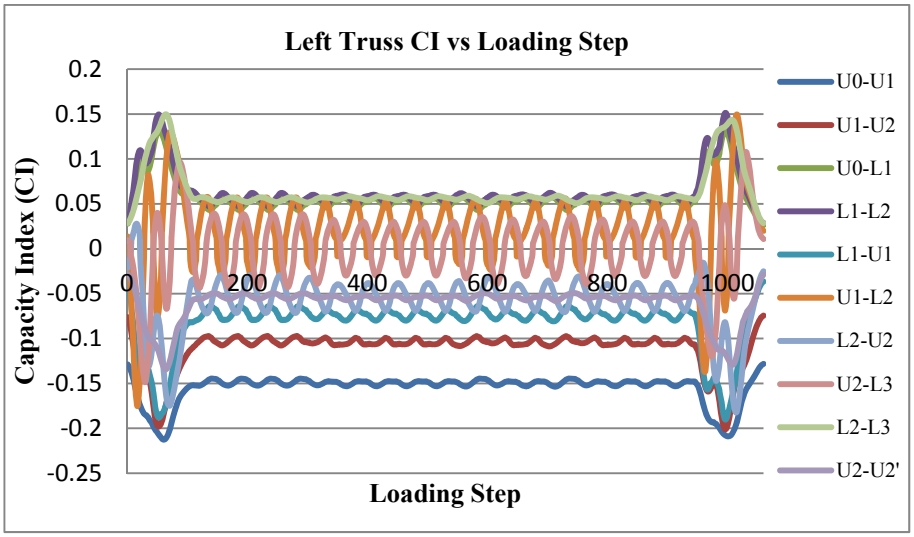

Figure 4.10: CombIV Right Truss CI vs. Loading Step (max=0.151, min=-0.202)

Upon analysis for actual train loading, critical combination for floor beams and lateral brace members is CombIV (Q + Q_c + W_{-y} + A + Self). For ComIV combination obtained maximum CI value is 0.130 from R0L1and minimum CI value is -0.203 from R1L1 (Table 4.12).

Table 4.12: CombIV CI Results for Floor Beams and Lateral Braces

Member	Max	Min
FB0	0.030	0.028
R0-L1	0.130	0.125
R1-L 1	-0.192	-0.203
R1-L2	0.119	0.115
FB1	-0.024	-0.025
R2-L 3	0.090	0.086
R3-L3	-0.073	-0.077
R3-L 4	0.075	0.072
FB2	-0.015	-0.016
R4-L 5	0.062	0.060
R5-L 5	-0.025	-0.025
System	**0.130**	**-0.203**

Upon analysis for actual train loading, critical combination for vertical members is CombIV **(**$Q + Q_c + W_{-y} + A +$ Self). For ComIV combination obtained maximum CI value is 0.115 from L2U2 (Table 4.13).

Table 4.13: CombIV CI Results for Vertical Braces

Member	**Max**	**Min**
L1-U1	0.033	0.030
U1-L2	0.106	0.101
L2-U2	0.115	0.109
U2-L3	0.012	0.012
System	**0.115**	**0.012**

Upon analysis for actual train loading, for all combinations, maximum CI value for truss members' connection is 0.321 from U2U2' (Table 4.14).

Table 4.14:CI Results for Connections

Member	**Maximum Axial Member Force (kN)**	**Connection Capacity (kN)**	**Capacity Index (CI)**
U0-U1	601.522	2825.062	0.213
U1-U2	889.798	2897.651	0.307
U0-L1	717.725	2796.364	0.257
L1-L2	830.267	3081.656	0.269
L1-U1	422.565	2032.573	0.208
U1-L2	226.340	893.169	0.253
L2-U2	367.019	2032.573	0.181
U2-L3	186.521	1027.354	0.182
L2-L3	949.547	3152.979	0.301
U2-U2'	1045.651	3254.266	0.321
		System	**0.321**

4.5 Summary of CI Results

Upon analysis three different train loading used for capacity analyses. In table 4.15 summary of results of capacity index analyses presented. Analyses have resulted that critical loading is LM 71 loading. Analyses of LM71 loading has resulted maximum CI as 0.61 and minimum CI as -0.48 therefore system CIs are 0.61 for tension and -0.48 for compression.

Table 4.15:Summary CI Results

	LM 71		Service Goods Train		Actual Train	
	Max	Min	Max	Min	Max	Min
Truss Members	0.40	-0.48	0.24	-0.30	0.20	-0.25
Truss Connections	0.61	0.21	0.40	0.18	0.32	0.18
Lateral Braces and Floor Beams	0.14	-0.25	0.14	-0.24	0.13	-0.20
Vertical Braces	0.08	0.01	0.12	0.01	0.12	0.01
System	0.61	-0.48	0.40	-0.30	0.32	-0.25

CHAPTER 5

RELIABILITY INDEX (β) CALCULATIONS

5.1 Philosophy of RI

Upon the study scope bridge existing structural state is studied. This study has two parts, the first capacity indices calculations introduced in chapter 4 and the second reliability indices calculations. Reliability index (β) calculations are included in chapter 5.

β's are the ratio values that indicate existing condition of structure in statistical approach, in comparison with the CIs, that are the ratios evaluate design condition of structure. Several uncertainties such as; strength of structure, moving load conditions etc. are taken in to account with the statistical parameters in β calculations. Upon study it is assumed that strength condition (R), loading condition (Q) are the variants that are normally distributed with standard deviations σ_R and σ_Q and, coefficient of variations V_R and V_Q, respectively.

Strength condition (R) determination is done according to Eurocode regulations stated in chapter 4. Strength condition (R) is 0.9 for compression members and 1.0 for tension members which are the right hand side of equations (4.1), (4.2) and (4.3). For connection, it is assumed that the R value of each connection is equal to the maximum axial force of connected member, created by loading. Therefore failure of structure is restricted by the failure of member.

Loading condition (Q) determination is done according to Eurocode regulations stated in chapter 4. Loading conditions (Q) are simply CI value of each members and connections for several moving load conditions and loading steps.

Due to lack of R and Q statistical measurements, coefficient of variation values are obtained from earlier study supported by NATO "Rehabilitation of Old Railway Bridges" conducted by Uzgider et al. in 1996. According to measurements, are done in study stated, coefficient of variation values are for strength condition V_R equal to 0.16 (V.AKAR, E.UZGİDER, 2006), and for loading condition V_Q equal 0.1256 (V.AKAR, E.UZGİDER, 2006).

Combination of strength condition and loading condition with statistical parameters done by the equation (5.1) stated below. β calculations are done for 60% LM71 loading, ultimate service goods train and actual goods train crossing the bridge moving load conditions and loading steps. Structural system of bridge is statically determined system, losing function of one member refers to failure of structure. Due to statically determined condition of bridge, it is assumed that the minimum β value obtained for member and connection is the system β value

.

$$\beta = \frac{(R - Q)}{\sqrt{(\sigma_R)^2 + (\sigma_Q)^2}} \qquad (5.1)$$

$$\sigma_R = \bar{V}_R \cdot R$$
$$\sigma_Q = V_Q \cdot Q \qquad (5.2)$$

Where;

β = Reliability Index

R = Strength Condition = (if compression 0.9, if tension 1.0)

Q = Loading Condition

V_R = Strength Coefficient of Variation =0.16

V_Q = Loading Coefficient of Variation =0.1256

σ_R = Strength Standard Deviation

σ_Q = Loading Standard Deviation

5.2 60% LM71 β Results

According to regulation and assumptions β analysis are completed for 60 % LM71. 60% LM71 load is better representation of real loading condition of bridge than LM71 type load that is used for design check. The 60% LM71 load determination is done by observations and calculations explained below.

During studies conducted, it is observed that maximum loading of span is created by locomotives of trains. Types of locomotives used on subjected railroad route are DE 22000, DE 24000 and DE 33000. DE 33000 type locomotive is the maximum axle load one upon others with 200 kN axle load. Length of DE 33000 is 20.74 m.

For the purpose of increasing load carrying capacity, two locomotives are used back to back before wagons are connected in studied bridge included railroad route. Two locomotives back to back bridge crossing is created maximum span loading. For span length with 30 meter one and half locomotives can be crossed simultaneously from bridge. One and half locomotives crossing bridge have totally 9 axles with 200 kN each which corresponds 60 % of LM 71 design train load for 30 meter span length. Calculation of explained loading is shown with the equations and figures below.

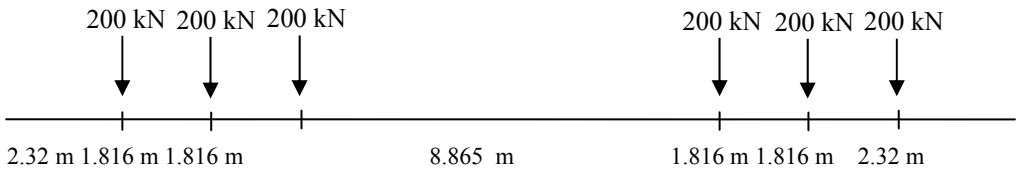

Figure 5.1: DE 33000 Locomotive axle load and distances

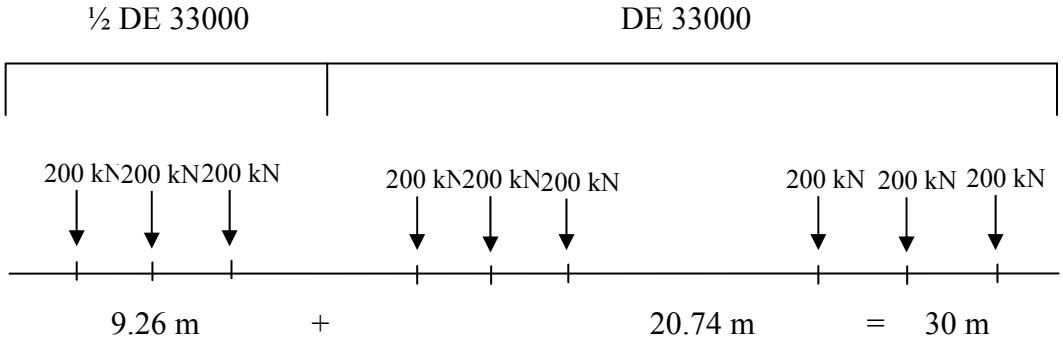

Figure 5.2:1+½ DE 33000 Locomotive axle load and distances

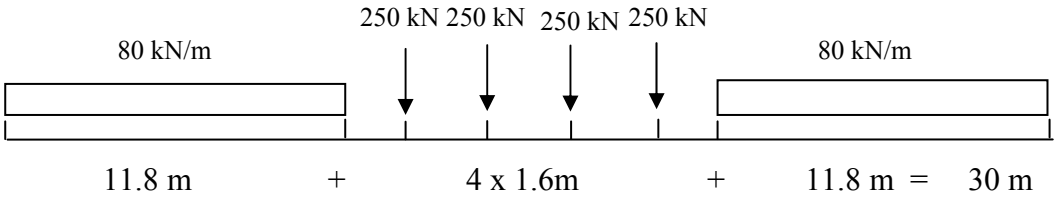

Figure 5.3:LM71 loading for corresponding 30 m span length

Σ load by 1 + ½ DE 33000 Locomotive = 200 kN x 9

= 1800 kN

Σ load by 30 m LM71 loading = 80 kN/m x 11.8 m x 2 + 4 x 250 kN

= 2888 kN

$$\frac{\textbf{Σ load by (1 + ½)DE 33000 Locomotive}}{\textbf{Σ load by 30 m LM71 loading}} = \frac{\textbf{1800 kN}}{\textbf{2888 kN}} \textbf{ x 100} \cong \textbf{60 \%}$$

β results of critical combination for truss members, lateral braces, and vertical braces are tabulated with maximum and minimum values and graph of whole train cross are given for truss members. β results of connections are also tabulated. In addition, the remaining β results of members for other combinations are given Appendix B, as table of maximum and minimum values for members and graphs of whole train cross for truss members.

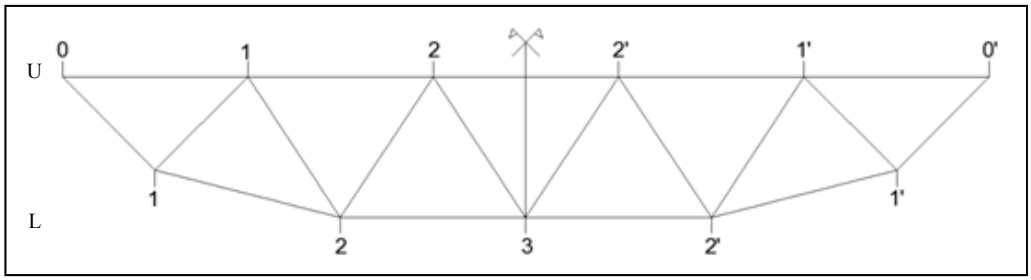

U : Upper L : Lower

Figure 5.4**:** Representative view of truss members

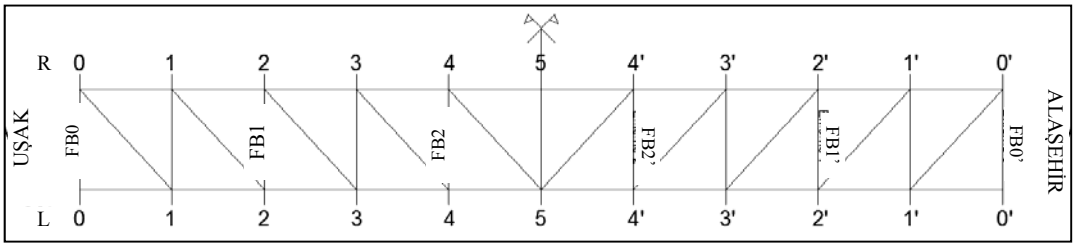

FB : Floor Beam R : Right L : Left

Figure 5.5**:** Representative view of lateral braces and floor beams members

Upon analysis for 60% LM71 train loading critical combination for truss members is CombIV **(**$Q + Q_c + W_{-y} + A + Self$). For CombIV combination obtained system β value is 3.980 from right truss U1U2 compression member.

Table 5.1: CombIV β Results for Truss Members

	Member	**Max**	**Min**		**Member**	**Max**	**Min**
RIGHT TRUSS	U0-U1	5.685	4.383	**LEFT TRUSS**	U0-U1	5.329	4.515
	U1-U2	5.617	3.980		U1-U2	5.724	4.650
	U0-L1	6.085	4.912		U0-L1	6.087	5.247
	L1-L2	6.070	4.699		L1-L2	6.072	5.097
	L1-U1	5.995	4.115		L1-U1	5.997	4.618
	U1-L2	6.202	5.278		U1-L2	6.197	5.513
	L2-U2	6.207	4.420		L2-U2	6.207	4.885
	U2-L3	6.227	5.214		U2-L3	6.224	5.500
	L2-L3	6.074	4.610		L2-L3	6.075	5.022
	U2-U2'	5.778	4.370		U2-U2'	6.036	5.021
	System	6.227	**3.980**		**System**	6.224	**4.515**

Upon analysis for 60% LM71 train loading, critical combination for truss members is CombIV **(**$Q + Q_c + W_{-y} + A + Self$). For CombIV combination obtained β results

are presented in graphical form for whole train cross for right truss (Figure 5.6) and left truss (Figure 5.7).

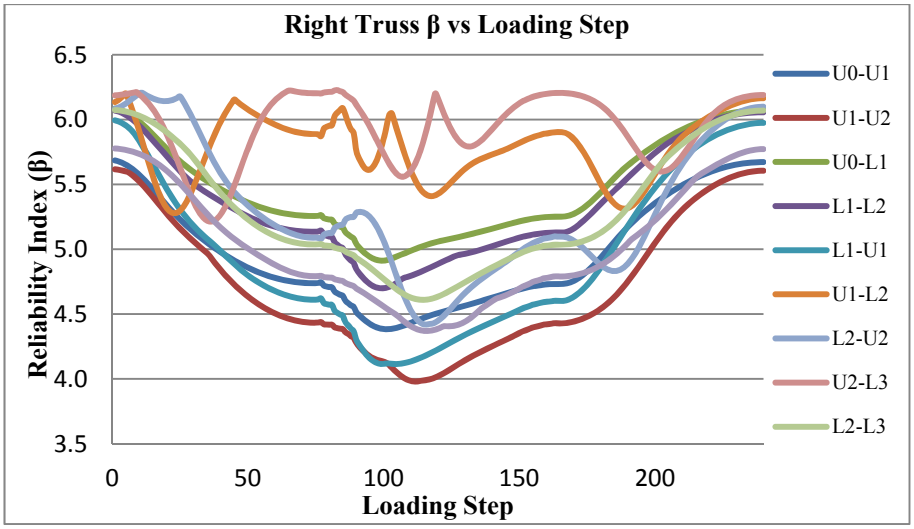

Figure 5.6: CombIV Right Truss β vs. Loading Step (min=3.980)

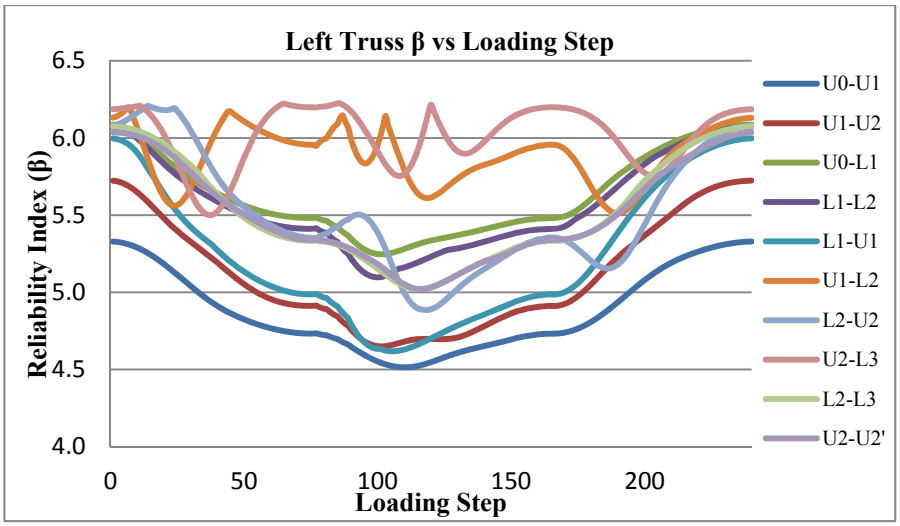

Figure 5.7: CombIV Left Trussβ vs. Loading Step (min=4.515)

Upon analysis for 60% LM71 train loading, critical combination for floor beams and lateral brace members is CombIV (Q + Q_c + W_{-y} + A + Self) . For CombIV combination obtained minimum β value is 4.495 from R1L1 (Table 5. 2).

Table 5.2: CombIV β Results for Floor Beams and Lateral Braces

Member	Max	Min
FB0	5.970	5.956
R0L1	5.419	5.381
R1L 1	4.600	4.495
R1L2	5.417	5.380
FB1	6.099	6.089
R2L 3	5.671	5.646
R3L3	5.661	5.622
R3L 4	5.729	5.704
FB2	6.154	6.149
R4L 5	5.886	5.874
R5L 5	6.067	6.066
System	**6.154**	**4.495**

Upon analysis for 60% LM71 train loading, critical combination for vertical brace members is CombIV **(**$Q + Q_c + W_{-y} + A +$ Self). For CombIV combination obtained minimum β value is 5.747 from L2U2 (Table 5.3).

Table 5.3: CombIV β Results for Vertical Braces

Member	Max	Min
L1-U1	6.120	6.107
U1-L2	5.812	5.784
L2-U2	5.777	5.747
U2-L3	6.201	6.198
System	**6.201**	**5.747**

Upon analysis for 60% LM71 train loading, for all combinations, minimum value for truss members' connection is 3.587 from U2U2' (Table 5.4).

Table 5.4:β Results for Connections

Member	Maximum Axial Member Force (kN)	Connection Capacity (kN)	Reliability Index(β)
U0-U1	721.040	2825.062	4.564
U1-U2	1117.444	2897.651	3.675
U0-L1	859.404	2796.364	4.208
L1-L2	995.400	3081.656	4.101
L1-U1	506.601	2032.573	4.605
U1-L2	160.661	893.169	5.075
L2-U2	378.317	2032.573	5.033
U2-L3	129.130	1027.354	5.438
L2-L3	1180.927	3152.979	3.750
U2-U2'	1297.153	3254.266	3.587
		System	**3.587**

5.3 Ultimate Service Goods Train Load β Results

According to regulation and assumptions β analysis are completed for ultimate service moving load. β Results of critical combination for truss members, lateral braces, and vertical braces are tabulated with maximum and minimum values and graph of whole train cross are given for truss members. β results of connections are tabulated. In addition, the β results of members for other combinations are given Appendix B as table of maximum and minimum values and graphs of whole cross of train.

Upon analysis for ultimate service goods train loading, critical combination is CombIV **(**$Q + Q_c + W_{-y} + A + Self$). For CombIV combination obtained minimum β value is 4.064 from right truss L1U1compresion-tension member (Table 5.5).

Table 5.5: CombIV β Results for Truss Members

	Member	Max	Min		Member	Max	Min
RIGHTTRUSS	U0-U1	5.915	4.590	**LEFTTRUSS**	U0-U1	5.328	4.509
	U1-U2	5.682	4.091		U1-U2	5.723	4.584
	U0-L1	6.086	4.897		U0-L1	6.086	5.225
	L1-L2	6.071	4.684		L1-L2	6.071	5.080
	L1-U1	5.996	4.064		L1-U1	5.996	4.583
	U1-L2	6.177	4.415		U1-L2	6.199	4.936
	L2-U2	6.207	4.253		L2-U2	6.206	4.758
	U2-L3	6.236	4.739		U2-L3	6.231	5.153
	L2-L3	6.073	4.648		L2-L3	6.074	5.050
	U2-U2'	5.776	4.428		U2-U2'	6.053	5.079
	System	**6.236**	**4.064**		**System**	**6.231**	**4.509**

Upon analysis for ultimate service goods train loading, critical combination for truss members is CombIV **(**Q + Q_c + W_{-y} + A + Self). For CombIV combination obtained β results are presented in graphical form for whole train cross for right truss (Figure 5.8) and left truss (Figure 5.9).

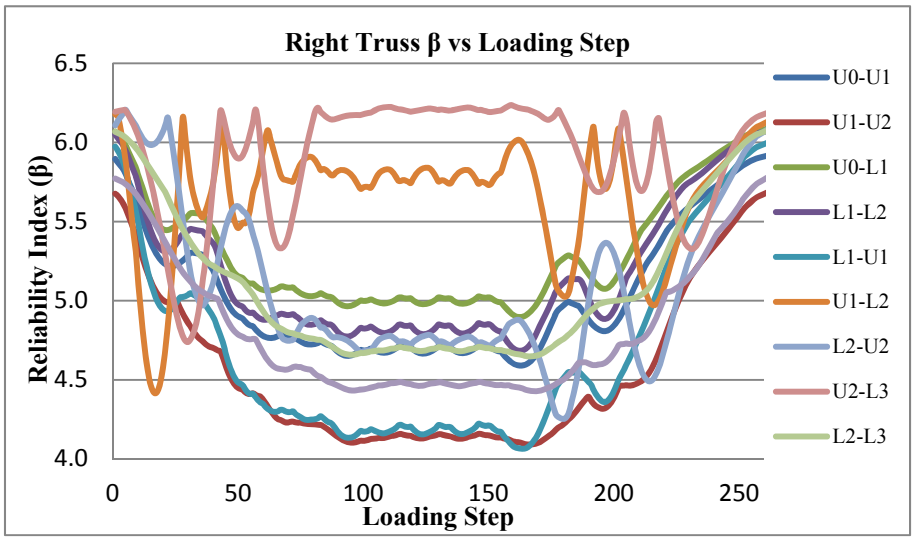

Figure 5.8: CombIV Right Truss β vs. Loading Step (min=4.064)

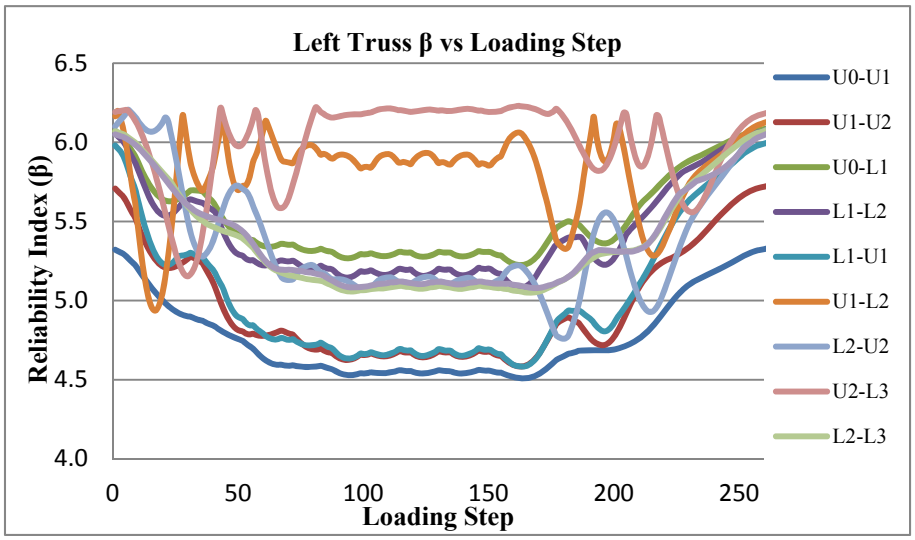

Figure 5.9: CombIV Right Truss β vs. Loading Step (min=4.059)

Upon analysis for ultimate service goods train loading, critical combination for floor beams and lateral brace members is CombIV (Q + Q_c + W_{-y} + A + Self). For CombIV combination obtained minimum β value is 4.491 from R1L1 (Table 5. 6).

Table 5.6: CombIV β Results for Floor Beams and Lateral Braces

Member	Max	Min
FB0	5.970	5.954
R0-L1	5.419	5.379
R1-L 1	4.600	4.491
R1-L2	5.417	5.378
FB1	6.099	6.089
R2-L 3	5.671	5.646
R3-L3	5.662	5.623
R3-L 4	5.729	5.705
FB2	6.154	6.150
R4-L 5	5.887	5.875
R5-L 5	6.067	6.066
System	**6.154**	**4.491**

Upon analysis for ultimate service goods train loading, critical combination for vertical brace members is CombIV (Q + Q_c + W_{-y} + A + Self). For CombIV combination obtained minimum β value is 5.502 from L2U2 (Table 5.7).

Table 5.7: CombIV β Results for Vertical Braces

Member	Max	Min
L1-U1	6.058	6.040
U1-L2	5.599	5.558
L2-U2	5.547	5.502
U2-L3	6.178	6.173
System	**6.178**	**5.502**

Upon analysis for ultimate service goods train loading, for all combinations, minimum value for truss members' connection is 3.599 from U2U2' (Table 5.8).

Table 5.8: β Results for Connections

Member	Maximum Axial Member Force (kN)	Connection Capacity (kN)	Reliability Index(β)
U0-U1	714.600	2825.062	4.580
U1-U2	1096.636	2897.651	3.724
U0-L1	876.725	2796.364	4.166
L1-L2	1015.778	3081.656	4.056
L1-U1	516.894	2032.573	4.570
U1-L2	225.525	893.169	4.583
L2-U2	409.235	2032.573	4.930
U2-L3	186.177	1027.354	5.066
L2-L3	1157.217	3152.979	3.801
U2-U2'	1291.399	3254.266	3.599
		System	**3.599**

5.4 Actual Train Crossing the bridge β Results

According to regulation and assumptions β analysis are completed for actual train crossing the bridge. β Results of critical combination for truss members, lateral braces, and vertical braces are tabulated with maximum and minimum values and graph of whole train cross are given for truss members. β results of truss members' connections are tabulated. In addition, the β results of members for other combinations are given Appendix B as table of maximum and minimum values for members and graphs of whole cross of train for trusses.

Upon analysis for actual train loading, critical combination is CombIV (Q + Q_c + W_{+y} + A + Self). For CombIV combination obtained minimum β value is 4.405 from right truss U1U2 compression member (Table 5.9).

Table 5.9: CombIV β Results for Truss Members

	Member	Max	Min		Member	Max	Min
RIGHTTRUSS	U0-U1	5.912	4.865	**LEFTTRUSS**	U0-U1	5.326	4.693
	U1-U2	5.677	4.405		U1-U2	5.721	4.782
	U0-L1	6.083	5.125		U0-L1	6.084	5.398
	L1-L2	6.068	4.941		L1-L2	6.069	5.268
	L1-U1	5.991	4.438		L1-U1	5.993	4.863
	U1-L2	6.196	4.469		U1-L2	6.199	4.975
	L2-U2	6.208	4.482		L2-U2	6.206	4.922
	U2-L3	6.215	4.768		U2-L3	6.223	5.175
	L2-L3	6.069	4.962		L2-L3	6.071	5.278
	U2-U2'	5.771	4.688		U2-U2'	6.050	5.281
	System	**6.215**	**4.405**		**System**	**6.223**	**4.693**

Upon analysis for actual train loading, critical combination for truss members is CombIV (Q + Q_c + W_{-y} + A + Self). For CombIV combination obtained β results are presented in graphical form for whole train cross for right truss (Figure 5.10) and left truss (Figure 5.11).

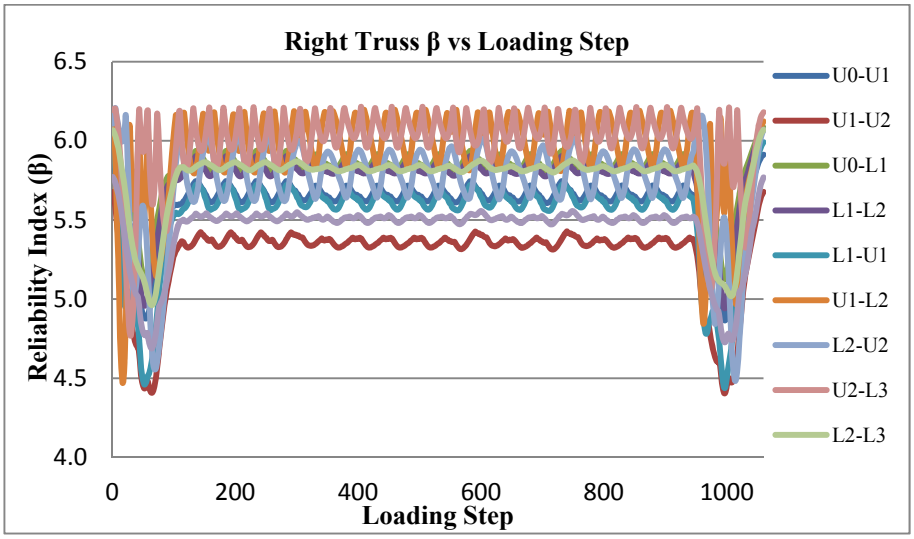

Figure 5.10: CombIV Right Truss β vs. Loading Step (min=4.405)

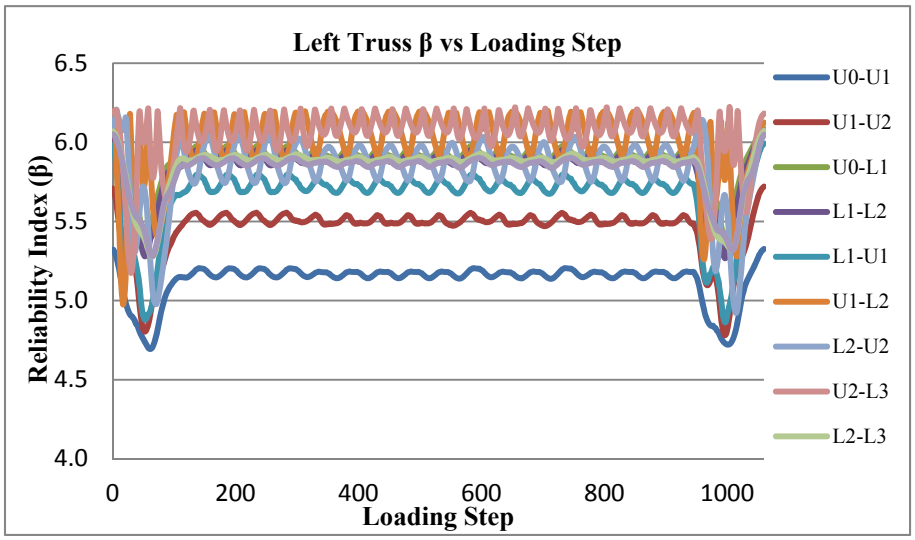

Figure 5.11: CombIV Right Truss β vs. Loading Step (min=4.693)

Upon analysis for actual train loading, critical combination for floor beams and lateral brace members is CombIV (Q + Q_c + W_{-y} + A + Self). For CombIV combination obtained minimum β value is 4.516 from R1L1 (Table 5. 10).

Table 5.10: CombIV β Results for Floor Beams and Lateral Braces

Member	Max	Min
FB0	5.970	5.957
R0-L1	5.418	5.388
R1-L 1	4.600	4.516
R1-L2	5.417	5.387
FB1	6.099	6.091
R2-L 3	5.671	5.651
R3-L3	5.662	5.630
R3-L 4	5.729	5.710
FB2	6.154	6.151
R4-L 5	5.887	5.875
R5-L 5	6.067	6.066
System	**6.154**	**4.516**

Upon analysis for actual train loading, critical combination for vertical brace members is CombIV (Q + Q_c + W_{-y} + A + Self). For CombIV combination obtained minimum β value is 5.511 from L2U2 (Table 5.11).

Table 5.11: CombIV β Results for Vertical Braces

Member	Max	Min
L1-U1	6.058	6.042
U1-L2	5.599	5.566
L2-U2	5.547	5.511
U2-L3	6.178	6.174
System	**6.178**	**5.511**

Upon analysis for actual train loading, for all combinations, minimum value for truss members' connection is 4.113 fromU2U2'(Table 5.12).

Table 5.12: β Results for Connections

Member	Maximum Axial Member Force (kN)	Connection Capacity (kN)	Reliability Index(β)
U0-U1	601.522	2825.062	4.852
U1-U2	889.798	2897.651	4.210
U0-L1	717.725	2796.364	4.554
L1-L2	830.267	3081.656	4.467
L1-U1	422.565	2032.573	4.886
U1-L2	226.340	893.169	4.576
L2-U2	367.019	2032.573	5.071
U2-L3	186.521	1027.354	5.064
L2-L3	949.547	3152.979	4.251
U2-U2'	1045.651	3254.266	4.113
		System	**4.113**

5.5 Summary of β Results

Upon analysis three different train loading used for reliability analyses. In table 5.13 summary of reliability analyses results are presented. Analyses have resulted that critical loading is 60% LM 71 loading. 60% LM71 loading has resulted minimum reliability index as 3.59; therefore system reliability index is 3.59.

Table 5.13: Summary of β Results

	60% LM 71	Service Goods Train	Actual Train
	β_{min}	β_{min}	β_{min}
Truss Members	3.98	4.06	4.41
Truss Connections	3.59	3.60	4.11
Lateral Braces and Floor Beams	4.50	4.49	4.52
Vertical Braces	5.75	5.50	5.51
System	3.59	3.60	4.11

CHAPTER 6

PROPOSED INSTRUMENTATION BASED EVALUATION PRINCIPLES

6.1 Introduction

In the scope of study, instrumentation based evaluation principles for railroad bridges are proposed. Upon study; SHM studies, condition evaluation studies' results and difficulties faced during studies have resulted a series of principle that can be applicable to all types of bridges rather than only steel truss type bridges.

6.2 Proposed Instrumentation Based Evaluation Principles

Proposed principles are listed as follows;

1. SHM studies should be conducted, if one of the stated condition exists;
   - **a.** Detection of unfavorable structural damage during routine inspection works such as; cracks, settlements, deflections etc.
   - **b.** Extraordinary design conditions such as; larger span length or pier height than as usual, pier located in detrimental hydraulic conditions,
   - **c.** Extraordinary design principles such as; different support condition and material properties than as usual,
   - **d.** Bridges located on highly important railroad route.
2. Depends on condition of bridge stated in principle 1; structural system and detail, connection, support condition etc. of bridge should be examined according to technical drawings, if exist.

3. Preliminary field studies should be conducted. In preliminary studies, researchers should compare technical drawings with the applications, determine if any changes done on structural parts of bridge, maintenance or strengthening work done that is not mentioned in drawings. These field studies are important for the visual understanding of condition that creates necessities of SHM application and logistic organization of SHM system.
4. In preliminary field study, some initial data collection can be conducted such as; dynamic measurements for determination bridge stiffness, resonance frequency, schmit hammer test, slope measurements etc. In addition to measurement, if possible, collection of sample material from structural material could be useful for material testing.
5. FEM construction of bridge should be done for getting idea about structural behavior of bridge. In this stage data collected in preliminary field study could be compared with the FEM analyses results. Initial calibration studies could be conducted with comparison done. Creation of FEMs should be done in steps, starting by simplest modeling then end more complex FEMs and sensitivity analyses are recommended.
6. With calibrated FEM should be used for determination of critical members of bridge structure.
7. Market research for purchasing of sensors and data logger should be done according to ;
   a. Observations in preliminary field study,
   b. FEMs structural analyses,
   c. Mechanical, material properties etc. of members that are decided to be monitored,
   d. Structural properties of bridge such as type; arch bridge, truss bridge or support condition etc.,
   e. Budget of study,
   f. Frequency of measurement such as dynamic or static measurement, data collecting speed, channel amount of data logger etc.

8. Purchasing of SHM system needs should be completed. It should be also noted that most of equipments are imported from abroad. Therefore order, delivery, custom works could take 2-3 months.
9. Programming studies of data logger should be done according to the required connection type for all the sensors work together (voltage and current needs, analog or digital data etc.), calibration constants of sensors, data collecting speed etc.
10. Complete system and software laboratory tests should be done to be sure about system correct data collection. Sensor calibration constants can be controlled by simple member testing in laboratory.
11. Installation of sensors, data logger etc. should be planned carefully for second field study. It could be possible to need extra technical personnel or firms. In addition to technical personnel, to be in contact with regional authorities who are responsible for bridge is also very important due to need of permissions and to have access to needed equipment for installation such as small cranes.
12. After installation studies, data collection while test train cross and service train cross should be done for controlling system, that works properly before living system for long term monitoring.
13. Remote access to data logger is important issue. Today, remote access to data logger via GSM modems and mobile phone operators` data communication sim cards if the bridge is in base station access region is possible. By remote connection, some possible problems about software can be detected and fixed remotely, such as reloading or improving software.
14. Test train loading information could be used in FEM analyses. Therefore unmonitored members loading condition can be found indirectly.
15. FEM detailed recalibration should be done with the measured data while test train cross, which has known loading information. If FEM analyses and monitored data are approximately repeated in same results, FEM and unmonitored members` analyses results could be more reliable.

16. Next step is condition assessment of bridge in accordance with monitored and FEM analyses by capacity analyses under design loads and reliability analyses under service loads.
17. In the condition of unsatisfactory results is obtained in capacity and reliability analyses, strengthening solution should be proposed.
18. In the condition of satisfactory results is obtained in capacity and reliability analyses, by long term monitoring; sustainability of satisfactory condition can be monitored continuously.

CHAPTER 7

EARTHQUAKE ANALYSES OF STEEL TRUSS RAILROAD BRIDGE

7.1 Introduction

In the scope of this study, bridge earthquake analyses and design checks are conducted. Two approaches are used for earthquake analyses; the first approach is linear time history analysis, and the second one is response spectrum analysis. Design check of structure conducted according to Eurocodes 3 and 8. Analyses and design checks are completed with analyses and design software SAP2000 v10. Analyses and design details are given in following subsections.

7.2 Finite Element Model of Bridge

3D Finite element model of bridge, without curve is used in earthquake analyses and design studies; 3D modeling is introduced in section 3.2. Technical drawings are available only for two span and 19 m height pier. Remaining 4 piers are modeled with the same height and structural properties of first 19 m height pier and 4 span is also modeled with the same structural properties of first two spans, due to lack of technical drawings of these piers and spans. 3D finite element model view given in Figure 7.1.

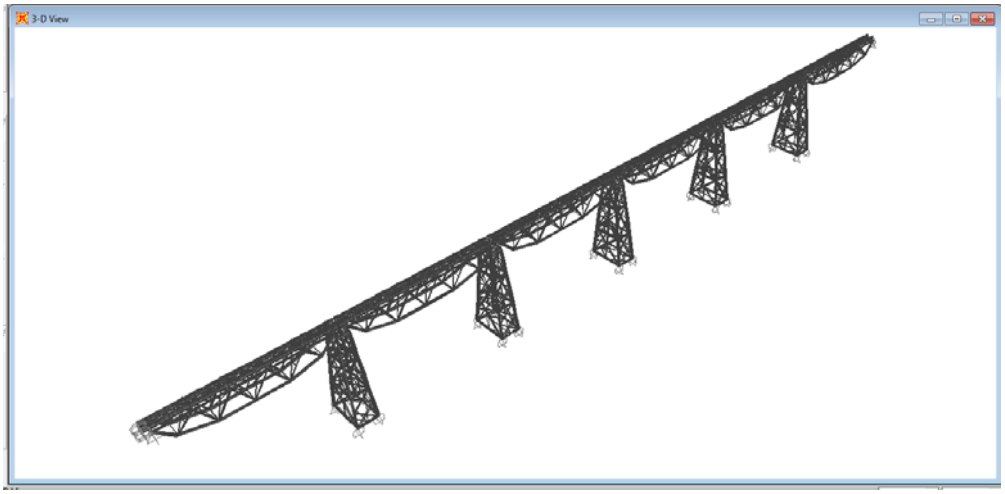

Figure 7.1: 3D view of earthquake model of bridge

7.3 Earthquake characteristics of bridge location

Steel Truss Railroad bridge location is introduced in section 2.1.1. According to Earthquake zoning map of Turkey published by Republic of Turkey Ministry of Public Works and Settlement, 1996, bridge location is corresponds to the first degree of earthquake zone (Figure 7.2 and 7.3).

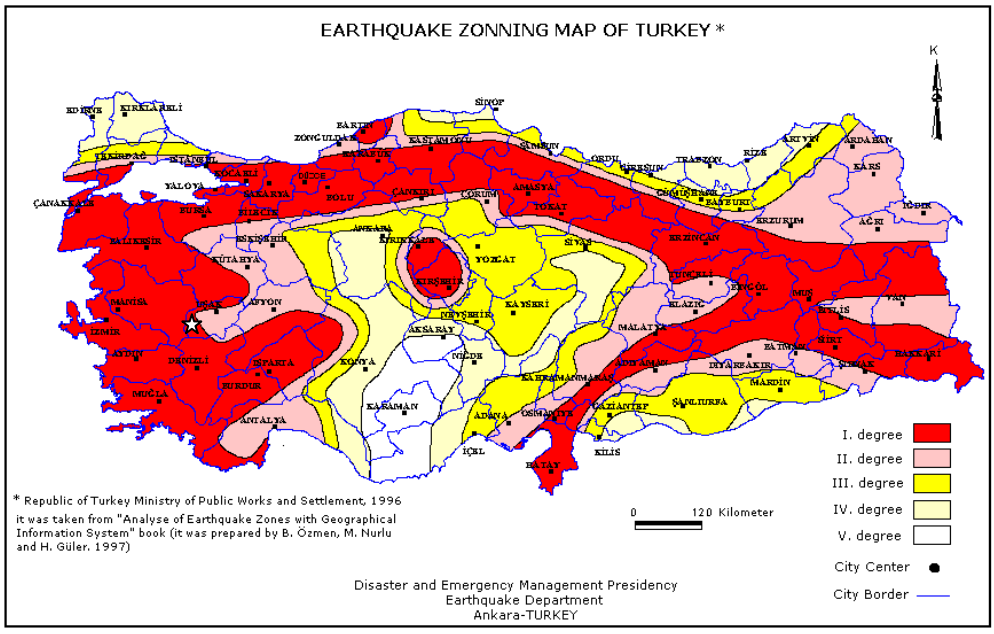

Figure 7.2: Earthquake zoning map of Turkey from www.deprem.gov.tr

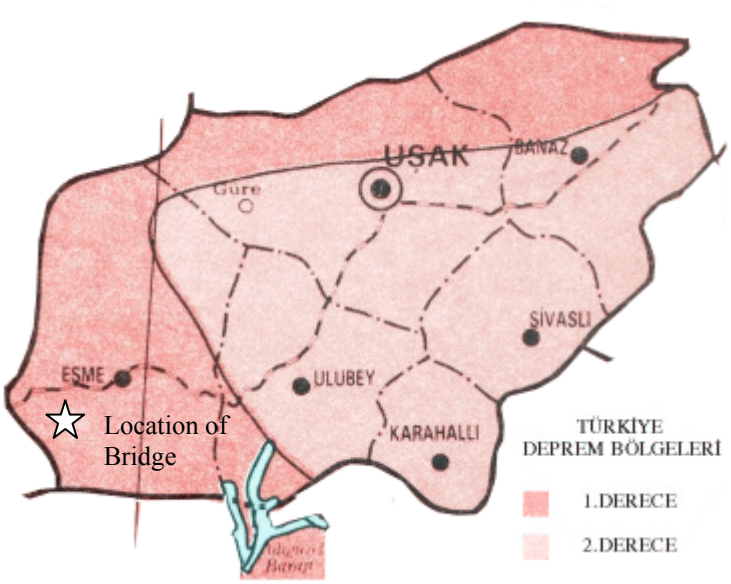

Figure 7.3: Earthquake zoning map of Uşak from www.deprem.gov.tr

According to Turkish earthquake code, Earthquake Design Regulations for Buildings Constructed in Earthquake Zones-2007 (DBYBHY-2007), peak ground acceleration (PGA) value for the first degree of earthquake zone is equal to 0.4g (g : gravitational acceleration value = 9.81 m/s^2).

Local geological characteristic of bridge structure is assumed as rock formation. Assumption is done due to absence of soil investigation studies.

7.4 Analyses Methods

7.4.1 Time History Analyses

Five real earthquake horizontal ground acceleration data is used for analyses. Data are chosen according to their location, peak ground acceleration value (PGA), and local geological characteristic. Four earthquakes' data are from Turkey`s destructive earthquakes and remaining one is from United States. Earthquakes have PGA values between 0.24g and 0.92g. All chosen data are from rock formation local geological characteristic, same as assumption introduced in section 7.3. Earthquake information details are;

- İzmit Earthquake;

Date:	17/08/1999
Magnitude:	7.6 Mw
Fault mechanism:	Strike-Slip
Station:	Gebze-Tubitak Marmara Research Center
Horizontal PGA:	0.24 g
Epicentral Distance:	47 km
Fault Distance:	30 km

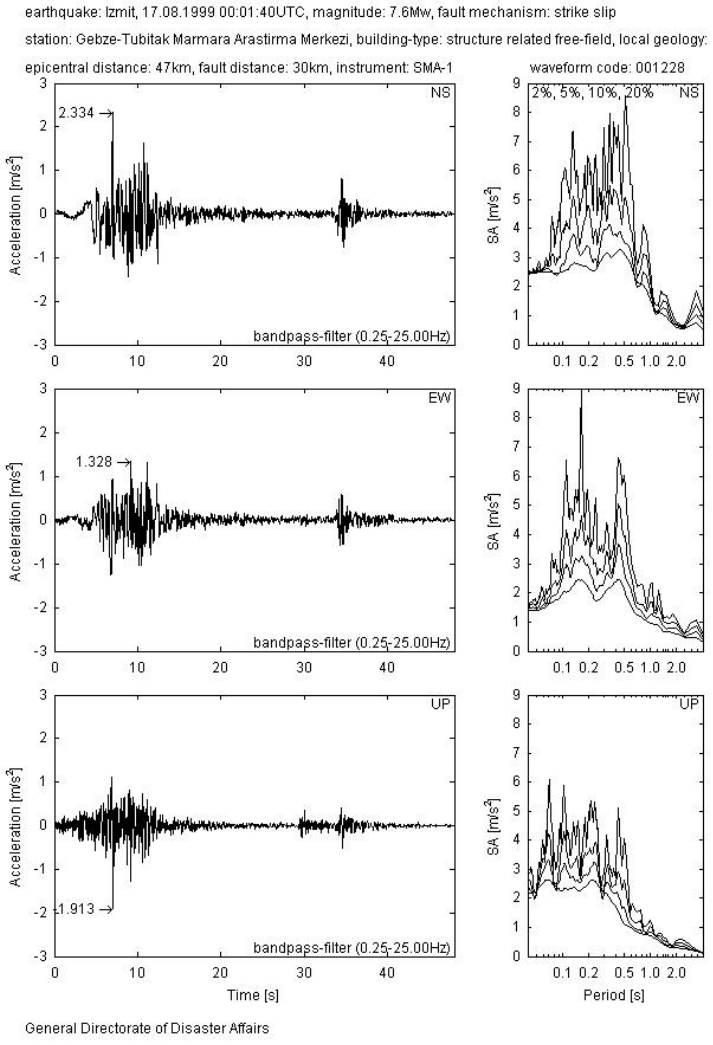

Figure 7.4: Graphical representation of İzmit Earthquake ground acceleration data (from the European Strong-Motion Database)

- İzmit (aftershock) Earthquake;

Date:	13/09/1999
Magnitude:	5.8 Mw
Fault mechanism:	Oblique
Station:	İzmit- Meteorological Station
Horizontal PGA:	0.32 g
Epicentral Distance:	15 km

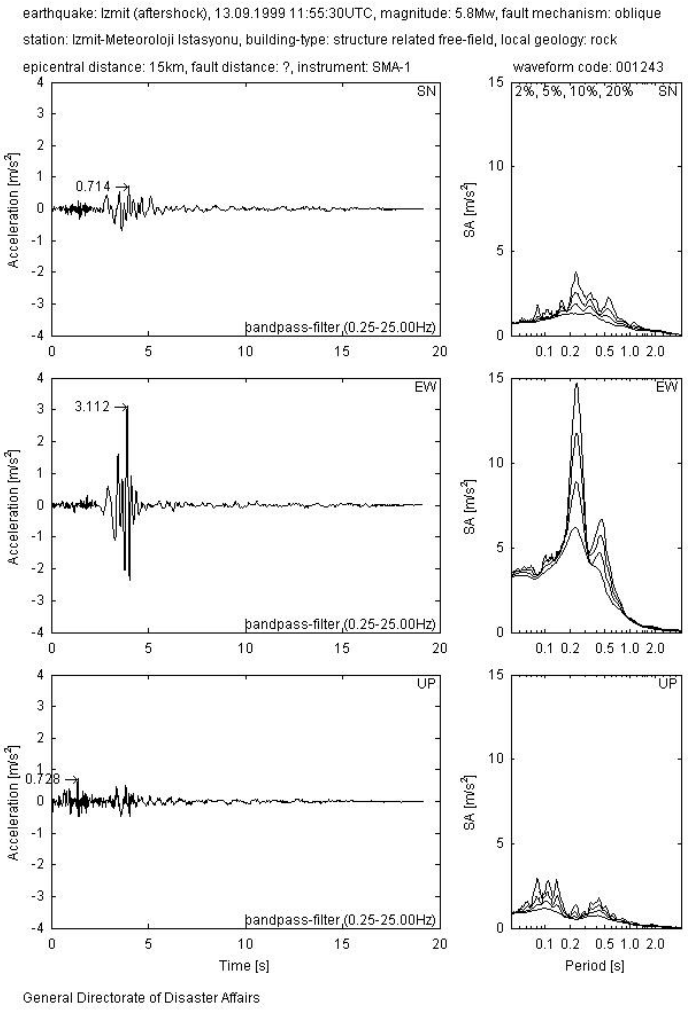

Figure 7.5: Graphical representation of İzmit (aftershock) Earthquake ground acceleration data (from the European Strong-Motion Database)

- Bingöl Earthquake;

Date:	01/05/2003
Magnitude:	6.3 Mw
Fault mechanism:	Strike Slip
Station:	Bingöl Public Works Directorate
Horizontal PGA:	0.52 g
Epicentral Distance:	14 km
Fault Distance:	10

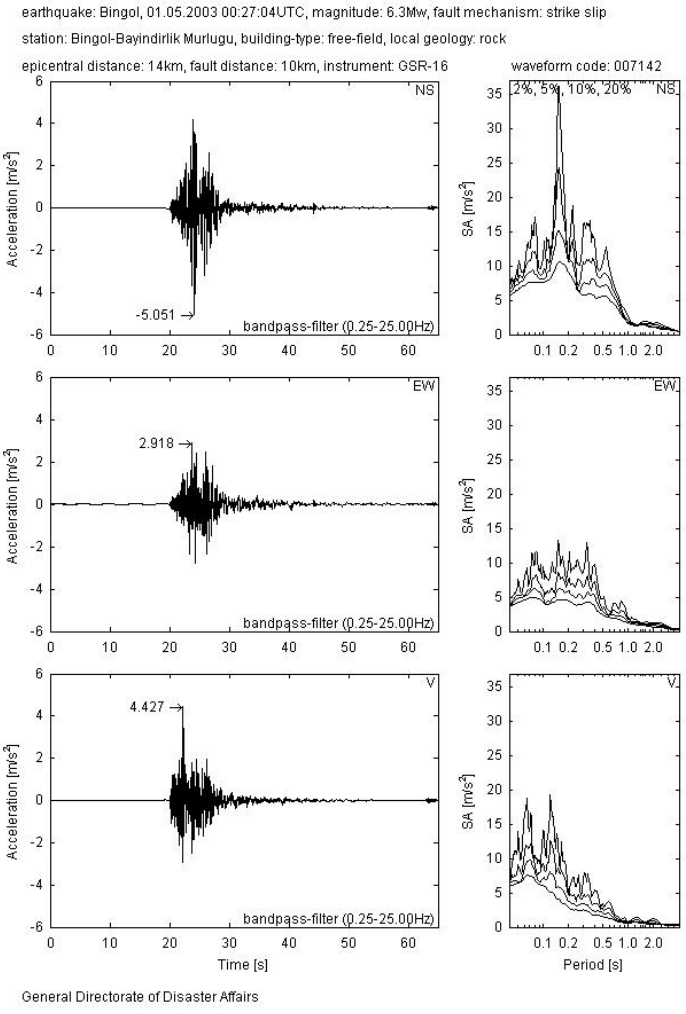

Figure 7.6: Graphical representation of Bingöl Earthquake ground acceleration data (from the European Strong-Motion Database)

- Düzce Earthquake;

Date:	12/11/1999
Magnitude:	7.2 Mw
Fault mechanism:	Oblique
Station:	LDEO Station No.C0375 VO
Horizontal PGA:	0.92 g
Epicentral Distance:	23 km
Fault Distance:	9 km

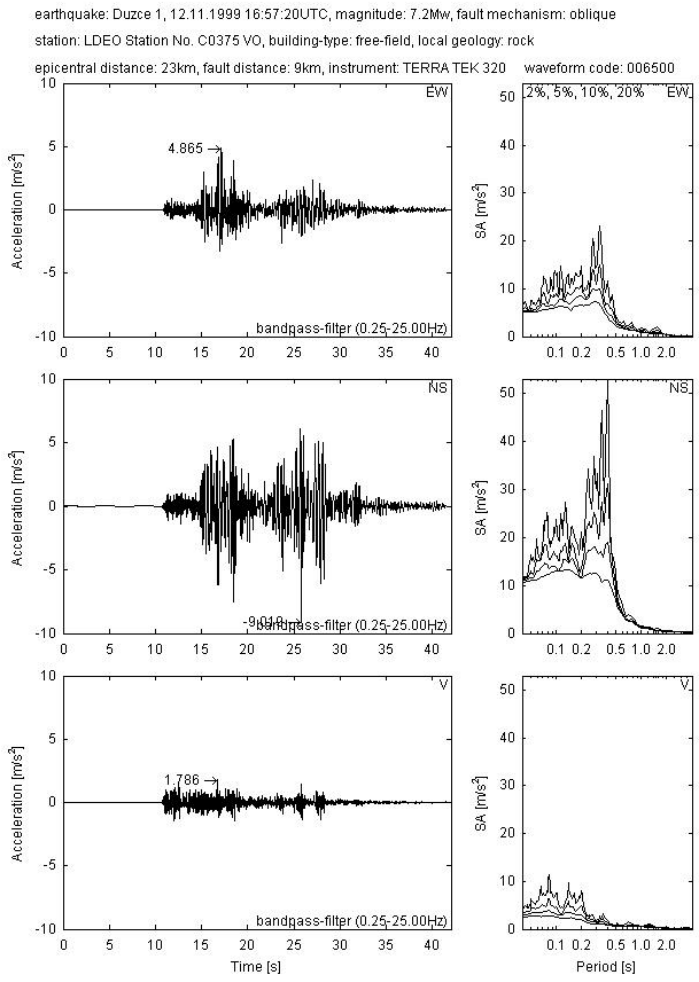

Figure 7.7: Graphical representation of Düzce Earthquake ground acceleration data (from the European Strong-Motion Database)

- Northridge (US) Earthquake;

Date:	17/01/1994
Magnitude:	6.7 Mw
Fault mechanism:	Strike Slip
Station:	CDMG 24207 Pacoima Dam
Horizontal PGA:	0.434 g
Epicentral Distance:	20.36 km

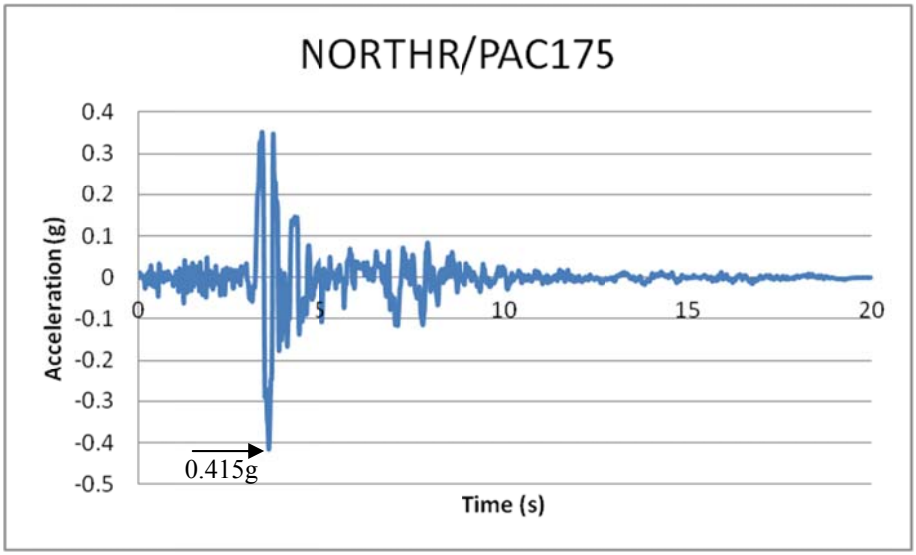

Figure 7.8: Graphical representation of Northridge Earthquake ground acceleration PAC175 data

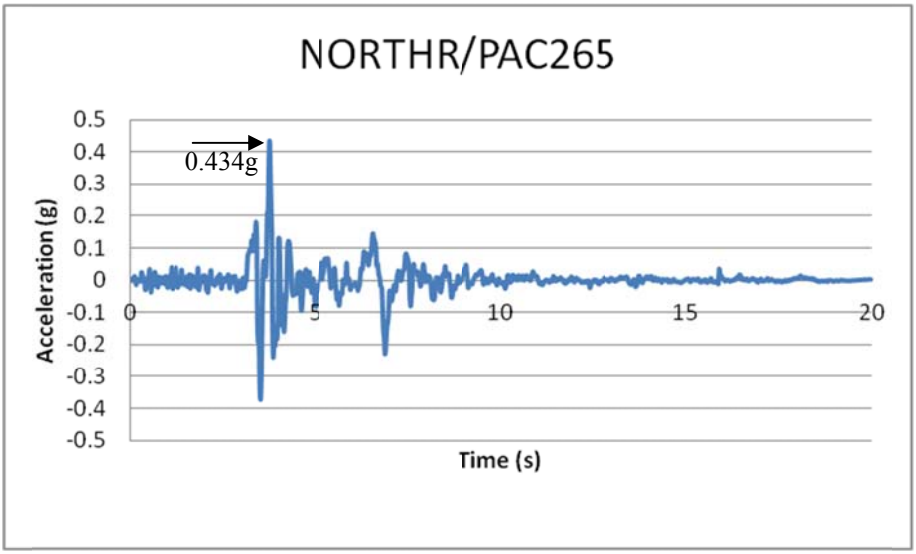

Figure 7.9: Graphical representation of Northridge Earthquake ground acceleration PAC265 data

7.4.2 Response Spectrum Analyses

Three types of design spectrum are used for response spectrum analysis. The first design spectrum is spectrum defined in Eurocode-8 (EC-8), the second design spectrum is spectrum defined in Design Regulations for Buildings Constructed in Earthquake Zones-2007 (DBYBHY-2007), and the third one is AASTHO 2002. Earthquake force reduction factor (q for EC-8, R for DBYBHY) is equal to 1.5 for limited ductile piers with normal bracings according to Eurocode-8 Part: 2. Seismic Design of Bridges same value of reduction is used for DBYBHY response spectrum. Properties of two response spectra are;

EC-8 Type-1 Response Spectrum;

Ground Type : A (Rock)

Soil Factor, S : 1.0

Damping correction factor, η : 1.0

Lower limit of the period of the constant spectral acceleration branch, T_B : 0.15 s

Upper limit of the period of the constant spectral acceleration branch, T_C : 0.40 s

Beginning of the constant displacement response range of the spectrum, T_D: 2 s

Design ground acceleration on Type A ground Ag: 0.4 g

Modification factor to account for special regional situations, k : 1.0

Ordinate of the elastic response spectrum, Se (T)

Response Spectrum Equations;

$0 \le T \le T_B$: $Se(T) = a_g\, k\, S\, [1 + \frac{T}{T_B}(\eta\, 2.5 - 1)]$ (7.1)

$T_B \le T \le T_C$: $Se(T) = a_g\, k\, S\, \eta\, 2.5$ (7.2)

$T_C \le T \le T_D$: $Se(T) = a_g\, k\, S\ \eta\, 2.5\, \frac{T_c}{T}$ (7.3)

$T_D \le T \le 4$ sec: $Se(T) = a_g\, k\, S\ \eta\, 2.5\, \frac{T_c\, T_D}{T^2}$ (7.4)

DBYBHY-2007 Response Spectrum;

Ground Type : Z1 (Rock)

Importance Factor, I : 1.0

Lower limit of the period of the constant spectral acceleration branch, T_A : 0.15 s

Upper limit of the period of the constant spectral acceleration branch, T_B : 0.3 s

Effective ground acceleration constant A_o : 0.4

Period, T

Elastic Spectral Acceleration, Sae (T)

Response Spectrum Equations;

$0 \leq T \leq T_A$: $\text{Sae}\,(T) = A_0\, I \left[1 + 1.5\, \frac{T}{T_A}\right]$ (7.5)

$T_A \leq T \leq T_B$: $\text{Sae}\,(T) = A_0\, I\ 2.5$ (7.6)

$T_C \leq T$: $\text{Sae}\,(T) = 2.5\, (\frac{T_B}{T})^{0.8}$ (7.7)

AASTHO 2002 Response Spectrum;

Soil Profile Type : I (Rock)

Ground Acceleration Coefficient, A : 0.4

Period, T

The elastic seismic response coefficient C_s,

Response Spectrum Equation;

$\text{Cs}\,(T) = \frac{1.2\, A\, S}{T^{2/3}} < 2.5A$ (7.8)

Response spectra are given in Figure 7.10.

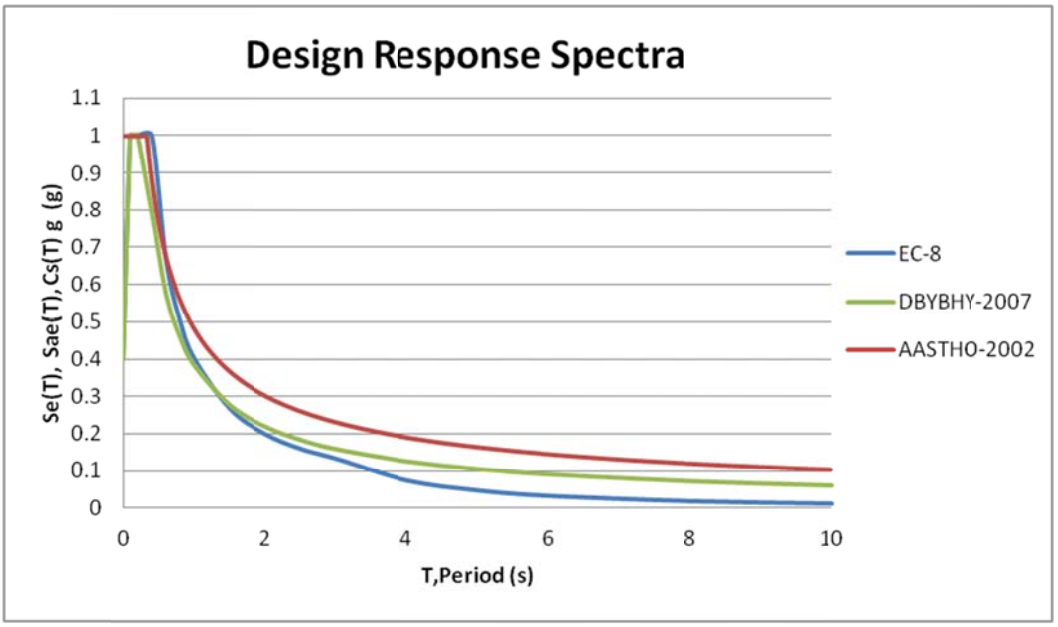

Figure 7.10: Response Spectra for EC-8, DBYBHY-2007, AASTHO-2002

7.5 Analyses and Design Results

Structural analyses and design is completed by the structural analyses and design software Sap2000 v15.

Dead loads and earthquake loads are combined for analyses. Combination coefficients are unity for dead load and related earthquake direction, and 0.3 for perpendicular direction.

As a result of earthquake analyses, the pier members and span members are within the limit indicated in Eurocode-3 regulations for recorded earthquake base accelerations of İzmit (17/08/1999), İzmit (aftershock-13/09/1999), Bingöl (01/05/2003), Northridge (17/01/1994), and design response spectra of EC-8, DBYBHY-2007, and AASTHO-2002 (Figure 7.11-12).

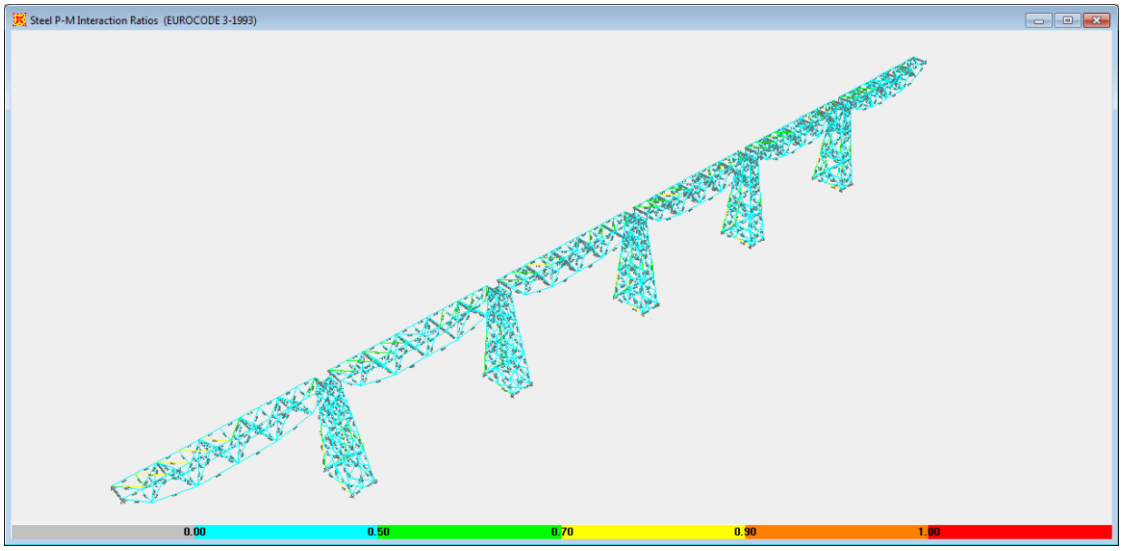

Figure 7.11: Earthquake design of bridge without Düzce Earthquake

Closer view of bridge span and pier design result is given in Figure 7.12 for İzmit, İzmit (aftershock), Bingöl, Northridge Earthquakes and both response spectra of EC-8 and DBYHY-2007. Members stress ratios are smaller than the limit value of 1.00.

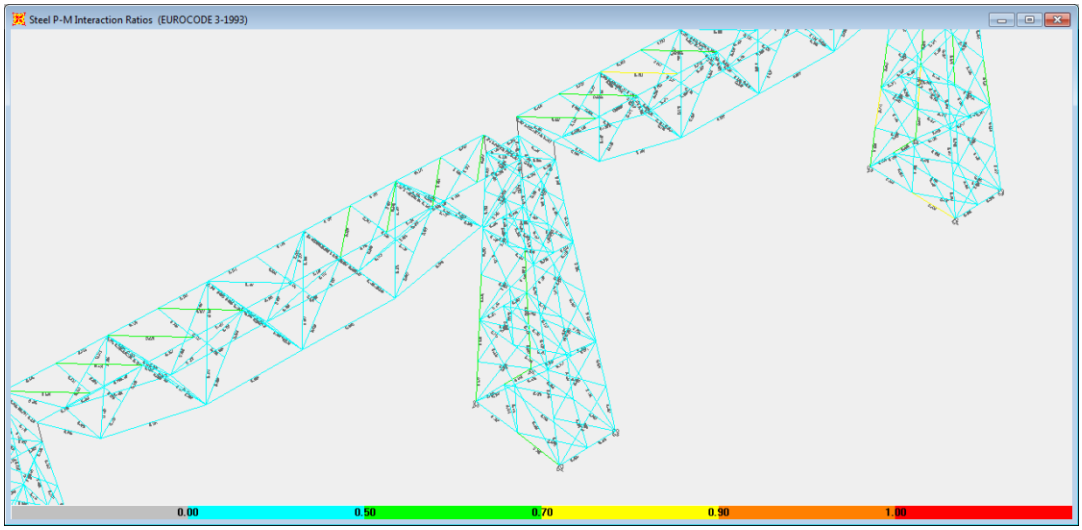

Figure 7.12: Earthquake design of bridge span and pier without Düzce Earthquake

The pier members and span members are within the limit indicated in Eurocode-3 regulations for recorded earthquake base accelerations Düzce (12/11/1999), but lateral brace member force levels are exceeding the limit of Eurocode-3 for this Earthquake. Maximum limit excess of lateral brace members is founded as 264%.

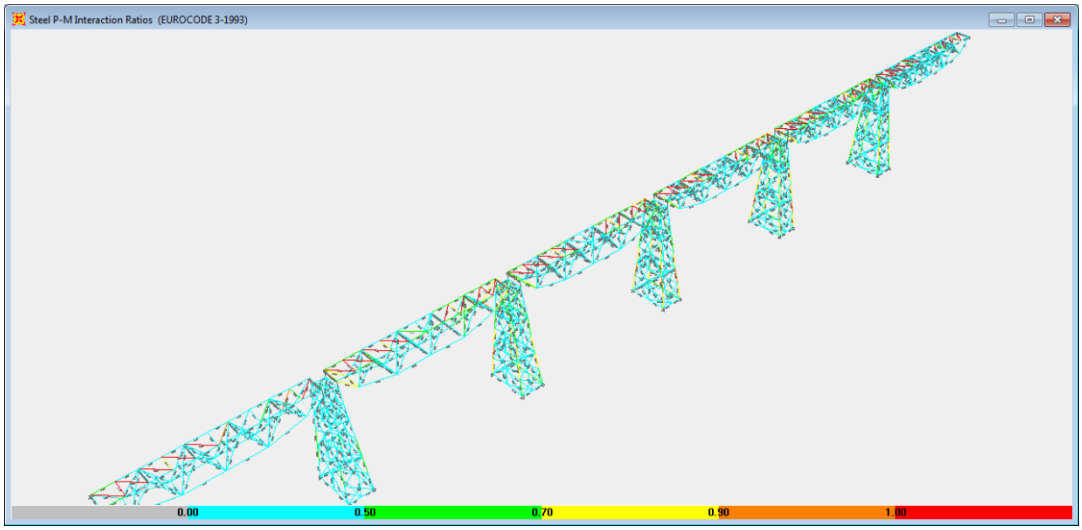

Figure 7.13: Earthquake design of bridge for Düzce Earthquake

Closer view of bridge span and pier member design result is given in Figure 7.14 for Düzce Earthquake.

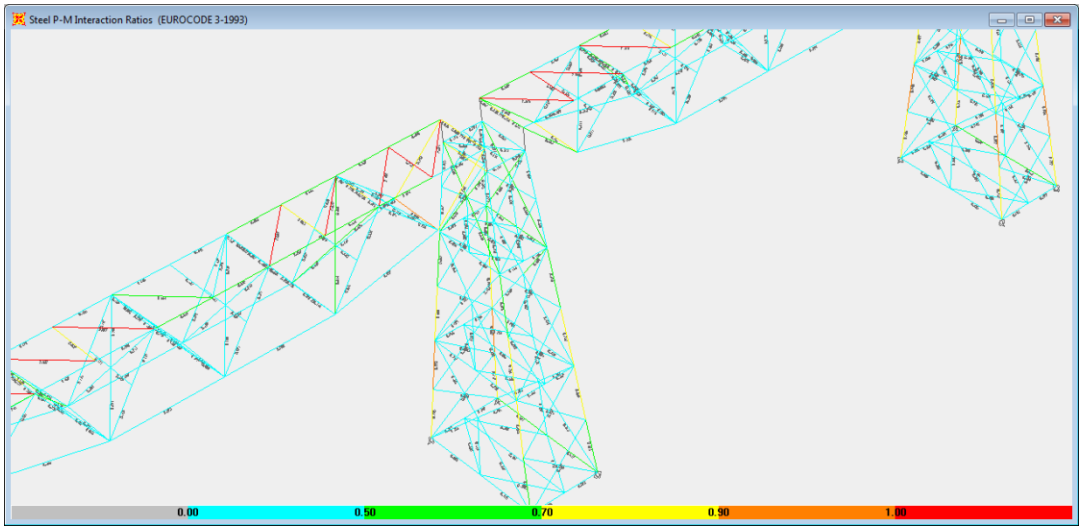

Figure 7.14: Earthquake design of bridge span and pier for Düzce Earthquake

View of bridge failed lateral brace members design result is given in Figure 7.15 for Düzce Earthquake.

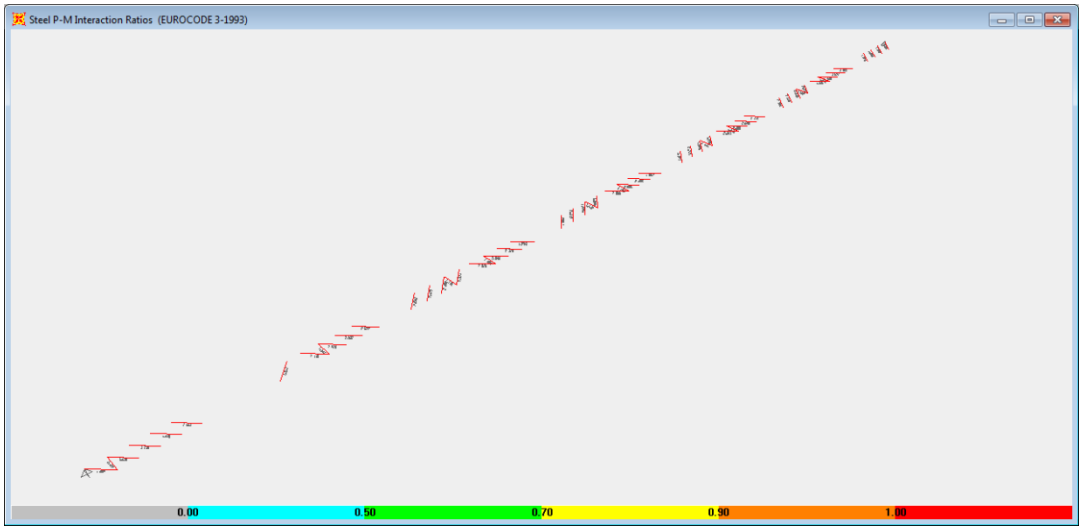

Figure 7.15: Earthquake design of bridge lateral braces for Düzce Earthquake

CHAPTER 8

SUMMARY AND CONCLUSIONS

8.1 Summary

Railroad conveyance is one of the major and effective ways of transportation for both passenger and goods transfer. Railroad bridges are the most crucial part of railroad conveyance. Consequently, inspection and maintenance works for these bridges are essential. These works become more important especially in Turkey due to aged structural condition of railroad bridges.

In this study, application of structural health monitoring (SHM) and conducting reliability analysis of a selected pilot steel railroad bridge were studied and their combination was introduced as one of the superior inspection techniques over generally used visual inspection techniques. In addition to SHM studies and reliability analysis, earthquake analyses and design checks are included.

Case study was performed by choosing a relatively old bridge located on Basmahane-Dumlupınar Railroad route Km: 199+352 in Uşak, Turkey. This bridge was constructed over hundred years ago. However, original documentation and plans could not be found. On the other hand, the first two spans of the total six spans bridge were rebuilt in 1960s with proper documentation and plans. Rebuilt two spans are located on the Dumlupınar side of bridge. Substructure of bridge consists of six spans with 30 m span length each. Maximum pier height is 52 m long and piers are also steel truss type. Superstructure is one lane with ballastless

railroad track and wooden log sleepers. Bridge is horizontally curved with 300 m radius and vertically sloped with 2.5% inclination.

Installation of SHM system, dynamic and static data collection and various difficulties faced during the installation/application studies were included and discussed in this study. Sensor technologies were explored and explained for SHM applications. Programming studies which were used in the SHM system to obtained data from sensors and also store collected data are given in the form of flowcharts. Finite element modeling (FEM) study of the selected truss bridge was conducted and compared with the monitored and collected strain and deflection data during train passage. FEM studies were initially carried out using 2D simplified models and then full 3D model was constructed and used for the analyses. The 2D FEM analyses were targeted for both connection condition evaluation of truss members and determining critical truss members in the first span of the bridge. Initial comparison of 3D FEM and 2D FEM analyses under static train loading were close enough and therefore decision was made to continue analysis with the simpler 2D FEM. Bridge 2D FEM analysis results and monitored data are compared to validate analytical model since the results were close to each other. 3D FEM was mainly used for earthquake simulations since the 3D geometry may have effects on the structural behavior.

Member forces were obtained and connection checks were done under design train loads and real train loads. Capacity index calculations were done for truss members, lateral bracing, vertical bracing members, floor beams, and connection in trusses for each moving load step, moved at 0.40 m intervals, and evaluated according to Eurocode regulations. For the condition assessment of bridge span, reliability analysis was completed for members stated in capacity index calculation section. In reliability analysis loading condition's and material condition's uncertainties are included by some statistical parameters.

In the light of SHM and reliability studies, instrumentation based evaluation principles were proposed for SHM application for all type of bridge structures,

such as; beam, truss, cantilever, arch, tied arch, suspension and cable-stayed type bridges.

Earthquake analyses and design checks are also carried out. Two types of analyses methods are used: linear time history analyses and response spectrum analyses. Time history analyses are conducted for 5 different real earthquake data, and response spectrum analyses are conducted for 3 different design response spectrum.

8.2 Conclusions

The conclusions were drawn based on structural health monitoring (SHM) studies, finite element model analyses, condition assessment studies, and earthquake simulations are carried out in this study. The conclusions made here are valid only for the scope of this study since some of the conclusions are case specific and may change based on the bridge type or location.

- SHM field studies showed that installation of sensors and programming of data logger is one of the most critical parts of these studies. Proper integration of sensors and DAS as well as relevant programming is important. Environmental conditions should be determined and interaction between existing load swings due to environmental conditions should be obtained. In addition, arrangement of sensor location should be managed before field studies, such as; critical members should be given priority for installation.

- As a part of SHM studies, rail load sensor development was completed. Rail load sensor was shown in laboratory testing that the sensor can measure load on a rail by measuring vertical strain created on web of rail. However, the developed sensors did not work properly for the long term measurements in the field due to harsh environmental conditions; whereas, it is understood that rail load sensors are useful sensors for identification of crossing train type and axle loads. Rail load sensors are also useful for

determining number of train crossing the bridge. In addition to measurement ability of rail load sensors, these sensors could be used for triggering the SHM system for fast measurements.

- Span midpoint deflections and members' axial and bending strains can be measured using SHM system, which was successfully, tested using installed sensor system on the pilot steel truss railroad bridge. Determined structural parameters were used in the analytical modeling load simulations of the first span of the steel truss bridge, which is identical to other simply supported spans.

- 2D FEM analyses are carried out for determination of differences in connections force distributions. Truss midpoint deflection and member stresses are compared between four models with different connection properties. It is concluded by the analyses that midpoint deflection differences among models are around 1 % under train loading. Another conclusion of analyses is related to the moment contributions in member total stresses. Average moment contributions in member stresses are 11 % for tension members, 8% for compression members and 20% for tension-compression members which can not be considered as negligible.

- Capacity index calculations were carried out for the major and the critical members of the selected steel truss railroad bridge's first span on Dumlupınar side, located on Basmahane-Dumlupınar Railroad route Km: 199+352 in Uşak, Turkey. Various loading conditions such as train vertical, centrifugal, acceleration, braking, and wind loading were defined on the analytical model in accordance with the regulations stated in Eurocodes. Obtained maximum and minimum structural capacity indices were 0.61 and -0.48 respectively, where the corresponding boundary levels were 1.0 and -0.9. These analysis results have shown that truss members, lateral bracing members, floor beams, vertical bracing members and truss

connection are in acceptable safety levels according to Eurocode regulations.

- Reliability index calculations were carried out for the major members of the selected steel truss railroad bridge's first span on Dumlupınar side, located on Basmahane-Dumlupınar Railroad route Km: 199+352 in Uşak, Turkey. Uncertainties about loading conditions and bridge's steel material properties are included to simulate existing condition of bridge structure by statistical parameters, during conducted reliability index calculations. The material test results carried out in metallurgical department laboratories were also incorporated. The minimum reliability index values for the structural members were obtained as 3.98 and minimum of 3.59 was obtained for member connections. These values are within acceptable levels as defined in the AASTHO LRFD code which have the minimum acceptable value of 3.5. On the other hand, EUROCODE 1990:2002(E) considers that if the consequences class assumed to be "CC2" and corresponding reliability class is taken as RC2, then the minimum acceptable level for 50 years old structure is 3.8. Therefore, the minimum reliability indices obtained for the connections is lower than acceptable level according to Eurocode, while it satisfies AASTHO LRFD; also the index value for members exceeds the acceptable level for both codes. TCDD also introduced an acceptable index level based on previous research as 3.0, which is smaller than both connection and member reliability indices categorizing the bridge in an acceptable level of reliability. It should be noted that reliability index is not an exact indication of structural safety; it is just a factor giving indication of probability of failure parameter as stated in EUROCODE 1990:2002(E) Annex C subsection C6.

- Throughout the conducted studies, bridge condition is analyzed with two evaluation methods named as "capacity" and "reliability". The comparison

of those two methods reveals the difference that capacity analysis is the determination of design conditions on existing structure according to current code regulations for both loading conditions and bridge material strength, while reliability analysis considers the loading condition and bridge material strength are the normally distributed random variables and includes unfavorable effects of random variables' standard deviations, means that includes uncertainties of loading and resistance condition of bridge structure. As a result of comparison, the capacity calculations yielded a higher bridge safety result in comparison to the reliability calculations. In the consideration of the ultimate service goods train loading, Critical capacity index value was obtained to be 0.40 where the critical upper boundary level was equal to 1.00; meanwhile critical reliability index value was 3.60 for same condition, where the upper boundary limit was equal to 3.00. Bridge safety level was 60% lower than acceptable maximum capacity level, whereas 20% higher than the acceptable minimum reliability level according to analyses of ultimate service goods train loading.

- When the members and member connections are evaluated separately, it would have been expected to have member connections to have a higher capacity and reliability index as compared to the members. The evaluation of the pilot Usak bridge results showed that connections are more critical than the members. In a consideration of capacity index calculations; maximum capacity index is obtained from LM 71 loading condition calculations. LM71 loading condition capacity index calculations have resulted maximum capacity index values as 0.48 for members, while 0.61 for connections which is 27% higher than members' capacity index value. Meanwhile in a consideration of reliability index calculations; minimum reliability index is obtained from 60% LM 71 loading condition calculations. 60% LM 71 loading condition reliability index calculations have resulted minimum reliability index values as 3.98 for members, while

3.59 for connections which is 10% lower than members' minimum reliability index value.

- Instrumentation based evaluation principles for all types of bridges (i.e., beam, truss, cantilever, arch, tied arch, suspension and cable-stayed type bridges) are proposed based on the experience obtained Uşak bridge and intuition. Principles are included suggestions for determination of monitoring needs, preparation and application of monitoring system installation studies, data collection from monitoring system, and analyses of data. In addition to structural monitoring suggestions, structural condition assessment methods of monitored structure are suggested such as capacity and reliability analyses.

- As a result of earthquake analyses, the pier members and span members, except lateral braces, are within the limit indicated in Eurocode-3 regulations for recorded earthquake base accelerations of İzmit (17/08/1999), İzmit (aftershock-13/09/1999), Bingöl (01/05/2003), Düzce (12/11/1999), Northridge (17/01/1994), and design response spectra of EC-8, DBYBHY-2007, and AASTHO-2002. Lateral brace member force levels are found to be exceeding the limit of Eurocode-3 for Düzce Earthquake. Maximum limit excess of lateral brace members is founded as 264%. Although the limits are exceeded for lateral brace members, the PGA value of Düzce Earthquake is considerably high when compared to the PGA values presented in design regulations. Düzce Earthquake has PGA value of 0.92 g which is 2.3 times higher than the design PGA (A_0.g) value of 0.4 g accepted for earthquake zone 1. Other earthquake records and response spectrum analyses yields results within acceptable limits.

REFERENCES

AASTHO LRFD (2010). *Bridge Design Specifications 6th Edition.* American Association of State Highway and Transportation Officials, Washington, DC.

AASTHO LRFD (2002). *Standard Specifications for Highway Bridges 17th Edition.* American Association of State Highway and Transportation Officials, Washington, DC.

Akar, V., Uzgider E. (2006). Determination of reliability indices of railway bridges. itüdergisi/d, 5, 93-104.

AS-GA/GB Acceleration Transducers.*Specifications*. http://www.kyowa-ei.co.jp, Last visited January 22th 2012.

BCD-E-70S Concrete Surface Displacement Transducer. *Specifications*. http://www.kyowa-ei.co.jp, Last visited January 22th 2012.

BDI ST350 Strain Transducer. *Instruction Manual*. Campbell Scientific, INC, North Logan.

Catbas,F. N., Susoy, M., Frangopol, D. M. (2008).*Structural health monitoring and reliability estimation: Long span truss bridge application with environmental monitoring data.* Engineering Structures, 30, 2347-2359.

CR5000 Measurement and Control System. *Operator`s Manual*. Campbell Scientific, INC, North Logan.

CS215 Temperature and Relative Humidity Probe. *Instruction Manual*. Campbell Scientific, INC, North Logan.

Czarnecki,A. A., Nowak, A. S. (2007).*Reliability Based Evaluation of Steel Girder Bridges*. Bridge Engineering, 160, 9-15.

DissanayakeP.B.R, andKarunananda, P. A. K. (2008). *Reliability Index for Structural Health Monitoring of Aging Bridges*. http://shm.sagepub.com-/content/7/2/175.full.pdf. Last visited on January 22th, 2012

Enckell-El Jemli,M., Karoumi, R. and Lanaro,F. (2003).*Monitoring of the New Årsta Railway Bridge using traditional and fibre optic sensors.* SPIE Symposium on Smart Structures and Materials, 2–6 March, San Diego, USA, 5057, 279–288.

EN1990 (2002). *Eurocode - Basis of Structural Design*. European Committee for Standardization (CEN), Brussels.

EN1991-2 (2003). *Eurocode 1 - Actions on Structures – Part 2: Traffic loads on bridges.* European Committee for Standardization (CEN), Brussels.

EN1991-1-4 (2004). *Eurocode 1 - Actions on Structures – General actions - Part 1.4: Wind actions*. European Committee for Standardization (CEN), Brussels.

EN1993-1-1 (2005). *Eurocode 3 -Design of Steel Structures- Part 1.1: General Rules and Rules for Buildings*. European Committee for Standardization (CEN), Brussels.

EN1993-2 (2006). *Eurocode 3 -Design of Steel Structures- Part 2: Steel Bridges*. European Committee for Standardization (CEN), Brussels.

EN1993-1-8 (2003). *Eurocode 3 -Design of Steel Structures- Part 1.8: Design of Joints.* European Committee for Standardization (CEN), Brussels.

EN1998-1 (2001). *Eurocode 8 -Design of Structures for Earthquake Resistance-Part 1: General rules, seismic actions and rules for buildings.* European Committee for Standardization (CEN), Brussels.

EN1998-1 (2001). *Eurocode 8 -Design of Structures for Earthquake Resistance-Part 1: General rules, seismic actions and rules for buildings.* European Committee for Standardization (CEN), Brussels.

EN1998-2 (2001). *Eurocode 8 -Design of Structures for Earthquake Resistance-Part 2: Bridges.* European Committee for Standardization (CEN), Brussels.

Earthquake zoning map of Turkey. http://www.deprem.gov.tr/SarbisEng/Shared/DepremHaritalari.aspx, Last visited August 16th 2012.

Goods wagon catalog 2006, Turkish State Railway (TCDD) loads department, Ankara.

KFG Gages for General Stress Measurements. *Specifications*. http://www.kyowa-ei.co.jp,Last visited January 22th 2012

Nowak, A.S. and Collins, K.R. (2000). *Reliability of Structures*. McGraw-Hill, New York.

NRG#200P Wind Direction Vane. *Product Specifications*. http://www.-nrgsystems.com,Last visited January 22th 2012.

NRG#40C Anemometer. *Product Specifications*. http://www.nrgsystems.com,Last visited January 22th 2012.

Resistive Linear Position Transducers LPM. *Technical specifications*. http://www.opkon.com.tr Last visited January 22th 2012.

SAP2000.v10. Integrated software for structural analysis & Design. *User's Manual*, http://www.csiberkeley.com/products SAP.html, Last visited January 22th 2012..

Sustainable Bridges Project Reports, Guideline_MON. *Monitoring Guidelines for Railway Bridges.*http://www.sustainablebridges.net/. Last visited January 22th, 2012.

DBYBHY-2007. *Earthquake Design Regulations for Buildings Constructed in Earthquake Zones*. http://www.deprem.gov.tr/sarbis/Doc/Yonetmelik/DBYBHY-2007.pdf, Last visited August 20th 2012.

Uzgider,E. et al (2004). *Safety Evaluation of Railway Bridges in Turkey, Edirne-Ankara-Irmak route project report vol.1*. Istanbul Technical University, Istanbul.

APPENDIX A

MEASURED DATA DURING FIELD STUDIES

A.1 First Field Study Measurements

A.1.1 Passenger Train Cross Dynamic Measurements

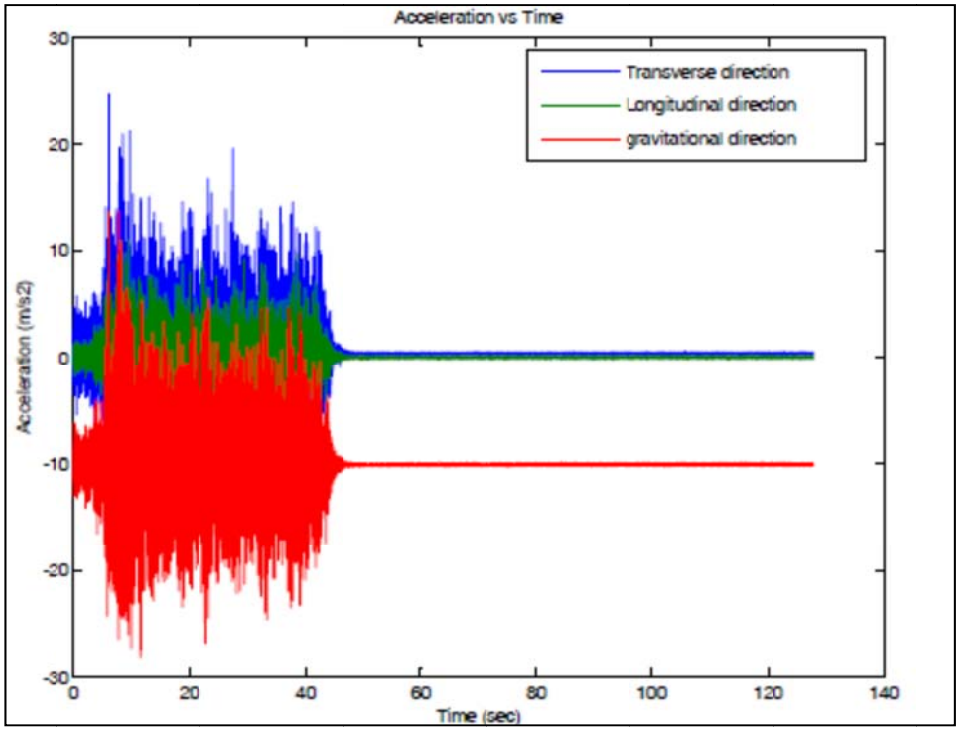

Figure A.1: Acceleration vs. Time graph of first measurement from wireless sensor node229

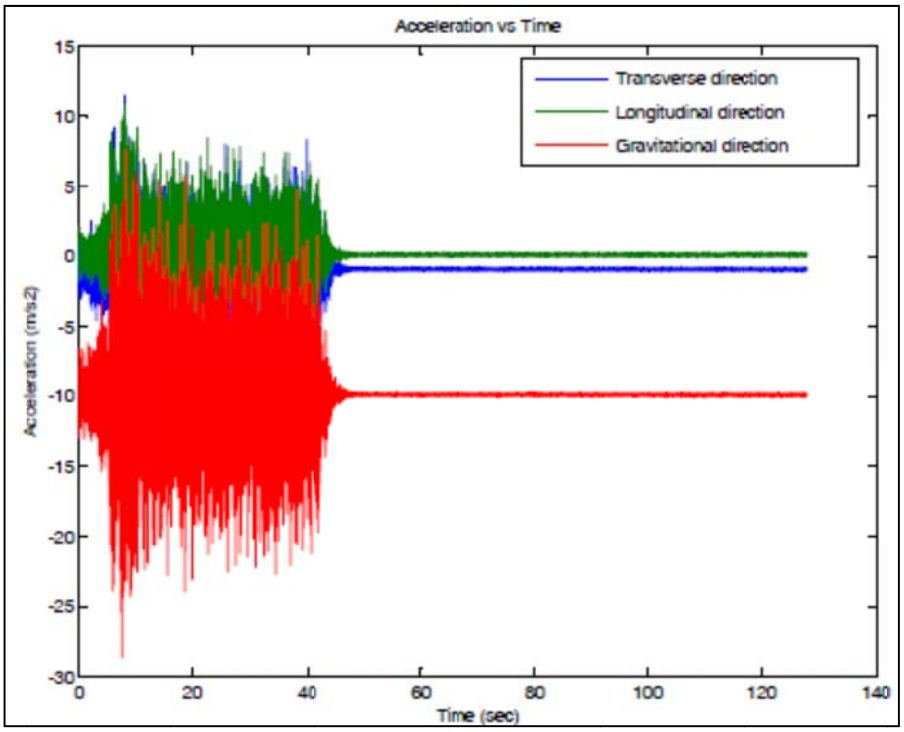

Figure A.2: Acceleration vs. Time graph of first measurement from wireless sensor node237

A.1.2 Locomotive First Cross Dynamic Measurements

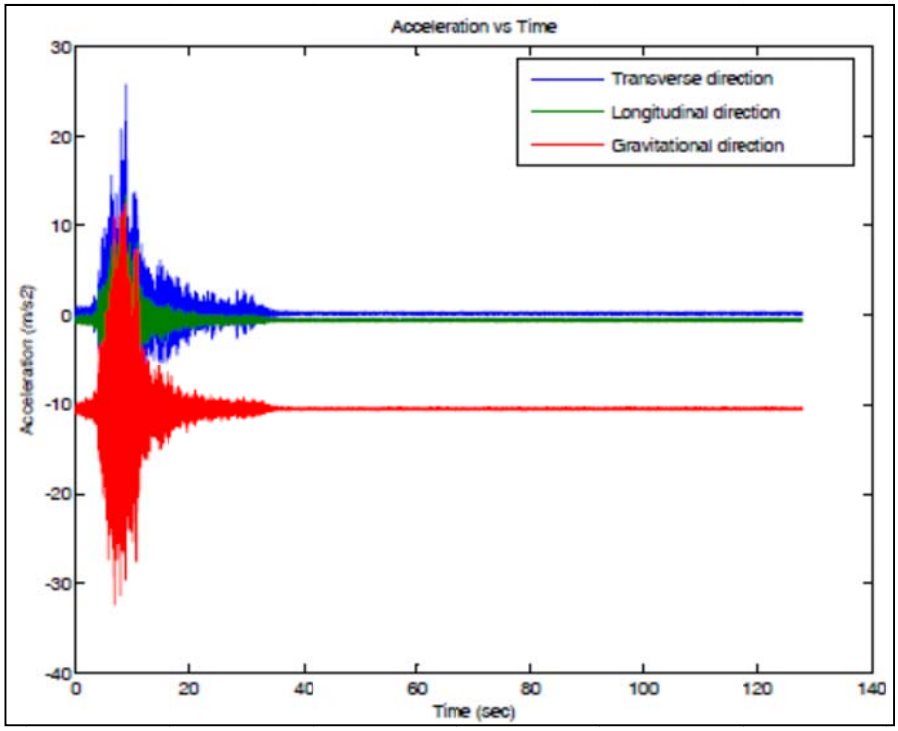

Figure A.3: Acceleration vs. Time graph of second measurement from wireless sensor node229

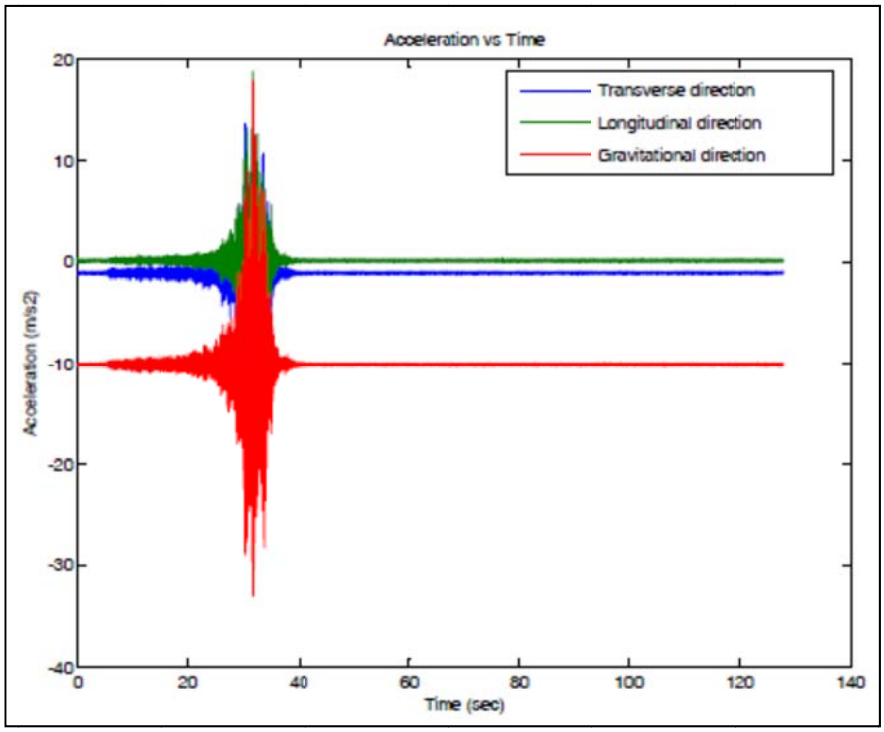

Figure A.4: Acceleration vs. Time graph of second measurement from wireless sensor node237

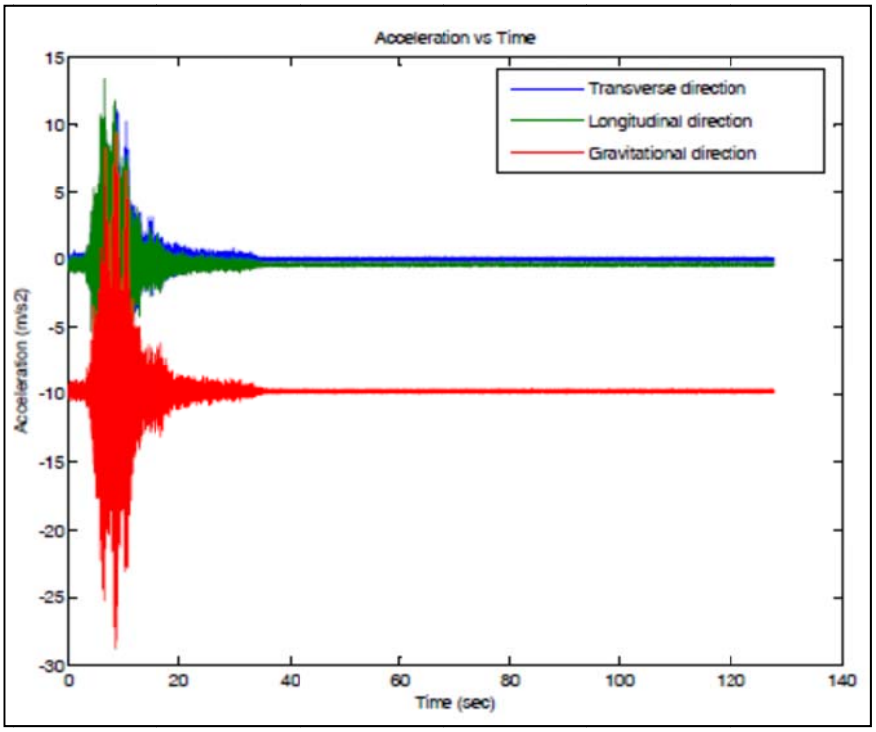

Figure A.5: Acceleration vs. Time graph of second measurement from wireless sensor node242

A.1.3 Locomotive Second Cross Dynamic Measurements

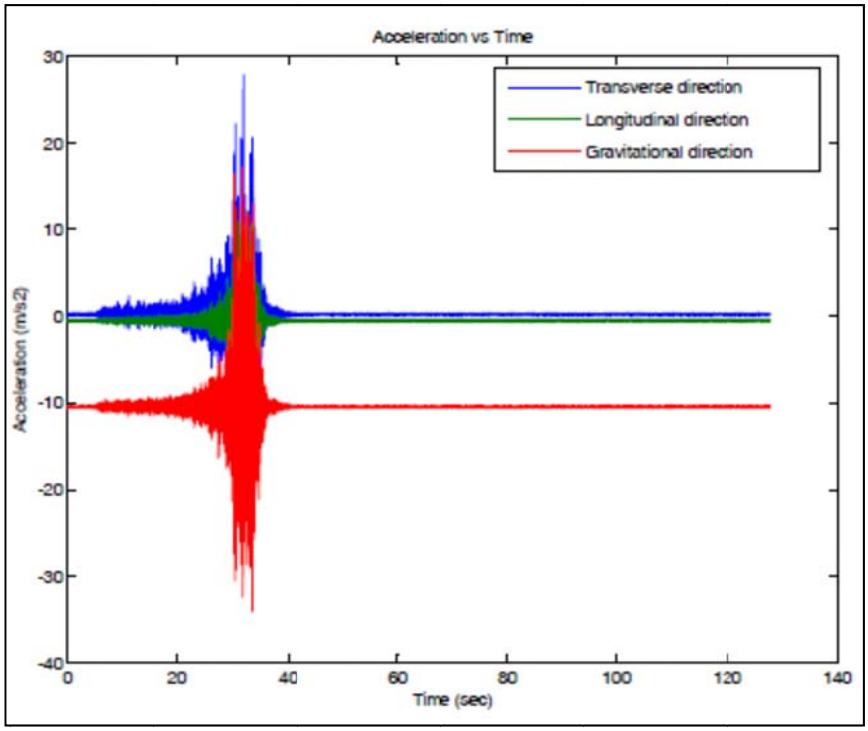

Figure A.6: Acceleration vs. Time graph of third measurement from wireless sensor node229

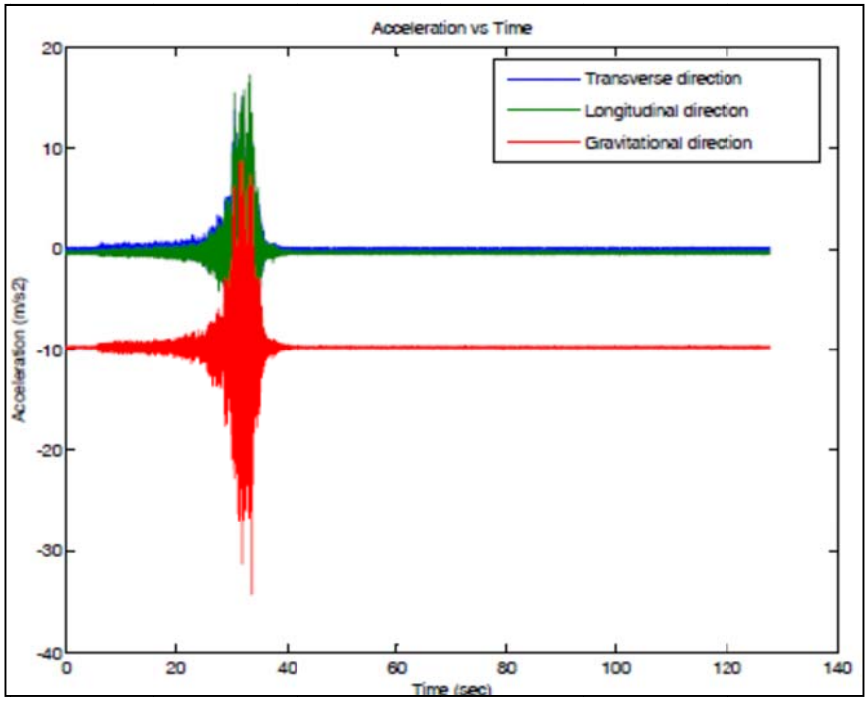

Figure A.7: Acceleration vs. Time graph of third measurement from wireless sensor node242

A.2 Third Field Study Measurements

A.2.1 Passenger Train Cross on 17.12.2010 at 12:08

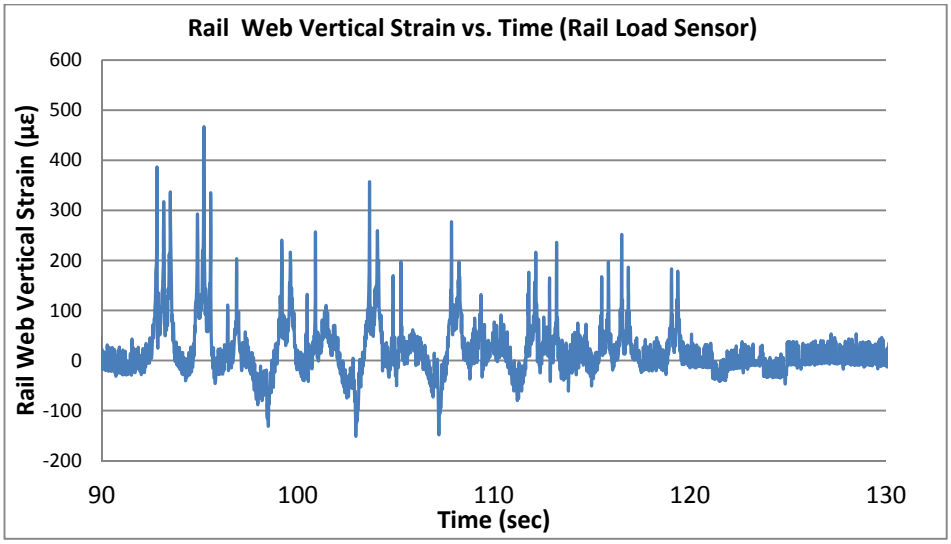

Figure A.8: Rail Load Sensor rail web vertical strain measurements results

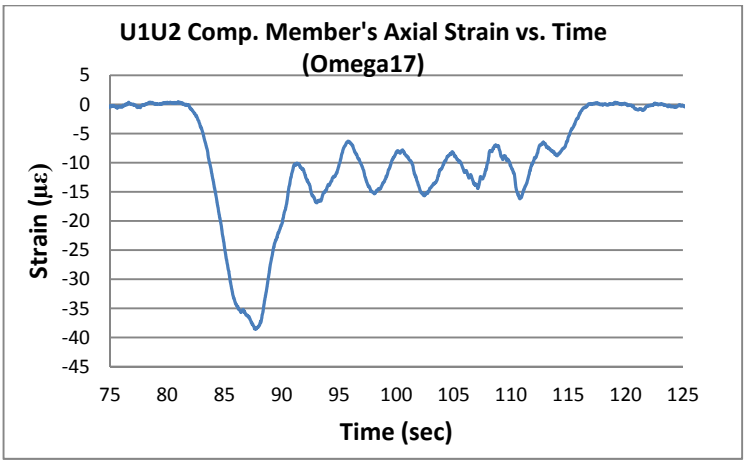

Figure A.9: Compression member Gage17 strain measurements results

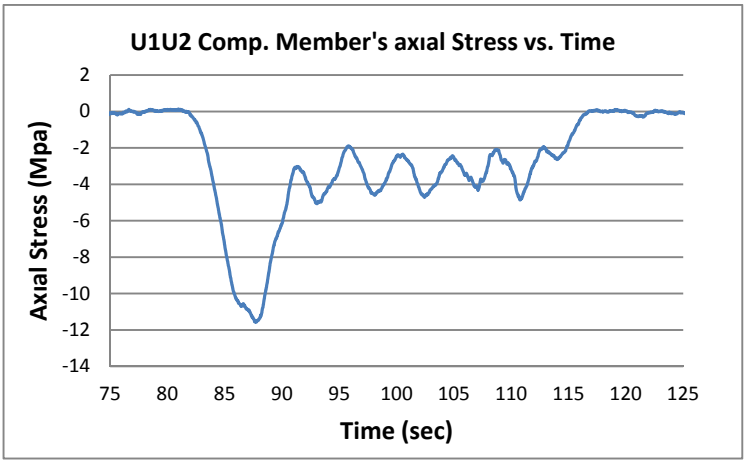

Figure A.10: Compression member calculated stress by strain measurements results

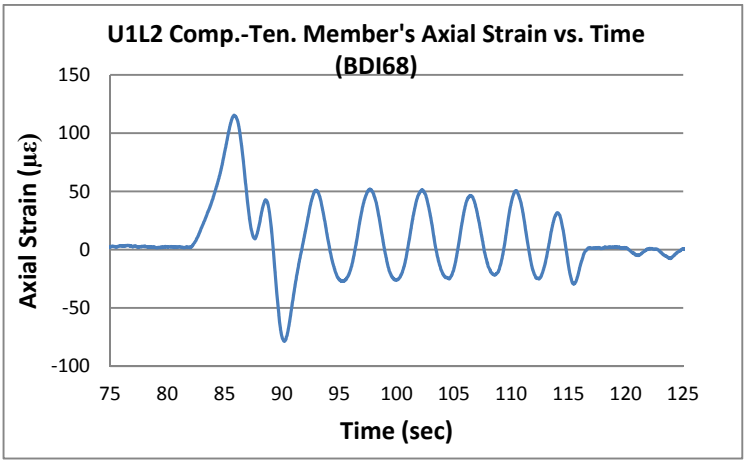

Figure A.11: Comp-ten member BDI68 strain measurements results

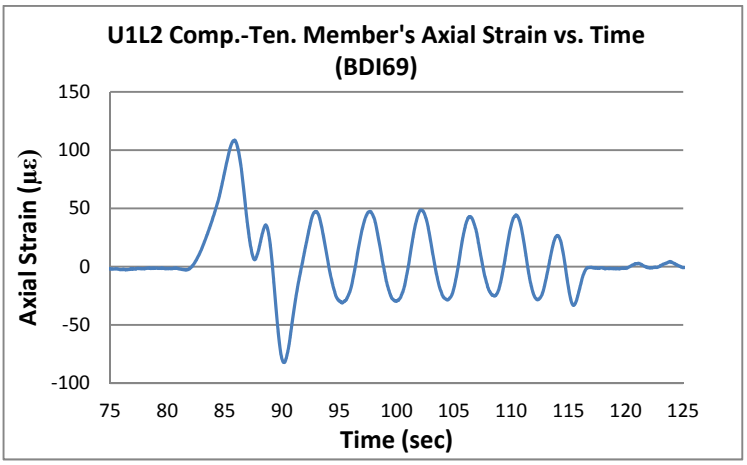

Figure A.12: Comp-ten member BDI69 strain measurements results

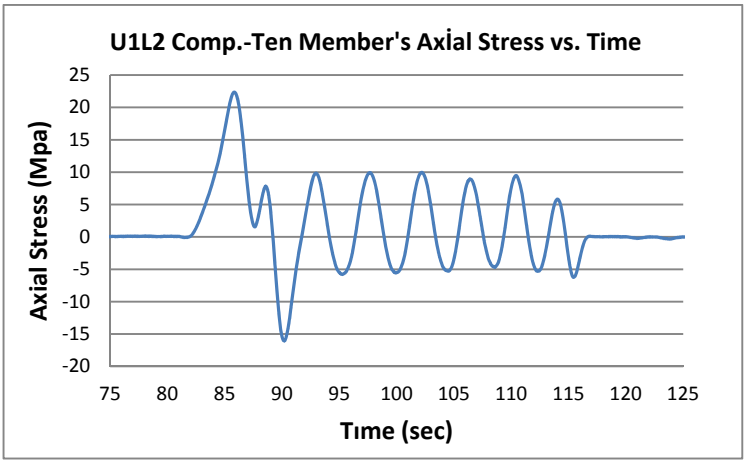

Figure A.13: Comp-ten member calculated stress by strain measurements results

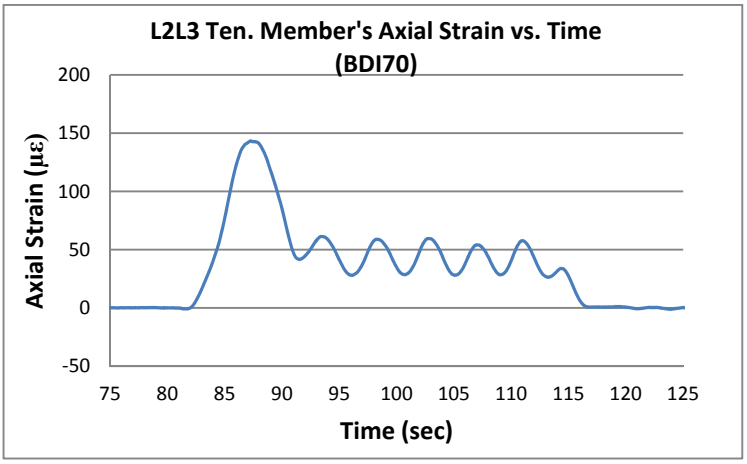

Figure A.14: Tension member BDI70 strain measurements results

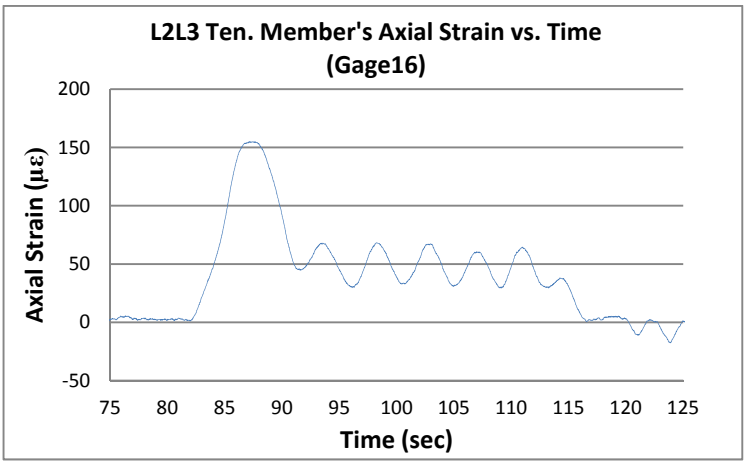

Figure A.15: Tension member Gage16 strain measurements results

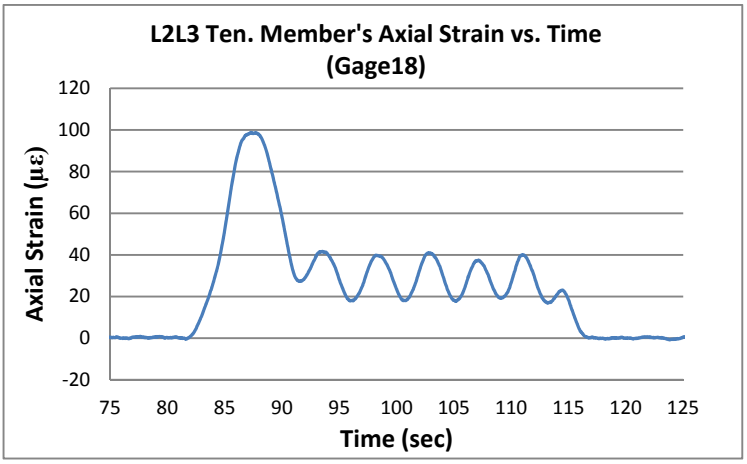

Figure A.16: Tension member Gage18 strain measurements results

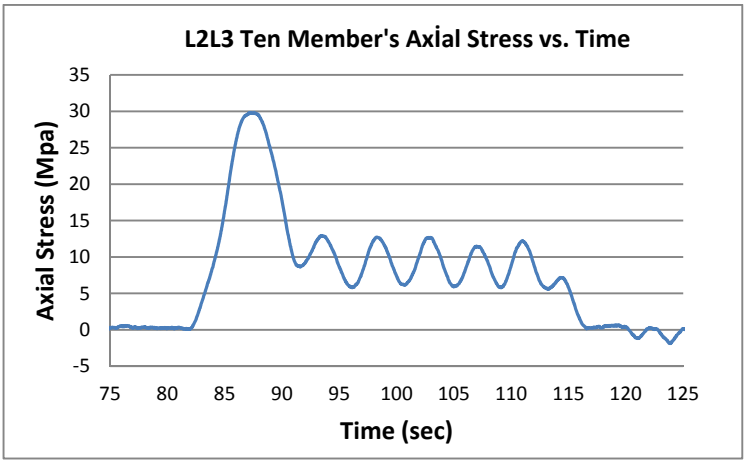

Figure A.17: Tension member calculated stress by strain measurements results

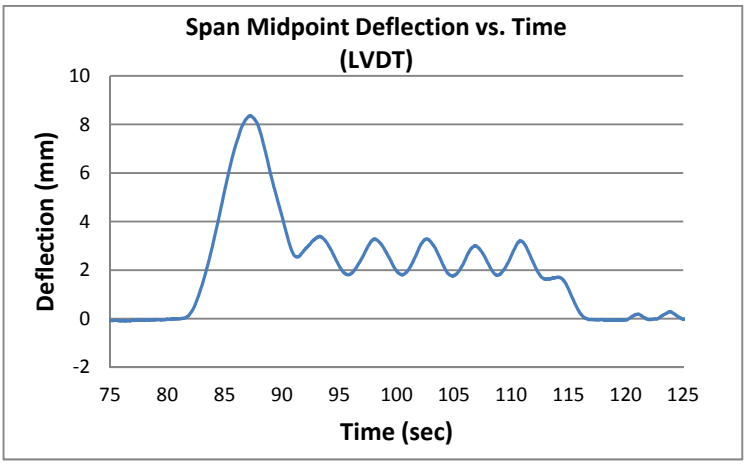

Figure A.18: Truss midpoint deflection measurements results

A.2.2 Goods Train Cross on 17.12.2010 at 12:50

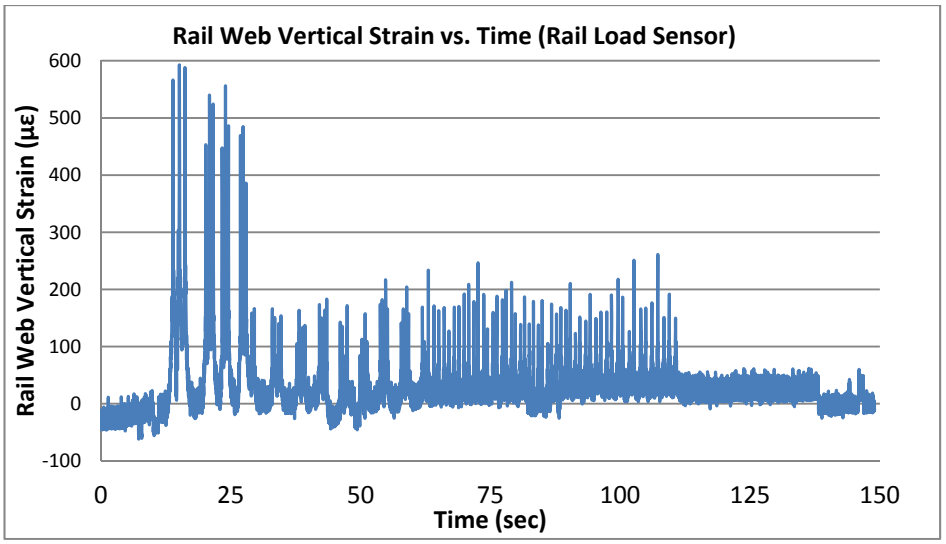

Figure A.19: Rail Load Sensor rail web vertical strain measurements results

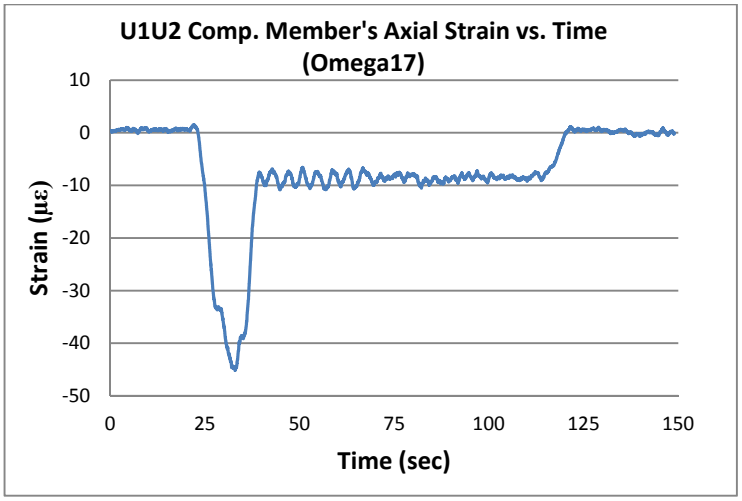

Figure A.20: Compression member Gage17 strain measurements results

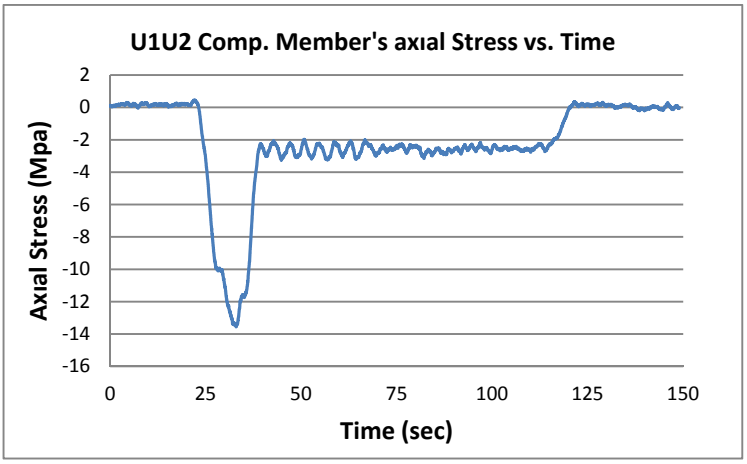

Figure A.21: Compression member calculated stress by strain measurements results

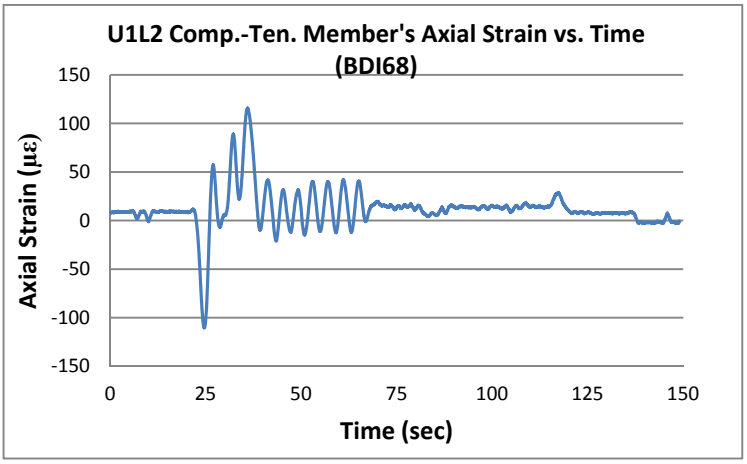

Figure A.22: Comp-ten member BDI68 strain measurements results

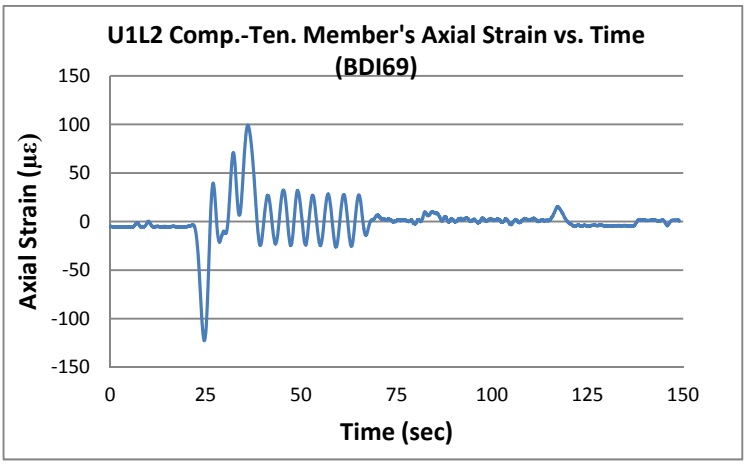

Figure A.23: Comp-ten member BDI69 strain measurements results

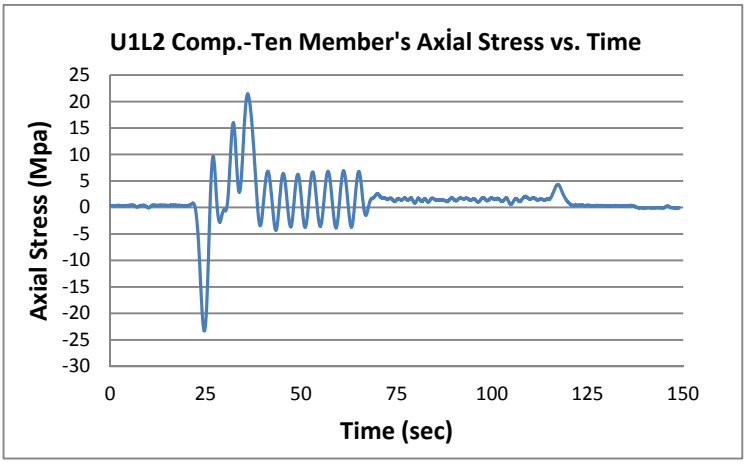

Figure A.24: Comp-ten member calculated stress by strain measurements results

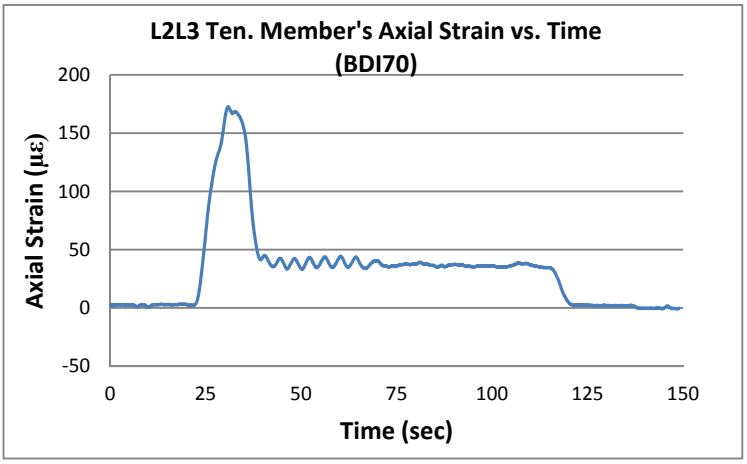

Figure A.25: Tension member BDI70 strain measurements results

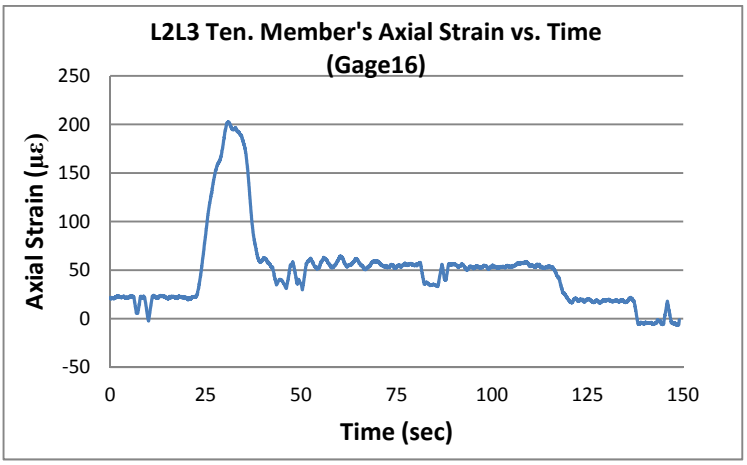

Figure A.26: Tension member Gage16 strain measurements results

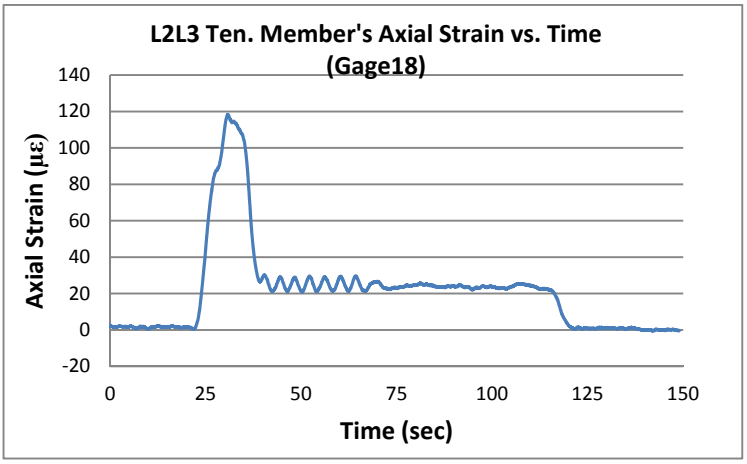

Figure A.27: Tension member Gage18 strain measurements results

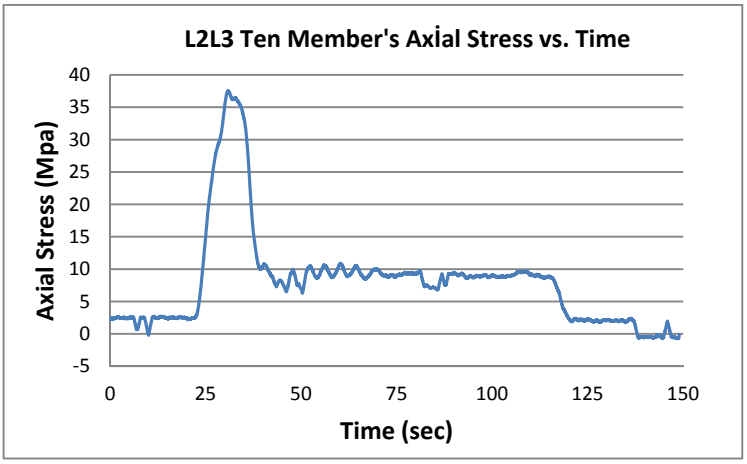

Figure A.28: Tension member calculated stress by strain measurements results

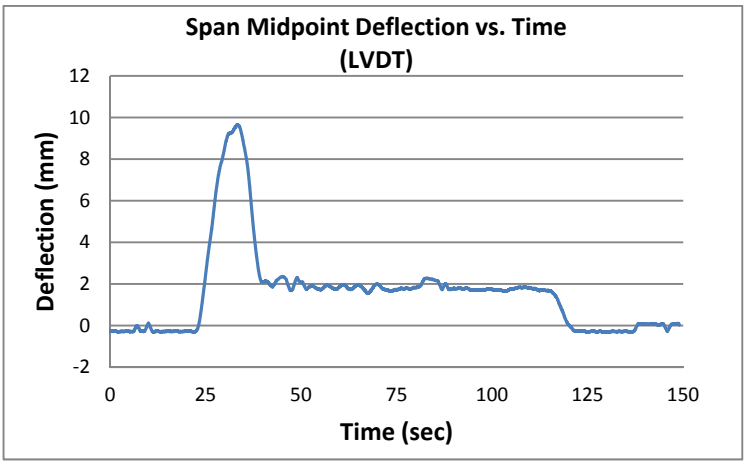

Figure A.29: Truss midpoint deflection measurements results

A.2.3 Goods Train Cross on 17.12.2010 at 14:51

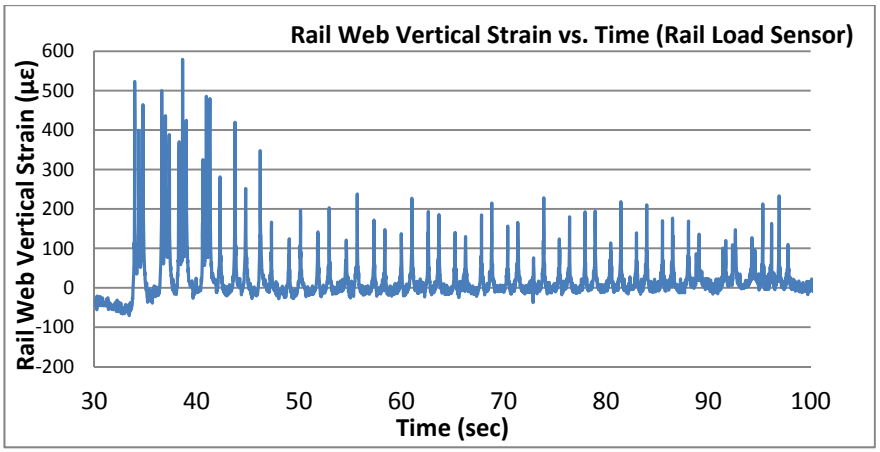

Figure A.30: Rail Load Sensor rail web vertical strain measurements results

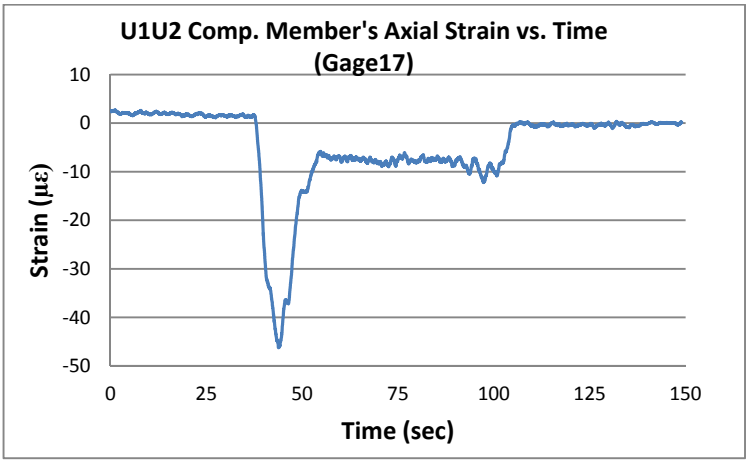

Figure A.31: Compression member Gage17 strain measurements results

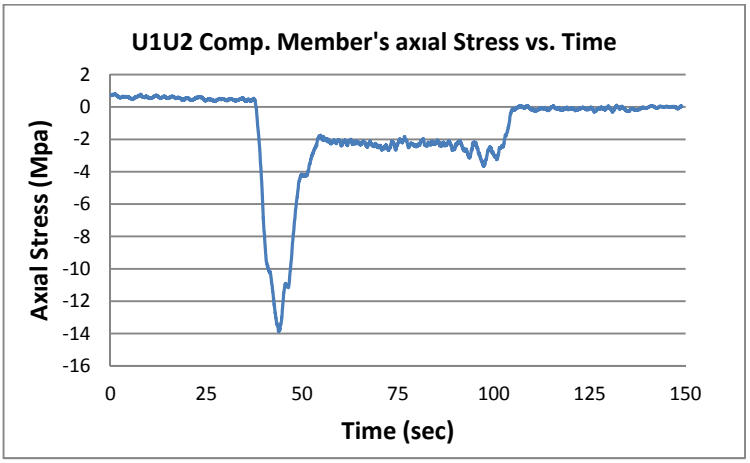

Figure A.32: Compression member calculated stress by strain measurements results

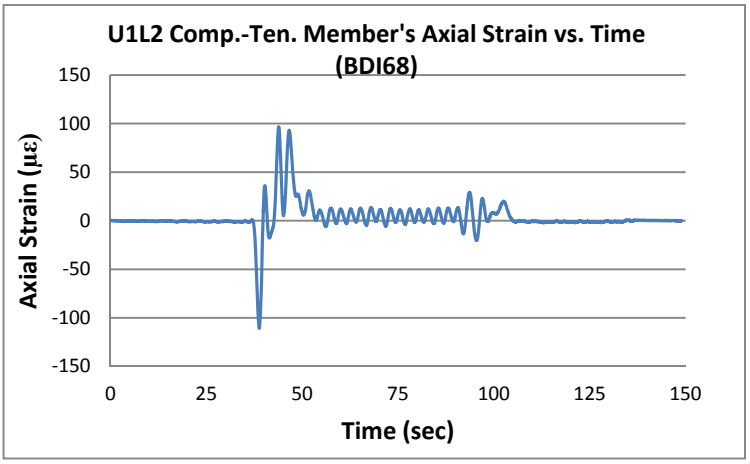

Figure A.33: Comp-ten member BDI68 strain measurements results

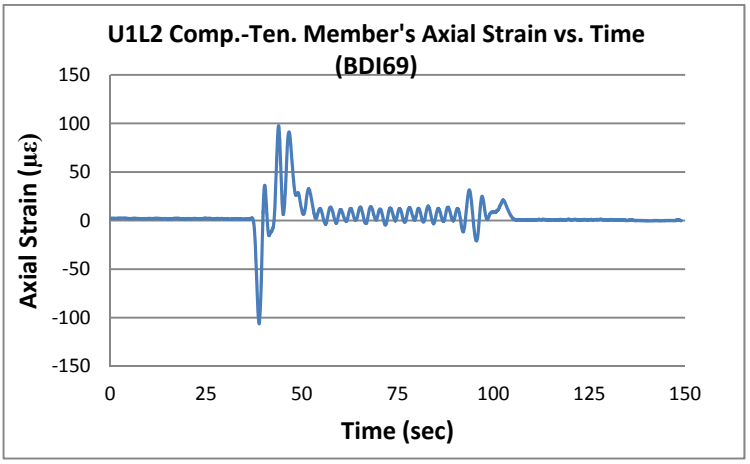

Figure A.34: Comp-ten member BDI69 strain measurements results

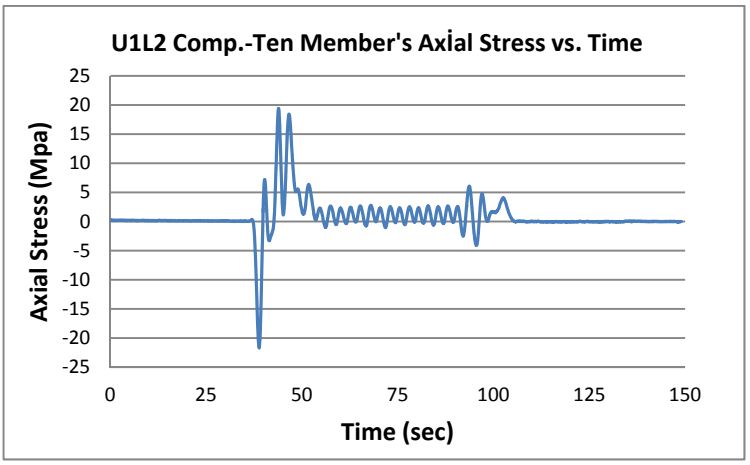

Figure A.35: Comp-ten member calculated stress by strain measurements results

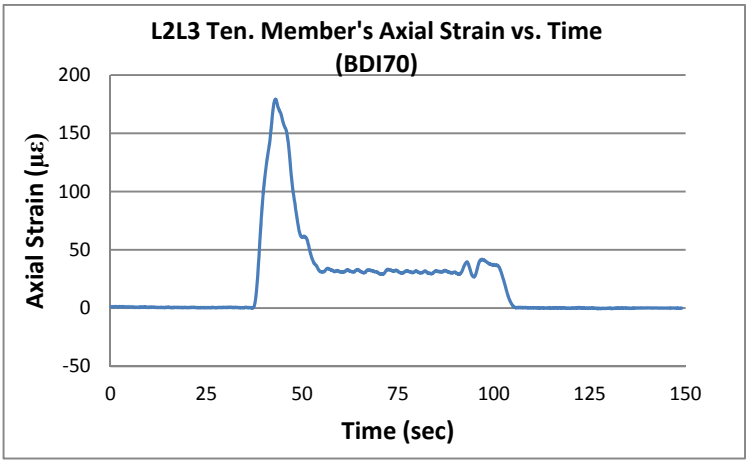

Figure A.36: Tension member BDI70 strain measurements results

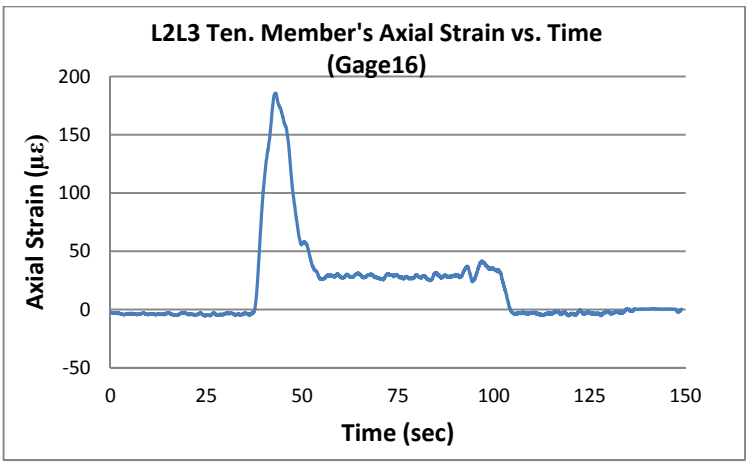

Figure A.37: Tension member Gage16 strain measurements results

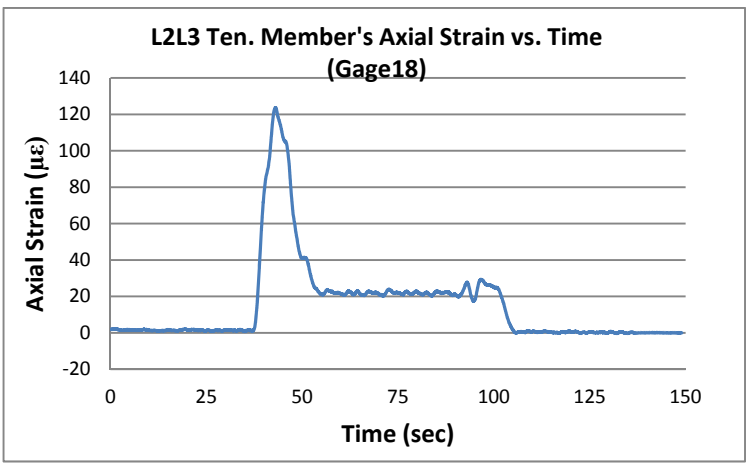

Figure A.38: Tension member Gage18 strain measurements results

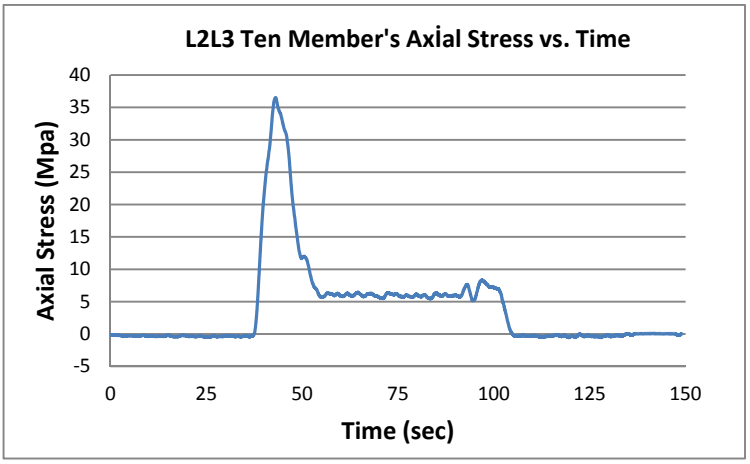

Figure A.39: Tension member calculated stress by strain measurements results

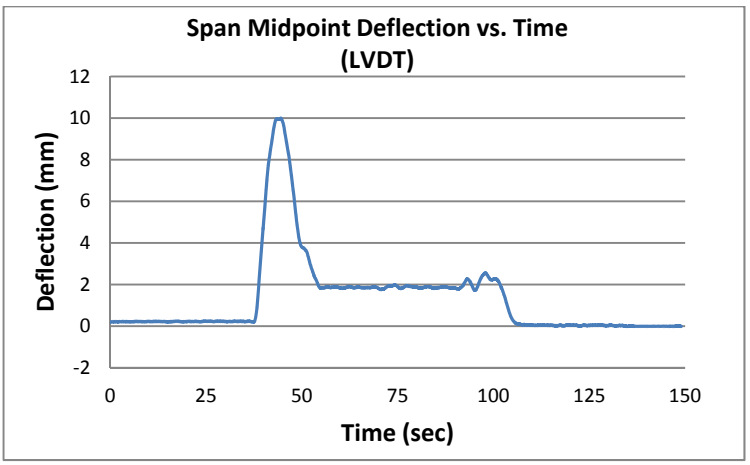

Figure A.40: Truss midpoint deflection measurements results

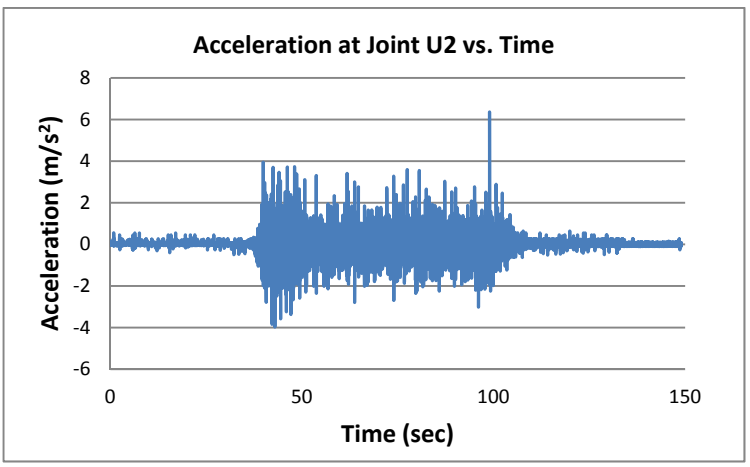

Figure A.41: Joint U2 acceleration measurements results

A.2.4 Locomotive Cross on 18.12.2010 at 02:36

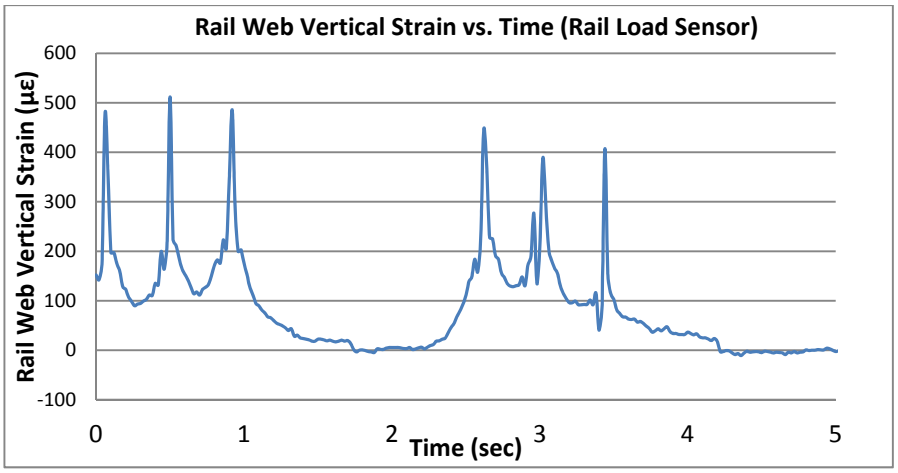

Figure A.42: Rail Load Sensor rail web vertical strain measurements results

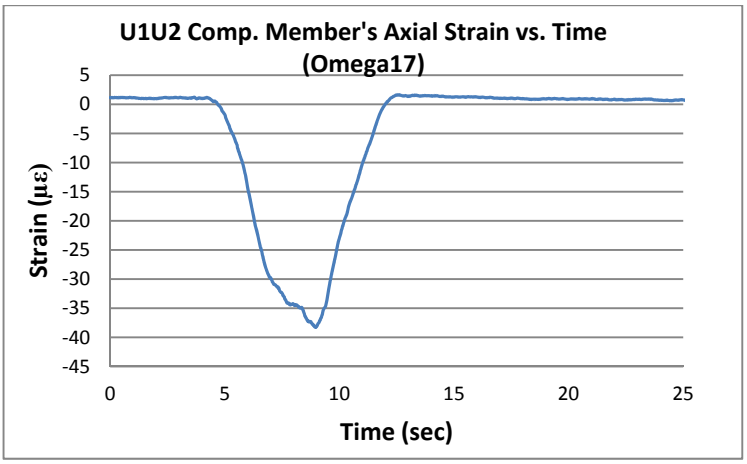

Figure A.43: Compression member Gage17 strain measurements results

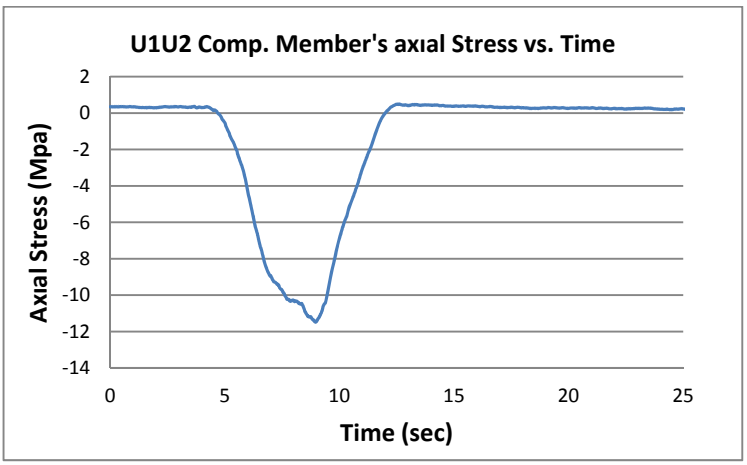

Figure A.44: Compression member calculated stress by strain measurements results

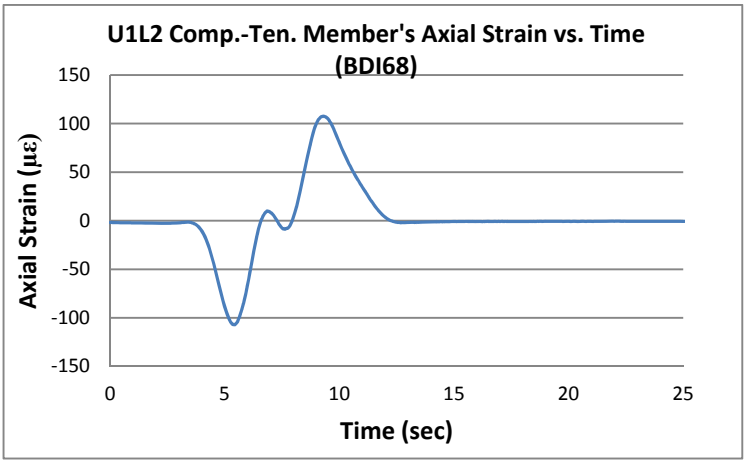

Figure A.45: Comp-ten member BDI68 strain measurements results

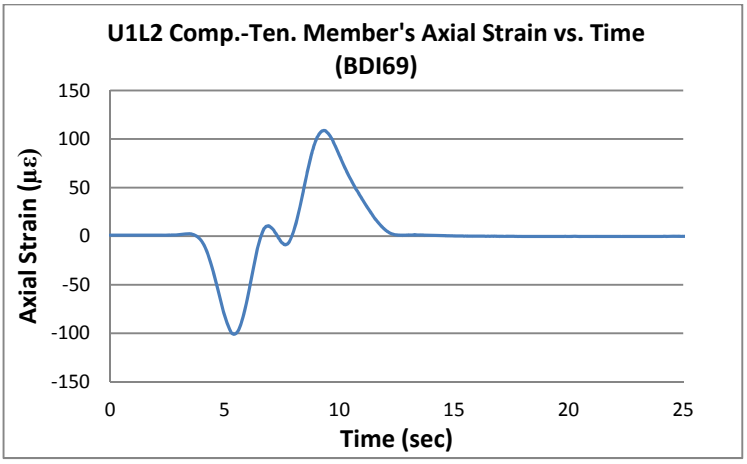

Figure A.46: Comp-ten member BDI69 strain measurements results

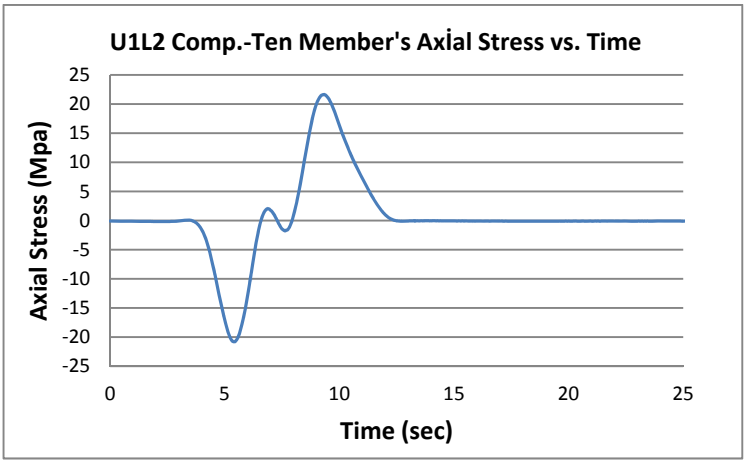

Figure A.47: Comp-ten member calculated stress by strain measurements results

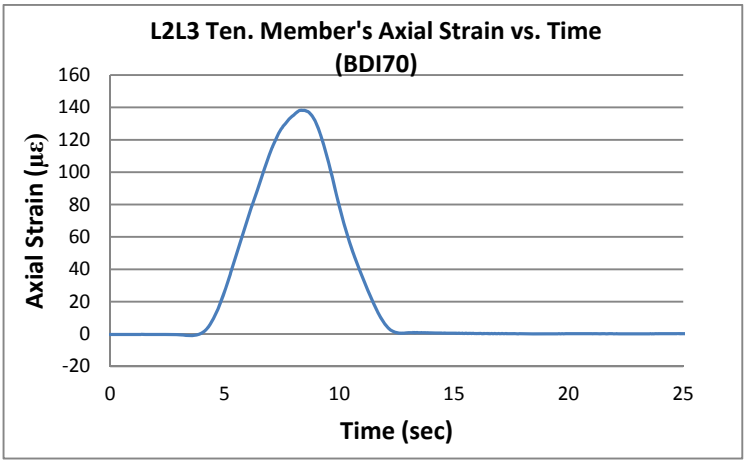

Figure A.48: Tension member BDI70 strain measurements results

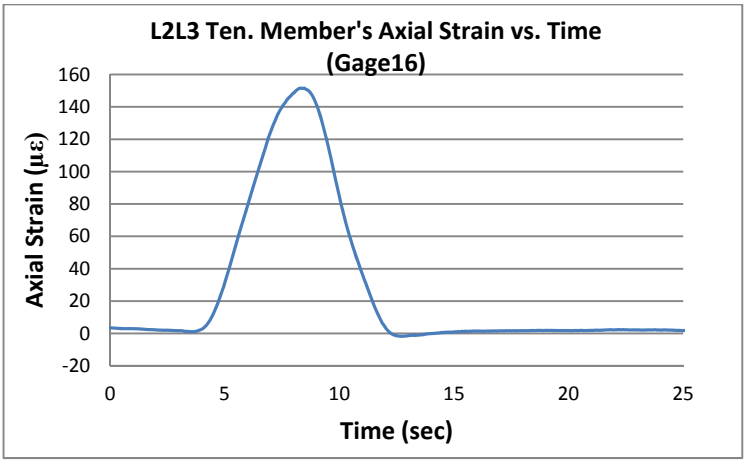

Figure A.49: Tension member Gage16 strain measurements results

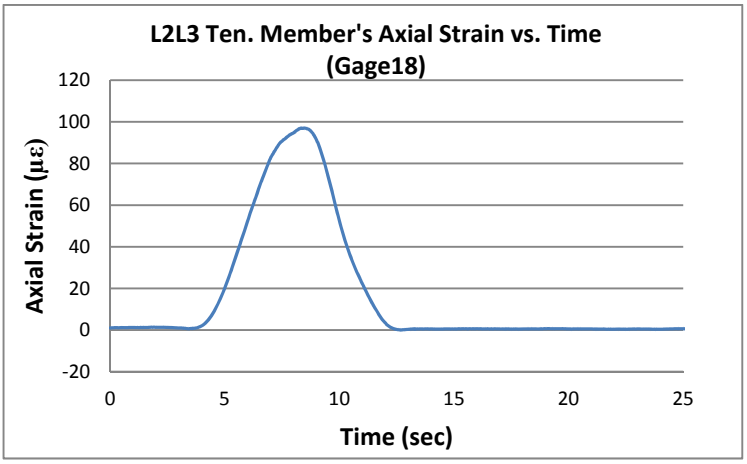

Figure A.50: Tension member Gage18 strain measurements results

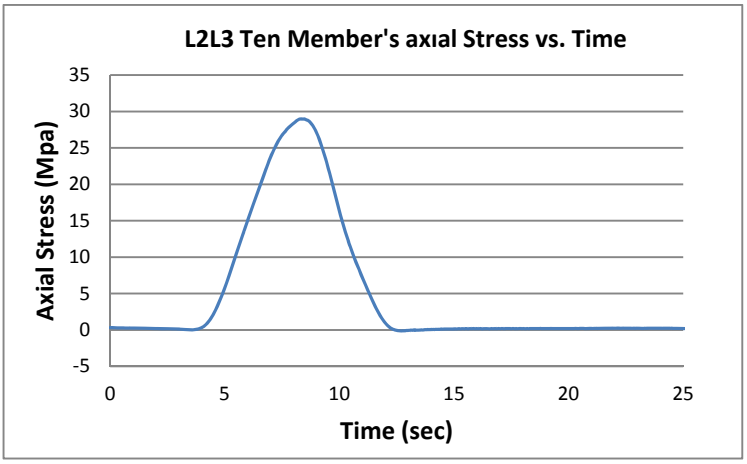

Figure A.51: Tension member calculated stress by strain measurements results

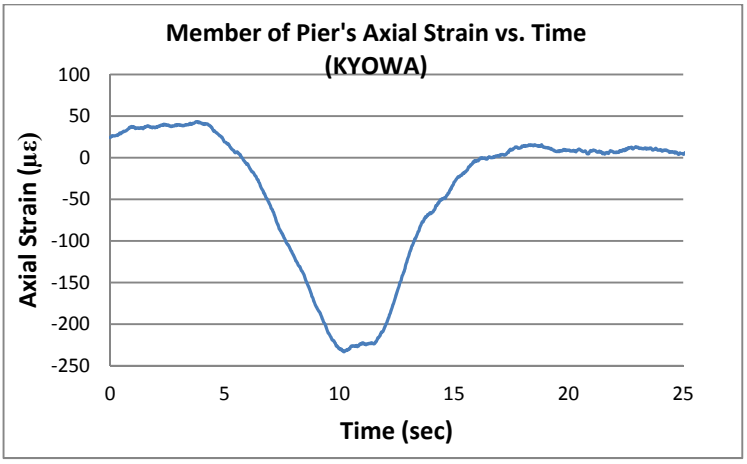

Figure A.52: Member of pier Kyowa gage strain measurements results

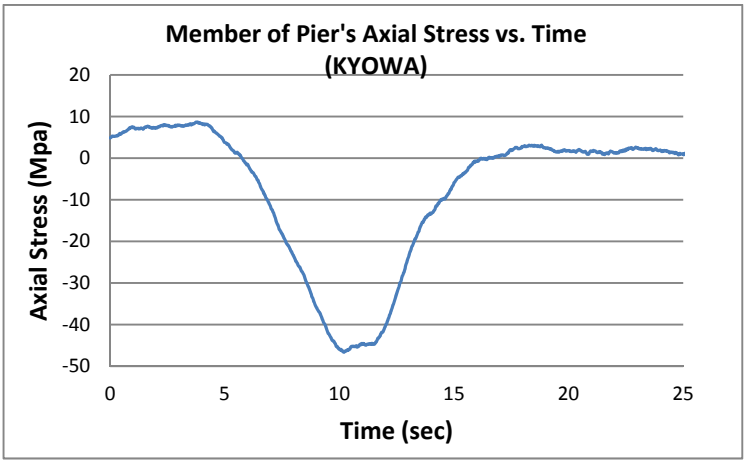

Figure A.53: Member of pier calculated stress by strain measurements results

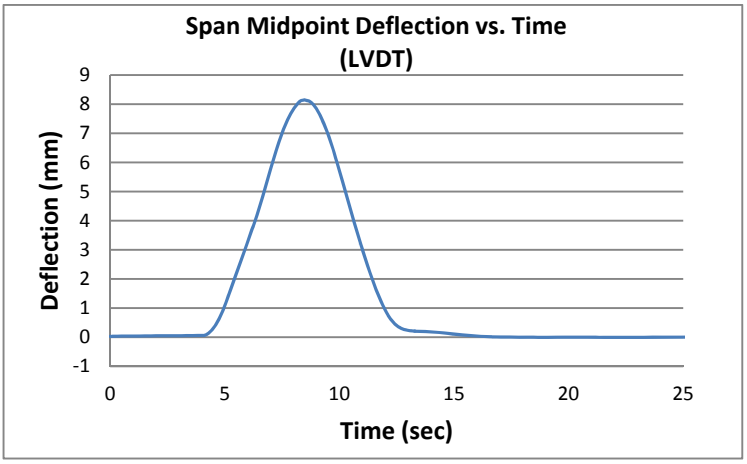

Figure A.54: Truss midpoint deflection measurements results

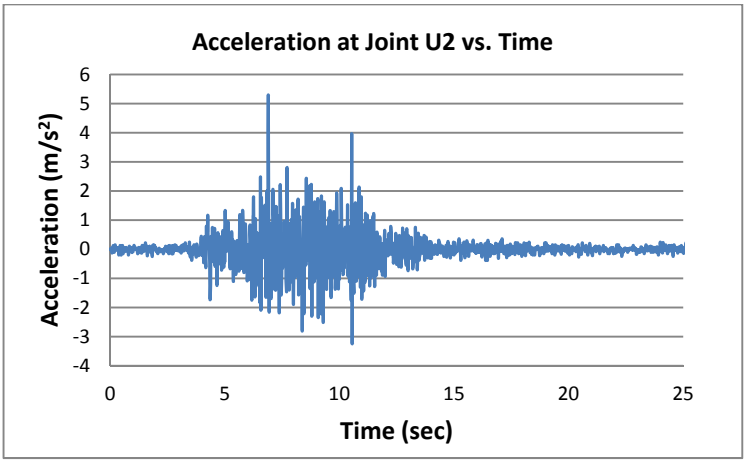

Figure A.55: Joint U2 acceleration measurements results

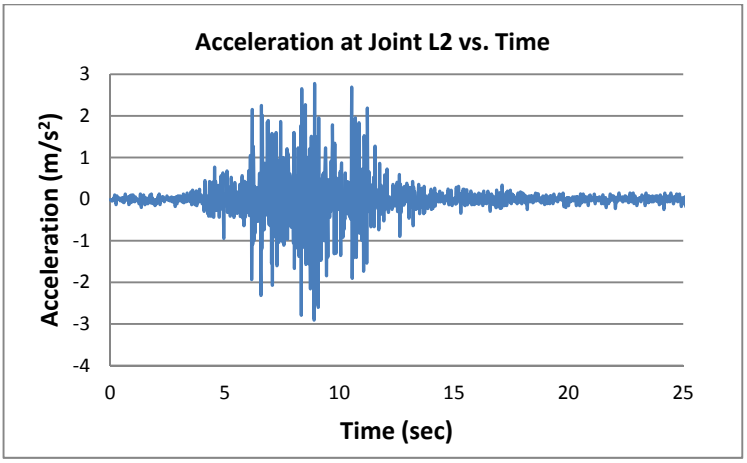

Figure A.56: Joint L2 acceleration measurements results

A.2.4 Goods Train Cross on 18.12.2010 at 04:30

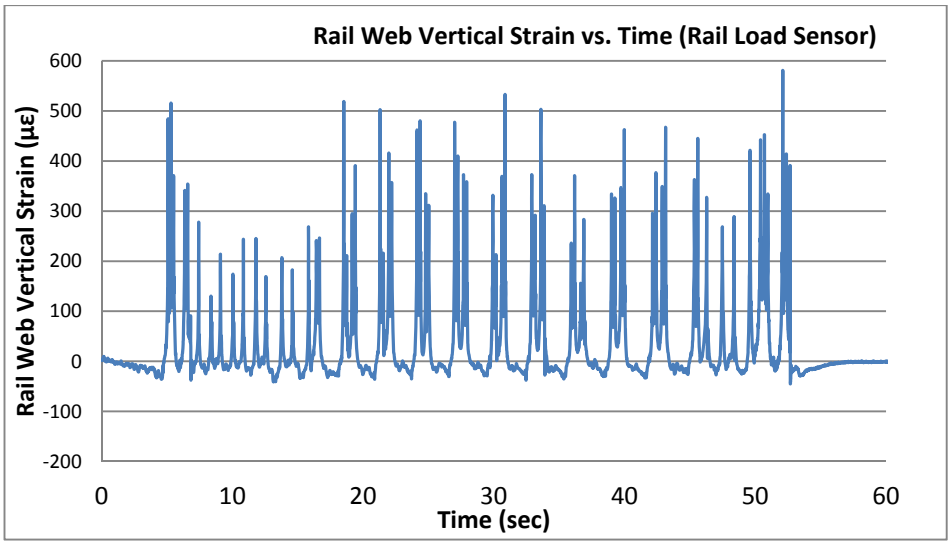

Figure A.57: Rail Load Sensor rail web vertical strain measurements results

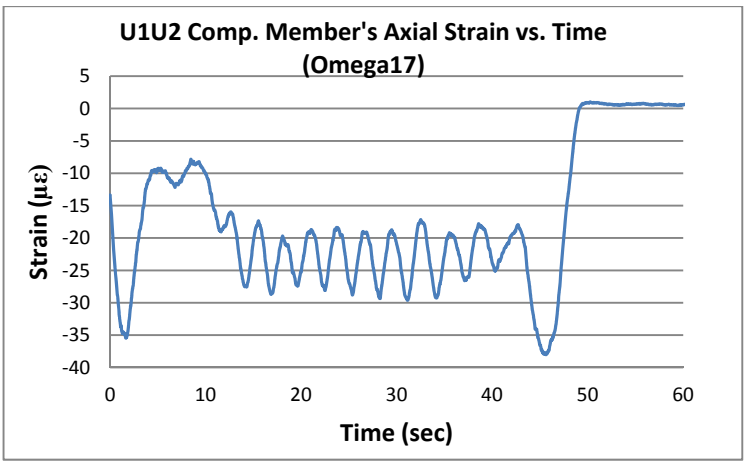

Figure A.58: Compression member Gage17 strain measurements results

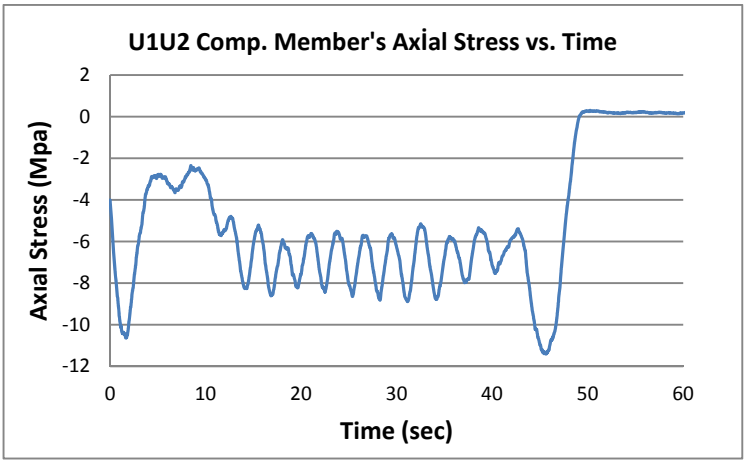

Figure A.59: Compression member calculated stress by strain measurements results

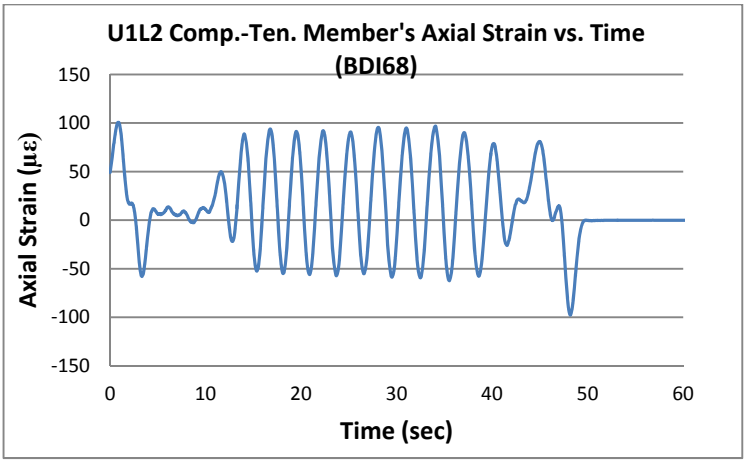

Figure A.60: Comp-ten member BDI68 strain measurements results

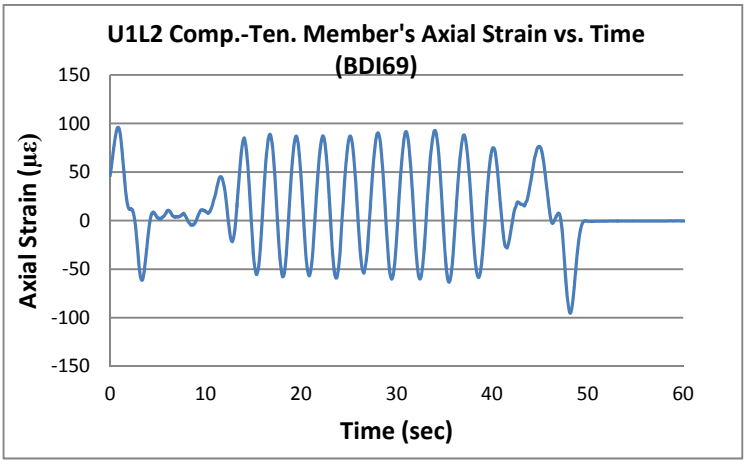

Figure A.61: Comp-ten member BDI69 strain measurements results

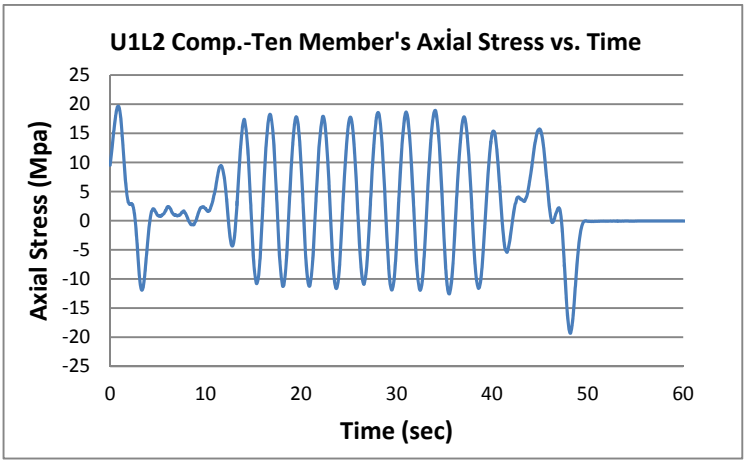

Figure A.62: Comp-ten member calculated stress by strain measurements results

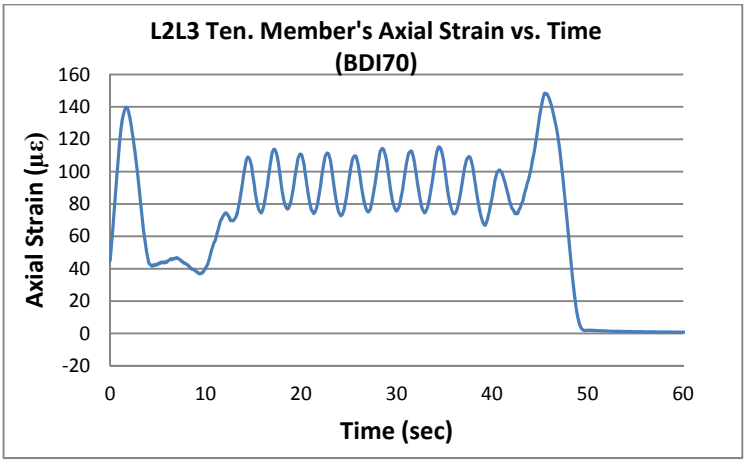

Figure A.63: Tension member BDI70 strain measurements results

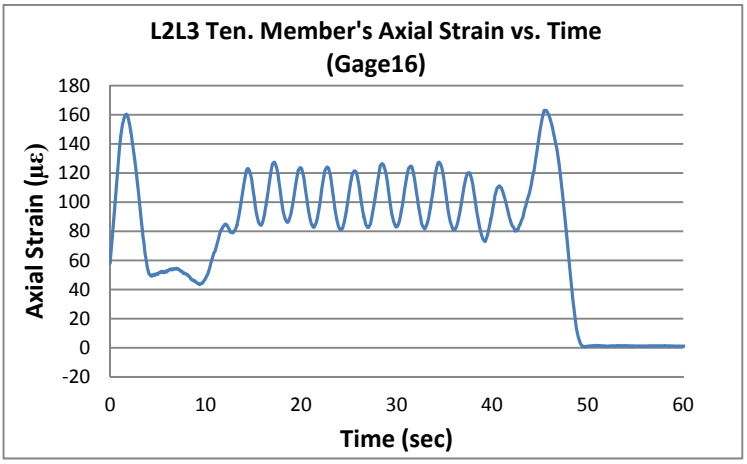

Figure A.64: Tension member Gage16 strain measurements results

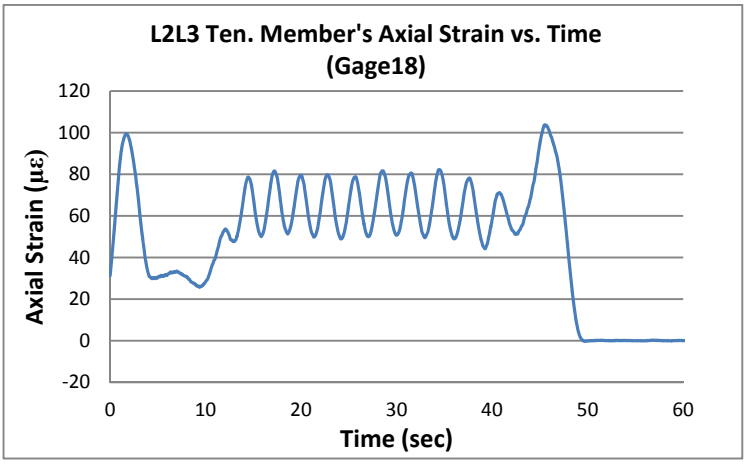

Figure A.65: Tension member Gage18 strain measurements results

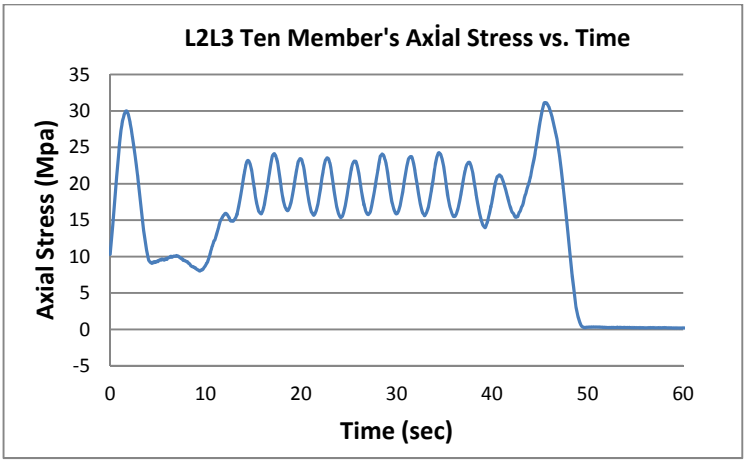

Figure A.66: Tension member calculated stress by strain measurements results

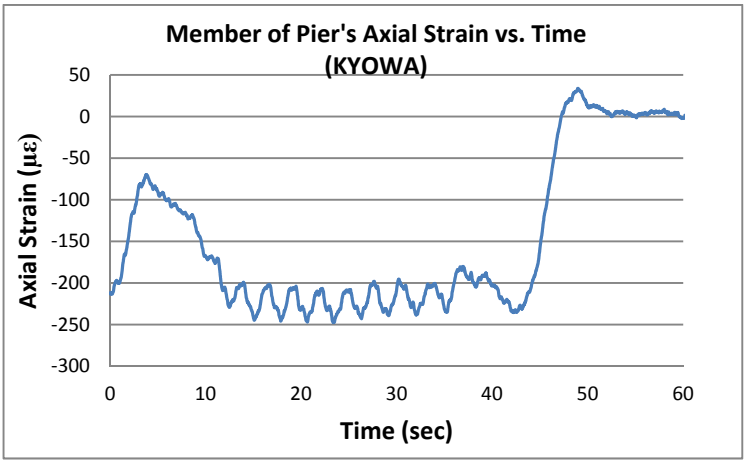

Figure A.67: Member of pier Kyowa gage strain measurements results

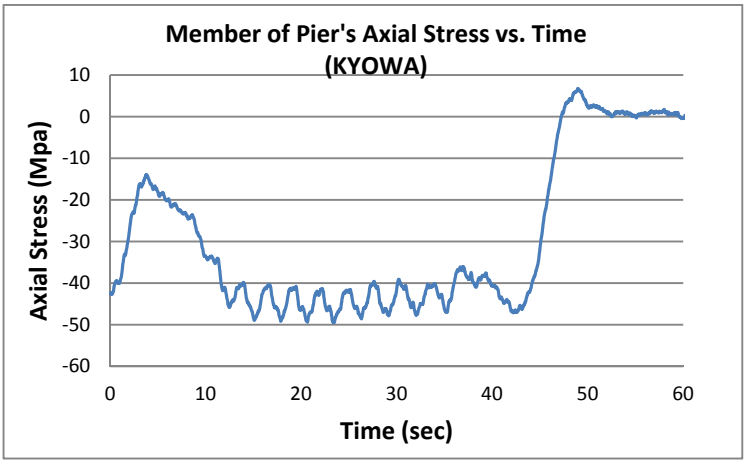

Figure A.68: Member of pier calculated stress by strain measurements results

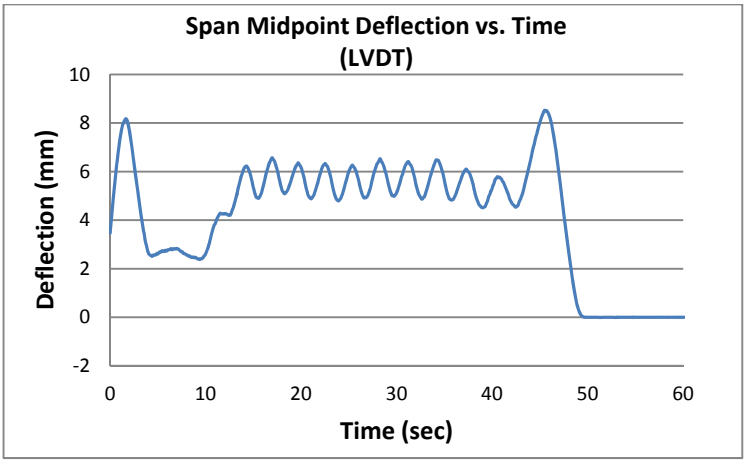

Figure A.69: Truss midpoint deflection measurements results

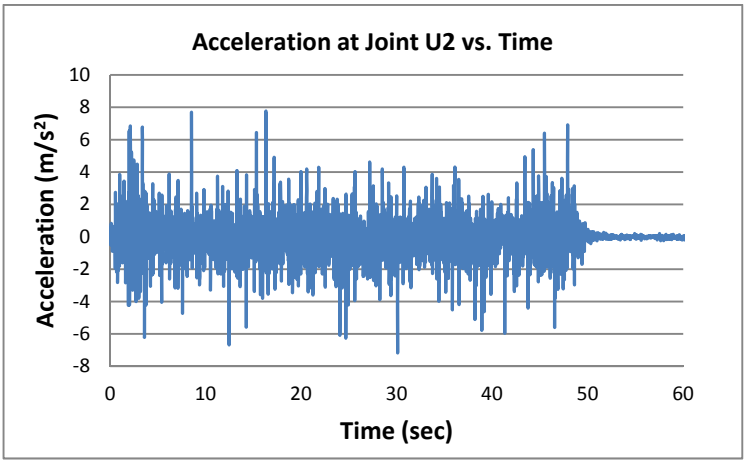

Figure A.70: Joint U2 acceleration measurements results

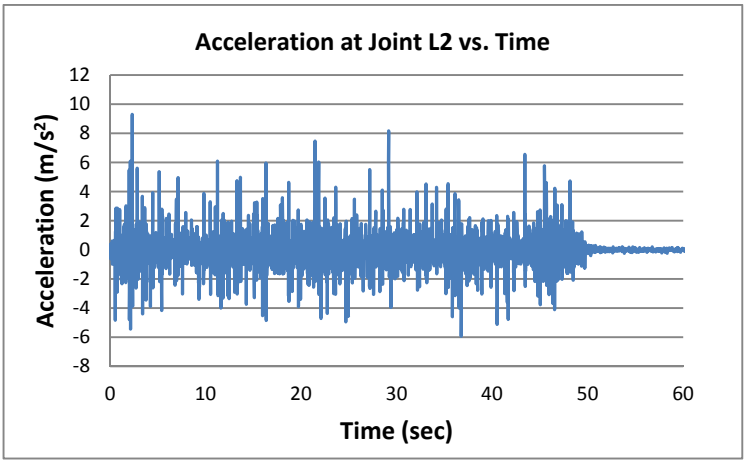

Figure A.71: Joint L2 acceleration measurements results

APPENDIX B

CAPACITY INDEX (CI) AND RELIABILITY INDEX (β) RESULTS

B.1 CI Results for Members

B.1.1 LM71 (Design Train Moving Load) CI Results

B.1.1.1 CombI ($Q + Q_c + W_{+y} + B + Self$) CI Results for Members

Table B.1: CombI CI Results for Truss Members

	Member	Max	Min		Member	Max	Min
RIGHT TRUSS	U0-U1	-0.054	-0.333	**LEFT TRUSS**	U0-U1	0.068	-0.221
	U1-U2	-0.034	-0.425		U1-U2	-0.079	-0.343
	U0-L1	0.331	0.026		U0-L1	0.246	0.026
	L1-L2	0.382	0.029		L1-L2	0.284	0.028
	L1-U1	-0.037	-0.459		L1-U1	-0.036	-0.347
	U1-L2	0.228	-0.234		U1-L2	0.178	-0.168
	L2-U2	0.033	-0.407		L2-U2	0.023	-0.303
	U2-L3	0.162	-0.241		U2-L3	0.122	-0.176
	L2-L3	0.402	0.028		L2-L3	0.301	0.028
	U2-U2'	-0.016	-0.358		U2-U2'	-0.065	-0.297
	System	**0.402**	**-0.459**		**System**	**0.301**	**-0.347**

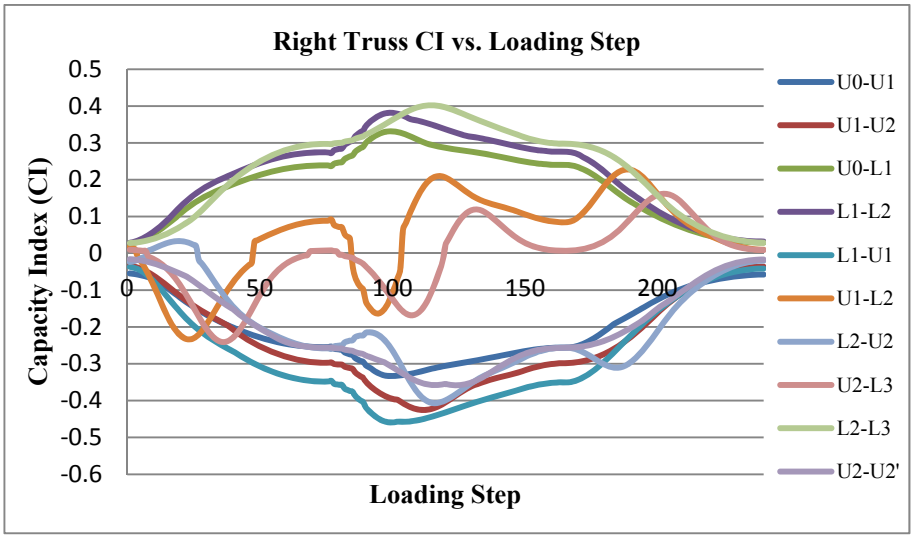

Figure B.1: CombI Right Truss CI vs. Loading Step (max=0.402, min=-0.459)

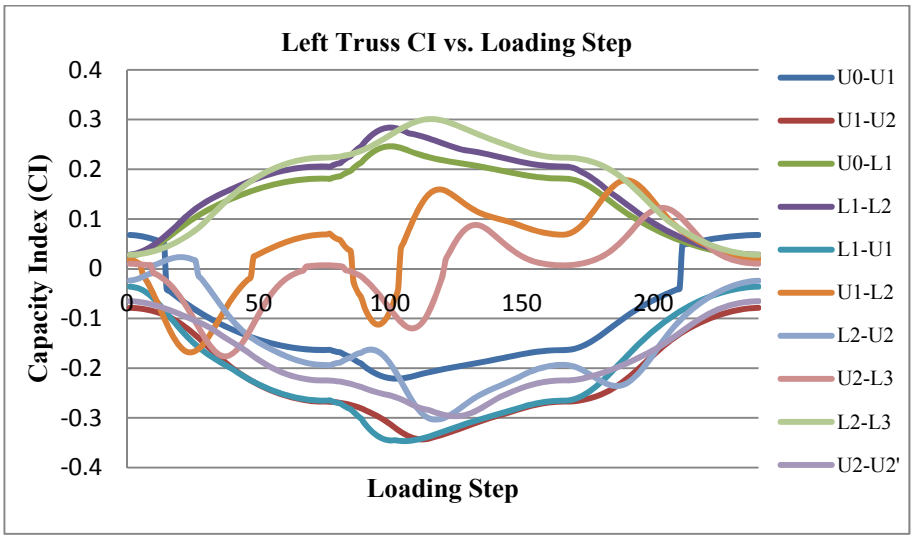

Figure B.2: CombI Left Truss CI vs. Loading Step (max=0.301, min=-0.347)

Table B.2: CombI CI Results for Floor Beams and Lateral Braces

Member	Max	Min
FB-0	-0.014	-0.017
R0-L1	-0.271	-0.300
R1-L 1	0.074	0.065
R1-L2	-0.242	-0.271
FB-1	0.019	0.016
R2-L 3	-0.188	-0.207
R3-L3	0.033	0.028
R3-L 4	-0.142	-0.161
FB-2	0.013	0.012
R4-L5	-0.093	-0.102
R5-L5	0.011	0.010
System	**0.074**	**-0.300**

Table B.3: CombI CI Results for Vertical Braces

Member	Max	Min
L1-U1	0.021	0.018
U1-L2	0.066	0.058
L2-U2	0.071	0.063
U2-L3	0.008	0.007
System	**0.071**	**0.007**

B.1.1.2 CombII ($Q + Q_c + W_{+y} + A + Self$) CI Results for Members

Table B.4: CombII CI Results for Truss Members

	Member	Max	Min		Member	Max	Min
RIGHT TRUSS	U0-U1	-0.092	-0.352	**LEFT TRUSS**	U0-U1	-0.032	-0.246
	U1-U2	-0.060	-0.436		U1-U2	-0.075	-0.348
	U0-L1	0.331	0.026		U0-L1	0.246	0.026
	L1-L2	0.382	0.029		L1-L2	0.284	0.028
	L1-U1	-0.037	-0.459		L1-U1	-0.036	-0.347
	U1-L2	0.228	-0.234		U1-L2	0.178	-0.168
	L2-U2	0.033	-0.407		L2-U2	0.023	-0.303
	U2-L3	0.162	-0.241		U2-L3	0.122	-0.176
	L2-L3	0.402	0.028		L2-L3	0.301	0.028
	U2-U2'	-0.030	-0.373		U2-U2'	-0.066	-0.301
	System	**0.402**	**-0.459**		**System**	**0.301**	**-0.348**

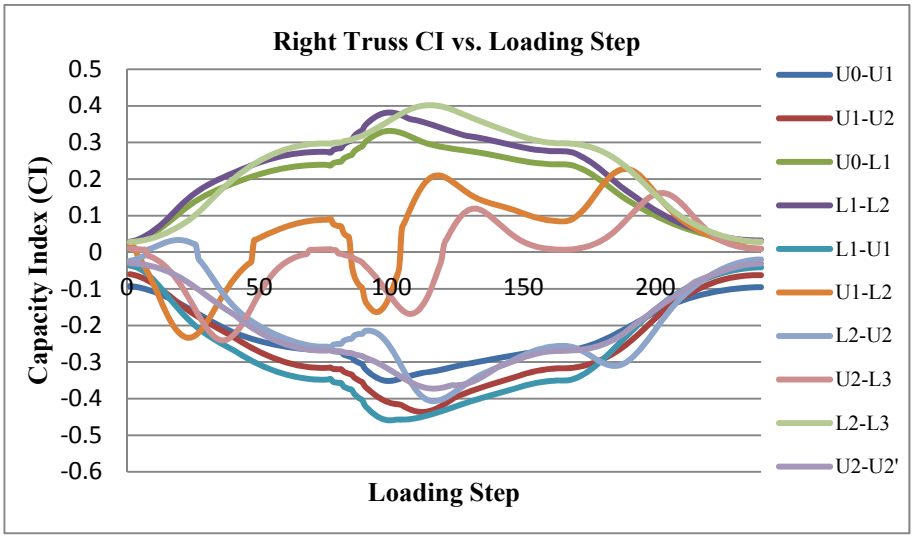

Figure B.3: CombII Right Truss CI vs. Loading Step (max=0.402, min=-0.459)

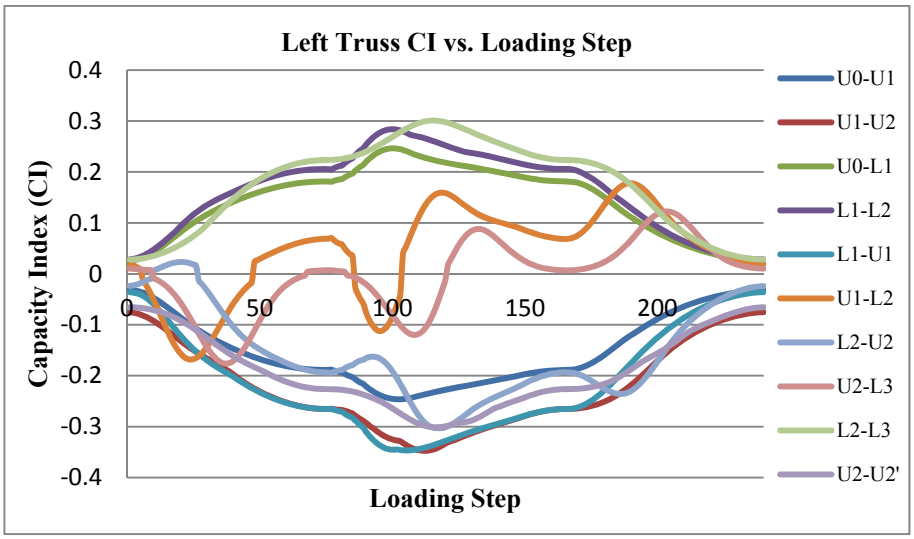

Figure B.4: CombII Left Truss CI vs. Loading Step (max=0.301, min=-0.348)

Table B.5: CombII CI Results for Floor Beams and Lateral Braces

Member	Max	Min
FB-0	0.012	-0.012
R0-L1	-0.232	-0.261
R1-L 1	0.062	0.053
R1-L2	-0.219	-0.249
FB-1	0.017	0.015
R2-L 3	-0.170	-0.188
R3-L3	0.029	0.025
R3-L 4	-0.133	-0.152
FB-2	0.009	0.008
R4-L5	-0.100	-0.109
R5-L5	0.011	0.011
System	**0.062**	**-0.261**

Table B.6: CombII CI Results for Vertical Braces

Member	Max	Min
L1-U1	0.020	0.017
U1-L2	0.055	0.048
L2-U2	0.059	0.051
U2-L3	0.007	0.006
System	**0.059**	**0.006**

B.1.1.3 CombIII ($Q + Q_c + W_{-y} + B + Self$) CI Results for Members

Table B.7: CombIII CI Results for Truss Members

	Member	Max	Min		Member	Max	Min
RIGHT TRUSS	U0-U1	0.050	-0.331	**LEFT TRUSS**	U0-U1	-0.072	-0.277
	U1-U2	-0.061	-0.469		U1-U2	-0.036	-0.308
	U0-L1	0.331	0.026		U0-L1	0.246	0.026
	L1-L2	0.382	0.029		L1-L2	0.284	0.028
	L1-U1	-0.037	-0.460		L1-U1	-0.036	-0.347
	U1-L2	0.228	-0.234		U1-L2	0.178	-0.168
	L2-U2	0.033	-0.407		L2-U2	0.023	-0.303
	U2-L3	0.162	-0.241		U2-L3	0.122	-0.176
	L2-L3	0.402	0.028		L2-L3	0.301	0.028
	U2-U2'	-0.057	-0.394		U2-U2'	-0.018	-0.261
	System	**0.402**	**-0.469**		**System**	**0.301**	**-0.347**

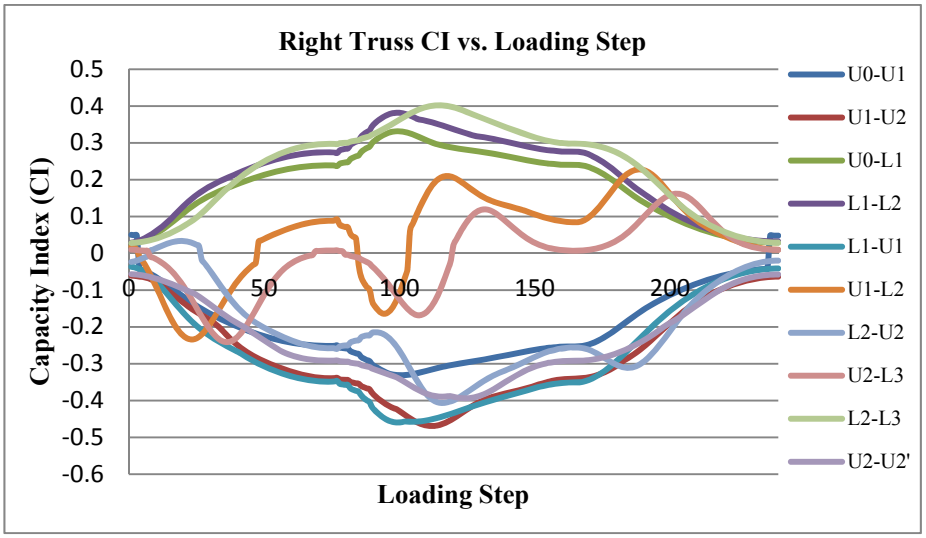

Figure B.5: CombIII Right Truss CI vs. Loading Step (max=0.402, min=-0.469)

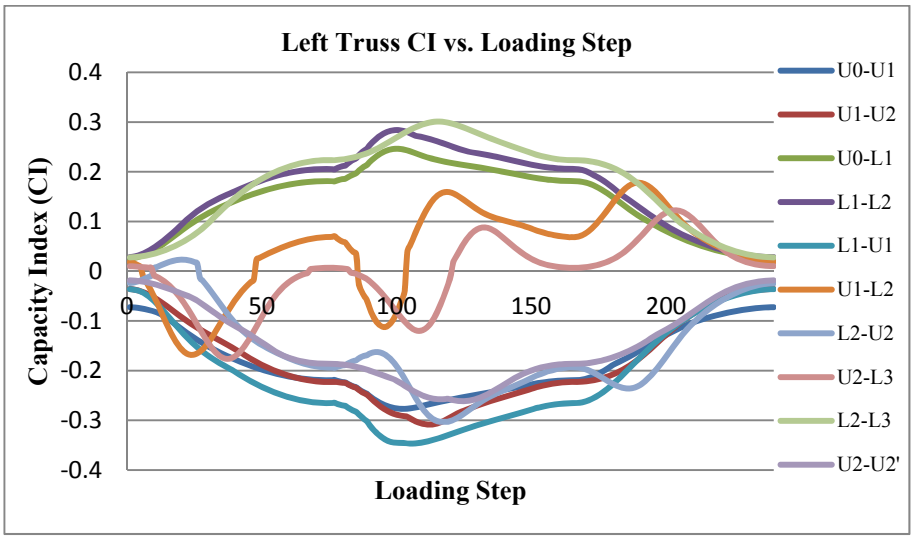

Figure B.6: CombIII Left Truss CI vs. Loading Step (max=0.301, min=-0.347)

Table B.8: CombIII CI Results for Floor Beams and Lateral Braces

Member	Max	Min
FB-0	0.031	0.028
R0-L1	0.135	0.125
R1-L 1	-0.192	-0.215
R1-L2	0.124	0.115
FB-1	-0.024	-0.026
R2-L 3	0.093	0.086
R3-L3	-0.073	-0.082
R3-L 4	0.078	0.072
FB-2	-0.015	-0.016
R4-L5	0.063	0.060
R5-L5	-0.025	-0.025
System	**0.135**	**-0.215**

Table B. 9: CombIII CI Results for Vertical Braces

Member	Max	Min
L1-U1	0.023	0.020
U1-L2	0.065	0.058
L2-U2	0.070	0.062
U2-L3	0.008	0.007
System	**0.070**	**0.007**

B.1.2 Ultimate Service Goods Train Load CI Results

B.1.2.1 CombI (Q + Q_c + W_{+y} + B + Self) CI Results for Members

Table B.10: CombI CI Results for Truss Members

	Member	Max	Min		Member	Max	Min
RIGHT TRUSS	U0-U1	-0.054	-0.221	LEFT TRUSS	U0-U1	0.068	-0.139
	U1-U2	-0.034	-0.246		U1-U2	-0.079	-0.231
	U0-L1	0.206	0.026		U0-L1	0.158	0.026
	L1-L2	0.238	0.028		L1-L2	0.179	0.028
	L1-U1	-0.036	-0.296		L1-U1	-0.036	-0.227
	U1-L2	0.195	-0.249		U1-L2	0.149	-0.180
	L2-U2	0.042	-0.271		L2-U2	0.029	-0.204
	U2-L3	0.142	-0.207		U2-L3	0.108	-0.151
	L2-L3	0.243	0.028		L2-L3	0.184	0.028
	U2-U2'	-0.016	-0.203		U2-U2'	-0.065	-0.195
	System	**0.243**	**-0.296**		**System**	**0.184**	**-0.231**

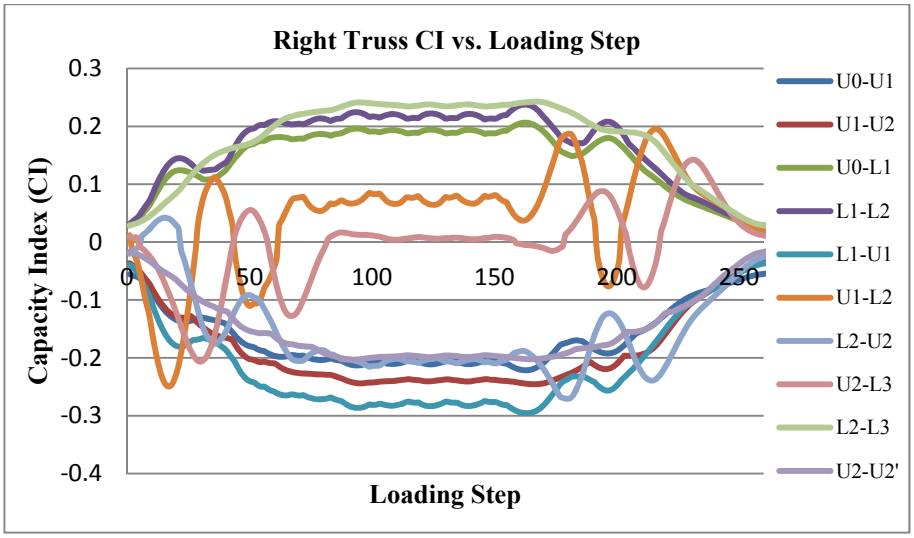

Figure B.7: CombII Right Truss CI vs. Loading Step (max=0.243, min=-0.296)

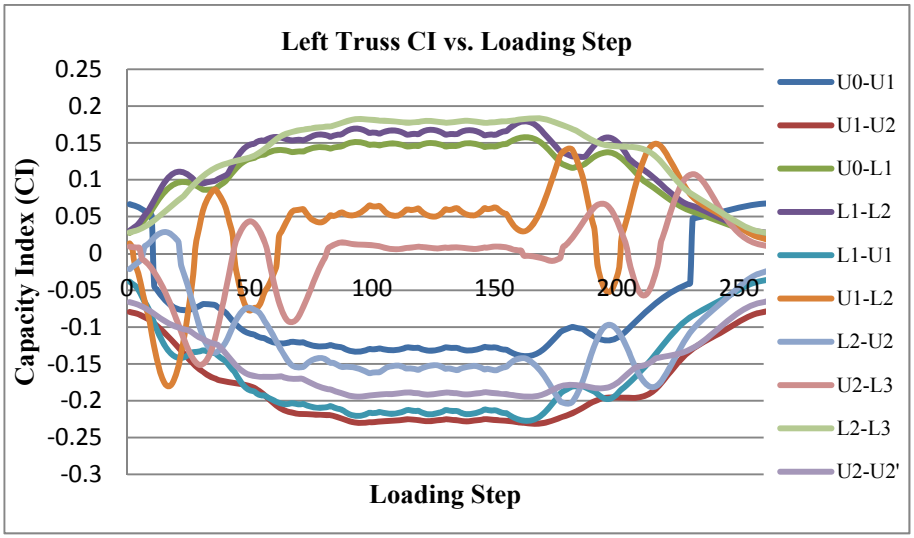

Figure B.8: CombII left Truss CI vs. Loading Step (max=0.184, min=-0.231)

Table B.11: CombI CI Results for Floor Beams and Lateral Braces

Member	Max	Min
FB-0	-0.015	-0.017
R0-L1	-0.281	-0.300
R1-L 1	0.074	0.069
R1-L2	-0.253	-0.271
FB-1	0.019	0.017
R2-L 3	-0.196	-0.207
R3-L3	0.033	0.030
R3-L 4	-0.150	-0.161
FB-2	0.013	0.012
R4-L5	-0.096	-0.102
R5-L5	0.011	0.010
System	**0.074**	**-0.300**

Table B.12: CombI CI Results for Vertical Braces

Member	Max	Min
L1-U1	0.031	0.028
U1-L2	0.097	0.090
L2-U2	0.104	0.097
U2-L3	0.011	0.010
System	**0.104**	**0.010**

B.1.2.2 CombII (Q + Q_c + W_{+y} + A + Self) CI Results for Members

Table B.13: CombII CI Results for Truss Members

	Member	Max	Min		Member	Max	Min
RIGHT TRUSS	U0-U1	-0.092	-0.235	LEFT TRUSS	U0-U1	-0.032	-0.164
	U1-U2	-0.060	-0.270		U1-U2	-0.075	-0.230
	U0-L1	0.206	0.026		U0-L1	0.158	0.026
	L1-L2	0.238	0.028		L1-L2	0.179	0.028
	L1-U1	-0.036	-0.296		L1-U1	-0.036	-0.227
	U1-L2	0.195	-0.249		U1-L2	0.149	-0.180
	L2-U2	0.042	-0.271		L2-U2	0.029	-0.204
	U2-L3	0.142	-0.207		U2-L3	0.108	-0.151
	L2-L3	0.243	0.028		L2-L3	0.184	0.028
	U2-U2'	-0.030	-0.216		U2-U2'	-0.066	-0.195
	System	**0.243**	**-0.296**		**System**	**0.184**	**-0.230**

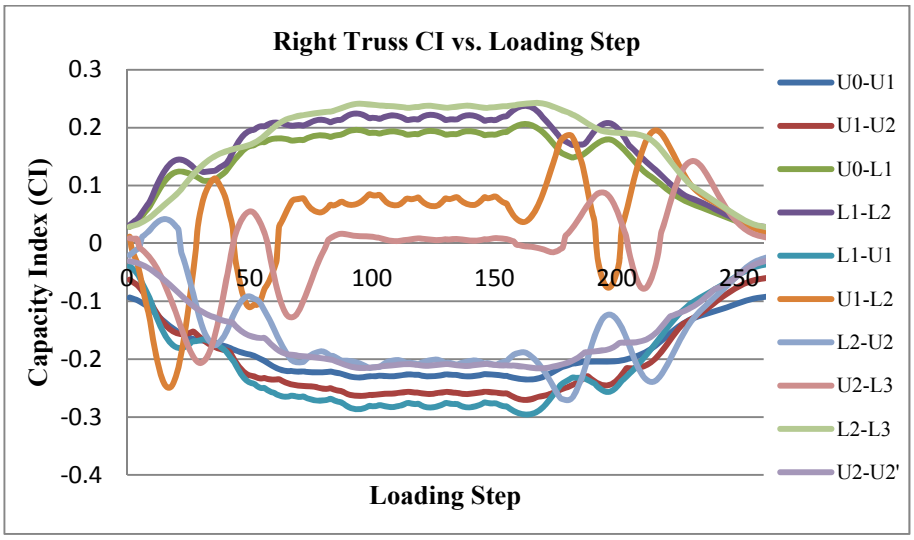

Figure B.9: CombII Right Truss CI vs. Loading Step (max=0.243, min=-0.296)

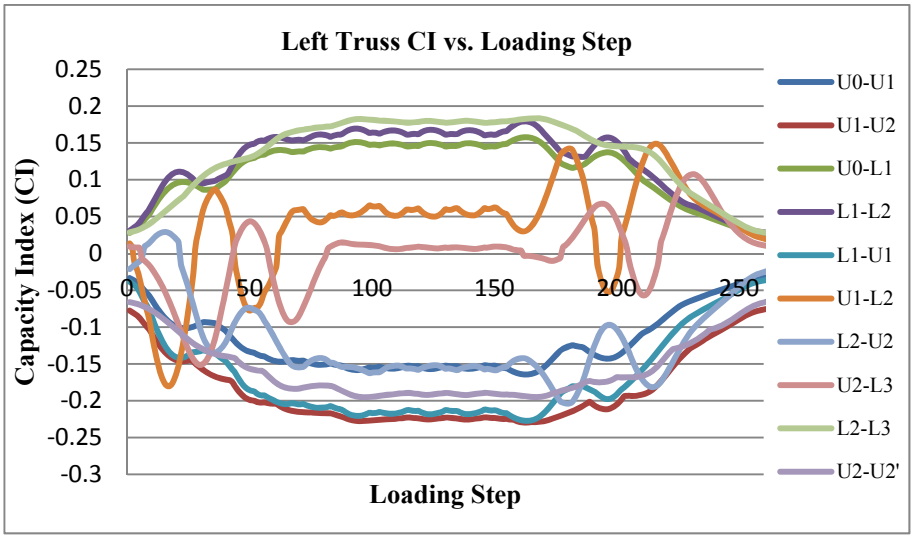

Figure B.10: CombII left Truss CI vs. Loading Step (max=0.184, min=-0.230)

Table B.14: CombII CI Results for Floor Beams and Lateral Braces

Member	Max	Min
FB-0	-0.010	-0.012
R0-L1	-0.243	-0.261
R1-L 1	0.062	0.057
R1-L2	-0.230	-0.249
FB-1	0.017	0.016
R2-L 3	-0.177	-0.188
R3-L3	0.029	0.027
R3-L 4	-0.141	-0.152
FB-2	0.009	0.009
R4-L5	-0.103	-0.109
R5-L5	0.011	0.011
System	**0.062**	**-0.261**

Table B.15: CombII CI Results for Vertical Braces

Member	Max	Min
L1-U1	0.030	0.027
U1-L2	0.081	0.075
L2-U2	0.087	0.080
U2-L3	0.010	0.009
System	**0.087**	**0.009**

B.1.2.3 CombIII (Q + Q_c + W_{-y} + B + Self) CI Results for Members

Table B.16: CombIII CI Results for Truss Members

RIGHT TRUSS	Member	Max	Min	LEFT TRUSS	Member	Max	Min
	U0-U1	0.050	-0.218		U0-U1	-0.072	-0.195
	U1-U2	-0.061	-0.278		U1-U2	-0.036	-0.190
	U0-L1	0.206	0.026		U0-L1	0.158	0.026
	L1-L2	0.238	0.028		L1-L2	0.179	0.028
	L1-U1	-0.036	-0.296		L1-U1	-0.036	-0.227
	U1-L2	0.195	-0.250		U1-L2	0.149	-0.180
	L2-U2	0.042	-0.271		L2-U2	0.029	-0.204
	U2-L3	0.142	-0.207		U2-L3	0.108	-0.151
	L2-L3	0.243	0.028		L2-L3	0.184	0.028
	U2-U2'	-0.057	-0.239		U2-U2'	-0.019	-0.148
	System	**0.243**	**-0.296**		**System**	**0.184**	**-0.227**

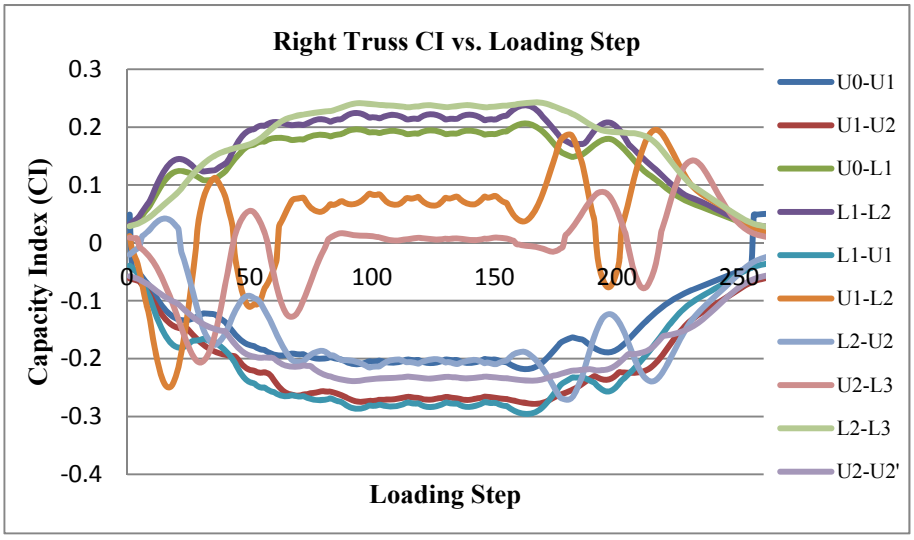

Figure B.11: CombIII Right Truss CI vs. Loading Step (max=0.243, min=-0.296)

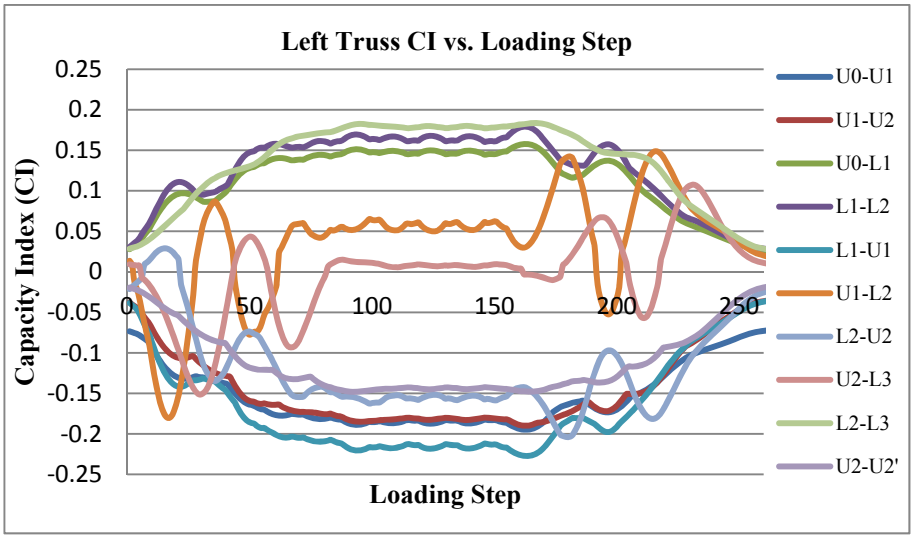

Figure B.12: CombIII left Truss CI vs. Loading Step (max=0.184, min=-0.227)

Table B.17: CombIII CI Results for Floor Beams and Lateral Braces

Member	Max	Min
FB-0	0.030	0.028
R0-L1	0.131	0.125
R1-L 1	-0.192	-0.206
R1-L2	0.120	0.115
FB-1	-0.024	-0.025
R2-L 3	0.090	0.086
R3-L3	-0.073	-0.078
R3-L 4	0.076	0.072
FB-2	-0.015	-0.016
R4-L5	0.062	0.060
R5-L5	-0.025	-0.025
System	**0.131**	**-0.206**

Table B.18: CombIII CI Results for Vertical Braces

Member	Max	Min
L1-U1	0.032	0.030
U1-L2	0.092	0.085
L2-U2	0.098	0.091
U2-L3	0.011	0.010
System	**0.098**	**0.010**

B.1.3 Actual Goods Train Load Crossing the Bridge

B.1.3.1 CombI (Q + Q_c + W_{+y} + B + Self) CI Results for Members

Table B.19: CombI CI Results for Truss Members

RIGHT TRUSS				LEFT TRUSS			
	Member	**Max**	**Min**		**Member**	**Max**	**Min**
	U0-U1	-0.055	-0.185		U0-U1	0.068	-0.112
	U1-U2	-0.034	-0.208		U1-U2	-0.079	-0.202
	U0-L1	0.172	0.026		U0-L1	0.132	0.026
	L1-L2	0.200	0.029		L1-L2	0.151	0.029
	L1-U1	-0.037	-0.246		L1-U1	-0.037	-0.190
	U1-L2	0.196	-0.242		U1-L2	0.149	-0.175
	L2-U2	0.040	-0.241		L2-U2	0.028	-0.182
	U2-L3	0.143	-0.203		U2-L3	0.108	-0.149
	L2-L3	0.197	0.029		L2-L3	0.150	0.028
	U2-U2'	-0.017	-0.161		U2-U2'	-0.066	-0.171
	System	**0.200**	**-0.246**		**System**	**0.151**	**-0.202**

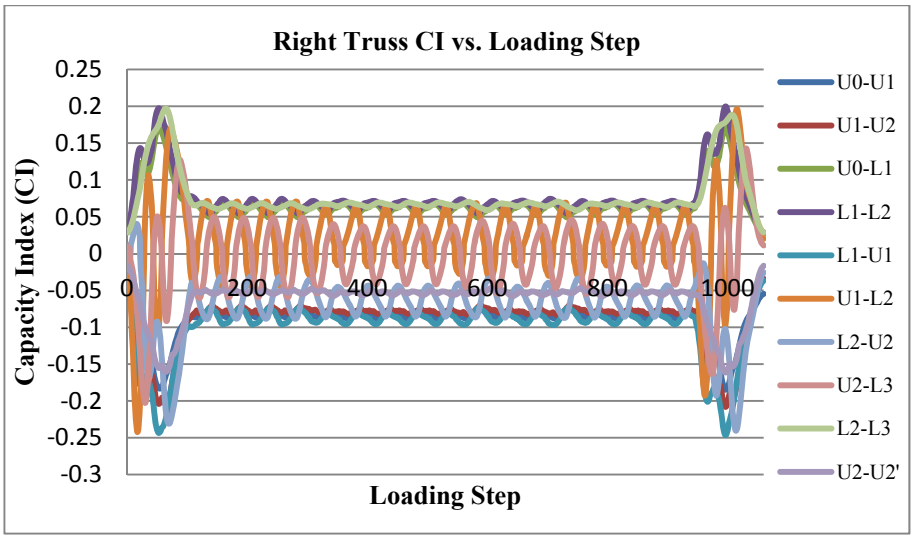

Figure B.13: CombI Right Truss CI vs. Loading Step (max=0.200, min=-0.246)

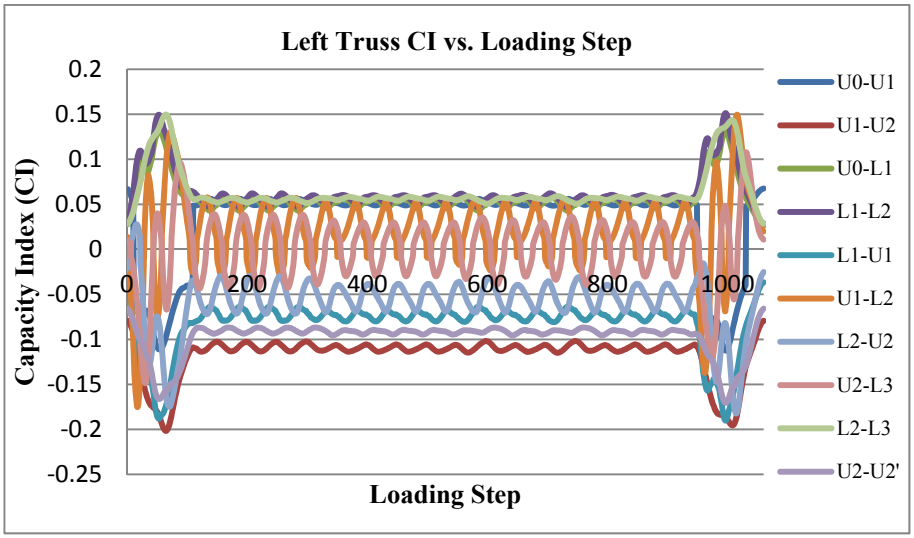

Figure B.14: CombI left Truss CI vs. Loading Step (max=0.151, min=-0.202)

Table B.20: CombI CI Results for Floor Beams and Lateral Braces

Member	Max	Min
FB-0	-0.015	-0.017
R0-L1	-0.286	-0.299
R1-L 1	0.074	0.070
R1-L2	-0.257	-0.271
FB-1	0.019	0.018
R2-L 3	-0.198	-0.207
R3-L3	0.033	0.031
R3-L 4	-0.152	-0.161
FB-2	0.013	0.012
R4-L5	-0.096	-0.102
R5-L5	0.011	0.010
System	**0.074**	**-0.299**

Table B.21: CombI CI Results for Vertical Braces

Member	Max	Min
L1-U1	0.031	0.028
U1-L2	0.097	0.092
L2-U2	0.104	0.099
U2-L3	0.011	0.011
System	**0.104**	**0.011**

B.1.3.2 CombII (Q + Q_c + W_{+y} + A + Self) CI Results for Members

Table B.22: CombII CI Results for Truss Members

RIGHT TRUSS	Member	Max	Min	LEFT TRUSS	Member	Max	Min
	U0-U1	-0.093	-0.203		U0-U1	-0.033	-0.137
	U1-U2	-0.060	-0.234		U1-U2	-0.076	-0.203
	U0-L1	0.172	0.026		U0-L1	0.132	0.026
	L1-L2	0.200	0.029		L1-L2	0.151	0.029
	L1-U1	-0.037	-0.246		L1-U1	-0.037	-0.190
	U1-L2	0.196	-0.242		U1-L2	0.149	-0.175
	L2-U2	0.040	-0.241		L2-U2	0.028	-0.182
	U2-L3	0.143	-0.203		U2-L3	0.108	-0.149
	L2-L3	0.197	0.029		L2-L3	0.150	0.028
	U2-U2'	-0.031	-0.176		U2-U2'	-0.066	-0.172
	System	**0.200**	**-0.246**		**System**	**0.151**	**-0.203**

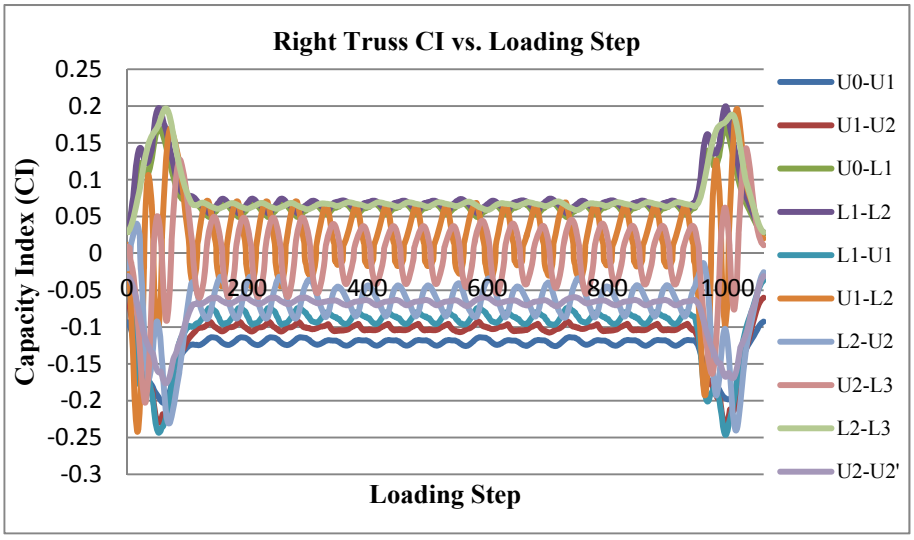

Figure B.15: CombII Right Truss CI vs. Loading Step (max=0.200, min=-0.246)

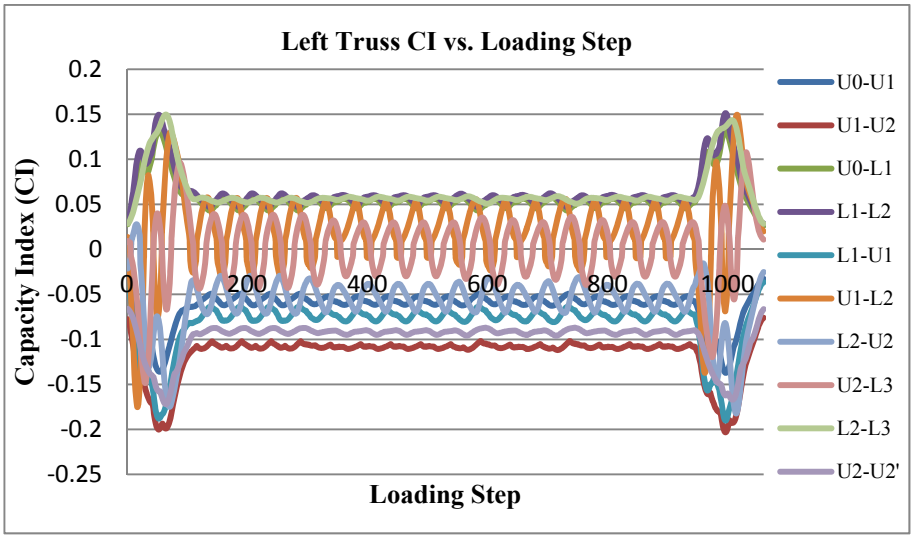

Figure B.16: CombII left Truss CI vs. Loading Step (max=0.151, min=-0.203)

Table B.23: CombII CI Results for Floor Beams and Lateral Braces

Member	Max	Min
FB-0	-0.010	-0.012
R0-L1	-0.247	-0.261
R1-L 1	0.062	0.058
R1-L2	-0.235	-0.249
FB-1	0.017	0.016
R2-L 3	-0.179	-0.188
R3-L3	0.029	0.027
R3-L 4	-0.143	-0.152
FB-2	0.009	0.009
R4-L5	-0.103	-0.109
R5-L5	0.011	0.011
System	**0.062**	**-0.261**

Table B.24: CombII CI Results for Vertical Braces

Member	Max	Min
L1-U1	0.030	0.028
U1-L2	0.081	0.076
L2-U2	0.087	0.081
U2-L3	0.010	0.009
System	**0.087**	**0.009**

B.1.3.3 CombIII (Q + Q_c + W_{-y} + B + Self) CI Results for Members

Table B.25: CombIII CI Results for Truss Members

RIGHT TRUSS				LEFT TRUSS			
	Member	**Max**	**Min**		**Member**	**Max**	**Min**
	U0-U1	0.050	-0.182		U0-U1	-0.073	-0.168
	U1-U2	-0.061	-0.233		U1-U2	-0.036	-0.164
	U0-L1	0.172	0.026		U0-L1	0.132	0.026
	L1-L2	0.200	0.029		L1-L2	0.151	0.029
	L1-U1	-0.037	-0.247		L1-U1	-0.037	-0.190
	U1-L2	0.196	-0.243		U1-L2	0.149	-0.175
	L2-U2	0.040	-0.241		L2-U2	0.028	-0.182
	U2-L3	0.143	-0.203		U2-L3	0.108	-0.149
	L2-L3	0.197	0.029		L2-L3	0.150	0.028
	U2-U2'	-0.057	-0.203		U2-U2'	-0.019	-0.124
	System	**0.200**	**-0.247**		**System**	**0.151**	**-0.190**

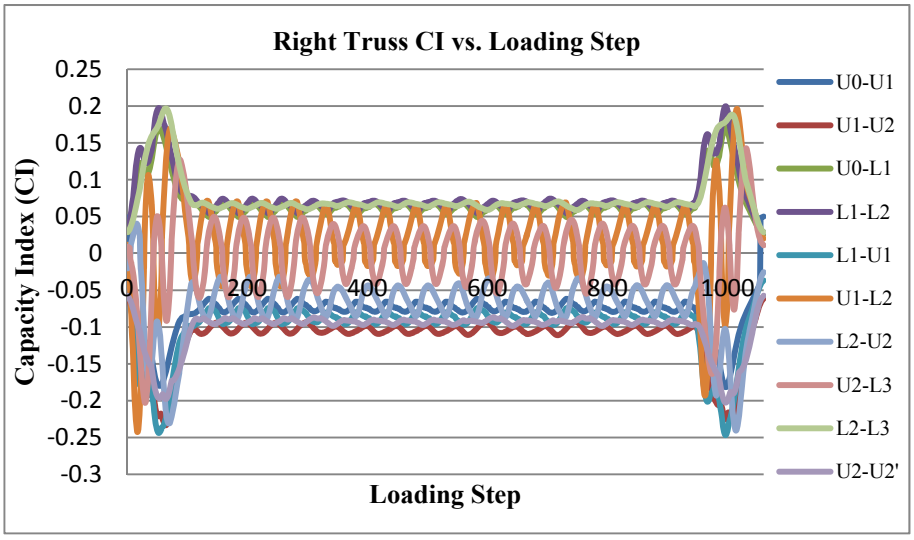

Figure B.17: CombII Right Truss CI vs. Loading Step (max=0.200, min=-0.247)

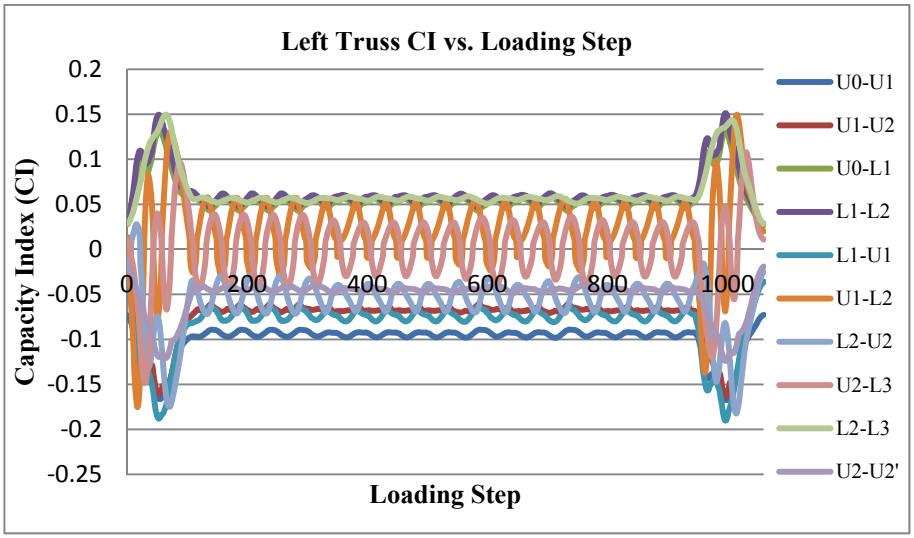

Figure B.18: CombII left Truss CI vs. Loading Step (max=0.151, min=-0.190)

Table B.26: CombIII CI Results for Floor Beams and Lateral Braces

Member	Max	Min
FB-0	0.030	0.028
R0-L1	0.130	0.125
R1-L 1	-0.192	-0.203
R1-L2	0.119	0.115
FB-1	-0.024	-0.025
R2-L 3	0.090	0.086
R3-L3	-0.073	-0.077
R3-L 4	0.075	0.072
FB-2	-0.015	-0.016
R4-L5	0.062	0.060
R5-L5	-0.025	-0.025
System	**0.130**	**-0.203**

Table B.27: CombIII CI Results for Vertical Braces

Member	Max	Min
L1-U1	0.032	0.030
U1-L2	0.091	0.085
L2-U2	0.097	0.091
U2-L3	0.011	0.010
System	**0.097**	**0.010**

B.2 β Results For Members

B.2.1 %60 LM71 (Design Train Moving Load) β Results

B.2.1.1 CombI (Q + Q_c + W_{+y} + B + Self) β Results for Members

Table B.28: CombI β Results for Truss Members

	Member	Max	Min		Member	Max	Min
RIGHT TRUSS	U0-U1	5.866	4.660	LEFT TRUSS	U0-U1	5.753	4.797
	U1-U2	6.014	4.406		U1-U2	5.546	4.374
	U0-L1	6.085	4.912		U0-L1	6.087	5.247
	L1-L2	6.070	4.699		L1-L2	6.072	5.097
	L1-U1	5.995	4.115		L1-U1	5.997	4.618
	U1-L2	6.202	5.278		U1-L2	6.197	5.513
	L2-U2	6.207	4.420		L2-U2	6.207	4.885
	U2-L3	6.227	5.214		U2-L3	6.224	5.500
	L2-L3	6.074	4.610		L2-L3	6.075	5.022
	U2-U2'	6.141	4.715		U2-U2'	5.788	4.831
	System	**6.227**	**4.115**		**System**	**6.224**	**4.374**

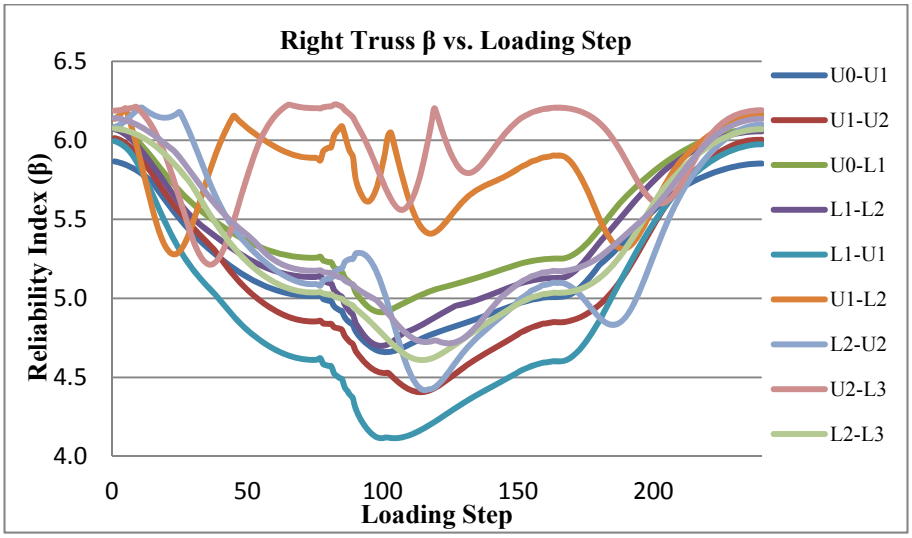

Figure B.19: CombI Right Truss β vs. Loading Step (min=4.115)

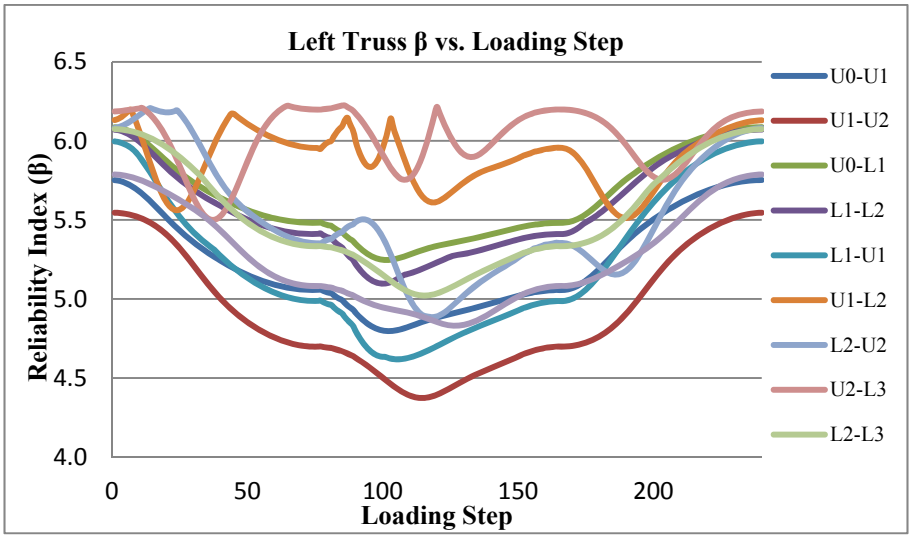

Figure B.20: CombI Left Truss β vs. Loading Step (min=4.374)

Table B.29: CombI β Results for Floor Beams and Lateral Braces

Member	Max	Min
FB-0	6.144	6.131
R0-L1	4.166	4.034
R1-L 1	5.812	5.779
R1-L2	4.383	4.247
FB-1	6.140	6.129
R2-L 3	4.822	4.738
R3-L3	6.061	6.045
R3-L 4	5.165	5.081
FB-2	6.174	6.172
R4-L5	5.566	5.526
R5-L5	6.184	6.184
System	**6.184**	**4.034**

Table B.30: CombI β Results for Vertical Braces

Member	Max	Min
L1-U1	6.131	6.119
U1-L2	5.860	5.832
L2-U2	5.829	5.799
U2-L3	6.206	6.203
System	**6.206**	**5.799**

B.2.1.2 CombII (Q + Q_c + W_{+y} + A + Self) β Results for Members

Table B. 31: CombII β Results for Truss Members

	Member	Max	Min		Member	Max	Min
RIGHT TRUSS	U0-U1	5.592	4.534	**LEFT TRUSS**	U0-U1	5.843	4.896
	U1-U2	5.828	4.261		U1-U2	5.691	4.518
	U0-L1	6.085	4.912		U0-L1	6.087	5.247
	L1-L2	6.070	4.699		L1-L2	6.072	5.097
	L1-U1	5.995	4.115		L1-U1	5.997	4.618
	U1-L2	6.202	5.278		U1-L2	6.197	5.513
	L2-U2	6.207	4.420		L2-U2	6.207	4.885
	U2-L3	6.227	5.214		U2-L3	6.224	5.500
	L2-L3	6.074	4.610		L2-L3	6.075	5.022
	U2-U2'	6.042	4.610		U2-U2'	5.786	4.826
	System	**6.227**	**4.115**		**System**	**6.224**	**4.518**

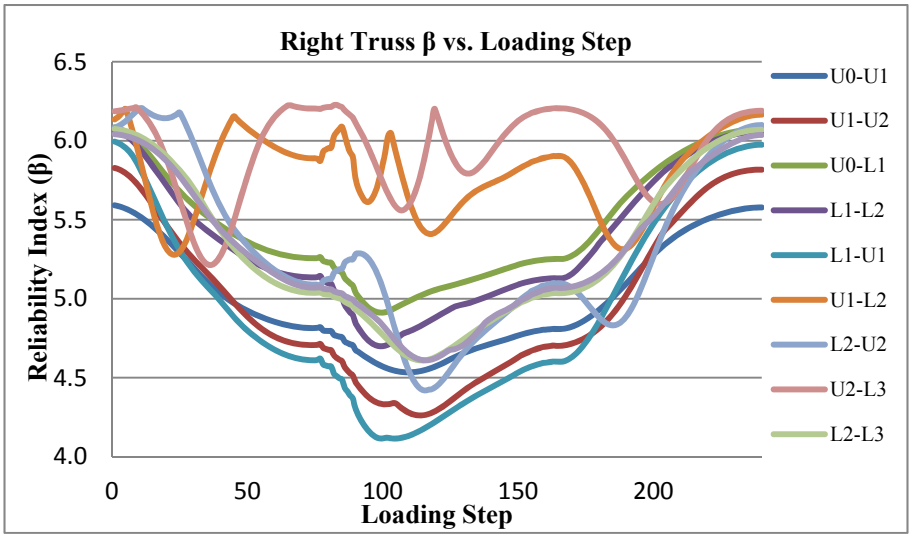

Figure B.21: CombII Right Truss β vs. Loading Step (min=4.115)

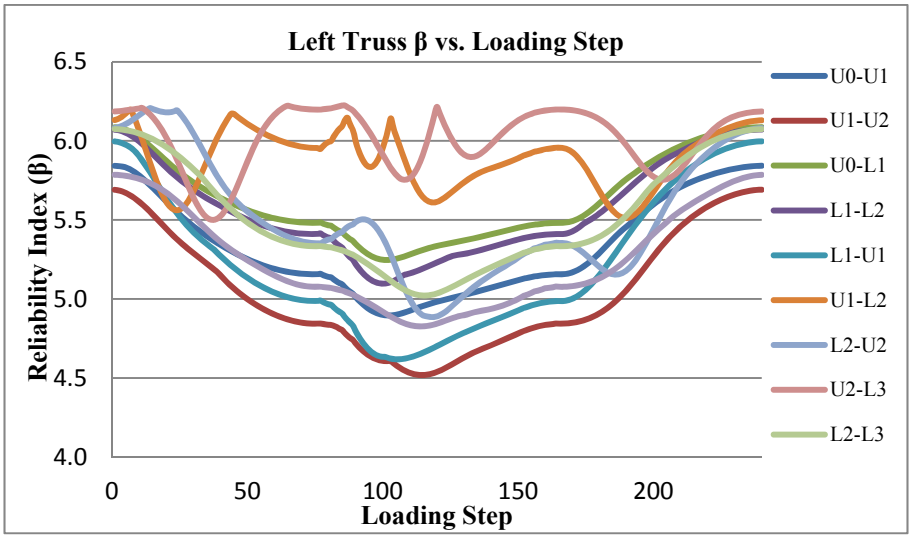

Figure B.22: CombI Left Truss β vs. Loading Step (min=4.518)

Table B.32: CombII β Results for Floor Beams and Lateral Braces

Member	Max	Min
FB-0	6.178	6.169
R0-L1	4.461	4.329
R1-L 1	5.890	5.857
R1-L2	4.553	4.418
FB-1	6.151	6.140
R2-L 3	4.963	4.879
R3-L3	6.082	6.066
R3-L 4	5.235	5.151
FB-2	6.195	6.192
R4-L5	5.512	5.472
R5-L5	6.182	6.181
System	**6.195**	**4.329**

Table B.33: CombII β Results for Vertical Braces

Member	Max	Min
L1-U1	6.135	6.122
U1-L2	5.929	5.901
L2-U2	5.907	5.877
U2-L3	6.211	6.208
System	**6.211**	**5.877**

B.2.1.3 CombIII (Q + Q_c + W_{-y} + B + Self) β Results for Members

Table B.34: CombIII β Results for Truss Members

	Member	Max	Min		Member	Max	Min
RIGHT TRUSS	U0-U1	5.636	4.324	LEFT TRUSS	U0-U1	5.736	4.856
	U1-U2	5.705	3.999		U1-U2	5.956	4.817
	U0-L1	6.085	4.912		U0-L1	6.087	5.247
	L1-L2	6.070	4.699		L1-L2	6.072	5.097
	L1-U1	5.995	4.114		L1-U1	5.997	4.618
	U1-L2	6.202	5.277		U1-L2	6.197	5.513
	L2-U2	6.207	4.420		L2-U2	6.207	4.885
	U2-L3	6.227	5.213		U2-L3	6.224	5.500
	L2-L3	6.074	4.610		L2-L3	6.075	5.022
	U2-U2'	5.850	4.444		U2-U2'	6.101	5.118
	System	**6.227**	**3.999**		**System**	**6.224**	**4.618**

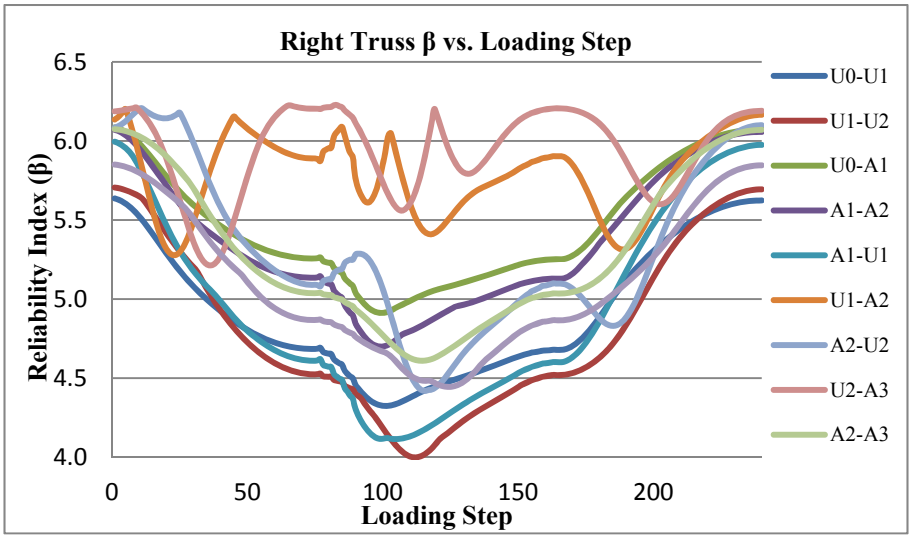

Figure B.23: CombIII Right Truss β vs. Loading Step (min=3.999)

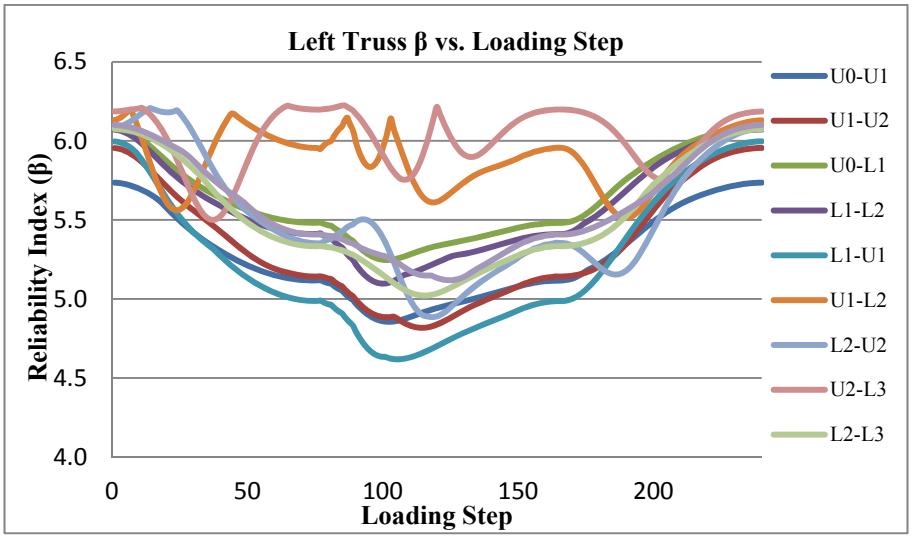

Figure B.24: CombIII left Truss β vs. Loading Step (min=4.618)

Table B.35: CombIII β Results for Floor Beams and Lateral Braces

Member	Max	Min
FB-0	6.076	6.062
R0-L1	5.442	5.404
R1-L 1	4.850	4.745
R1-L2	5.512	5.474
FB-1	6.083	6.073
R2-L 3	5.697	5.671
R3-L3	5.733	5.695
R3-L 4	5.791	5.766
FB-2	6.143	6.139
R4-L5	5.869	5.857
R5-L5	6.076	6.075
System	**6.143**	**4.745**

Table B.36: CombIII β Results for Vertical Braces

Member	Max	Min
L1-U1	6.123	6.111
U1-L2	5.881	5.853
L2-U2	5.855	5.825
U2-L3	6.206	6.203
System	**6.206**	**5.825**

B.2.2 Ultimate Service Goods Train Load β Results

B.2.2.1 CombI (Q + Q_c + W_{+y} + B + Self) β Results for Members

Table B.37: CombI β Results for Truss Members

RIGHT TRUSS	Member	Max	Min	LEFT TRUSS	Member	Max	Min
	U0-U1	5.866	4.628		U0-U1	5.968	5.243
	U1-U2	6.014	4.443		U1-U2	5.689	4.552
	U0-L1	6.086	4.897		U0-L1	6.086	5.225
	L1-L2	6.071	4.684		L1-L2	6.071	5.080
	L1-U1	5.996	4.064		L1-U1	5.996	4.583
	U1-L2	6.177	4.415		U1-L2	6.199	4.936
	L2-U2	6.207	4.253		L2-U2	6.206	4.758
	U2-L3	6.236	4.739		U2-L3	6.231	5.153
	L2-L3	6.073	4.648		L2-L3	6.074	5.050
	U2-U2'	6.139	4.765		U2-U2'	5.787	4.830
	System	**6.236**	**4.064**		**System**	**6.231**	**4.552**

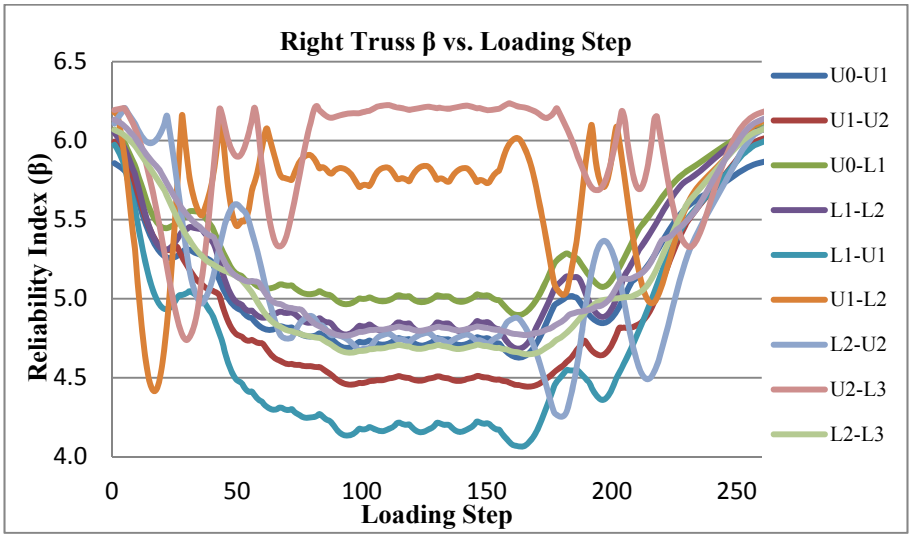

Figure B.25: CombI Right Truss β vs. Loading Step (min=4.064)

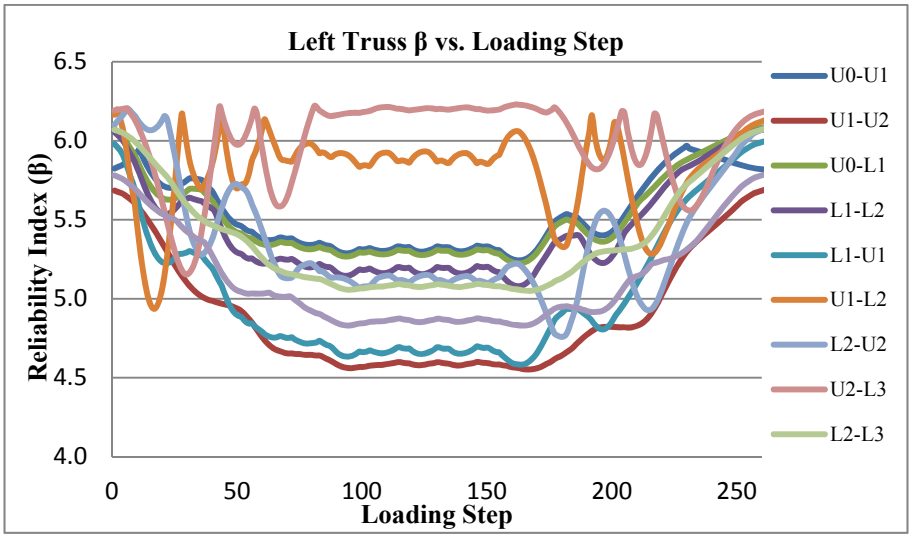

Figure B.26: CombI Left Truss β vs. Loading Step (min=4.552)

Table B.38: CombI β Results for Floor Beams and Lateral Braces

Member	Max	Min
FB-0	6.145	6.131
R0-L1	4.171	4.034
R1-L 1	5.813	5.779
R1-L2	4.388	4.247
FB-1	6.141	6.129
R2-L 3	4.821	4.738
R3-L3	6.060	6.045
R3-L 4	5.163	5.080
FB-2	6.174	6.172
R4-L5	5.564	5.523
R5-L5	6.184	6.184
System	**6.184**	**6.184**

Table B.39: CombI β Results for Vertical Braces

Member	Max	Min
L1-U1	6.073	6.055
U1-L2	5.670	5.629
L2-U2	5.625	5.580
U2-L3	6.185	6.180
System	**6.185**	**5.580**

B.2.2.2 CombII (Q + Q_c + W_{+y} + A + Self) β Results for Members

Table B.40: CombII β Results for Truss Members

	Member	Max	Min		Member	Max	Min
RIGHT TRUSS	U0-U1	5.592	4.523	LEFT TRUSS	U0-U1	6.022	5.057
	U1-U2	5.827	4.256		U1-U2	5.713	4.565
	U0-L1	6.086	4.897		U0-L1	6.086	5.225
	L1-L2	6.071	4.684		L1-L2	6.071	5.080
	L1-U1	5.996	4.064		L1-U1	5.996	4.583
	U1-L2	6.177	4.415		U1-L2	6.199	4.936
	L2-U2	6.207	4.253		L2-U2	6.206	4.758
	U2-L3	6.236	4.739		U2-L3	6.231	5.153
	L2-L3	6.073	4.648		L2-L3	6.074	5.050
	U2-U2'	6.040	4.669		U2-U2'	5.784	4.825
	System	**6.236**	**4.064**		**System**	**6.231**	**4.565**

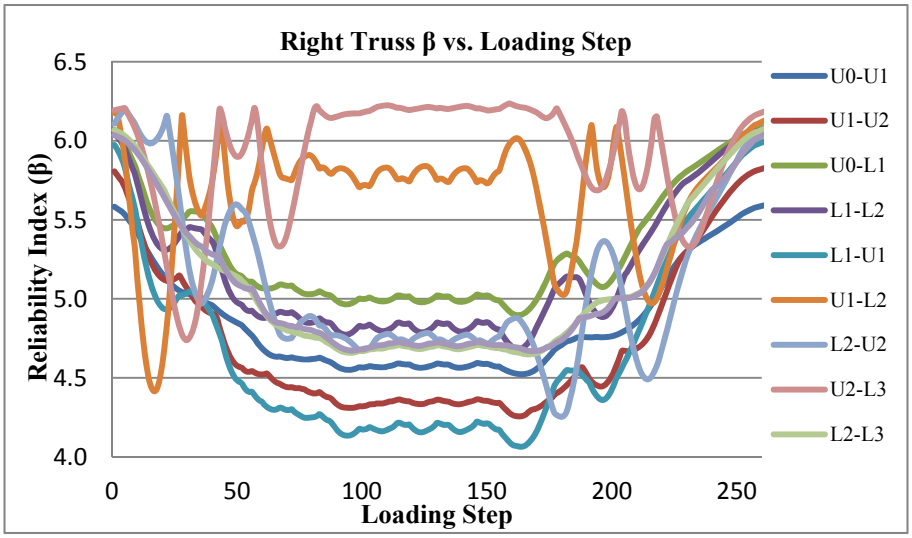

Figure B.27: CombII Right Truss β vs. Loading Step (min=4.064)

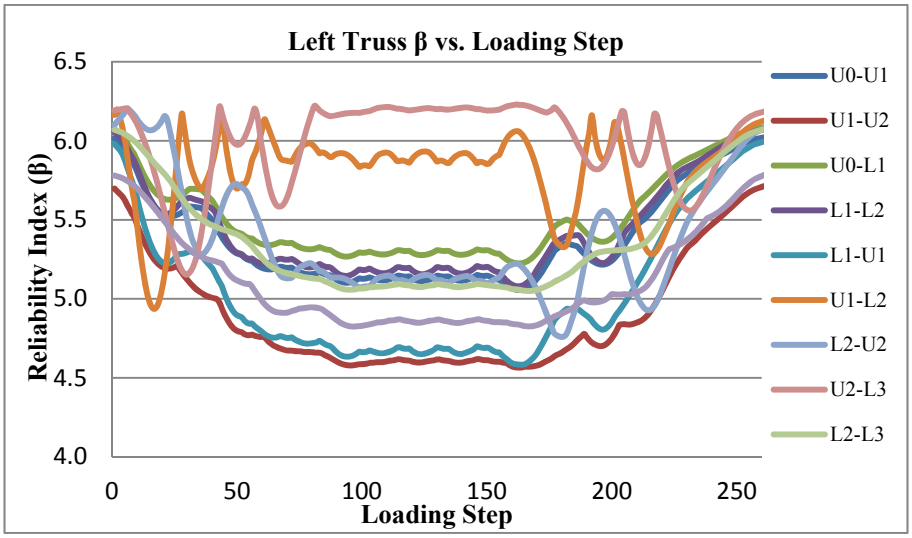

Figure B.28: CombII Left Truss β vs. Loading Step (min=4.565)

Table B.41: CombII β Results for Floor Beams and Lateral Braces

Member	Max	Min
FB-0	6.179	6.169
R0-L1	4.466	4.329
R1-L 1	5.891	5.857
R1-L2	4.559	4.418
FB-1	6.152	6.140
R2-L 3	4.961	4.879
R3-L3	6.082	6.066
R3-L 4	5.233	5.151
FB-2	6.195	6.192
R4-L5	5.510	5.469
R5-L5	6.182	6.181
System	**6.195**	**4.329**

Table B.42: CombII β Results for Vertical Braces

Member	Max	Min
L1-U1	6.079	6.061
U1-L2	5.774	5.733
L2-U2	5.741	5.696
U2-L3	6.192	6.187
System	**6.192**	**5.696**

B2.2.3 CombIII (Q + Q_e + W_{-y} + B + Self) β Results for Members

Table B.43: CombIII β Results for Truss Members

RIGHT TRUSS				LEFT TRUSS			
	Member	**Max**	**Min**		**Member**	**Max**	**Min**
	U0-U1	5.952	4.653		U0-U1	5.736	4.828
	U1-U2	5.820	4.196		U1-U2	5.999	4.865
	U0-L1	6.086	4.897		U0-L1	6.086	5.225
	L1-L2	6.071	4.684		L1-L2	6.071	5.080
	L1-U1	5.996	4.064		L1-U1	5.996	4.583
	U1-L2	6.177	4.412		U1-L2	6.199	4.936
	L2-U2	6.207	4.251		L2-U2	6.206	4.758
	U2-L3	6.236	4.737		U2-L3	6.231	5.153
	L2-L3	6.073	4.648		L2-L3	6.074	5.050
	U2-U2'	5.849	4.495		U2-U2'	6.120	5.179
	System	**6.236**	**4.064**		**System**	**6.231**	**4.583**

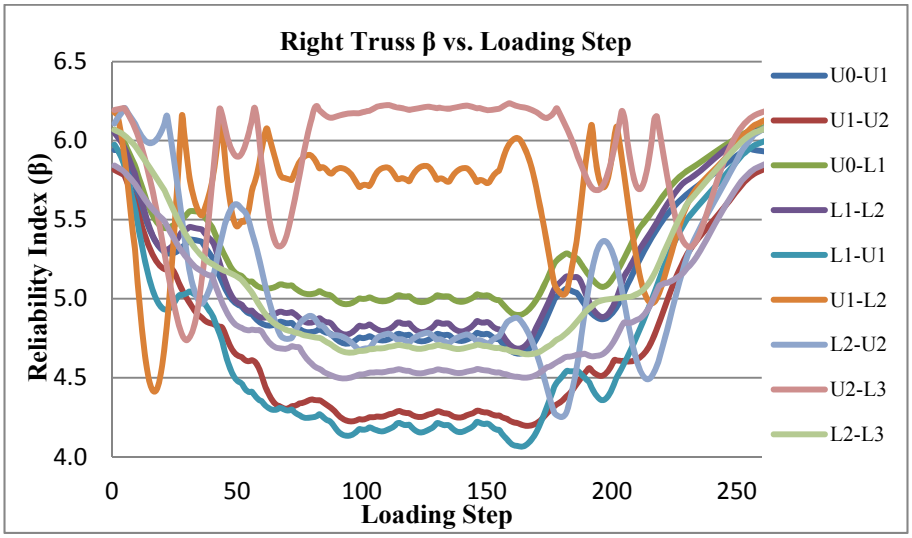

Figure B.29: CombIII Right Truss β vs. Loading Step (min=4.064)

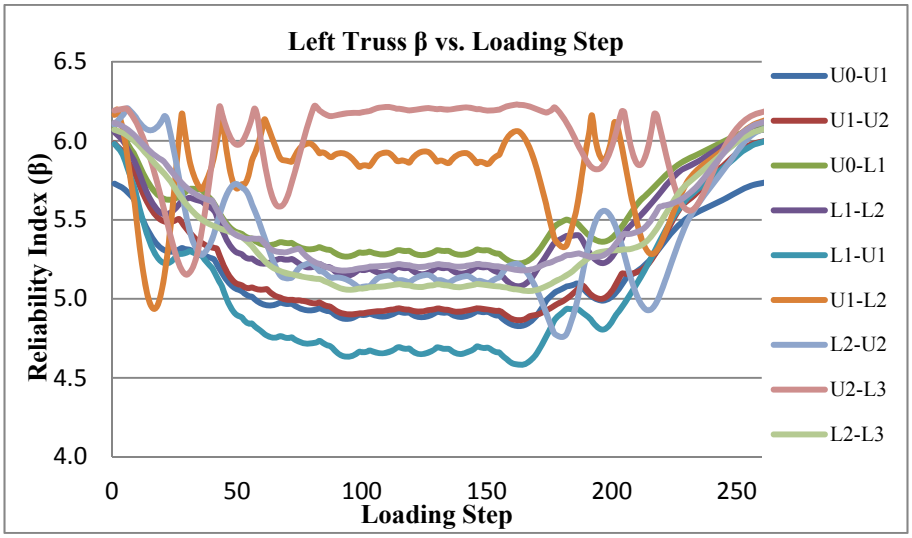

Figure B.30: CombIII Left Truss β vs. Loading Step (min=4.583)

Table B.44: CombIII β Results for Floor Beams and Lateral Braces

Member	Max	Min
FB-0	6.076	6.060
R0-L1	5.442	5.403
R1-L 1	4.849	4.741
R1-L2	5.512	5.473
FB-1	6.083	6.073
R2-L 3	5.697	5.672
R3-L3	5.734	5.695
R3-L 4	5.791	5.767
FB-2	6.143	6.139
R4-L5	5.870	5.858
R5-L5	6.076	6.076
System	**6.143**	**4.741**

Table B.45: CombIII β Results for Vertical Braces

Member	Max	Min
L1-U1	6.063	6.045
U1-L2	5.703	5.662
L2-U2	5.664	5.619
U2-L3	6.185	6.180
System	**6.185**	**5.619**

B.2.3 Actual Goods Train Load Crossing the Bridge β Results

B.2.3.1 CombI (Q + Q_c + W_{+y} + B + Self) β Results for Members

Table B.46: CombI β Results for Truss Members

	Member	Max	Min		Member	Max	Min
RIGHT TRUSS	U0-U1	5.864	4.903	LEFT TRUSS	U0-U1	5.973	5.443
	U1-U2	6.011	4.728		U1-U2	5.686	4.776
	U0-L1	6.083	5.125		U0-L1	6.084	5.398
	L1-L2	6.068	4.941		L1-L2	6.069	5.268
	L1-U1	5.991	4.438		L1-U1	5.993	4.863
	U1-L2	6.196	4.469		U1-L2	6.199	4.975
	L2-U2	6.208	4.482		L2-U2	6.206	4.922
	U2-L3	6.215	4.768		U2-L3	6.223	5.175
	L2-L3	6.069	4.962		L2-L3	6.071	5.278
	U2-U2'	6.135	5.079		U2-U2'	5.783	5.010
	System	**6.215**	**4.438**		**System**	**6.223**	**4.776**

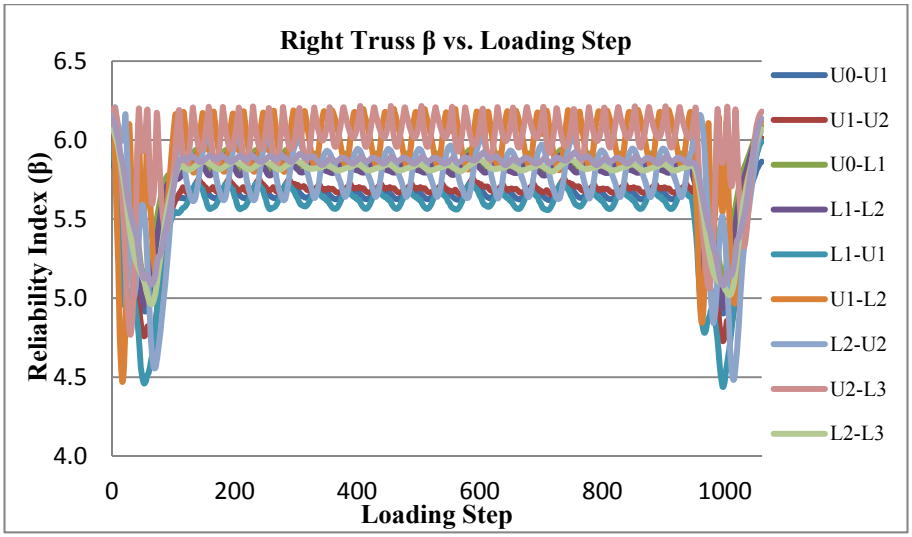

Figure B.31: CombI Right Truss β vs. Loading Step (min=4.438)

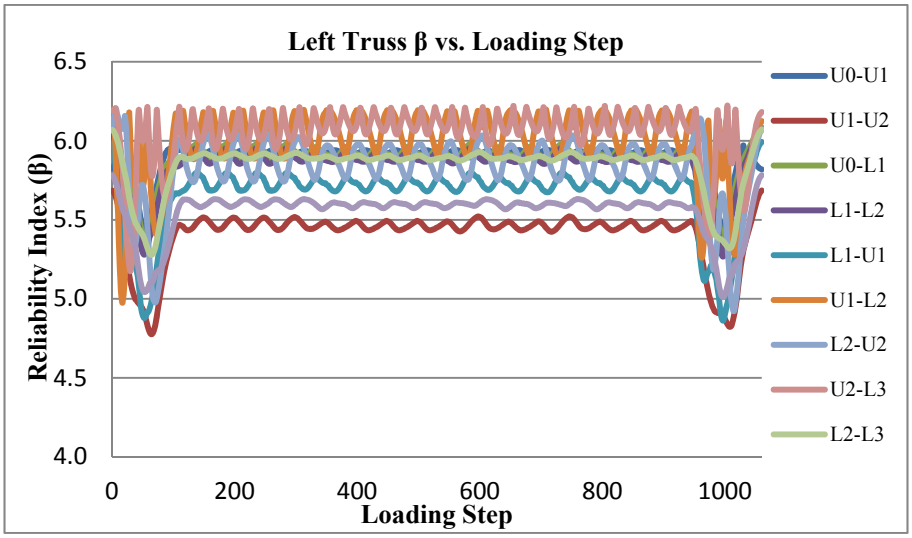

Figure B.32: CombI Left Truss β vs. Loading Step (min=4.776)

Table B.47: CombI β Results for Floor Beams and Lateral Braces

Member	Max	Min
FB-0	6.143	6.131
R0-L1	4.140	4.035
R1-L 1	5.805	5.779
R1-L2	4.356	4.248
FB-1	6.138	6.129
R2-L 3	4.805	4.738
R3-L3	6.057	6.045
R3-L 4	5.148	5.080
FB-2	6.174	6.172
R4-L5	5.563	5.523
R5-L5	6.184	6.184
System	**6.184**	**4.035**

Table B.48: CombI β Results for Vertical Braces

Member	Max	Min
L1-U1	6.071	6.055
U1-L2	5.662	5.629
L2-U2	5.616	5.580
U2-L3	6.184	6.180
System	**6.184**	**5.580**

B.2.3.2 CombII (Q + Q_c + W_{+y} + A + Self) β Results for Members

Table B.49: CombII β Results for Truss Members

	Member	Max	Min		Member	Max	Min
RIGHT TRUSS	U0-U1	5.589	4.766	**LEFT TRUSS**	U0-U1	6.020	5.260
	U1-U2	5.824	4.532		U1-U2	5.710	4.765
	U0-L1	6.083	5.125		U0-L1	6.084	5.398
	L1-L2	6.068	4.941		L1-L2	6.069	5.268
	L1-U1	5.991	4.438		L1-U1	5.993	4.863
	U1-L2	6.196	4.469		U1-L2	6.199	4.975
	L2-U2	6.208	4.482		L2-U2	6.206	4.922
	U2-L3	6.215	4.768		U2-L3	6.223	5.175
	L2-L3	6.069	4.962		L2-L3	6.071	5.278
	U2-U2'	6.035	4.966		U2-U2'	5.781	5.000
	System	**6.215**	**4.438**		**System**	**6.223**	**4.765**

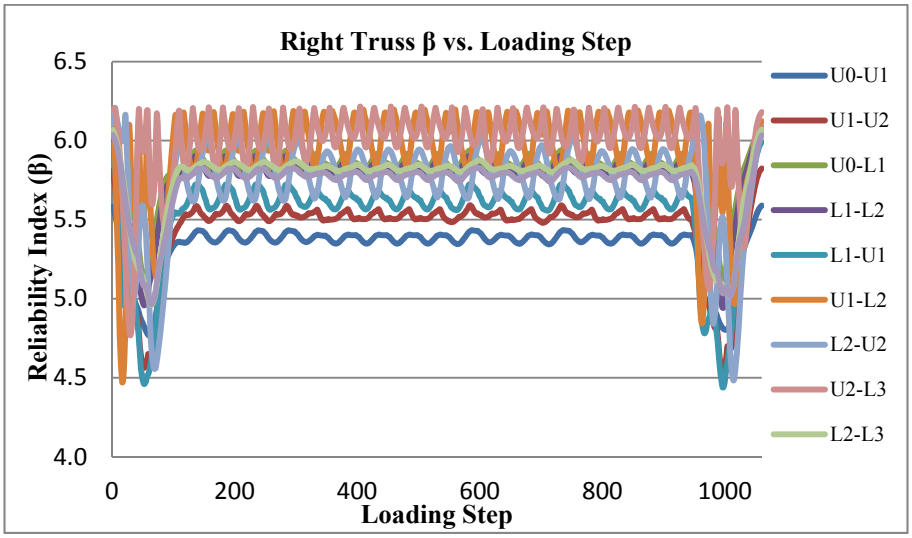

Figure B.33: CombII Right Truss β vs. Loading Step (min=4.438)

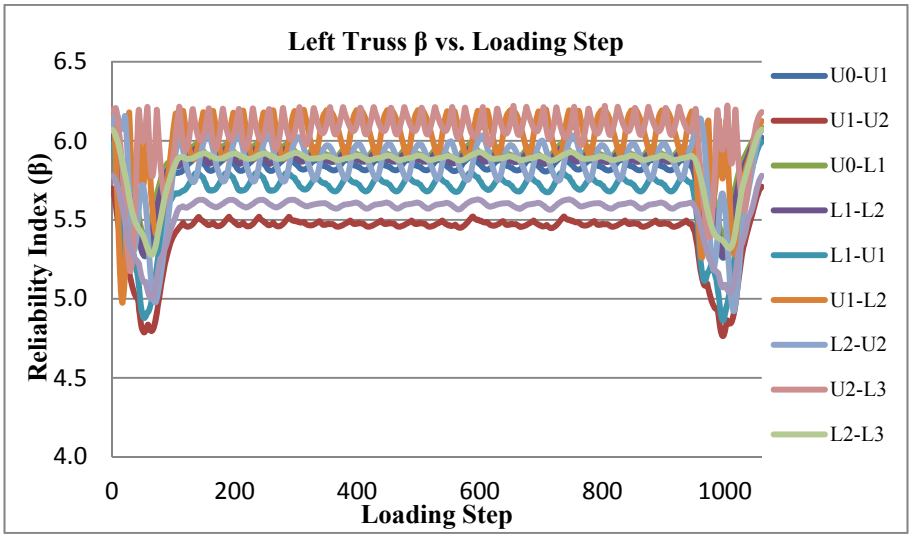

Figure B.34: CombII Left Truss β vs. Loading Step (min=4.765)

Table B.50: CombII β Results for Floor Beams and Lateral Braces

Member	Max	Min
FB-0	6.177	6.169
R0-L1	4.435	4.329
R1-L 1	5.883	5.857
R1-L2	4.526	4.419
FB-1	6.149	6.140
R2-L 3	4.945	4.879
R3-L3	6.079	6.066
R3-L 4	5.218	5.151
FB-2	6.194	6.192
R4-L5	5.509	5.469
R5-L5	6.182	6.181
System	**6.194**	**4.329**

Table B.51: CombII β Results for Vertical Braces

Member	Max	Min
L1-U1	6.077	6.061
U1-L2	5.766	5.733
L2-U2	5.732	5.696
U2-L3	6.191	6.187
System	**6.191**	**5.696**

B.2.3.3 CombIII (Q + Q_c + W_{-y} + B + Self) β Results for Members

Table B.52: CombIII β Results for Truss Members

	Member	Max	Min		Member	Max	Min
RIGHT TRUSS	U0-U1	5.948	4.928	LEFT TRUSS	U0-U1	5.733	5.033
	U1-U2	5.815	4.538		U1-U2	5.996	5.063
	U0-L1	6.083	5.125		U0-L1	6.084	5.398
	L1-L2	6.068	4.941		L1-L2	6.069	5.268
	L1-U1	5.991	4.435		L1-U1	5.993	4.863
	U1-L2	6.196	4.467		U1-L2	6.199	4.975
	L2-U2	6.208	4.482		L2-U2	6.206	4.922
	U2-L3	6.215	4.767		U2-L3	6.223	5.175
	L2-L3	6.069	4.962		L2-L3	6.071	5.278
	U2-U2'	5.844	4.770		U2-U2'	6.117	5.358
	System	**6.215**	**4.435**		**System**	**6.223**	**4.863**

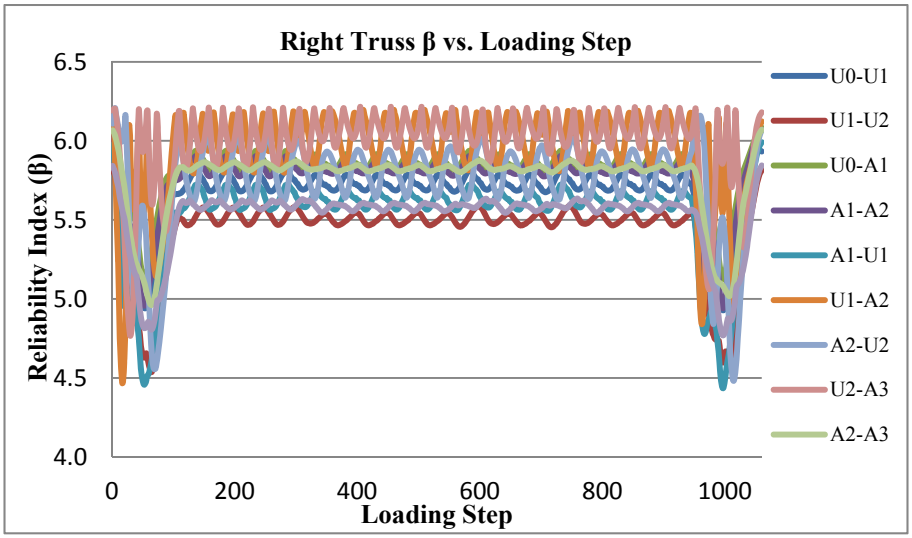

Figure B.35: CombIII Right Truss β vs. Loading Step (min=4.435)

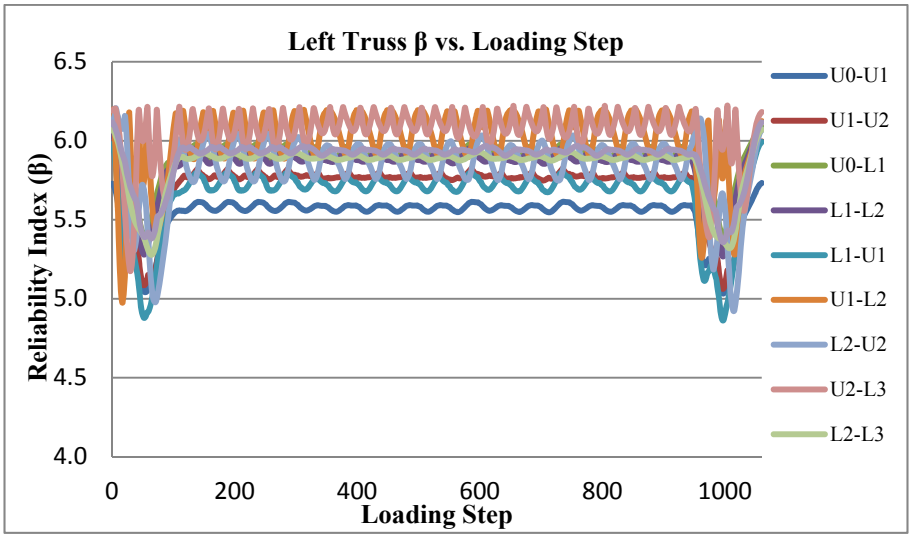

Figure B.36: CombIII Left Truss β vs. Loading Step (min=4.863)

Table B.53: CombIII β Results for Floor Beams and Lateral Braces

Member	Max	Min
FB-0	6.076	6.063
R0-L1	5.442	5.412
R1-L 1	4.849	4.766
R1-L2	5.511	5.482
FB-1	6.083	6.075
R2-L 3	5.697	5.676
R3-L3	5.734	5.702
R3-L 4	5.791	5.772
FB-2	6.143	6.140
R4-L5	5.870	5.859
R5-L5	6.076	6.076
System	**6.143**	**4.766**

Table B.54: CombIII β Results for Vertical Braces

Member	Max	Min
L1-U1	6.063	6.048
U1-L2	5.703	5.670
L2-U2	5.664	5.628
U2-L3	6.185	6.181
System	**6.185**	**5.628**